AD NUMBER
AD855747
LIMITATION CHANGES

TO:

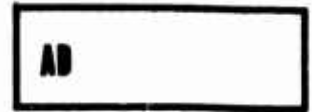Approved for public release; distribution is unlimited.

FROM:

Distribution authorized to U.S. Gov't. agencies and their contractors; Administrative/Operational Use; MAY 1969. Other requests shall be referred to Army Aviation Materiel Labs., Fort Eustis, VA 23604.

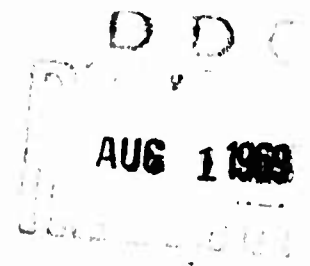AUTHORITY

USAMRDL ltr 23 Jun 1971

USAAVLABS TECHNICAL REPORT 68-57

INSTALLATION OF A
HIGH-REDUCTION-RATIO TRANSMISSION
IN THE UH-1 HELICOPTER

By

C. W. Bowen
C. E. Braddock
R. D. Walker

D D C

AUG 1 1969

May 1969

U. S. ARMY AVIATION MATERIEL LABORATORIES
FORT EUSTIS, VIRGINIA

AD855747

306

BLANK PAGES
IN THIS
DOCUMENT
WERE NOT
FILMED

Disclaimers

The findings in this report are not to be construed as an official Department of the Army position unless so designated by other authorized documents.

When government drawings, specifications, or other data are used for any purpose other than in connection with a definitely related Government procurement operation, the United States Government thereby incurs no responsibility nor any obligation whatsoever; and the fact that the Government may have formulated, furnished, or in any way supplied the said drawings, specifications, or other data is not to be regarded by implication or otherwise as in any manner licensing the holder or any other person or corporation, or conveying any rights or permission, to manufacture, use, or sell any patented invention that may in any way be related thereto.

Disposition Instructions

Destroy this report when no longer needed. Do not return it to the originator.

DEPARTMENT OF THE ARMY
U. S. ARMY AVIATION MATERIEL LABORATORIES
Fort Eustis, Virginia 23604

ERRATUM

USAAVLABS Technical Report 68-57
TITLE: Installation of a High-Reduction-Ratio Transmission in the
UH-1 Helicopter

Delete the statement on cover, title page, and block 10 of DD Form 1473
which reads

> "This document has been approved for public release
> and sale; its distribution is unlimited. "

and replace with the following statement:

> "This document is subject to special export controls
> and each transmittal to foreign governments or
> foreign nationals may be made only with prior approval
> of US Army Aviation Materiel Laboratories, Fort
> Eustis, Virginia 23604. "

This report represents a part of a continuing research program for investigation of new concepts of high-speed gear reducers for use as main transmissions in helicopters. The main efforts of this particular study were directed toward the investigation of the roller gear transmission concept for installation in a UH-1 type helicopter.

The results obtained from this study are considered to be applicable to a UH-1 type helicopter and will not necessarily apply to other helicopter drive trains.

Demonstration of the conclusions reported herein requires the implementation of a fully integrated program that would include design, manufacture, bench test, and flight test of the roller gear transmission.

Task 1G121401D14414
Contract DA 44-177-AMC-411(T)
USAAVLABS Technical Report 68-57
May 1969

INSTALLATION OF A
HIGH-REDUCTION-RATIO TRANSMISSION
IN THE UH-1 HELICOPTER

Bell Helicopter Report 299-099-112
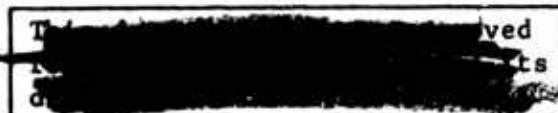

By

C. W. Bowen
C. E. Braddock
R. D. Walker

Prepared by

BELL HELICOPTER COMPANY
A Division of Bell Aerospace Corporation
Fort Worth, Texas

U. S. ARMY AVIATION MATERIEL LABORATORIES
FORT EUSTIS, VIRGINIA

SUMMARY

This report presents the results of an engineering design
study to determine the feasibility of utilizing a high-speed
roller gear transmission in a turbine-powered helicopter drive
system.

In such a transmission, the total speed reduction from the en-
gine power turbine to the main rotor is through one bevel gear
stage and a single "planetary" stage. The salient advantages
of this concept are derived from the use of pitch-line rollers
in lieu of antifriction bearings in the "planetary" stage.

The study was directed toward the design of an optimized
system adaptable to the UH-1 helicopter. Five different
roller gear planetary systems were devised and analyzed during
this refinement period. Manufacturing tolerance requirements
commensurate with reliable operation were also determined.
The primary study criteria were cost, weight, efficiency, and
reliability as compared to the existent UH-1 system.

The comparison results were greatly influenced by the obvious
inherent inefficiencies of the two separate speed reduction
units and lubrication systems now employed in the UH-1. How-
ever, the magnitude of the gains achieved through elimination
of the integral engine gearbox was surprisingly large. This
fact suggested the need for the further study of a relatively
conventional planetary system designed within a comparable
premise and utilization of current technological skills.

As an extension of the scope of this study, a three-stage
planetary adaptation of the UH-1 transmission was designed in
order to provide a credible comparative basis for evaluating
the roller gear system.

The relative rankings of the three systems with respect to
the noted criteria were found to be:

	UH-1	Roller Gear	Triple Planetary
Effective Weight Index	3	2	1
Power Transmission Efficiency	3	1	2
Potential Reliability	3	1	2
Manufacturability/Cost	2	3	1

FOREWORD

This report presents the results of an engineering design study to determine the feasibility of utilizing a high-speed roller gear transmission in a turbine-powered helicopter drive system (UH-lB). The study was accomplished at Bell Helicopter Company for the U. S. Army Aviation Materiel Laboratories (USAAVLABS), under Contract DA 44-177-AMC-411(T), Refe.ence 3, during the period 28 June through 17 April 1967. This contract resulted from a proposal submitted in May 1966 by BHC, containing Technical Report No. 299-099-314, to conduct an analysis, design, and feasibility study for installation of a high-speed roller gear transmission in the UH-1 helicopter, in response to RFQ AMC(T)44-177-66 (Neg. 59) of April 1966. An amendment to this contract, Reference 4, expanding the scope of this study to include the investigation of a three-stage planetary transmission system, authorized the work accomplished during the period 6 February 1968 through 30 April 1968. The entire study effort was conducted under the technical cognizance of Mr. W. Hudgins, USAAVLABS representative.

Technical assistance was provided by Messrs. W. R. Stapper, C. N. Warren, C. A. Turner, D. J. Cleveland, and F. A. Green of BHC Transmission Design Group. Mr. C. W. Bowen was Project Engineer for the study.

Acknowledgement of appreciation for technical contribution is given Mr. R. Fox and G. Knudsen of BHC Reliability Group, Mr. R. G. Nicoll of Lord Manufacturing Company, and Dr. A. L. Nasvytis, Mr. W. M. Shipitalo, and Mr. P. Rountree of TRW.

LIST OF ILLUSTRATIONS

LIST OF TABLES

INTRODUCTION

Recent developments in the high-speed roller gear transmission have demonstrated the feasibility of accomplishing large speed reductions in a single compound stage without the usual relatively high power loss. This capability may give the helicopter drive-train designer greater freedom in the use of high-speed, lightweight main drive and accessory components, in order to obtain increased overall operational efficiency for the complete drive system. The basic concepts involved have been explored by the TRW Company, in programs supported by USAAVLABS, and reported in References 1 and 2.

An adaptation of this drive system to the UH-1 helicopter is presented in this report. A further extension of the high-speed reduction approach is also presented in the form of a more conventional multiple-stage planetary transmission, in order to better evaluate the intrinsic characteristics of the RGT viewed apart from the advantages gained solely in combining all main rotor speed reduction gearing in one gearbox.

The comparisons of these two drives with the existent UH-1 drive system with regard to the study objective criteria of weight, efficiency, reliability, and cost, are developed, in detail, in the appropriate discussion sections following the design discussions. A brief description of the three drive systems follows.

A schematic of the existent UH-1 power transmission system is shown in Figure 1. The T-53 free-turbine engine incorporates an integrally housed gear reduction unit which reduces N_{II} turbine speed of 21,016 rpm to an output speed of 6,600 rpm. The main input drive shaft transmits engine power at this speed through crowned tooth gear coupling joints capable of absorbing the misalignment between engine output and the flexibly mounted main transmission. The multiple power paths to the main rotor, the antitorque rotor, and various electrical and hydraulic accessories are split within the main transmission. The 324-rpm main rotor drive is provided by a 90° 29/62 spiral bevel gear reduction and two planetary speed reduction stages of 3.087:1 each. Figure 2 is a detailed drawing of this transmission. The antitorque rotor drive from the main transmission output and along the top of the boom is through five thin-wall tubular aluminum drive shafts operating at 4,300 rpm, well below the first critical speed. Three hanger bearing/flexible coupling assemblies, a 42° 1:1 ratio spiral bevel gearbox (which redirects the drive line from the top of the boom to the leading edge of the ventral fin), and a 90° 15/39 ratio spiral bevel reduction gearbox connected by

1

MAIN ROTOR
324 RPM

2-STAGE PLANETARY REDUCTION
9.53 : 1

90° BEVEL DRIVE
2.14 : 1

SUMP & TA
DRIVE ASS

PYLON SUPPORT (
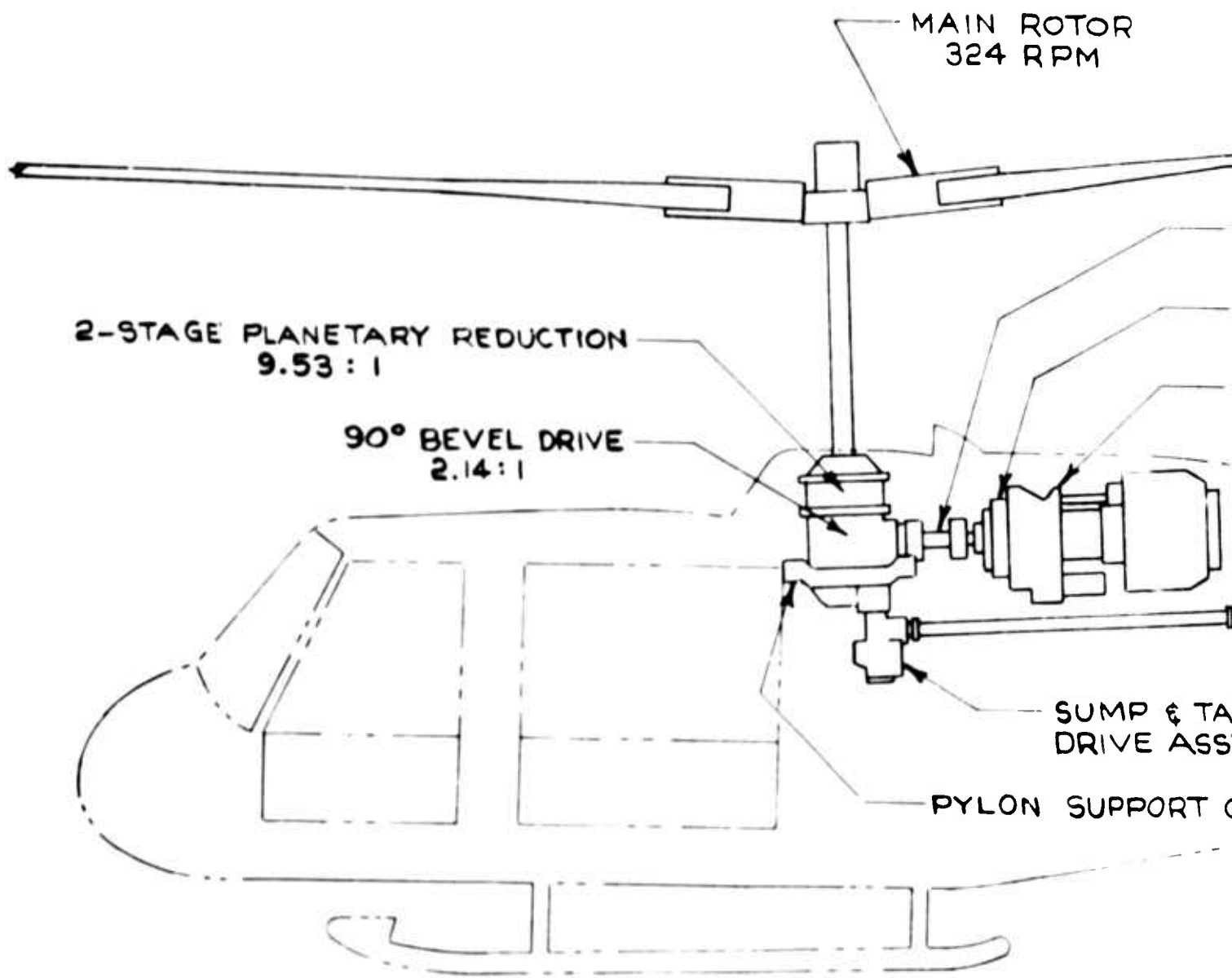
Figure 1. UH-1 Drive System

3

A

OR

MAIN INPUT DRIVE SHAFT
6600 RPM

INTEGRAL REDUCTION GEARBOX
3.19:1

T-53 ENGINE

BEARING HANGER
& GEAR COUPLING ASSY

MP & TAIL ROTOR
IVE ASSY

UPPORT CASE

TUBULAR ALUMINUM
DRIVE SHAFTS
4300 RPM

b.

90° TAIL ROTOR
GEARBOX
2.60:1

SHAFT

N GEARBOX

BEARING HANGER
& GEAR COUPLING ASSY

TAIL ROTOR
1654 RPM

42° GEARBOX
1:1

TUBULAR ALUMINUM
DRIVE SHAFTS
4300 RPM

B.

Figure 2. Main Transmission Cross Section

B.

SECTION A-A

SECTION C-C

204-040-355-1 DRIVE & QUILL ASSY (DN -7 & -9)
204-040-355-5 DRIVE & QUILL ASSY (DN -8, 10)
204-040-355-7 DRIVE & QUILL ASSY (DN -88)
204-040-355-9 DRIVE & QUILL ASSY (DN -11 & -4)

204-075-143-3 BRACKET
BKT IDENTIFICATION NUMBER AT THIS
LOCATION

AN100056 COVER
AN4044 GASKET

NUT   12 REQD
WASHER   12 REQD
WASHER   12 REQD

GASKET

PLUG

'O'RING

BEARING

AN345-68 NUT   4 REQD
AN960C816 WASHER 4 REQD

AN100043 COVER
AN4040-1 GASKET

204-040-254-1 SET SCREW
WASHER
LOCKWIRE

AN345-46 NUT   4 REQD
AN960C46 WASHER   4 REQD

204-040-353 CASE ASSY (REF)

CASE, ASSY OF (DN -4)
CASE ASSY (DN -9)
CASE ASSY (DN -6)
RING

RETAINING RING

RETAINING RING

BEARING

AN5-12A   BOLT   6 REQD
AN960-616   WASHER   6 REQD
NAS KEY-616   WASHER   6 REQD

204-040-354-1 QUILL ASSY (DN -7, -9 & -11)
204-040-360-1 QUILL ASSY (DN -88)
204-040-379-1 QUILL ASSY (DN -11 & -4)

AN100044 COVER
AN4047-1 GASKET

MS 27801-046 'O'RING

AN960C816 WASHER   6 REQD
AN345-816 NUT   6 REQD

SECTION G - G

D.

a short mast to the antitorque rotor are also employed in this drive.

The proposed roller gear transmission (hereafter referred to as the RGT) system, designed for adaptation to the UH-1 as a specific task of this study, is shown schematically in Figure 3. In this system, the reduction gearing is removed from the T-53 engine, and the main input drive shaft operates at the full turbine N_{II} speed of 21,016 rpm. The 324-rpm main rotor drive speed is achieved by a 90° 37/56 spiral bevel gear reduction drive and a 42.847:1 roller gear planetary reduction unit. The antitorque rotor drive system is essentially unchanged from the existent UH-1.

The three-stage planetary reduction system, designed as a specific task of the expanded scope study effort, is shown schematically in Figure 4. This system combines the modified T-53 engine, the high-speed input drive shaft, and the 37/56 bevel reduction gearing designed for the RGT system, with the two UH-1 3.087:1 ratio final planetary stages, by inserting a new high-speed planetary stage of 4.5:1 reduction ratio between the RGT bevel output and the first UH-1 planetary.

The general procedures used in this investigation closely follow those normally used at BHC in the design of a conventional helicopter transmission drive system. Extensive use is made of the high-speed digital computer as a design optimization tool for evaluating gear tooth and antifriction bearing parameters. Optimization areas include: efficiency (power loss), life, weight, and cost. The reliability analysis makes use of gear life/load relationships, established from extensive test work conducted at Bell Helicopter Company and the review of UH-1 transmission overhaul data. The results of all work performed under this contract are reported herein.

MAIN ROTOR
324 RPM

PYLON SUPPORT CASE

ROLLER GEAR REDUCTION
42.86 : 1

90° BEVEL DRIVE
1.51 : 1

SUMP & T
DRIVE AS
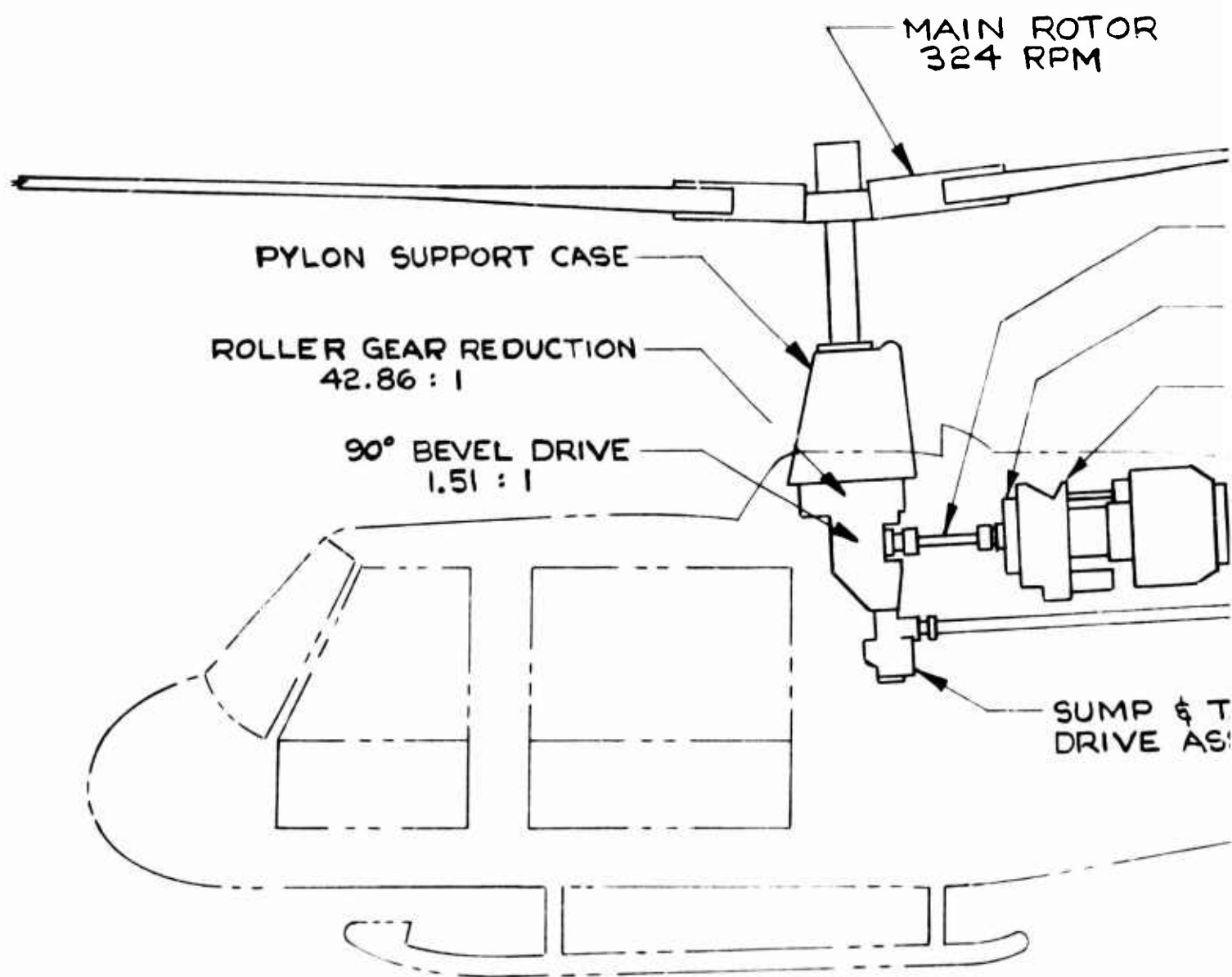
Figure 3. RGT Drive System

9

A.

TOR
M

MAIN INPUT DRIVE SHAFT
21,016 RPM

ELECTRONIC TORQUE METER

T-53 ENGINE

BEARING HANGER
& GEAR COUPLING ASSY

MP & TAIL ROTOR
RIVE ASSY

TUBULAR ALUMINUM
DRIVE SHAFTS
4300 RPM

B.

90° TAIL ROTOR
GEARBOX
2.60 : 1

SHAFT

E METER

BEARING HANGER
& GEAR COUPLING ASSY

TAIL ROTOR
1654 RPM

42° GEARBOX
1 : 1

TUBULAR ALUMINUM
DRIVE SHAFTS
4300 RPM

C.

MAIN ROTOR
324 RPM

PYLON SUPPORT CASE

3-STAGE PLANETARY REDUCTION
42.88 : 1

90° BEVEL DRIVE
1.51 : 1

MA

ELE

T-5

SUMP & TAIL R
DRIVE ASSY

Figure 4. TSPT Drive System

11

A

MAIN INPUT DRIVE SHAFT
    21,016 RPM

ELECTRONIC TORQUE METER

T-53 ENGINE

BEARING HANGER
& GEAR COUPLING ASSY

IL ROTOR
SY

TUBULAR ALUMINUM
DRIVE SHAFTS
+300 RPM

42°

B.

90° TAIL ROTOR
GEARBOX
2.60 : 1

FT

TER

BEARING HANGER
& GEAR COUPLING ASSY

TAIL ROTOR
1654 RPM

42° GEARBOX
1 : 1

TUBULAR ALUMINUM
RIVE SHAFTS
4300 RPM
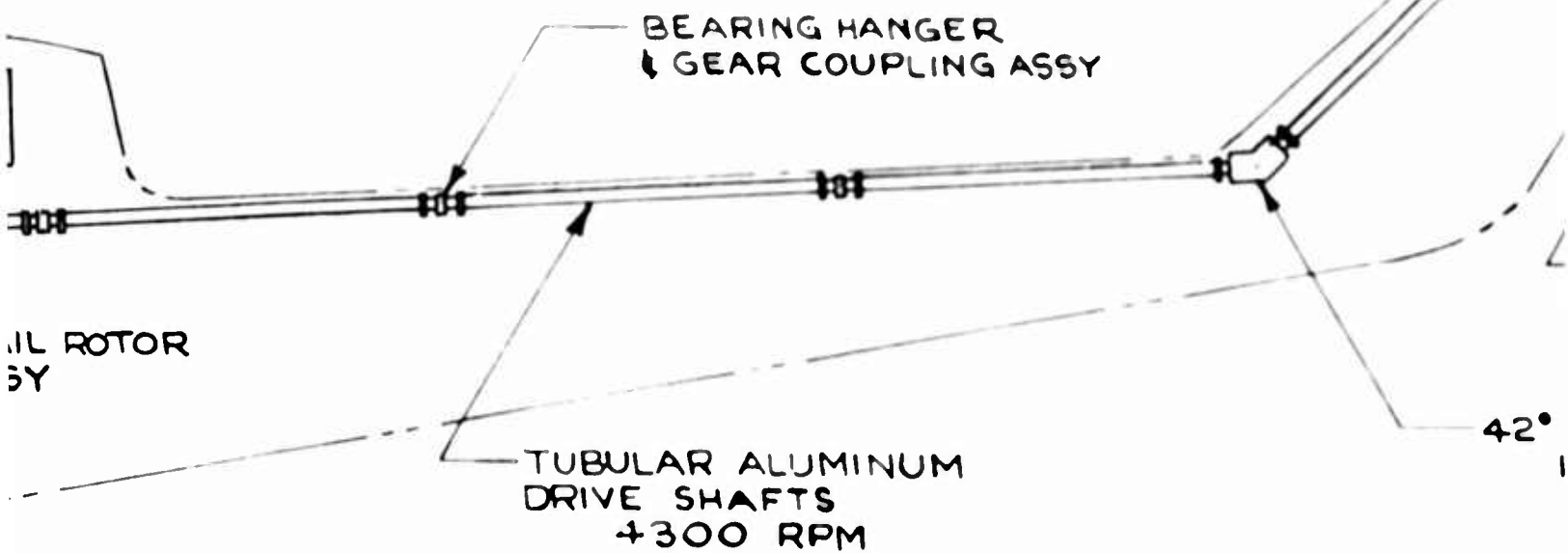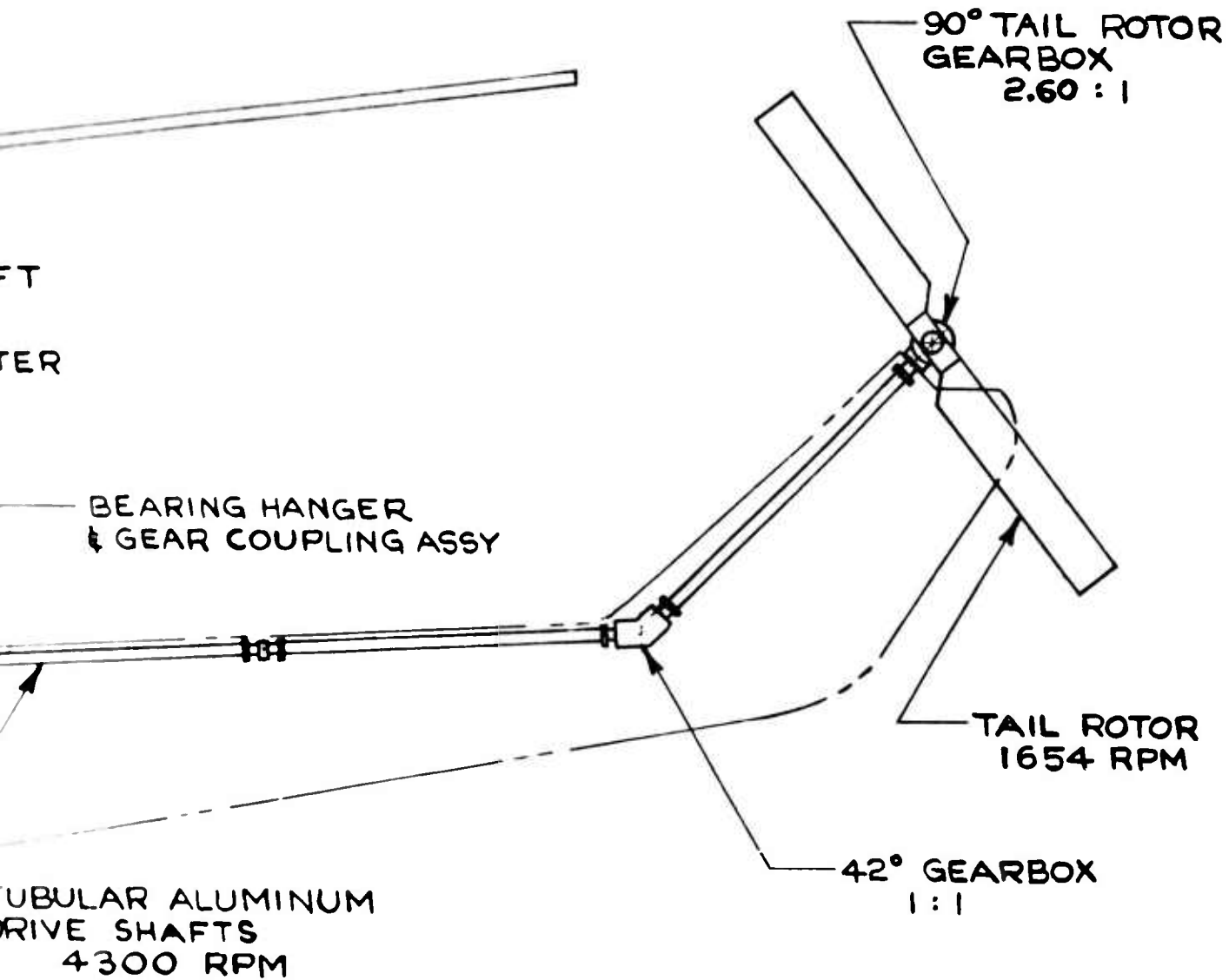
ROLLER GEAR TRANSMISSION AND DESIGN ANALYSIS

DESCRIPTIVE ANALYSIS OF A ROLLER GEAR REDUCTION DRIVE

A roller gear reduction drive is basically a nested multiple-reduction gear unit which utilizes split multiple power paths and a unique torque reaction system. Figure 5 shows a typical roller gear reduction drive of the type studied in this report. It is a nested gear unit since one reduction stage straddles another reduction stage. It is a triple-reduction gear unit. It has 6 power paths at the first reduction mesh point, 12 power paths at the second reduction mesh point, and 6 power paths at the third (final) reduction mesh point. Each of these power paths is split axially to form two coincident power paths. The gears and pinions at the first reduction mesh point are also staggered in groups of three, since the circumferential space does not permit single-plane meshing for each of the two axial power paths.

Figure 5 shows a two-row design. The rows are circular in form. The first row contains the axes of the first-stage reduction gears and the second-stage reduction pinions; the second row contains the axes of the second-stage reduction gears and the third-stage reduction pinions. The number of rows will usually be one less than the number of reduction stage.

The sun pinion is in the center of the roller gear reduction drive unit and has four sets of gear teeth. (It is sometimes called a sun gear even though it usually has less teeth than the member it drives.) The gears that the sun pinion drives are attached to shafts on which the second-stage pinions are also attached. Each one of these shaft assemblies is called a cluster. Those in the first row are called first-row clusters; those in the second row are called second-row clusters. In the two-row design shown in Figure 5, each row contains six clusters. The six clusters in the second row (last row) are all identical, whereas the first row contains three widely spaced clusters and three closely spaced clusters. The two different types of first-row clusters result from the staggering requirement of the first reduction mesh point. This is also the reason why the sun pinion requires four sets of gear teeth instead of only two sets.

The uniqueness of the torque reaction system of a roller gear reduction drive lies in the method by which the torque is reacted at each of the reduction stages except the final stage. The torque reaction in the final stage is accomplished by conventional cylindrical roller bearings attached to the

13

First-Row Cluster
(Widely Spaced)
3 Req'd.

Ring Gear
2 Req'd.

Output Adap-
ter

Conventional
Roller Brg.
6 Req'd.

Sun Pinion

Second (Last)
Row Cluster
6 Req'd.

First-Row Cluster
(Closely Spaced)
3 Req'd.

Typical
Pitchline
Rollers

Input Shaft

SECTION A-A

Figure 5.   Schematic of a Roller Gear Reduction Drive,
Typical of Type Studied in This Report.

14

drive housing. To react the torque at the first and second reduction stages, pitch-line rollers attached closely to each pinion and each gear are utilized. These pitch-line rollers are disc-like in shape, and each is equal in diameter to the pitch diameter of the pinion or gear to which it is attached. The sun pinion has four of these rollers, each first-row cluster has four, and each second-row cluster has only two.

When torque is applied to the sun pinion and transmitted through the roller gear reduction drive, each first-row cluster is retained in position by the action of its rollers wedging between the sun-pinion rollers and the second-row cluster rollers. This wedging reaction replaces the requirement for a fixed spider and conventional cylindrical roller bearings to retain the first-row clusters in their true geometric positions.

If the geometric location of the clusters (in each row) causes the resultant load (produced by gear tooth reaction forces) on the last-row cylindrical roller bearings to have an inward component, then the roller gear reduction drive is called a self-preloaded system. If the geometry causes the resultant load to be either purely tangential or to have only a very small outward or inward component, then the drive is called a nonpreloaded system. If the resultant load has a significant outward component necessitating an externally applied radial load to balance or overcome the outward component, then the drive is called an externally preloaded system. Both the self-preloaded and the nonpreloaded systems may be made into externally preloaded systems by applying external radial loads.

In this report, the designations of different roller gear reduction drives by symbols such as 6x6 signify that the drive contains two rows of clusters with six in the first row and six in the last row.

SYSTEM REQUIREMENTS FOR THE PROPOSED ROLLER GEAR TRANSMISSION

The system is required to reduce engine power turbine speed of 21,000 rpm (engine speed decreaser gearbox removed) to main rotor speed of 324 rpm and tail rotor speed of 1656 rpm at a rated input takeoff power of 1250 hp. The power input to the roller gear transmission is from an engine-to-transmission drive shaft and through a high-speed one-way clutch into a right-angle spiral bevel gear set which has a reduction ratio of 56:37 (1.513:1). The 1138 hp is transmitted through the roller gear reduction unit (ratio = 42.857:1) to the main rotor shaft, which operates at 324 rpm. The total reduction ratio is then 64.843:1. The remaining power is transmitted through an auxiliary drive train to the accessory and tail rotor take-off drives.

15

DESCRIPTION OF PROPOSED RGT SYSTEM (Figures 6 and 7)

The tail rotor takeoff, hydraulic pump, tachometer, and oil pump (single element) drives are mounted in an accessory bevel gearbox (identical to that of the UH-1 helicopter) attached to the offset spur gear reduction box, which in turn is suspended from the main bevel gear reduction box. The accessory bevels are driven by a single offset spur gear reduction, with the driving pinion mounted on the lower end of the main bevel gear shaft.

Also mounted on the main bevel gear shaft is a small bevel gear for driving the generator.

Immediately above the main bevel gearbox is the roller gear reduction unit, which is attached to the main rotor shaft and transmission support unit. (See Tables I and II for ratios and horsepower requirements.)

ROLLER GEAR REDUCTION UNIT

Roller Gearbox Parameters

Early in the study, it became apparent that the minimum diameter of the roller gear sun drive must not be restricted to a size permitting the main rotor shaft to pass through concentrically, as in the existent UH-1 series transmission, if any weight or size advantages were to be demonstrated. The existent sun gear diameters of the UH-1 planetary system cannot be beneficially reduced since the present tooth loads are quite high; consequently, little weight penalty is incurred in this design. However, in the roller gear system, the sun gear torque is much less due to the very high input speed, and full advantage of this characteristic requires elimination of the "through mounted" main rotor shaft. Since the weight of the roller gear drive varies roughly as the square of the diameter for constant power transmission (the axial envelope cannot be significantly altered due to maintenance of reasonable bearing and gear thicknesses), a 185-percent weight penalty would be paid for retaining the "through mounted" rotor shaft. See "Types of Configurations Studied" on page 26 for further explanation of this weight penalty.

The roller gear study was originally restricted to the existent TRW demonstration system featuring a two-row externally preloaded system with fixed spider and rotating outer ring drive gear. This restriction was subsequently removed when it became evident that a properly designed nonpreloading system should function as well as a self-preloading system and should

16
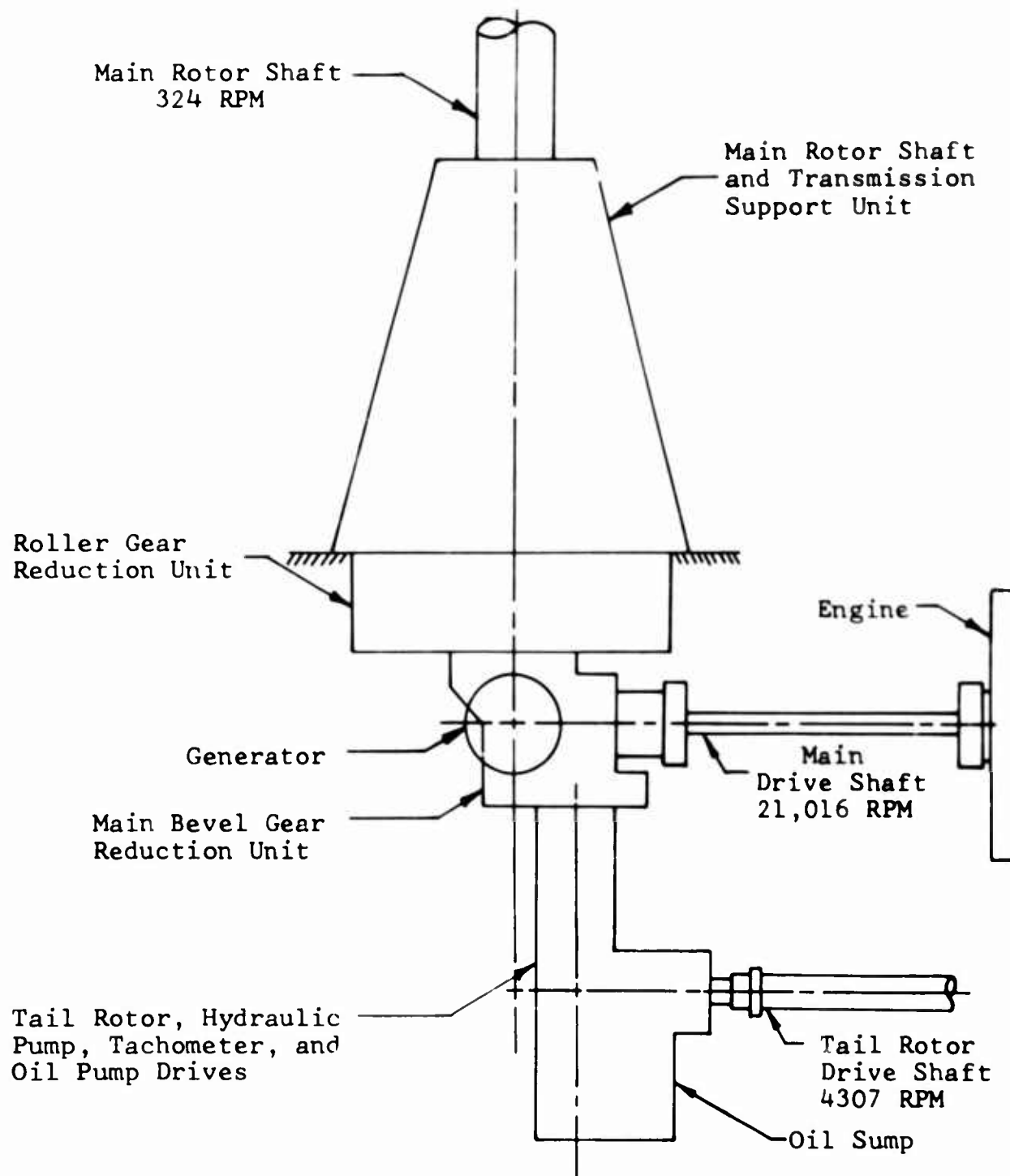
Figure 6.   Proposed RGT System.

TYPICAL ROLLER GEAR TRAIN

SECTION A-A

VIEW B-B
(ABBREVIATED)

ROLLER GEAR REDUCTION UNIT GEOMETRY

Figure 7. Roller Gear Transmission

19

A.

C.

NATIONAL SEAL
4/S07-N

SS9-040-2C- PLATE

SPIDER MOUNTING DETAILS

SS9-040-3S8-1
SS9-040-S08-S MAST ASSY

SS9 DR8 27-1 BEARING

SS9-040-808-1 SPACER

SS9-040-208-1
TOP CASE ASSY

B.

B

I2 BEARING

NATIONAL SEAL
BCM03

A

ROLLER BEARING

ROLLER GEAR REDUCTION UNIT
RATIO : 61.887 : 1

72111G BEARING

INPUT BEVEL GEAR
RATIO 1.5.5 : 1

13,000 RPM

2CT BEARING

200 BE

BEARING

503-040-808-1 SPACER

BR RM 34-1 BEARING

B

503-040-431-1 PACKING

FIXTURE
81.20KTE.50 BEARING

RING JET MANIFOLD

6/41 BEARING
2 REQD

INPUT QUILL - 21,040 RPM

BORG WARNER : 3.646
ONE WAY CLUTCH

A

C

SECTION C-C
THROUGH ROLLER GEAR
REDUCTION UNIT

C

D.

TABLE I. HP AND RPM SUMMARY FOR RGT (NO EFFICIENCY LOSSES CONSIDERED)

	Individual Max HP	Cruise Max HP	RPM
Engine Output Shaft	1250	1220	21016
Roller Gearbox Input	1138	1138	13886
Generator	30	15	12059
Input to Sump Case	119	67	13886
Hydraulic Pumps	12	6	4307
Oil Pump	1	1	4148
Tail Rotor Shafting	106	60	4307
Main Rotor Shaft	1138	1138	324
Tachometer Drive	-	-	4307

TABLE II. RATIOS AND RPM FOR RGT*

	Main Rotor Shaft	Eng. Output Shaft	RPM
Main Rotor Shaft	1	.0154	324
Eng. Output Shaft	64.864	1	21016
Roller Gearbox Input	42.847	.6607	13886
Main Bevel Gear Shaft	42.857	.6607	13886
Input to Sump Case	12.802	.1974	4148
Tail Rotor Shafting	13.293	.2049	4307
Oil Pump	12.802	.1974	4148
Hydraulic Pump	13.293	.2049	4307
Tachometer Drive	13.293	.2049	4307
Generator	37.219	.5738	12059
Tail Rotor Blades	5.113	.0788	1656

* RGT = Roller Gear Transmission

be more desirable from the standpoint of predicting roller
loads and improving load-sharing characteristics of the drive.

Stability Requirements

A fundamental requirement for a helicopter or most any other
type of mechanical drive train is that it remain stable, i.e.,
operate in a non-self-destructive mode, everywhere within its
normal or expected speed and power spectrum. It has virtually
become a standard procedure during the early design phase to
attempt an analysis of the entire drive train with respect to
various manifestations of elasto-inertial systems. The more
common analyses define whirling critical speeds for shafts,
natural torsional vibration frequencies for overall system
and subsystem spring-inertia coupling, locations of nodes and
antinodes for expected forced vibrations, and, more recently,
cymbal vibrations for gear rims and shafts when forced by
tooth meshing frequencies. However, previous experience by
TRW on roller gear reduction drives indicates that some of
the drive components tend toward an apparent intrinsic in-
stability or vibration mode caused by unknown or unpredicted
elasto-inertial force systems.

Such a vibration had been observed in the first-row cluster
during the early testing stage of a roller gear reduction
drive that was built and tested by TRW. The axial distance
between the rollers at each of the sun roller and first-row
cluster roller contact points was increased, and the vibration
was eliminated. Since this modification appeared to stabilize
the first-row clusters, it follows that the original axial
span between the roller contact points did not provide suf-
ficient rigidity for cluster stability.

Also, in a roller gear reduction drive stability study per-
formed by TRW, it became evident that the location of the
last-row clusters had to be held within set limits since all
other rows of clusters depend upon the last-row clusters for
the geometric location of the stabilizing load application
points.

During this study, the stability analysis of a typical non-
preloaded roller gear reduction drive predicted that if in-
stability did occur, it would be caused by erratic motion of
the momentarily "free" first-row clusters during torque
direction changes, or the variation of load distribution
between the two axially split power paths resulting from un-
equal drag forces on the cluster support thrust surfaces.

22

Thus, major efforts were directed throughout the study toward the elimination of the above two possible causes of instability in the proposed RGT system. The results of these efforts are covered in the following pages of this report and are summarized below.

- The use of gears in the second and third (last) reduction stages with opposing helix angles allows the ring gears to axially support both rows of clusters, thus eliminating the necessity for thrust surfaces on each roller for cluster support. The sliding action between two thrust washers on only one end of a cluster could become erratic during certain helicopter maneuvers and create a possible cause of roller gear instability.

- The use of gears in the second and third (last) reduction stages with opposing helix angles in conjunction with high gea tooth pressure angles should force all clusters downward and inward in a non-preloaded system the instant that the torque direction changes from engine driving to main rotor driving during autorotation. This downward and inward action of each cluster results in a slight but significant damping load at each roller contact during the time that roller gear instability would be most apt to occur.

Whether or not these proposed modifications to the non-preloaded type RGT reduction drive will prevent the occurrence of any instability can be determined only by actually building and testing a unit similar to the proposed RGT reduction drive.

Basic Design Requirements

The following requirements were set forth at the beginning of the study:

- Reduction Ratio - 40±4 (for roller reduction stage)

- RPM to Main Rotor Drive Shaft - 324 rpm

- Torque to Main Rotor Drive Shaft - 221,222 in.-lb (1138 hp at 324 rpm)

- Hertz Stress on Rollers - 225,000 psi maximum

23

- K-factor for Gear Teeth - 1000 maximum

- Bearing Life - 2400 hours minimum B_{10}

The following additional requirements were established as the study progressed:

- All fixed joints should be electron-beam welded, and all separable joints should be of the Gleason curvic teeth type.

- The first gear mesh (sun gear mesh: $S-X_1$) should be spur gear teeth; the second gear mesh (Y_1-X_2) and the third gear mesh (ring gear mesh Y_2-R) should be helical gear teeth. Several benefits are realized from helical gear teeth at the Y_1-X_2 and Y_2-R gear meshes: the elimination of thrust wear surfaces; the relaxation of the gear teeth alignment requirements on the ring gears, since these two helical gears will be operating as a single herringbone gear with all the mating second-row clusters free to float axially not individually, but in unison (thus any alignment error between the teeth on the two helical ring gears will not further aggravate the split-multiple-power-path gear unit such as the roller gear drive); the possible solution to any instability problem during load direction changes, since the weight of each cluster in conjunction with its helix angle will produce a radial force necessary to keep all rollers in contact during rotation with zero torque; the reduction of the bending moment along the second-row cluster from X_2 gear to Y_2 gear to approximately zero; and the increased gear capacity at the lower pitch line velocity ring gear mesh, where axial size reduction affords the greatest weight savings.

- The stationary spider should be splined into the magnesium housing in order for the change in relative size, due to the temperature rise from assembly to operation applied to the coefficient of expansion of the dissimilar housing gear materials, not to adversely affect the roller gear assembly.

- The roller bearings in the second-row cluster should be self-aligning because the spider post deflection, due to the necessary overhang, would be excessive for any non-self-aligning bearing.

- These roller bearings should have increased radial clearance in order for the self-preloading action to be effective. A nonpreloaded system could use standard internal clearances.

24

- The rollers should be crowned (form ground-constant radius crowning).

- The numbers of teeth on all gears should be of such a value that each mesh is a nonsynchronous hunting tooth ratio type, even though this is not preferable from a manufacturing and installation point of view. The wear life advantages of this type mesh are well proven.

All of the above requirements were reasonably adhered to in the final design except for the self-aligning second-row cluster roller bearing and the nonsynchronous gear meshes. Since the capacity requirement of the bearing was excessive for a self-aligning bearing that would fit into the limited space, a simple roller bearing was used in conjunction with the ball joint spider concept which absorbs the spider post deflection without transference of these deflections into misaligned gear tooth contacts.

This system for flexible retention of a carrier structure, which affords extremely high compliance (and, hence, load sharing of the various idler gears) without any gear axis skewing as a result of the moment reaction, is protected under U. S. Patent Number 3,227,006, awarded to Bell Helicopter Company in 1966. This system is presently employed in all current UH-1 series transmission first-stage planetary reduction units.

The nonsynchronous gear mesh requirement was not followed because the assembly process for such gears in a split multiple power path system would require a timing procedure or an assembly fixture. Each cluster in each row would have to be installed with a marked tooth inserted in a marked tooth space on its mating cluster. This process would have to continue until all 12 clusters were installed, while being careful not to rotate any of them an entire revolution before the last one was installed. Further study of this problem may reveal that the second-row cluster would have to be unequally spaced also.

Unfortunately, this necessary concession to practicality is not without penalty. Some adjustment in ultimate tooth load capability consistent with adequate wear life must be made. Experience has shown a reduction on the order of 10 percent to be generally adequate for 10^7 to 10^8 wear cycles. This would fix the limit design K-factor nearer to 900 than the customary 1000 used in a conventional BHC planetary design.

Types of Configurations Studied

In the following discussion, a self-preloaded system is one in which the geometry causes the resultant load on the second-row cluster roller bearing to have an inward component. A non-preloaded system is one in which the geometry causes the resultant load either to be purely tangential or to have a very slight outward component.

An 8x8 self-preloaded system (Figure 8) proposed by TRW for this application was studied primarily for familiarization purposes. It was proposed prior to the decision not to require that the sun gear be large enough for a through main rotor shaft. The large sun gear caused only a slight reduction in ratio at the first mesh, resulting in a 29.5:1 reduction ratio in the roller gear unit and a large diameter envelope. A greater ratio could be obtained by using a smaller sun gear, but this phase was not studied because of the large quantity of gears required in an 8x8 system (64 gears excluding the sun gear and the ring gear).

A 6x6A self-preloaded system (Figure 9) was studied. It is only slightly self-preloaded and has a ratio of 37.4:1.

A 5x5 self-preloaded system (Figure 10) was studied. It is more heavily self-preloaded than the 6x6A and has a ratio of 39.4:1.

The 6x6B nonpreloaded system (Figure 11) with a slight outward load component was also studied. It has a ratio of 43.33:1.

A 6x6C nonpreloaded system (Figure 12) with only a tangential load component was studied and selected to be the system used in the final design proposal. It has a ratio of 42.857:1.
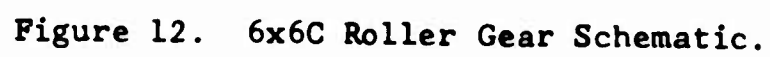
A 6x6D system (Figure 13) with a ratio of 42.726:1 was studied only to the extent of enabling a weight comparison to be made between a 6x6 unit with a large sun gear (for a through main rotor shaft) and a 6x6 unit with a small sun gear, both units having the same ratio. By comparing the enveloping diameter of the 6x6D in Figure 13 to the enveloping diameter of the 6x6C in Figure 12, and by noting that the weight varies as the square of the diameter (the axial envelope remains the same), it is concluded that the 6x6D is 185 percent heavier than the 6x6C. This 6x6D will not be discussed below in the "Comparison of Types Studied."

26

Figure 8. 8x8 Roller Gear Schematic.

Figure 9. 6x6A Roller Gear Schematic.

Figure 10. 5x5 Roller Gear Schematic.

Figure 11. 6x6B Roller Gear Schematic.

Figure 12. 6x6C Roller Gear Schematic.

Comparison of Types Studied

Number of gears and rollers (excluding sun and ring gears):

8x8	64 gears and 48 rollers
6x6A	48 gears and 36 rollers
5x5	40 gears and 30 rollers
6x6B	48 gears and 36 rollers
6x6C	48 gears and 36 rollers

Pitch diameter of ring gear:

8x8	18.400 inches
6x6A	16.846 inches
5x5	16.800 inches
6x6B	14.738 inches
6x6C	14.389 inches

Estimated weight:

8x8	Heaviest
6x6A	Next heaviest
5x5	Equal to 6x6B
6x6B	Equal to 5x5
6x6C	Lightest

Preliminary problem areas:

8x8	None in particular
6x6A	None in particular
5x5	The odd number of first-row clusters will not fit in a simple staggered system; therefore, the gear teeth and rollers on the fifth first-row cluster have to be located axially in a 5th and 6th meshing rolling plane.
6x6B	The addendum of the gear teeth on the X_2 gears and the Y_2 gears has to be decreased for running clearance to such an extent that optimum gear design cannot be accomplished.
6x6C	None in particular

Estimated cost:

8x8	Most expensive
6x6A	Next most expensive
5x5	Equal to 6x6B
6x6B	Equal to 5x5
6x6C	Least expensive

Figure 13. 6x6D Roller Gear Schematic

All conclusions drawn on the above comparisons would show that
the 6x6C is the superior system. Thus, the 6x6C system was
selected to be used in the detailed analysis and design.

Comparison of the Self-Preloaded System With the Nonpreloaded System

TRW maintains that although its own 6x6 roller gear trans-
mission (TRW drawing number 263800) utilized an externally
activated roller preload system to obtain stability, a system
which is self-preloaded from the gear tooth reaction forces
will work just as well.

The intent of this discussion is to show that if a self-
preloaded system such as the 5x5 above, will function properly
as a helicopter main reduction system, then so will a non-
preloaded system such as the 6x6C, above.

In the self-preloaded systems studied, each X_1 roller (see
Figure 14) has one contact, each Y_1 roller has two contacts,
and each X_2 roller has two contacts. All of these contacts
except one of the two X_2-Y_1 contacts are caused primarily by
the transmitted torque, while this one X_2-Y_1 is caused solely
by the inward component of the torque reaction at the second-
row cluster bearing. In order for this inward component to
be effective, two design factors must be incorporated. First,
the second-row roller bearing must have in "increased" radial
internal clearance of about .003 inch total to allow the X_2
roller to move inward and make contact with the Y_1 roller.
Second, the radial location of this roller bearing must be
positioned slightly inward, about .001 inch relative to true
position, in order that the majority of the internal clearance
(.002 inch) is on the inward side of the roller bearing inner
race. Thus, the direction of the resultant load vector on
the roller bearing will be in the third quadrant of the x_2-
axis and y_2-axis coordinate system, shown in Figure 14, as
torque is initially applied to the system. As the torque is
increased, the resultant load vector will rotate counterclock-
wise from the third quadrant toward the second quadrant, thus
increasing the inward component simultaneously to produce
.0005 inch radial self-preload on the system when the resul-
tant is parallel to the x_2-axis. Since the amount of self-
preloading is entirely dependent upon the radial location of
the second-row roller bearing relative to true position, the
manufacturing tolerance band on that location must be extremely
small. If not, then what is intended to be a properly designed
self-preloaded unit will be either a nonpreloaded unit or an
overloaded self-preloaded unit.

34

The following data apply to 6x6C only:

C_1 = 3.6000 Inches α = 30°
C_2 = 3.6000 Inches β = 30°
C_3 = 6.2354 Inches γ = 30°

Figure 14. Roller Gear Geometry.

35

In a nonpreloaded system, each X_1, Y_1, and X_2 roller has only one contact, and each of these is caused solely by the transmitted torque. These contacts are the only contacts necessary to load the system as torque is being transmitted. The manufacturing tolerance band on the radial location of the second-row roller bearing in the nonpreloaded system may be approximately twice the tolerance band required on the self-preloaded unit, providing the roller bearing is positioned slightly outward relative to true geometric position. In comparing the two systems (self-preloaded vs. nonpreloaded), it appears that no additional benefit is gained toward precluding instability by providing for an additional increase (self-preloading) in roller loads as torque is being applied to the system. It would appear that if any instability is encountered, it will become evident during the helicopter autorotation process when the load changes from the drive sides of the gear teeth to the coast sides of the gear teeth. Since this momentary no-load condition could exist on both the self-preloaded and the non-preloaded systems, there are no apparent advantages of the self-preloaded system over the nonpreloaded system. Also, because the roller load in a self-preloaded system is more heavily dependent upon the manufacturing tolerances than the roller loads in a nonpreloaded system, and since there are six less roller contacts on the latter system, the nonpreloaded system is considered to be the better of the two.

Conclusion

The combined conclusions of sections "Comparison of Types Studied" and "Comparison of Self-Preloaded System with Non-Preloaded System" indicate that the 6x6C nonpreloaded system is superior to the other systems studied in the areas of weight, cost, and possibly performance. Thus, the 6x6C system was selected to be used in the detailed analysis and design of this report.

Although TRW maintains that a self-preloaded system will work as well as an externally preloaded system, the 6x6C system proposed in this report contains a design feature which may solve the potential instability problem which may be encountered during the transition from engine driving to rotor driving or vice versa. This design feature was mentioned briefly in "Basic Design Requirements," page 24. Essentially, the concept depends on the weight of each first-row and each second-row cluster in conjunction with the opposing helix angles and the high pressure angles to force all clusters downward and inward the instant that the torque is reversed. Providing this downward and inward movement of all the clusters can take place within the necessary time limit, then the system will always be preloaded to some extent. The results of this particular

36

design feature are described more fully in "Functional Analysis, page 52.

The use of gears with opposing helix angles to support the clusters was the result of a major effort directed toward the elimination of thrust washers. The following two reasons justify the effort expended:

- The method of supporting the clusters in a 6x6 externally preloaded roller gear unit that has been built and tested consists of thrust lips on one side of each roller. A thorough inspection of these thrust surfaces after approximately 25 hours of operation revealed what appeared to be burnished areas caused by rather high thrust loads. Since that unit was operating in the horizontal position as compared to the necessary vertical position on a UH-1 helicopter, it is questionable whether the thrust lips would adequately support the weight of the clusters with the reduction unit in the vertical position.

- Also, it could be that this type of cluster support might be the cause of previously observed instability, since this condition is analogous to the tricks that a flat plate plays when, after spinning on end and before it falls flat, it "walks" or progresses in the direction opposite to its own rotational vector.

Roller Gear Unit Design

Roller Gear Unit Geometry (See Figure 14)

Ratio. The reduction ratio across the roller gearbox is determined as follows:

$$\text{Ratio} = \frac{N_{X_1}}{N_S} \times \frac{N_{X_2}}{N_{Y_1}} \times \frac{N_R}{N_{Y_2}}$$

Upon substitution of the tooth numbers, the resulting ratio is

$$\text{Ratio} = \frac{48}{24} \times \frac{60}{21} \times \frac{150}{20} = 42.857$$

Tooth Number Relationships. In order to maintain a high probability of equal load sharing, and to be able to assemble the gears without different indexing requirements for each cluster in each row, the following tooth number criteria must be met:

37

- The number of teeth in the sun gear must be an integer multiple of the number of first-row clusters

$$\frac{N_S}{K_1} = I_S \ : \ \frac{24}{6} = 4$$

- The number of teeth in the Y_1 gear must be such that the circular arc $180° - 2\alpha$ contains an integer multiple

$$(180° - 2\alpha)\left(\frac{N_{Y_1}}{360°}\right) = I_{Y_1}$$

$$\left[180° - 2(30°)\right]\left[\frac{21}{360°}\right] = 7$$

where $\quad \alpha = 90° - \dfrac{180°}{K_1} - \gamma \ = 90° - \dfrac{180°}{6} - 30°$

$$\alpha = 30°$$

- The number of teeth in the X_2 gear must be such that the circular arc 2γ contains an integer multiple

$$(2\gamma)\left(\frac{N_{X_2}}{360°}\right) = I_{X_2}$$

$$(2)(30°)\left(\frac{60}{360°}\right) = 10$$

where $\quad \gamma = \sin^{-1}\left[\left(\frac{c_1}{c_2}\right)\left(\sin\frac{180°}{K_1}\right)\right]$

$$\gamma = \sin^{-1}\left[\left(\frac{3.6}{3.6}\right)\left(\sin\frac{180°}{6}\right)\right] = 30°$$

- The number of teeth in the ring gear must be an integer multiple of the number of clusters in the second row

$$\frac{N_R}{K_2} = I_R \ : \ \frac{150}{6} = 25$$

- The number of teeth in the X_1 and Y_2 gears is independent of any required tooth number relationship necessary for assembly.

38

Center Distance. The basic center distances were deter-
mined by the number of teeth of each of two meshing gears and
by using a basic diametral pitch of 10 for all gear tooth pro-
portions. However, the center distances for the Y_1 and X_2
gear mesh and the Y_2 and R gear mesh were changed from basic
in order to maintain the selected ratio and to give the angles
α and Y the necessary values required for assembly and equal
load sharing of the gears, as described above in "Tooth Number
Relationships."

The center distances were determined as follows:

- The center distance for S and X_1 gear mesh was not changed
  from basic.

$$C_1 = \frac{N_S + N_{X_1}}{2\ P_1} = \frac{24 + 48}{2(10)} = 3.6000$$

- The center distance for Y_1 and X_2 gears was changed from
  basic.

$$C_2 = \left(\frac{C_1}{\sin Y}\right)\left(\sin \frac{180°}{K_1}\right) = \left(\frac{3.6}{\sin 30°}\right)\left(\sin \frac{180°}{6}\right)$$

$$= 3.6000$$

- C_2 was changed instead of C_1, in order to reduce the diam-
  eter of the overall roller gearbox.

- The center distance for Y_2 and R gears was also changed
  from basic.

$$C_3 = C_1 \cos \frac{180°}{K_2} + C_2 \cos Y$$

$$C_3 = 3.6 \cos \frac{180°}{6} + 3.6 \cos 30°$$

$$C_3 = 7.2 \cos 30° = 6.23538$$

Diametral Pitch. A basic diametral pitch of 10 was se-
lected for all gear meshes while realizing that it would prob-
ably be different from 10 at one or all three meshes, because
the number of teeth and the center distances are fixed for a
specific ratio and specific values for the angles α and Y,
which are required to allow the assembly and the equal load
sharing of the gears.

39

The operating diametral pitch is a function of the number of teeth of two meshing gears and the center distance between them. For the sun gear and X_1 gear mesh, the diametral pitch is

$$P_1 = \frac{N_S + N_{X_1}}{2C_1} = \frac{24 + 48}{2(3.6)} = 10$$

For the Y_1 and X_2 gear mesh, the diametral pitch is

$$P_2 = \frac{N_{Y_1} + N_{X_2}}{2C_2} = \frac{21 + 60}{2(3.6)} = 11.2500$$

and for the Y_2 and ring gear mesh, the diametral pitch is

$$P_3 = \frac{N_R - N_{Y_2}}{2C_3} = \frac{150 - 20}{2(6.2354)} = 10.4244$$

Pressure Angles. The pressure angle at all three distinct gear meshes was selected to be 25°. It was anticipated that the pressure angle Φ_3 of the Y_2 and R gears might have to change from the basic 25°, in order for the resultant load on the roller bearing, which restrains the second-row cluster, to be purely tangential. However, this was not necessary in the proposed 6x6C unit since, in using $\Phi_3 = 25°$, the inward component of the resultant load is 6.8 pounds, as compared to the tangential component of 5776 pounds (with maximum torque applied to the system).

Thus, $\Phi_1 = 25°$ = Pressure angle at S and X_1 gear mesh

$\Phi_2 = 25°$ = Pressure angle at Y_1 and X_2 gear mesh

$\Phi_3 = 25°$ = Pressure angle at Y_2 and R gear mesh

Y_1 and X_2 Roller Loads. The load (R_2) on the Y_1 and X_2 rollers is a function of the sun gear torque, the pitch diameters of X_1 and Y_1 gears, and the angle α.

$$R_2 = \frac{W_t}{\cos\alpha} \left[1 + \left(\frac{D_{X_1}}{d_{Y_1}} \right) \sin\alpha \right]$$

40

where W_t = Tangential load on sun gear teeth per gear mesh

$$W_t = \frac{T_S}{K_1 d_S} = \frac{5162}{(6)(2.4)} = 358.5 \text{ lbs}$$

$$R_2 = \frac{358.5}{\cos 30°} \left[1 + \left(\frac{4.80000}{1.86667}\right) \sin 30° \right]$$

$$= 946 \text{ lbs}$$

<u>S and X_1 Roller Loads</u>. The load (R_1) on the sun and X_1 rollers is a function of the sun gear torque, the pitch diameters and pressure angles of X_1 and Y_1 gears, and the angle α.

$$R_1 = W_t \left[\left(\frac{D_{X_1}}{d_{Y_1}}\right) \sin \alpha \, \tan \Phi_2 - \tan \Phi_1 \right] + R_2 \sin \alpha$$

$$R_1 = 358.5 \left[\left(\frac{4.80000}{1.86667}\right) \sin 30° \tan 25° - \tan 25° \right]$$

$$+ 946 \sin 30° = 521 \text{ lbs}$$

<u>Roller Bearing Load</u>. The resultant load (R_3) on the roller bearing that restrains the second-row cluster is a function of the sun gear torque; the pitch diameters of X_1, Y_1, X_2, and Y_2 gears; the pressure angles of X_2 and Y_2 gears; and the angles α and γ.

The summation of the forces along the x_2-axis is

$$\Sigma F_{x_2} = 2 R_1 \sin \gamma - \frac{D_{X_1}}{d_{Y_1}} (2) W_t \left[\cos \gamma + \frac{D_{X_2}}{d_{Y_2}} \right]$$

$$= 2(946) \sin 30° - \frac{4.80000}{1.86667} (2)(358.5)$$

$$\left[\cos 30° + \frac{5.33333}{1.91858} \right]$$

$$\Sigma F_{x_2} = -5776 \text{ lbs}$$

41

The summation of the forces along the y_2-axis is

$$\Sigma F_{y_2} = 2 W_t \frac{D_{X_1}}{d_{Y_1}} \left[\frac{D_{X_2}}{d_{Y_2}} \tan \Phi_3 - \tan \Phi_2 \cos \Psi \right]$$

$$-2 R_2 \cos \Psi = 2(358.5)\left(\frac{4.80000}{1.86667}\right)$$

$$\left[\frac{5.33333}{1.91858} \tan 25° - \tan 25° \cos 30° \right]$$

$$- 2(946) \cos 30°$$

$$\Sigma F_{y_2} = 6.8 \text{ lbs}$$

Now the resultant load R_3 is

$$R_3 = \left[\Sigma F_{x_2}^{\ 2} + \Sigma F_{y_2}^{\ 2} \right]^{.5}$$

$$R_3 = \left[(-5776)^2 + (6.8)^2 \right]^{.5}$$

$$R_3 = 5776 \text{ lbs}$$

It should be noted that, since the inward component load of 6.8 lbs of R_3 is very small compared to the tangential load of 5776 lbs, this roller unit may be considered nonpreloaded.

Gear Design

A summary of the dimensional gear data is given in Table III, and the detailed gear stress analysis is given in Appendix III.

Appendix VII is a summary of Bell Helicopter Company's gear design technique and philosophy.

The following analyses briefly describe the basic gear design in the roller gear reduction unit, with particular emphasis on design factors peculiar to this unit.

A basic diametral pitch of 10 was selected as a compromise toward designing a reduction unit of the smallest diameter and length possible without undue sacrifice of gear tooth beam bending strength. During the final analysis, however,

the diametral pitch was adjusted to 11.25 at the Y_1-X_2 mesh and to 10.424 at the Y_2-R mesh in order to maintain a specific ratio and to allow for proper assembly. These values are equally satisfactory.

A pressure angle of 25° was selected as being the optimum for reducing the beam bending stresses, Hertz stresses, flash temperatures, and power losses. The gears were also studied using a 20° pressure angle; however, the 25° pressure angle was superior in all respects. The difference between the 20° and 25° pressure angles had negligible effects on the roller loads and roller bearing loads in the 6x6C reduction unit. This can be seen from the following comparison of the pressure angles with respect to the roller loads at each sun-X_1 contact, at each Y_1-X_2 contact, and with respect to the resultant load on each second-row cluster roller bearing.

	20°	25°
Sun-X_1	511 lbs	521 lbs
Y_1-X_2	946 lbs	946 lbs
Bearing	5787 lbs	5776 lbs

The helix angles at the Y_1-X_2 and Y_2-R gear meshes were selected for purposes of other than the basic gear design requirements. (See "Basic Design Requirements," page 24.) The 5° helix angle at the Y_1-X_2 mesh will have no appreciable effect on the gear capacity; however, the 30° helix angle at the Y_2-R mesh will show about 130 percent increase in capacity over the same mesh designed as spur gears. If the 5° helix angle at the Y_1-X_2 mesh were increased for additional gear capacity (which would allow a reduction in the gear teeth face width for a given strength level), then the thickness of the supporting web would have to be increased to minimize the lateral deflection of the gear rim produced by the axial force of a high-helix angle gear mesh. Thus, a high helix angle (in the area of 30°) at the Y_1-X_2 mesh would result in a weight increase rather than a weight reduction.

The gear teeth proportions were adjusted to give long addenda on the driving members and short addenda on the driven members in order to balance the flash temperature in the regions of recess action and approach action. The tooth thicknesses were varied to obtain equal bending strength. The whole depth is 2.30 divided by the diametral pitch for the full fillet form ground gear teeth.

TABLE III. DIMENSIONAL GEAR DATA - ROLLER GEARBOX

	S	X₁	Y₁	X₂	Y₂	R
Number of Teeth	24	48	21	60	20	150
Pressure Angle	25°	25°	25°	25°	25°	25°
Diametral Pitch	10.0000	10.0000	11.2500	11.2500	10.42438	10.42438
Pitch Diameter (In.)	2.4000	4.8000	1.86667	5.33333	1.91858	14.38934
Outside Diameter (or Inside) (In.)	2.6240	4.9760	2.0801	5.4755	2.1586	14.2455
Root Diameter (In.)	2.1640	4.5160	1.6713	5.0667	1.7166	14.6875
Face Width (In.)	.329	.329	.333	.333	1.158	1.158
Circular Tooth Thickness (In.)	.1727	.1353	.1498	.1239	.1701	.1254
Circular Pitch (In.)	.31416	.31416	.27925	.27925	.301370	.301370
Base Circle Diameter (In.)	2.175139	4.350277	1.691778	4.833539	1.738823	13.041171
Helix Angle, Upper	0	0	5° R.H.	5° L.H.	30° R.H.	30° R.H.
Helix Angle, Lower	0	0	5° L.H.	5° R.H.	30° L.H.	30° L.H.
Normal Pressure Angle	-	-	24.913°	24.913°	21.990°	21.990°
Normal Diametral Pitch	-	-	11.29297	11.29297	12.03704	12.03704
Normal Circular Pitch (In.)	-	-	.27819	.27819	.26099	.26099
Normal Circular Tooth Thickness (In.)	-	-	.1492	.1234	.1473	.1086

The involute profiles on all gear teeth were modified from true involute form in order to obtain an optimum balance between resistance to scoring and the gears running rough at low powers. Refer to the section on Gearbox Efficiency Comparison for an elaboration of this analysis.

The material for all the external gears is AMS 6260 steel, vacuum arc remelted to Bell Specification 299-947-032. The gear teeth are selectively carburized to an effective case depth of .030 to .038 inch. The maximum stock removal after carburizing is .006 inch; hence, the finished effective case depth is .024 to .037 inch. Case hardness is Rc 60-63 and core hardness is Rc 33-41 on the finished gears. The carburizing process is per BPS FW-4420, Class A, which includes carburizing, subcritical annealing, quenching, deep freezing, and tempering.

The material for the ring gears (R gears) is AMS 6475 steel, vacuum arc remelted to Bell Specification 299-947-042. The gear teeth are selectively nitrided to an effective case depth of .018 to .024 inch. The maximum stock removal allowed after nitriding is .005 inch; hence, the finished effective case depth is .013 to .023 inch. Case hardness is R_{15} 90.0 minimum (on ground surfaces), and core hardness is Rc 38-44 on finished parts. The nitriding process is per BPS FW-4304.

Roller Design

A summary of the dimensional and functional roller data is given in Tables IV and V. The detailed roller stress analysis and the method used to calculate the lives of the rollers are given in Appendixes III and IV.

Each set of contacting rollers will have one of its members fully crowned. The sun rollers and the Y_1 rollers were selected to be crowned since there are only 10 sun and Y_1 rollers as compared to 12 X_1 and X_2 rollers. The crown radius is 4.50 inches on the sun rollers and 15.00 inches on the Y_1 rollers. The resulting crown drop is .00044 inch on the sun rollers and .0003 inch on the Y_1 rollers. The method used to determine the crown radii is described in Appendix I (Power Loss). The crown will be produced by form grinding a constant curvature on the roller O.D.

The effective length of the rollers was based on a maximum allowable Hertz stress of 220,000 psi under maximum load. The total lengths are greater, to allow for dimensional mismatch in the system and edge breaks on the ends of the rollers. The calculated B_{10} life on each roller was determined using only 60 percent of the maximum load, in a manner consistent with the

TABLE IV. DIMENSIONAL ROLLER DATA

Roller	Diameter (In.)	Total Length (In.)	Effective Length (In.)
S	2.40000	.125	.070
X_1	4.80000	.125	.070
Y_1	1.86667	.188	.148
X_2	5.33333	.188	.148

TABLE V. FUNCTIONAL ROLLER DATA

Roller	Load (Lb)	RPM	Velocity (Ft/Min)	B_{10} Life (Hrs)
S	521	13886	8725	4,440
X_1	521	6943	8725	29,600
Y_1	946	6943	3393	18,150
X_2	946	2430	3393	51,800

life calculations used in the remaining conventional rolling contact bearings. This is justified since the life determination of the rollers, as well as the conventional bearings, is predicated on stress, cycles, material factors, and operating characteristics. The stress in the roller contact that contributes to fatigue failure is subsurface shear. This shear stress is produced by the two compound curved bodies contacting under normal load. The depth and magnitude of maximum subsurface shear stress is a function of contacting body subsurface shear stress is a function of contacting body curvature, normal load, and lubrication condition. Stress application cycles are determined by the speed of rotation of the contacting bodies. The above-mentioned operating characteristics normally involve tolerances, type of roller guiding, speed, and normal load. The pitch-line roller surfaces are expected to be well aligned because of the axial spread between upper and lower contacts; thus, the tendency to skid is minimized but not eliminated. The rollers were designed with the stress magnitude and cycles preset to yield specific life. That is, having determined a safe operating stress level based on imposed loads, the design reduced to a problem of selecting proper roller width and crown radii to produce the required stress.

The design and subsequent operation of the conventional UH-1 planet rollers are precisely the same as those of the pitch line rollers in the RGT. The rollers in the UH-1 planet bearings are crowned to relieve end-load concentration, and the rollers are guided by inner and outer flanges, which do not eliminate skidding but do minimize it. Subsurface shear stresses are again predicated on radii of curvature of the contacting bodies (without regard to relative size) and imposed loads (from whatever source they be generated). Life determination is also based on the relative number of contact cycles. The analogy is complete even to material factors, since fatigue is a function of material cleanliness and strength. Fatigue life of contacting bodies producing subsurface shear stress would be equal in two sets of roller contacts providing the stress magnitudes are equal and the materials are the same, regardless of geometry.

The material for all rollers is AMS 6260 steel, vacuum arc remelted to Bell Specification 299-947-032. The contacting surfaces are selectively carburized to an effective case depth of .030 to .038 inch. The maximum stock removal allowed after carburizing is .010 inch; hence, the finished effective case depth is .020 to .037 inch. Case hardness is Rc 60-63, and core hardness is Rc 33-41 on the finished rollers. The carburizing process is per BPS FW-4420, Class A, which includes

carburizing subcritical annealing, quenching, deep freezing, and tempering.

Spider Design

The spider consists of two parts: a splined base plate with six integral "posts" and a detachable upper plate. The space between the gears dictates the size of the spider posts. On the 6x6C unit, that space is so limited that the material selected for the spider base plate had to have a higher than ordinary fatigue endurance limit.

The material selected is CEVM H-11 Mod. tool steel, heat treated to 260,000 psi and shot peened all over. Since the only fully oscillatory load is caused by starts and stops of the helicopter, the allowable number of cycles to failure can be safely set at 100,000. As shown in Appendix III, the spider base plate has a sufficient margin of safety under the above conditions.

The upper spider plate houses the six second-row roller bearings and the six self-aligning bearings. The material is SAE 4340 steel, heat treated to 180,000 psi.

Roller Bearing Design

The bearing selected is a standard-dimension cylindrical roller bearing without an inner race. The inner race is integral with the second-row cluster. The bearing will be operating under near-perfect conditions, since the ball-joint spider design concept was employed to absorb the spider post deflections.

Also, since the nonpreloaded roller gear system is being proposed, this roller bearing does not have to have "increased" radial clearance which is required to make a self-preloaded system effective. The B_{10} life of a bearing reduces rapidly as the internal clearance is increased, since there will be less rollers in contact for a given load deformation.

The calculated B_{10} life of the bearing is 2524 hours. A detailed stress analysis of the bearing and the inner race is shown in Appendix III.

The material for the inner race is AMS 6260 steel, vacuum arc remelted to Bell Specification 299-947-032.

The race diameter is selectively carburized to an effective case depth of .070 to .080 inch. The maximum stock removal allowed after carburizing is .010 inch; hence, the finished effective case depth is .060 to .079 inch. Case hardness is

48

Rc 60-63 and core hardness is Rc 33-41 on the finished race.
The carburizing process is per BPS FW-4420, Class A.

Electron Beam (E.B.) Welded Joints Design

In the quest for a compact RGT, it was concluded early in this
study that all rollers and gears would be E.B. welded in posi-
tion, if they could not be manufactured integrally with the
shafts. This concept has been utilized throughout, except for
two separable joints on each second-row cluster, which are
necessary for assembly and disassembly.

The roller gear concept requires the rollers to be positioned
"close" to the gears. This necessitates the E.B. welding of
the rollers directly to the gear web. Since it was desirable
for the material to be SAE 9310 (AMS 6260) for the gears, and
since it was conventional for the material to be SAE 52100 for
the rollers, a search of the electron beam welding industry
was made for information on the feasibility of E.B. welding a
through-hardened SAE 52100 roller to the non-carburized area
of a 9310 gear. All sources indicated that even though it has
never been done, it would be feasible, provided the joint could
be stress relieved. The lowest relieving temperature proposed
was 385°F. This would draw the carburized gear teeth below
the desired hardness.

Since some of the E.B. welded joints in the RGT are necessarily
in the areas of high fatigue stresses, and since the magnitude
of the gear teeth stresses (both contact and beam bending
stresses) dictate the use of case-hardened gears, it was con-
cluded that all rollers and gears should be made from AMS 6260
carburizing steel. Extensive experience exists in E.B. welding
and subsequent operations of such joints. Experience also
exists in the E.B. welding of AMS 6475 nitriding steel to
AMS 6260 carburizing steel. The joining of these two different
materials would allow a carburized roller to be E.B. welded to
a nitrided gear should the development testing of the RGT show
the necessity for a particular gear to have a higher surface
hardness (Reference 6). (The average surface hardness of
nitrided AMS 6475 is about Rc 66, both hardnesses applying to
a finish-ground surface.)

The use of AMS 6260 as a rolling contact bearing raceway is
extensive in BHC transmission systems. In all cases, this
material has shown its suitability by exceeding the fatigue
life of SAE 52100 in similar applications.

E.B. welded joints in the proposed roller gear reduction unit
have been designed toward minimizing difficulties in the
welding process. The sun gear design was slightly compromised

49

in the interest of providing the central spline location. Experience has shown that an expandable arbor, located in the bore of the assembled parts to be welded and designed to operate in a vacuum, is required to hold the gears in line during the welding process. The internal spline teeth of the sun gear make the design of this arbor somewhat complicated but not impractical.

Experience has also dictated that the joint design give due consideration for the following requirements:

- Any potential obstruction to the E.B. welded joint must be at least .050 inch away, to allow undisturbed passage of the focused uniform electron beam.

- A minimum of .080 inch from the point of "good" weld to the expandable arbor (or the gear teeth for the axial welds) must be provided for the electron beam "runout." Otherwise, the part will be welded to the arbor.

All the joint designs meet the above two requirements with the exception of the sun gear shaft; it fails to meet the latter requirement. If, during the development of the E.B. welding process on the sun gear shaft, a workable expandable arbor cannot be utilized, then the internal spline may have to extend throughout the length of the shaft to provide a single piloting surface for the arbor and space for beam "runout."

Sun and Cluster Shaft Design

The sun gear shaft and the first-row cluster shaft are designed to be soft in torsion yet strong enough to show a suitable margin of safety across the electron beam welded joints.

The necessity for the torsionally soft shafting is straightforward. Compliance in excess of that inherent in the beam deflection of the gear teeth must be introduced to reduce the dynamic overloads inherent with the spacing errors.

An example of the magnitude of the misalignment that must be absorbed can be seen from the following discussion.

The section "Roller Gear Unit Manufacturing Process and Dimensional Requirements" specifies that the master teeth on both Y_1 gears must be in line within .0004 inch. Since a .0004-inch gear teeth accumulated spacing error is allowed on each Y_1 gear, and if the .0004 inch is in the advancing direction on Y_1 upper gear while being in the retarding direction on the Y_1 lower gear, then 180° from the master teeth, the gear teeth can be out of alignment .0012 inch.

50

Using this same analysis on the X_2 gear teeth on the second-row cluster, there can be a .0018-inch misalignment of the gear teeth 180° from the master teeth on the X_2 gears.

Now, mating the Y_1 gear teeth with the X_2 gear teeth, there can be a .003-inch total misalignment at the lower Y_1-X_2 gear mesh, relative to the upper Y_1-X_2 gear mesh.

Since the gear teeth in both these torsionally soft members are relatively short, no appreciable adverse effects from torsional windup is anticipated.

Also, since the rollers are crowned, no appreciable adverse effects from shaft bending are anticipated.

The second-row cluster shaft was designed to be relatively stiff in torsion because of the 1.160-inch face width of the Y_2 gear mesh with the ring member. Since the ring is quite stiff in torsion, appreciable windup in the X_2-Y_2 shaft and the section under the Y_2 mesh would necessitate an additional helical lead correction in final grind.

Assembly Process (See Figure 7)

The assembly of the roller gear reduction unit and installation in the main case can be accomplished as follows with the use of suitable holding fixtures and work aids.

Install the roller bearings and the self-aligning bearings in the spider plate. With this plate supported by a suitable fixture, install the first-row clusters and move each out from the center of the plate in order to get the last one in. Now, move all these clusters toward the center and install the roller bearing inner race and Y_2 gear portions of the second-row clusters. These must be held in place with a suitable fixture.

Install the lower ring gear from the bottom side and the upper ring gear from the top side. The master spline teeth on the ring gears must be in line. Clamp the two gears together with a suitable clamp. Now, install the sun gear by moving the first-row clusters out against the Y_2 gears. With the first-row clusters meshed with the sun gear, install the upper and lower X_2 gears with the master curvic coupling tooth on the end of each Y_2 gear inserted in the master curvic coupling tooth space on each proper mating X_2 gear. Insert the second-row cluster bolts, and torque the nuts to 800 to 1000 inch-pounds.

51

Press the reduction unit support ball bearing on the splined sun gear driving adaptor and in the rotor shaft adaptor support flange. Insert this subassembly in the sun gear until it bottoms on the upper sun roller. Now, place the upper ring jet loosely on top of the spider plate between the upper X_2 gears.

Install one of the two large retaining rings in the upper groove of the main rotor shaft adaptor and lower the adaptor down to engage the spline teeth on the ring gears, making certain that the master spline tooth on the upper ring gear is in line with the master tooth on the lower. Now, install the other large retaining ring in the lower groove of the adaptor.

With the six inner oil jets and the six oil transfer dowels in place, install and secure the spider to the main case. Now lower the above assembled clusters into the case until the self-aligning bearings in the spider plate are bottomed out on the shoulders of the spider posts. Install the retaining rings that secure the self-aligning bearings to the spider posts by reaching through the 2.25-inch diameter holes in the main rotor drive adaptor. Through these same holes, force the upper ring jet down into the spider posts and install the six small retaining rings.

Functional Analysis

The operational characteristics of the roller gear reduction unit discussed in this section are those relative to the axial position of the clusters during load direction changes and those relative to the possible instability problem.

In the static condition, the ring gears are supported axially by the rotor shaft driving adaptor, the second-row clusters are supported axially by the ring gears due to the opposing helix angles at the Y_2-R gear meshes, the first-row clusters are supported axially by the second-row clusters due to the opposing helix angles at the X_2-Y_1 gear meshes, and the sun gear shaft is supported axially by the main bevel gear shaft.

The 30° opposing helix angles in conjunction with the .006-inch backlash at the Y_2-R gear meshes allow the second-row clusters to drop down .0052 inch from a mean loaded position and make contact on the coast side of the gear teeth at the lower Y_2-R gear meshes, while contacting on the drive side of the gear teeth at the upper Y_2-R gear meshes. See Figure 15.

The 5° opposing helix angles in conjunction with the .006-inch backlash at the Y_1-X_2 gear meshes allow the first-row

52

Direction Of
Rotation

(a)   Load-On Condition
(Engine Driving)

.0060-inch Backlash

30°

.0052 inch

Helix Angle

Tooth Thickness
of Y_2 Gear

Tooth Thickness
of R Gear

(b)   Load-Off Condition

Direction of
Rotation

(c)   Load-Reversed Condition
(Rotor Driving - Autorotation)

Figure 15.   Axial Position of Y_2 Gear Relative to Ring
Gear During Loaded, Unloaded, and Reverse
Loaded Conditions With Ring Gear Fixed
Axially. (Sections are Taken From Along
the Pitch Circles and Show One Y_2 Gear
Tooth Meshing Between Two Ring Gear Teeth.)

53

clusters to drop down an additional .0344 inch and make contact on the drive side of the gear teeth at the lower Y_1-X_2 gear meshes, while contacting on the coast side of the gear teeth at the upper Y_1-X_2 gear meshes.

The 0° helix angles (spur gears) at the S-X_1 gear meshes allow the sun gear shaft to be supported by the main bevel gear shaft. With a ±.020-inch dimensional stackup from the sun gear shaft to the first-row clusters in addition to the .0052 inch and the .0344 inch above, there will be a maximum mismatch of .0596 inch at each S-X_1 gear mesh and roller contact.

As the sun gear shaft begins to rotate, all the S-X_1 gear meshes will theoretically share the transmitted torque equally. However, at the Y_1-X_2 gear mesh, the lower Y_1 and X_2 gears will theoretically carry all the transmitted torque until the torque is of such a magnitude that the resulting tangential load on the gear teeth in conjunction with the 5° helix angle will lift each first-row cluster up to force the upper Y_1 and and X_2 gears into mesh. The transmitted torque required to lift each first-row cluster is calculated as follows:

$$W_t = \frac{2T}{d_{Y_1}} \text{ where T is the torque of each first-row cluster;}$$

also,

$$W_t = \frac{W_x}{\tan\psi} \text{ where } W_x \text{ is the weight of each first-row cluster and } \psi \text{ is the helix angle at the } Y_1\text{-}X_2 \text{ mesh.}$$

Solving for T, the required torque is calculated

$$T = \frac{d_{Y_1}}{2}\left(\frac{W_x}{\tan\psi}\right) = \frac{1.8667}{2}\left(\frac{3.5}{\tan 5°}\right) = 37 \text{ in.-lb}$$

This 37 in.-lb is only 2.2 percent of the maximum torque of 1721 in.-lb on each first-row cluster. Since this unbalance of load between the upper Y_1 and X_2 gears and rollers and the lower Y_1 and X_2 gears and rollers is quite small, it was not considered in the gear and roller design and stress analysis.

The above condition is similar at the Y_2-R gear mesh except that the upper Y_2 and R gears will theoretically carry all the transmitted torque until the magnitude is such that the resulting tangential load on the gear teeth in conjunction with the 30° helix angle will lift each second-row cluster up to

54

force the lower Y_2 and R gears into mesh. This transmitted torque required to lift each second-row cluster is

$$T = \frac{d_{Y_2}}{2} \left(\frac{W_x}{\tan \psi} \right) = \frac{1.91858}{2} \left(\frac{7.4}{\tan 30°} \right) = 12.3 \text{ in.-lb}$$

which is negligible when compared to the maximum torque of 4916 in.-lb on each second-row cluster.

As the sun gear begins to rotate with torque applied to the system by the inertia of the rotor blades, all the clusters will shift upward to their mean loaded positions. This position will be maintained until a condition exists (such as during autorotation) that will allow the rotor blades to drive the unit instead of the engine driving. Figure 15 describes the axial position of the Y_2 gear relative to the ring gears during the load-on condition (engine driving), load-off condition, and load-reversed condition (rotor driving).

Since this proposed 6x6C roller gear reduction unit is not externally preloaded, all the first-row and second-row clusters will be "free" during the load-off condition (rotation with zero torque) and will possibly cause an instability problem. However, it is anticipated that the weight of the clusters in conjunction with the gear teeth pressure angles and helix angles will cause the clusters in both rows to move inward as they drop down, thereby providing the necessary preload to the rollers to maintain a stable system. (The internal clearance in the second-row cluster roller bearings will be such that the inward movement is not restricted.)

Roller Gear Unit Manufacturing Process and Dimension Requirement

The manufacturing process and dimension requirements for all the parts in the RGT reduction unit will be similar to those utilized for all the parts in the UH-1 transmission reduction units except in the areas of electron beam welding, gear teeth alignment, roller manufacturing, and gear teeth spacing. All but the latter of these exceptions are not required in the UH-1 transmission reduction units. The allowable gear teeth spacing errors on the smaller gears in the RGT reduction unit will be less than the comparable allowable errors in the UH-1 transmission gears because the gear teeth spacing errors are directly additive to the gear teeth alignment errors. Thus, the unequal load sharing caused by the gear teeth alignment errors will be increased by the gear teeth spacing errors. However, reducing the spacing errors should not affect the

55

cost of the RGT reduction unit, because, as the gears are
reduced in size, the manufacturing ability to reduce the gear
teeth spacing errors is inherently increased.

<u>Sun Gear Shaft</u> (See Figure 16)

<u>Manufacturing Process</u>. The two gears integral with the
shaft are hobbed, carburized, and hardened. The internal
spline is broached. Two other gears are hobbed, carburized,
and hardened and then clamped on the ends of the shaft with
a spacer (equal in length to the length of a sun roller but
with an outside diameter less than the root diameter of the
gears) between the shaft and each "loose" gear. The gear
teeth of this "subassembly" are now finish-ground in one
setup, and four teeth, in line, are marked as master teeth.
The four sun rollers are carburized and hardened.

With the two spacers replaced with the unfinished sun rollers
and the other two unfinished rollers placed on each end, this
"assembly" is now E.B. welded together while making certain
that the two loose gears are in the exact positions relative
to the integral gears as they were when finish-ground.

The four sun rollers are now finish-ground and super-finished.
The tolerance on the basic roller diameter is ±.0001 inch,
and the circumference of the diameter must not deviate from
a true circle more than .000025 inch.

<u>Dimensional Requirements</u>. When the finished sun gear is
mounted between centers and rotated such that each roller is
running true within .0001 inch total indicator reading
(T.I.R.), then the following requirements must be met con-
currently.

- The master teeth on the four gears must be in line within
  .0002 inch (measured along their pitch circles at their
  gage points).

- The tooth-to-tooth spacing error and the accumulated
  spacing error on each gear must not exceed .00015 inch
  and .0004 inch, respectively.

- Lead error on each gear must not exceed .0003 inch per
  inch of tooth length. Lead waviness must not exceed
  .000070 inch (from peak to valley).

- Involute error on each gear must not exceed ±.00015 inch
  from limit diameter to start of modification diameter and
  must not exceed ±.00015 inch from start of modification

56

Gage Points

Figure 16.   Sun Gear Shaft.

diameter to the outside diameter. Involute waviness must not exceed .000070 inch (from peak to valley).

First-Row Clusters (See Figures 17 and 18)

Manufacturing Process. Both X_1 gears (which are integral with the shaft) are hobbed, carburized, hardened, and finish-ground while maintaining the alignment of a master tooth of X_1 upper gear with a master tooth on X_1 lower gear within .0001 inch (measured along the pitch circles at gage points C and D).

The Y_1 gears are carburized, hardened, and finish-ground.

The X_1 and Y_1 rollers are carburized and hardened.

Both Y_1 gears, both X_1 rollers, and both Y_1 rollers are now E.B. welded to the X_1 gear shaft in their proper positions.

The master tooth on the Y_1 upper gear must be in line with the master tooth on Y_1 lower gear within .0003 inch (measured along the pitch circles at gage points B and E). Also, the master tooth on the Y_1 upper gear must be in line with the master tooth on X_1 upper gear within .0002 inch, and the master tooth on Y_1 lower gear must be in line with the master tooth on X_1 lower gear within .0002 inch (measured along the pitch circles of the X_1 gears at gage points C and D while zeroing along the pitch circles of the Y_1 gears at gage points B and E). Both X_1 rollers and both Y_1 rollers are now finish-ground and super-finished. The basic diameter of each roller has a tolerance of $\pm.0001$ inch, and the circumference of the diameter of each roller will not vary more than .000025 inch from a true circle.

Dimensional Requirements. When the finished cluster is mounted between centers and rotated such that both X_1 rollers and both Y_1 rollers are running true within .0002 T.I.R., then the following requirements must be met concurrently:

- The master gear teeth on the X_1 gears must be in line within .0002 inch (measured along their pitch circles at their gage points).

- The master gear tooth on the Y_1 upper gear must be in line with the master gear tooth on the Y_1 lower gear within .0004 inch (measured along the pitch circles at the gage points).

Gage Points

Figure 17. First-Row Cluster - X_1 Gears Narrowly Spaced.

59

Gage Points

Figure 18. First-Row Cluster - X_1 Gears Widely Spaced.

60
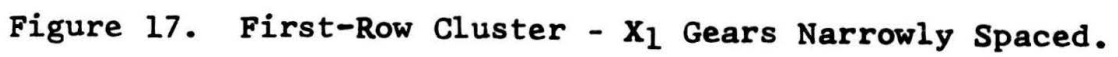
- The master gear tooth on each Y_1 gear must be in line with the master gear tooth on its adjacent X_1 gear within .0003 inch (measured along the pitch circles of the X_1 gears at their gage points while zeroing along the pitch circles of the Y_1 gears at their gage points).

- The tooth-to-tooth spacing error and the accumulated spacing error in each X_1 gear must not exceed .0002 inch and .0006 inch, respectively.

- The tooth-to-tooth spacing error and the accumulated spacing error in each Y_1 gear must not exceed .00015 inch and .0004 inch, respectively.

- Lead error on each X_1 and Y_1 gear must not exceed .0003 inch per inch of tooth length. Lead waviness must not exceed .000070 inch (from peak to valley).

- Involute error on each X_1 gear and each Y_1 gear must not exceed ±.00015 inch from limit diameter to start of modification diameter and must not exceed ±.00015 inch from start of modification diameter to the outside diameter. Involute waviness must not exceed .000070 inch (from peak to valley).

Second-Row Cluster (See Figure 19)

Manufacturing Process. The roller bearing inner race, all gear teeth, all curvic teeth, and both rollers are carburized and hardened. The Y_2 gears are now finish-ground (gear teeth and curvic teeth) while maintaining the alignment of a master tooth on the curvic coupling with a master tooth on the Y_2 gear within .0005 inch (measured along the pitch circle of Y_2 gear in the transverse plane at gage point C).

The curvic teeth on both X_2 gears are now finish-ground while maintaining the alignment of a master tooth space on the curvic coupling with a master tooth on the unground X_2 gear within .001 inch (measured along the pitch circle of X_2 gear in the transverse plane at gage point A).

An X_2 upper gear is now positioned on a Y_2 upper gear with the curvic coupling master tooth on the Y_2 gear inserted in the curvic coupling master tooth space on the X_2 gear.

This "subassembly" is now clamped together firmly and the X_2 gear is finish-ground while maintaining the alignment of the master tooth on the X_2 gear with the master tooth on the Y_2 gear within .0002 inch (measured along the point circle of X_2
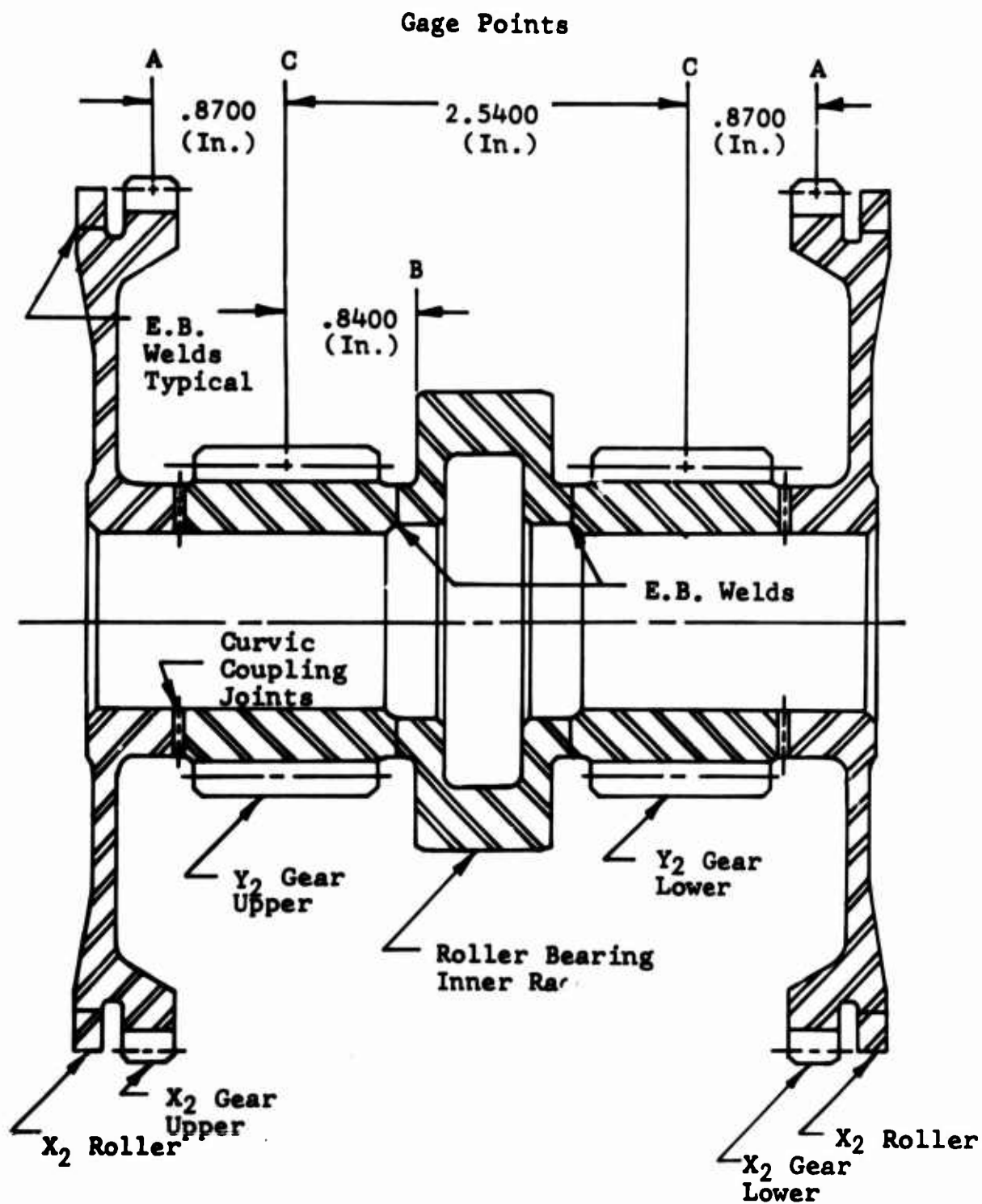
61

Gage Points

Figure 19.   Second-Row Cluster.

62

gear at gage point A, while zeroing at gage point C on the Y_2 gear along its pitch circle).

The X_2 lower gear and the Y_2 lower gear are now processed in the same manner described above for X_2 and Y_2 upper gears.

The X_2 upper gear and its mating Y_2 upper gear, the X_2 lower gear and its mating Y_2 lower gear, the roller bearing inner race, and both X_2 rollers are now positioned properly and E.B. welded where designated on Figure 19. The master tooth on the Y_2 upper gear must be in line with the master tooth on the Y_2 lower gear within .0002 inch (measured along the pitch circle at gage points C).

Both X_2 rollers and the roller bearing inner race are now finish-ground and super-finished.

The basic diameter of each X_2 roller and the roller bearing inner race have a tolerance of ±.0001 inch. The circumference of the diameters will not vary more than .000025 inch from a true circle.

Dimensional Requirements. When the finished cluster is firmly clamped together with both X_2 gears in their proper positions and mounted on an arbor such that when rotated, the roller bearing inner race is running true within .0002 inch T.I.R., then the following requirements must be met concurrently:

- Each X_2 roller diameter must run true within .0002 inch T.I.R.

- The master gear tooth on each X_2 gear must be in line with the master gear tooth on its mating Y_2 gear within .0003 inch (measured along the pitch circle of X_2 gears at gage point A, while zeroing at gage point C on the Y_2 gears along its pitch circle).

- The master gear teeth on both Y_2 gears must be in line within .0003 inch (measured at gage point C along the pitch circles).

- The master tooth on the X_2 upper gear must be in line with the master tooth on the X_2 lower gear within .0004 inch (measured along the pitch circles at their gear points).

- The tooth-to-tooth spacing error and the accumulated spacing error on each X_2 gear must not exceed .0002 inch and .0006 inch, respectively.

63

- The tooth-to-tooth spacing error and the accumulated spacing error on each Y_2 gear must not exceed .00015 inch and .0004 inch, respectively.

- Lead error on each X_2 and Y_2 gear must not exceed .0003 inch per inch of tooth length. Lead waviness must not exceed .000070 inch (from peak to valley).

- Involute error on each X_2 gear and each Y_2 gear must not exceed ±.00015 inch from limit diameter to start of modification diameter and must not exceed ±.00015 inch from start of modification diameter to the outside diameter. Involute waviness must not exceed .000070 inch (from peak to valley).

Ring Gears

Manufacturing Process. After the gear teeth are shaped and nitrided, the spline teeth are finish-hobbed and then the gear teeth are finish-ground.

At final inspection, a gear tooth will be selected that is in line with a spline tooth within .0008 inch (measured along the pitch circle of the gear teeth at a gage dimension of 1.2700 inch from the common mating surface of the upper gear and the lower gear, while zeroing along the pitch circle of the spline teeth).

The selected gear tooth and spline tooth are marked as master teeth. At assembly, the upper and lower gears are installed with their master spline teeth in line.

Note: Since the numbers of the gear teeth and spline teeth are prime, one to the other, then there will always be at least one gear tooth in line with a spline tooth within the .0008 inch noted above. The inspection fixture required to find the aligned teeth is not complicated.

Dimensional Requirements. When the finished ring gear is mounted on the common mating surface of the upper gear and lower gear and rotated such that the pitch diameter of the external spline teeth is running true within .001 inch T.I.R., then the following requirements must be met:

- The gear teeth tooth-to-tooth spacing error and the accumulated spacing error must not exceed .0002 inch and .0008 inch, respectively.

64

- The gear teeth lead error must not exceed .00025 inch per inch of tooth length. Lead waviness must not exceed .000070 inch (from peak to valley).

- The gear teeth involute error must not exceed ±.00015 inch from limit diameter to start of modification diameter to the inside diameter. Involute waviness must not exceed .000070 inch (from peak to valley).

- The spline teeth tooth-to-tooth spacing error and the accumulated spacing error must not exceed .0004 inch and .0015 inch, respectively.

- The spline teeth lead error must not exceed .0004 inch per inch of tooth length.

- The spline teeth involute error must not exceed ±.0010 inch from form diameter to the major diameter.

- The common mating surface of the upper gear and lower gear must be flat within .0010 inch T.I.R.

Main Bevel Gear Reduction Unit

Spiral Bevel Gear Design

The input spiral bevel gears in the RGT were designed with the aid of a Gleason Company computer program. Three main design features were given careful consideration in the bevel gear analysis: safe gear operating stresses consistent with the high-speed application, shaft mounting configuration, and imposed bearing loads (Appendix III).

Safe operating stresses, of course, are essential to successful long-life operation of the bevel teeth. It is recognized that the high spped of the RGT input pinion aggravates the operating stresses due to any dynamic tooth loading condition that exists in the teeth. In order to partially offset the dynamic loading condition and to prevent overstressing, the bevel gear teeth were designed with a high mismatch contact ratio. This coupled with relatively low calculated bending stresses, assures safe operation (Reference 7).

The mounting system of both the pinion and the gear member materially affects the operating stress conditions in the teeth. Both bevel gear members in the RGT are straddle-mounted. This arrangement yields less load deflection than an overhung gear mounting and provides more accurate conjugate tooth contact, thus minimizing pattern shift and reducing the applied design mounting factor. The low internal clearances held in the roller bearings and the rigidity of the duplex

and triplex ball bearings mounted as shown in Figure 7 also contribute to the accuracy and smooth operation of the bevel gears.

The third item given close design consideration in the bevel gear analysis was the component loads. High radial or axial loads can be generated by varying the helix angle and pressure angle of the bevel teeth. The tangential tooth load varies only with pitch, so a proper choice of helix and pressure angles for the bevel teeth will minimize the reaction loads on the support bearings. The various bevel gear configurations investigated are shown in Table VI, and the data for the final selected set are shown in Table VII. This set represents an optimum design, considering the above factors.

Bearing Design

The B_{10} lives shown in Table VIII were obtained with the aid of a high-speed digital computer program. Bearings operating at high rotational speeds have appreciable loads generated internally from centrifugal forces and gyroscopic moments, which are calculated by the computer program and included in the statistical treatment of the load-life relationship. Since the bearings supporting the input bevel pinion and gear shaft in the RGT rotate at very high rpm (21,000 and 13,886, respectively), the internal bearing geometry and associated effects of centrifugal and gyroscopic forces were given close consideration. The ball spin/roll axes are greatly influenced by speed-produced internal forces, and rapid catastrophic failure can occur if the controlling race changes at such high speed. Frictional heat causing rapid wear to occur during control transition leads to accelerated failure. These deleterious conditions were precluded by choosing proper preload, race curvatures, and contact angles.

A concurrent bevel gear analysis was conducted to obtain a spiral bevel gear configuration that produced the least bearing loads while maintaining proper contact ratios and allowable stresses (see Table VI). Several arrangements were investigated to attain an optimum bearing/bevel gear balance.

The material chosen for fabricating the RGT bearing rings and rolling elements was CEVM M50 steel (AMS 6490). Though about 50 percent more expensive than conventional SAE 52100 bearings, the advantages gained in reliability and fatigue life far offset the additional cost.

In deference to the high-speed application, it is essential that no distress appear in the bearings since the rate of failure progression is too high to ensure detection before

TABLE VI. SUMMARY OF INPUT SPIRAL 1

GEAR SET	DIAMETRAL PITCH	PITCH DIAMETER (IN.) PINION	GEAR	FACE WIDTH (IN.)	SPIRAL ANGLE (DEG)	PRESSURE ANGLE (DEG)	TANGENTIAL FORCE (LBS)	AXIA (PINIO
1	8.186	4.520	6.841	1.250	25	22.5	1,956	1,255
2	↑↓	↑	↑	↑	30	20	↑	1,398
3					30	22.5	↓	1,461
4	8.186	4.520	6.841	1.250	30	25	1,956	1,525
5	8.705	4.251	6.434	1.000	25	20	2,026	1,240
6	↑	↑	↑	↑	25	22.5	↑	1,300
7					25	25		1,364
8					30	20		1,446
9					30	22.5		1,510
10				↓	30	25	↓	1,577
11				1.000	35	20	2,026	1,682
12*				1.125	30	20	2,064	1,476
13				↑	30	22.5	↑	1,540
14					30	25		1,607
15					35	20		1,712
16				↓	35	22.5	↓	1,784
17				1.125	35	25	2,064	1,855
18	↓	↓	↓	1.250	25	22.5	2,104	1,349
19	8.705	4.251	6.434	1.250	30	25	2,104	1,641

* Indicates Selected Gear Set.

67

A.

AXIAL FORCE (LBS)		SEPARATING FORCE (LBS)		BENDING STRESS (PSI)	COMPRESSIVE STRESS (PSI)	MESH POINT TEMPERATURE RISE (°F)	MISMATCH CONTACT RATIO
PINION	GEAR	PINION	GEAR				
1,255	161	161	1,255	21,985	173,121	150	2.238
1,398	64	64	1,398	23,729	160,180	161	2.628
1,461	161	161	1,461	19,714	160,372	141	2.582
1,525	259	259	1,525	17,278	160,694	126	2.549
1,240	161	161	1,240	36,213	205,634	211	2.050
1,300	255	255	1,300	29,919	204,414	189	1.986
1,364	352	352	1,364	25,456	204,029	174	1.938
1,446	67	67	1,446	33,204	193,308	194	2.300
1,510	165	165	1,510	27,887	194,527	172	2.248
1,577	266	266	1,577	24,672	195,683	154	2.209
1,682	-34	-34	1,682	30,641	181,045	181	2.601
1,476	67	67	1,476	26,881	179,825	179	2.529
1,540	169	169	1,540	24,409	180,339	158	2.482
1,607	274	274	1,607	22,068	180,917	141	2.447
1,712	-34	-34	1,712	27,273	171,415	168	2.891
1,784	75	75	1,784	24,982	171,223	150	2.854
1,855	187	187	1,855	23,288	171,415	135	2.827
1,349	262	262	1,349	22,978	181,431	157	2.357
1,641	277	277	1,641	18,399	170,645	134	2.706

B.

TABLE VII. MAIN REDUCTION SPIRAL BEVEL GEAR DIMENSIONS

	Pinion	Gear
Number of Teeth	37	56
Part Number	-	-
Diametral Pitch	8.705	8.705
Face Width, inches	1.125	1.125
Pressure Angle, degrees (D), minutes (M)	20D 0M	20D 0M
Shaft Angle, degrees	90D 0M	90D 0M
Transverse Contact Ratio	1.346	1.346
Face Contact Ratio	2.141	2.141
Mismatch Contact Ratio	2.529	2.529
Outer Cone Distance, inches	3.856	3.856
Mean Cone Distance, inches	3.293	3.293
Circular Pitch, inches	0.361	0.361
Working Depth, inches	0.199	0.199
Whole Depth, inches	0.220	0.220
Clearance, inches	0.022	0.022
Pitch Diameter, inches	4.251	6.434
Addendum, inches	0.125	0.074
Dedendum, inches	0.096	0.146
Outside Diameter, inches	4.458	6.515
Pitch Apex to Crown, inches	3.149	2.064
Circular Thickness, inches	0.209	0.153
Mean Normal Top Land, inches	0.069	0.069
Outer Normal Top Land, inches	0.062	0.068
Pitch Angle, degrees	33D 27M	56D 33M
Face Angle of Blank, degrees	35D 45M	58D 5M
Root Angle, degrees	31D 55M	54D 15M
Dedendum Angle, degrees	1D 33M	2D 18M
Outer Spiral Angle, degrees	36D 56M	36D 56M
Mean Spiral Angle, degrees	30D 0M	30D 0M
Inner Spiral Angle, degrees	23D 20M	23D 20M
Hand of Spiral	LH	RH
Driving Member	PIN	
Direction of Rotation	CW	
Backlash, inches	MIN. 0.004	MAX. 0.006
Tooth Taper	TRLM	
Cutting Method		SB
Gear Type		GENERATED
Face Width in Percent of Cone Distance		29.181

TABLE VII - Continued

	Pinion	Gear
Theoretical Cutter Radius, inches	3.002	3.002
Cutter Radius, inches	3.000	3.000
Calc. Gear Finish. Pt. Width, inches	0.061	0.061
Gear Finishing Point Width, inches	0.060	0.060
Roughing Point Width, inches	0.045	0.050
Outer Slot Width, inches	0.057	0.060
Mean Slot Width, inches	0.063	0.060
Inner Slot Width, inches	0.058	0.060
Finishing Cutter Blade Point, inches	0.040	0.040
Stock Allowance, inches	0.012	0.010
Max. Radius-Cutter Blades, inches	0.033	0.039
Max. Radius-Mutilation, inches	0.045	0.051
Max. Radius-Interference, inches	0.023	0.028
Cutter Edge Radius, inches	0.020	0.020
Calc. Cutter Number	4	6
Max. No. Blades in Cutter	0.000	0.000
Cutter Blades Required	Std. Depth	Std. Depth
Duplex Sum of Dedendum Angle, inches	3D 50M	3D 50M
Roughing Radial, inches	3.157	3.157
Geometry Factor-Strength-J	0.3251	0.3240
Strength Factor-Q	6.522	4.323
Factor	MN 0.6858	
Strength Balance Desired	STRS	
Strength Balance Obtained	TPLD	0.008
Geometry Factor-Durability-I	0.1003	0.1003
Durability Factor-Z	2801.	2277.
111263H	0.0013	0.0002
111263Y	0.0166	0.0166
Profile Sliding Factor	0.0025	0.0023
Axial Factor-Driver CW	OUT 0.394	OUT 0.012
Axial Factor-Driver CCW	IN 0.138	OUT 0.244
Separating Factor-Driver CW	SEP 0.018	SEP 0.260
Separating Factor-Driver CCW	SEP 0.369	ATT 0.092

TABLE VIII. SUMMARY OF BALL AND ROLLER BEARING LIVES IN RGT

Bearing Name and Location	Rpm	B_{10} Life in Hrs.
Main Rotor Driveshaft		
Roller Bearing	324	15,200
Duplex Bearing	324	4,840
RG Reduction Unit		
Support Ball Bearings	13,562	30,000
Cluster Roller Bearing	2,430	2,524
Main Bevel Gear Shaft		
Duplex Ball Bearing	13,886	2,335
Roller Bearing	13,886	60,600
Input Bevel Pinion Shaft		
Triplex Ball Bearing	21,016	13,920
Roller Bearing	21,016	5,750
Generator Drive Quill		
Outer Ball Bearing	12,059	55,700
Inner Ball Bearing	12,059	11,140
Off-Set Spur Gear Unit		
Gear Roller Bearing	4,418	93,000
Gear Ball Bearing	4,418	1,665,000
Sump Input Quill		
Duplex Ball Bearing	4,418	9,740
Roller Bearing	4,418	7,630
Tail Rotor Drive Quill		
Duplex Ball Bearing	4,307	3,500
Roller Bearing	4,307	3,750

catastrophic failure. The normal sequence of events, as experienced with the UH-1 transmission bearings, is to detect a failure, either audibly or by magnetic chip sensor. to isolate the location, and to take corrective action by replacing a quill or the entire transmission assembly. However, with the high-speed RGT, the probability of having sufficient time for detection and correction before catastrophic failure occurs is greatly reduced. Consequently, the need for high reliability is paramount, and the CEVM M-50 bearing material contributes significantly to this requirement.

The inner rings of the RGT ball bearings are press fitted sufficiently to preclude occurrence of detrimental ring creep and fretting corrosion. The proper fit values can be calculated with excellent confidence by an experimentally derived method developed by BHC. When the elastic rings of duplex and triplex bearings are interference fitted, the inner raceways grow diametrally and induce additional axial preloading when the rings are clamped flush. These bearings must be fabricated with the proper endshake (I.R. face intrusion) to secure the desired mounted preload at the high interference fits. The shafting inside diameters are similarly fixed by the strain requirements in the inner rings (at the determined fits) to produce the required interfacial pressures to prevent creep. The resulting mounted preload is highly critical of tolerances. Therefore, the ABEC classes and shaft journal tolerances chosen must be compatible with system design requirements.

The most effective method of preventing inner ring creep in roller bearings is to eliminate the ring and to finish the raceway integrally with the shaft. This practice has been in extensive use on all UH-1 series transmissions, with excellent results. Not only is the tolerance range of internal clearance significantly reduced by this practice, but the fatigue endurance of the carburized vacuum arc remelted gear material far exceeds that of conventional through-hardened bearing materials. Additionally, cost and weight savings are realized by elimination of the inner rings and the associated spacers, nuts, and locking hardware.

The recommended tolerance grade is ABEC 7 for the RGT ball bearings and ABEC 5 for the roller bearings. Since preload, race control, and press-fitting tolerances of the ball bearings are interdependently critical, it is essential that the tolerance variations be minimized. All journals are to be super-finished to a CLA of 8. Considerable effort must be expended to ensure maintenance of the proper dimensions and tolerances, which in turn ensures successful bearing operation.

72

Input One-Way Clutch

The function of the input one-way, or freewheeling, clutch is to transmit engine torque to the transmission during normal operation, yet to allow free rotation of the transmission and other rotor-drive components in the event of engine stoppage.

A 26-sprag, full-phasing clutch manufactured by the Spring Division of Borg-Warner Corporation, Bellwood, Illinois (Part Number X-136466) was chosen for the roller gear transmission. This clutch has a normal torque capacity of 5112 in.-lb and features extra-wide drag springs for high-speed freewheeling. Design requirements of 3747 in.-lb continuous torque at 21,016 rpm are fully met by this unit.

Sprag design of this unit is such that the clutch is centrifugally engaging. That is, centrifugal force acting at the center of gravity of each sprag rotates the sprag into more intimate contact with the inner and outer races. This feature ensures continuous sprag-race contact and allows smooth engine reengagement, at speed, after a period of freewheeling.

Clutch lubrication is via a .28-gpm stream of oil injected into the end of the main input pinion. This quantity of oil lubricates both clutch assembly radial bearings in addition to the sprag clutch proper.

Drag torque during clutch freewheeling is only 13 in.-lb, so that sprag and race wear during freewheeling should be no problem. Both inner and outer clutch races are of carburized AMS 6260 steel.

Offset Spur Gears

The function of the offset spur train is to extract 119 hp from the 13,886 rpm main gear shaft and transmit this to the sump and accessory drive unit. Sump and accessory drive unit input speed must be approximately 4140 rpm, in order to obtain correct accessory speeds and a tail rotor drive shaft speed of about 4300 rpm.

Prior to designing the offset spur set, the following design parameters were specified:

- Transmitted hp = 119

- Reduction ratio approximately $\frac{13,886}{4140}$, or 3.354:1.

- Gear center distance of 4.8000 inches on the UH-1 transmission is to be maintained on the RGT.

- Diametral pitch is to be approximately 10.

- If possible, the set members are to have a hunting tooth ratio.

- Face width is to be based upon a "K" factor of 1000.

- The material for the gears is AMS 6475 steel, vacuum arc-remelted to Bell Specification 299-947-042. The gear teeth are selectively nitrided to an effective case depth of .018 to .024 inch. The maximum stock removal allowed after nitriding is .005 inch; hence, the finished effective case depth is .013 to .023 inch. Case hardness is R_{15N} 90.0 minimum (on ground surfaces), and core hardness is Rc 38-44 on finished part. The nitriding process is per BPS FW 4304.

The following summary defines the set designed to meet the above conditions:

Diametral Pitch = 10.4166

Pressure Angle = 25°

Gear	Pinion

Number Teeth = 77 | Number Teeth = 23

Pitch Diameter = 7.392 in. | Pitch Diameter = 2.208 in.

Face Width = .288 in. | Face. Width = .400 in.

RPM = 4,148 | RPM = 13,886

Max Bending Stress = 36,359 psi | Max Bending Stress = 39,168 psi

Max Hertz Stress = 166,326 psi (See Appendix II)

The pinion is internally splined and is piloted under load by a mating spline on the end of the main gear shaft. A radial ball bearing in the spacer case provides static support for the pinion, but once under load, the pinion is free to float both axially and radially until pilot is established on the spline. This system was utilized for three reasons:

- Pinion and gear can be installed in mesh as an assembled unit within the spacer case.

74

- The main gear shaft can be easily removed from the transmission without first removing the spacer case.

- The running axis of the pinion is definitely defined. There would not be the problem of inter-bearing eccentricities as would be the case if the pinion were not free to float and if it received its pilot from the lower ball bearing. Also, the inevitable eccentricities that would accumulate between the main gear shaft roller bearing and the pinion pilot ball bearing would drastically reduce the life of both bearings.

The 1007 roller bearing and a 6008 radial ball bearing in a straddle-mount configuration support the gear. The combined radial load on the roller bearing under design load is 605 pounds, while on the ball bearing it is 64.8 pounds. These low radial load levels and the absence of any appreciable axial load result in very long bearing B_{10} lives: 12,070 hours on the roller and 359,000 hours on the ball.

Lubrication of the gear set is provided by scavenged oil and oil mist. Lubrication by scavenged oil is also provided to the pinion static-stop bearing and the roller bearing on the upper end of the offset gear shaft. A small .3-gpm lube jet, integral with the main case, taps the input triplex bearing lube gallery to supply continuous lubrication to the offset gear shaft ball bearing.

Sump and Accessory Drive Unit

The sump and accessory drive case assembly used on the RGT is the same unit (with exception of oil pump) as the 204-040-365-21 assembly used on current UH-1B helicopter transmissions. This unit contains the tail rotor drive quill, dual hydraulic pump quill, tachometer generator mounting pad, lube pump, pump inlet screen, magnetic chip detector, 40-micron lube filter, and lube reservoir. The design power requirements of various drive components as used on the RGT are listed below:

Component	RPM	Design Horsepower
Tail Rotor Drive Quill	4,307	106
Tachometer Generator	4,307	-
Oil Pump	4,148	1
Dual Hydraulic Pump Quill	4,307	12
Input Quill	4,148	119

Design loads are nearly identical to those used for the component gear and bearing analysis in UH-1 transmission service. It can, therefore, be assumed that a similar performance will result.

75

Use of the 204-040-365 drive unit was made primarily in the interest of design and manufacturing expedience. Various dash numbers of the 204-040-365 sump and accessory drive case assembly, including the -21, are currently in production at BHC. With the exception of the 15-gpm oil pump, all components are off the shelf and will require no redesign.

The UH-1 transmission input quill centerline to tail rotor drive quill centerline separation of 16.250 inches was applied to the RGT in order that the relative positions of input and tail rotor drive shaft aboard the helicopter remain unchanged.

Bearings and gear meshes within the 204-040-365 unit are lubricated by scavenge oil draining to the sump and by a 1.16-gpm, 100-psi lube jet centrally located within the unit.

Generator Drive Quill

Of all the accessories studied, the generator was the only item deemed practical for high-speed operation on the RGT. The generator tentatively chosen is an abbreviated version of the Bendix Generator 28B262-1. This new generator weighs only 18 pounds (35 pounds total weight including off-transmission components) and can supply 28-volt, 300-amp D.C. electrical power. In comparison, the generator alone utilized on the UH-1 transmissions weighs about 46 pounds. Rated generator rpm is 12,000; hence, it was possible to design a generator drive train of minimum complexity.

The generator drive quill is of conventional accessory quill design. It features a generator mounting pad conforming to AND20002 specifications and a 38-tooth, 12.878-pitch spiral bevel drive gear. Power is taken from a mating 33-tooth spiral bevel gear on the 13,886-rpm main gear shaft. This single reduction results in a generator quill speed of 12,059 rpm, which is well within generator speed limits.

Both spiral bevel gears and the generator quill split-duplex bearing were sized for a 200-percent generator load at 75-percent generator efficiency. Specifically, this amounted to a transmitted torque of 157 in.-lb at the generator at 12,059 rpm. Gear stress and bearing B_{10} life calculations based upon a continuous operation under the above conditions are summarized below.

    Pinion (33-tooth) bending stress = 14,743 psi
    Gear (38-tooth) bending stress = 17,779 psi
    Hertz stress = 126,106 psi
    Inboard bearing B_{10} life = 2,400 hours
    Outboard bearing B_{10} life = 12,000 hours

76

See Table IX for the gear dimensions of this set.

Lubrication of the 7007 CG bearing is accomplished by injecting a .28-gpm stream of lubricant into an annular groove around the inside diameter of the generator quill gear shaft. Centrifugal force then routes the oil through radial holes in the gear shaft and inner bearing spacer to the bearing.

The generator drive gear mesh is splash lubricated by oil supplied to the input bevel ring gear and by oil draining from above the generator quill location.

Main Rotor Drive Shaft Unit and Support Structure

The 583-040-308 top case and related parts (all parts above the top case-main case interface) were designed previously as part of a 1800-hp transmission design program. This structure, with the 583-040-302-5 main rotor drive shaft assembly, is suitable for rigid-rotor utilization and for work with a conventional rotor with the 583-040-302-1 drive shaft. All weight penalties imposed upon the RGT by using this top case have been compensated for in the comparative weight analysis portion of the report. In this way, the type of top case utilized in the transmission will not reflect one way or another in the total system evaluation. The following paragraphs will explain briefly the primary reasons for using the 583-040-308 top case in the RGT preliminary design.

Stub Drive Shafts

As stated prior, the 583-040-308 top case was designed to use drive shafts for both rigid- and hinged-rotor studies. Both shafts, the 583-040-302-1 and -5, are stubbed. That is, they receive all their structural support from two bearings within the top case and do not extend down into the transmission gear area, as does the UH-1 mast. By using this arrangement in conjunction with the roller gear reduction unit, it was possible to use a very small sun gear, since main rotor drive shaft passage through the sun gear was not necessary. Reduction in required sun gear size greatly increased the number of roller gear reduction unit configurations possible within a given envelope size.

Top Case Transmission Mounting

Transmissions utilizing the 583-040-308 top case may be mounted in the helicopter by means of structure attached to the base flange of the case. It is, therefore, not necessary to transmit all the rotor torque and thrust loads through the adjacent transmission case structure as is required when using

77

	Pinion	Gear
TABLE IX. GENERATOR SPIRAL BEVEL GEAR DIMENSIONS		

	Pinion	Gear
Number of Teeth	33	38
Part Number	-	-
Diametral Pitch	12.878	12.878
Face Width, inches	0.250	0.250
Pressure Angle, degrees (D), minutes (M)	20D OM	20D OM
Shaft Angle, degrees	90D OM	90D OM
Transverse Contact Ratio	1.331	1.331
Face Contact Ratio	0.768	0.768
Mismatch Contact Ratio	1.536	1.536
Outer Cone Distance, inches	1.955	1.955
Mean Cone Distance, inches	1.830	1.830
Circular Pitch, inches	0.244	0.244
Working Depth, inches	0.136	0.136
Whole Depth, inches	0.150	0.150
Clearance, inches	0.015	0.015
Pitch Diameter, inches	2.563	2.951
Addendum	2.563	2.951
Dedendum	0.075	0.090
Outside Diameter, inches	2.676	3.030
Pitch Apex to Crown, inches	1.427	1.236
Circular Thickness, inches	0.134	0.111
Mean Normal Top Land, inches	0.046	0.045
Outer Normal Top Land, inches	0.043	0.049
Pitch Angle, degrees	40D 58M	49D 2M
Face Angle of Blank, degrees	44D 16M	51D 53M
Root Angle, degrees	38D 7M	45D 44M
Dedendum Angle, degrees	2D 51M	3D 17M
Outer Spiral Angle, degrees	35D 15M	35D 15M
Mean Spiral Angle, degrees	35D 0M	35D 0M
Inner Spiral Angle, degrees	34M 55M	34D 55M
Hand of Spiral	LH	RH
Driving Member	PIN	
Direction of Rotation	CW	
Backlash, inches	MIN. 0.002	MAX. 0.004
Tooth Taper	TRLM	
Cutting Method		SB
Gear Type		GENERATED
Face Width in Percent of Cone Distance		12.794

TABLE IX (Continued)

		Pinion	Gear
Theoretical Cutter Radius, inches		2.152	2.152
Cutter Radius, inches		3.000	3.000
Calc. Gear Finish. Pt. Width, inches		0.040	0.040
Gear Finishing Point Width, inches		0.040	0.040
Roughing Point Width, inches		0.035	0.040
Outer Slot Width, inches		0.042	0.040
Mean Slot Width, inches		0.040	0.040
Inner Slot Width, inches		0.037	0.040
Finishing Cutter Blade Point, inches		0.025	0.025
Stock Allowance, inches		0.002	0.000
Max. Radius-Cutter Blades, inches		0.018	0.025
Max. Radius-Mutilation, inches		0.034	0.042
Max. Radius-Interference, inches		0.015	0.017
Cutter Edge Radius, inches		0.010	0.015
Calc. Cutter Number		9	11
Max. No. Blades in Cutter		0.000	0.000
Cutter Blades Required		Std. Depth	Std. Depth
Duplex Sum of Dedendum Angle, inches		7D 48M	7D 48M
Roughing Radial, inches		2.460	2.460
Geometry Factor-Strength-J		0.2159	0.2154
Strength Factor-Q		98.302	85.574
Factor	KI	1.3023	
Strength Balance Desired	STRS		
Strength Balance Obtained	TPLD		0.017
Geometry Factor-Durability-I		0.0919	0.0919
Durability Factor-Z		10298.	9596.
111263H		0.0016	0.1027
Profile Sliding Factor		0.0018	0.0017
Axial Factor-Driver CW	OUT	0.684 IN	0.090
Axial Factor-Driver CCW	IN	0.198 OUT	0.576
Separating Factor-Driver CW	ATT	0.104 SEP	0.594
Separating Factor-Driver CCW	SEP	0.663 ATT	0.172

typical UH-1-type mounts. This greatly reduces the required size and weight of the RGT cases.

Availability

The 583-040-308-1 top case and related parts are now in limited production. Design and development time required for totally new parts is saved by using this structure.

Size

Base flange pilot diameter of the 583-040-308-1 top case is compatible with roller gear reduction unit requirements. Also, this case will not necessitate extensive rotor control mechanism redesign and relocation when the transmission is installed aboard a helicopter for flight test.

Lubrication System Analysis

This analysis concerns only the lubrication of and the lubrication hardware on, or contained within, the RGT. However, it is understood that such items as an oil-to-ambient air heat exchanger with some form of low-temperature oil-cooler bypass valve will be employed in the total lubrication system. The lubricant considered is MIL-L-7808 synthetic turbine engine oil supplied by a 15-gallon-per-minute pump from a 2-1/2-gallon sump integral with the transmission assembly. The UH-1 transmission uses the same type of oil with the same size sump but the oil is supplied by a 12.5-gpm pump instead of a 15-gpm pump. The additional pump capacity is required on the RGT because of the relatively large number of gear meshes in the roller gear reduction unit, as compared to the gear meshes in the 2-stage planetary in the UH-1 transmission. Each gear mesh in the RGT requires a jet-stream of lubricant because of the high tooth contact stresses (on the order of 180,000 psi Hertz stress). The size of the orifice in the jet must not be less than 0.030 inch in diameter (preferably 0.040 inch diameter minimum) because of the hazard of clogging with lint, O-ring chips, small specks of scale, or other foreign material. The velocity of this jet stream must be sufficient to overcome the wind resistance produced by the high pitch-line velocity gears. Thus, the quantity of oil forced in each gear mesh may be greater than that required for minimal lubrication and cooling; however, as noted above, this quantity is dictated by the minimum size of orifice, the number of orifices required, and the necessary oil pressure to obtain the needed stream velocity.

Although the lube flow requirements of the RGT are calculated to be 20 percent larger than those of the present UH-1 series

transmission, overall power-train lube requirements are actually reduced. This is due to the absence of the engine nose box along with its 5-gpm (2265 lbs/hr) lube requirement in an RGT installation. With the RGT, reproportionment of transmission and engine cooler core sizes will be required, but the total cooler area and weight will remain essentially unchanged. This is due to the reduction in convection cooling efficiency caused by the removal of the engine gear reduction unit from the engine air inlet area. This, however, results in an overall increase in efficiency when engine performance is considered. As the result of eliminating heat transfer from the engine nose box into the engine's air induction system by removing the engine gear reduction unit, it will be shown on page 141 of the Weight Comparison section that there would be an effective 2.5-pound weight savings in fuel (relative to a mission consuming 1,600 pounds of fuel), and it will be shown on page 146 of the same section that the hot-day takeoff gross weight capabilities of the UH-1 helicopter would be increased by 29.7 pounds.

Basic lubrication considerations in the case of this relatively high-speed roller gear transmission are threefold. Refer to Figure 20 and Table X for lubrication system identification.

Lubrication Per Se

Lubrication is accomplished by means of direct lubricant injection, pressure lubrication, and random "splash" or mist lubrication.

Lubrication under pressure must be provided to all heavily loaded, high-speed bearings and to all critical gear meshes. Roller and conventional gears are lubricated by impinging a stream of lubricant on the teeth immediately before mesh. Pressure-lubricated bearings receive lubricant from circumferential galleries feeding via radially slotted outer ring faces.

Other, less critical bearings and gears are "splash" lubricated by gravity return lube flowing enroute to the sump or, in confined areas, by lube jets as above.

Cooling

Oil must be provided as a cooling agent in areas of large frictional losses and excessive gear mesh flash temperature rises. This is accomplished either by increasing the supply above that needed for minimal lubrication or, where possible in the case of critical gears, by impinging an additional stream of lubricant against the teeth leaving mesh.

To Lube
Cooler

From Lube
Cooler
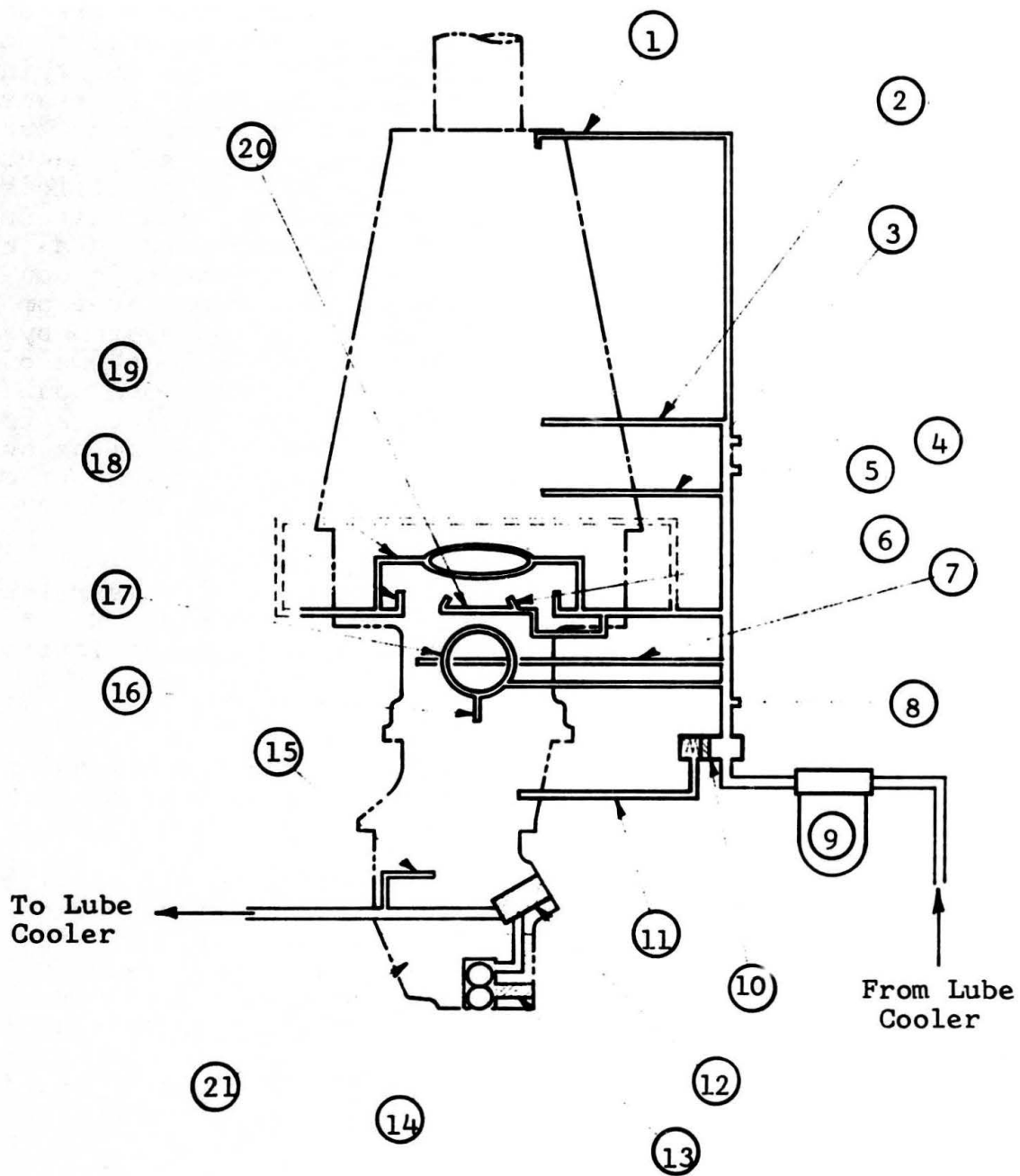
Figure 20. Lubrication System Schematic,
Roller Gear Transmission.

TABLE X.   IDENTIFICATION OF LUBE SYSTEM COMPONENTS
(REF. FIG. 20)

Item No.	Nomenclature	Function	Pressure (PSI)	Flow Rate (GPM)
1	Lube Jet	Lubricates: Main Rotor Drive Shaft Roller Bearing	47	.28
2	Lube Jet	Lubricates: Main Rotor Drive Shaft Thrust Bearing	50	.54
3	Lube Jet	Same as Item #2		
4	Thermoswitch, High Lube Temp. (230°F)			
5	Lube Temp. Bulb			
6	Lube Jet (Ring of Six Jets Supplied by Item 20)	Lubricates: Lower S-X$_1$ Roller and Gear Mesh - One Stream from Each of Six Jets	50	.76 (Total)
7	Lube Jet, Main Case	Lubricates: a) Generator Drive Quill - 1 Stream b) Main Bevel Set - 2 Streams c) Gear Shaft Roller Bearing - 1 Stream d) Input Pinion Roller Bearing - 1 Stream e) Freewheeling Unit - 1 Stream	5C	1.70 (Total)
8	Pressure Gage			
9	Filter, Paper Element, 10 Micron			
10	Valve, Pressure Regulator, 60 psi			

83

TABLE X - Continued

Item No.	Nomenclature	Function	Pressure (PSI)	Flow Rate (GPM)
11	Over-Pressure Discharge Duct from Item 10			
12	Filter, Wire Screen Cascade, 40 Micron			
13	Screen, Pump Inlet, 16 X 16 Wire Mesh			
14	Lube Pump, 15 GPM Gerotor			
15	Lube Jet, Sump Case	Lubricates: Tail Rotor and Hyd. Pump - Bevel Gear Drive - 3 Streams	100	1.16 (Total)
16	Lube Jet, (Supplied by Item 17)	Lubricates: Accessory Drive Spur Gear Ball Bearing	58	.30
17	Lube Gallery	Lubricates: a) Main Input Triplex Bearing b) Supplies Lube to Item #16	58	1.00 (To Brg.)
18	Lube Jet, Six Required	Lubricates: a) Lower Y2-R Gear Mesh - 1 Stream from Each of Six Jets b) Lower Y1-X2 Roller and Gear Mesh - 1 Stream from Each of Six Jets	50	1.52 (Total)

84

TABLE X - Continued

Item No.	Nomenclature	Function	Pressure (PSI)	Flow Rate (GPM)
19	Lube Jet (Ring Supplied by Six Jets)	Lubricates: a) Upper Y_2-R Gear Mesh - 1 Stream from Each of Six Jets b) Upper Y_1-X_2 Roller and Gear Mesh - One Stream from Each of Six Jets c) Upper S/X_1 Roller and Gear Mesh - Six Streams from Ring d) Second-Row-Cluster Roller Bearing - One Stream from Each of Six Jets e) Reduction Unit Support Ball Bearing - Three Streams from Ring	47 (Avg.)	3.31 (Total)
20	Lube Gallery	Lubricates: a) Gear Shaft Duplex Bearing b) Supplies Lube to Item #6	53	2.76 (To Brg.)
21	Lubricant Sump - 2-1/2-Gallon Capacity MIL-L-7808 Synthetic Lubricant			

85

Total heat generation due to various power losses in the RGT system is calculated to be 25.876 hp or 1,097 Btu/min. Of this, about 77 percent is estimated to be rejected via heat transfer through the oil-air heat exchanger.

The balance will be effectively handled by convection transfer through transmission cases into the surrounding air envelope, similar to the manner in which the convective heat is transferred from the existing UH-1 transmission. Table XI compares the RGT heat rejection rates with those of the UH-1 system. It is interesting to note that the conductive-convective heat rejection is 250 Btu/min (5.90 hp) for both the RGT and the UH-1 transmission. The 250 Btu/min convective heat rejection figure for the UH-1 transmission is an indirectly measured quantity determined from bench tests. The 250 Btu/min heat rejection figure for the RGT was calculated by using the same specific heat rejection number of 0.00135 Btu/min/in.^{2}/Δ °F which was derived from the test data on the UH-1 transmission, and by calculating the effective wetted area of the RGT. This area was found to be equal to that of the UH-1 transmission. Additional information concerning this specific heat rejection number may be found on page 178 in Gearbox Efficiency Comparison.

The quantity of lube circulated through the RGT is 2-1/2 gallons (exclusive of line and/or cooler containment) with a total circulation time of .17 minute (10 seconds).

Effective Scavenging

The quantity of lubricant injected into any high-speed machinery for cooling and actual lubrication must be held to a minimum, in order to avoid excessive churning and aeration of the lubricant accompanied by high "pumping" losses in the system.

With the exception of the main input spiral bevel gear, all components of high rotational speed have ample case-clearance for minimum pumping losses. The above bevel gear has about a .44-in. minimum radial case clearance (further arbitrary increase costs approximately .2 lb/.1 in. clearance) an operating speed of 13,826 rpm, which may restrict gravity oil return to the sump. Solution to this possible trouble area can be best obtained during initial development tests.

It should be noted that the power losses shown in Table XI represent the minimum loss condition, assuming a proper development cycle to eliminate such uncalculated oil churn losses.

86

TABLE XI.   COMPARATIVE HEAT REJECTION DATA

	Total Heat Rejection (HP) (BTU/MIN)		Rejection Through Oil (HP) (BTU/MIN)		Conductive-Convective Rejection to Air (HP) (BTU/MIN)	
RGT Total System	25.876	1097	19.98	847	5.90	250
UH-1 Total System	30.08	1275	20.73	879	9.35	396
T-53 Nose Box	12.20	517	8.75	371	3.45	146
UH-1 Transmission	17.88	758	11.98	508	5.90	250

Rotating Shaft Seals

A vented lube-filler cap is installed in the transmission top case to limit build-up of internal case pressure to about 2 psi above atmospheric pressure. This low-pressure differential, combined with low relative shaft-to-seal housing eccentricities, enables certain lip-type shaft seals to perform satisfactorily, even at the high rotational speeds they encounter.

In general, however, an exorbitant number of field reports concerning seal leaks is characteristic of all military helicopter operational experience with transmission systems operating in MIL-L-7808 or MIL-L-23699 synthetic lubricants. There are many factors contributing to these problems, which leaves the attainment of their solution somewhat out of grasp. BHC has conducted extensive tests with various oil qualifications and many seal elastomer compounds. The best production seals in use today are silicon compounds which unfortunately exhibit finite lives due to excessive wear rates. The problems are increased by tremendous differences in various oil qualifications, with respect to their elastomer compatibility characteristics. Compatibility criterion alone shows that the Viton-type elastomers are far superior to any others. However, efforts to produce satisfactory Viton lip seals have been erratic, the wear rate problem again being foremost.

The operation of a lip seal is paradoxical. Although its purpose is to prevent leakage, in order to function properly, it must be kept moist; this requires a designed and controlled small leakage. If this leakage is not present, the harder materials dry, shrink, and crack, while the softer materials wear at excessive rates. The elastomer deterioration as a result of exposure to the synthetic lubricants acts to change the hydrodynamic relationships governing proper controlled leakage; in effect, absolute compatibility must be achieved.

However, with the exception of the main input shaft seal, all roller gear transmission seals are of the lip type and are essentially off-the-shelf items, although the exact elastomer compounds utilized cannot be predicted as of this writing.

In the case of the input shaft seal, the high rotational speed (21,016 rpm), the large shaft diameter (3.350 in.), and the possibility of shaft-to-seal housing eccentricities greater than .006 inch appear to make the use of a lip seal in this application unwarranted. It was necessary to consider another type seal, namely, a face seal.

Ordinary face seals resemble the unit shown in Figure 21. They usually consist of a carbon seal nose "A" (keyed to the

Seal Nose "A"   Seal Housing

Required "Leakage" Route

Mating Ring "B"   Seal Cup

                            Shaft

Pressure   Atmosphere
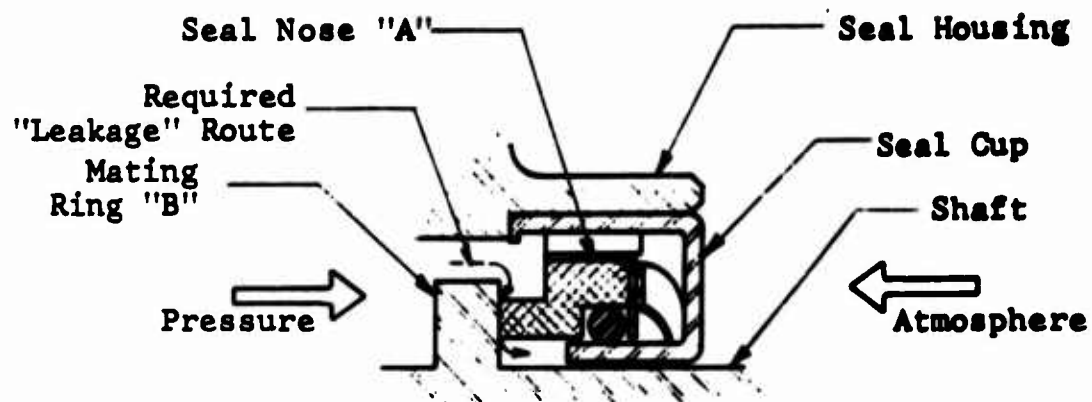
Conventional Face Seal Configuration and Typical Installation.

Normal Fluid Flow Route   Annular Seal Drain

Thrust Washer "C"   Shaft

Mating Ring Tab-Drive
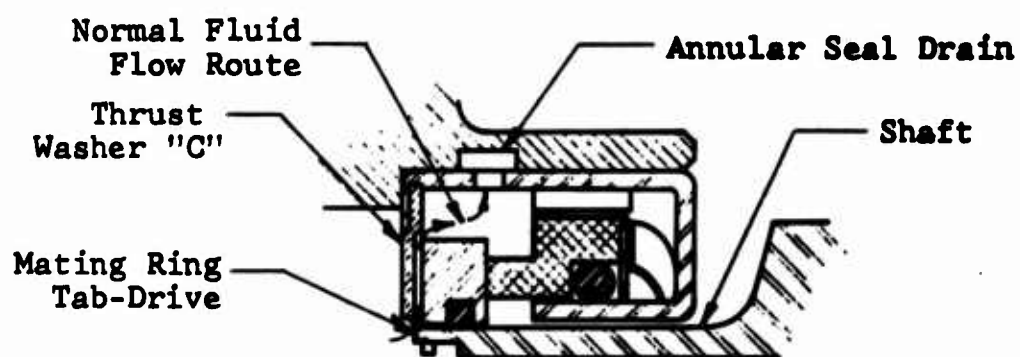
Cartriseal SK 6811 Configuration and Installation.

Figure 21.   Face Seal Types.

seal cup to prevent relative rotation) and a hardened steel mating ring "B" (fixed to the rotating shaft). Sealing is effected at the A-B interface. In order for the captive fluid to escape through the seal, it must follow the route shown and must have sufficient pressure to overcome both centrifugal force and the A-B sealing mechanism.

This system performs well at high rotational speeds and relatively large shaft-to-seal housing eccentricities as long as the shaft axis angular oscillations are of low amplitude and the installation forces the fluid to take the route shown in order to escape.

The input shaft seal operating and installation conditions require several modifications of the basic face seal in order to obtain an effective sealing unit. Figure 21 illustrates the seal design developed for this application.

The seal was developed by Bell Helicopter and the Cartriseal Corporation of Weeling, Illinois. It carries Cartriseal Design Number SK-6811 and is basically a carbon-seal-nose face seal with O-ring secondary seals. Sealing of MIL-L-7808 synthetic lube oil at 3-psi pressure differential can be effected at shaft speeds in excess of 21,000 rpm and at maximum anticipated radial and axial shaft-axis oscillations.

However, two areas exist in this seal design that may be potential problem areas:

- Thrust washer "C", now of AMCO 8 bronze, may require additional lubrication or a change of material, if wear problems arise at the mating-ring/thrust washer interface.

- Machining of the mating ring O-ring cavity must be closely controlled. An oversize cavity will allow the O-ring to deform excessively under high centrifugal forces and lift off the shaft, thereby greatly reducing seal effectiveness.

THREE-STAGE PLANETARY AND DESIGN ANALYSIS

This section presents the design, analysis, and substantiation of a transmission having the same reduction ratio as the RGT 6x6C, but utilizing three "conventional" planetary assemblies in place of the roller gear reduction unit. The engine input shaft, spiral bevel gears, and sump assembly are common to both. However, the spiral bevel gear output shaft drives the sun pinion of a high-speed planetary assembly with carrier output and fixed ring gear, rather than the RGT sun pinion. The carrier output drives the sun gear of the standard lower planetary of the UH-1 transmission. Thus, the three-stage planetary transmission is comprised of the bevel gear reduction stage designed for the RGT, a new high-speed planetary assembly, and the two planetary assemblies presently used in the UH-1 transmission. See Figure 22.

Since the bevel gears are discussed in detail in the RGT section, and the UH-1 planetary assemblies are an existent production design (operating data shown in Table XXIV), only the design and analysis of the new high-speed planetary assembly are treated in this section. The cross-section schematic of the three-stage planetary reduction unit is shown in Figure 23.

HIGH-SPEED PLANETARY DESIGN

The high-speed reduction unit consists of sun gear (input), planet idlers, idler bearings, fixed ring gear, and carrier (output). The carrier embodies the same design characteristics as the UH-1 four planet ball joint carrier.

The high-speed planetary carrier assembly is comprised of 3 planets, 3 sets of planet rollers, 3 inner rings and support shafts, a spider, 3 spherical ball Teflon fabric lined swaged outer ring gearings, 2 parallel plates, and 3 attaching bolts and nuts. The spider has 3 legs positioned 120° apart into which the 3 spherical ball bearings are fitted. The spider is attached to the 2 carrier plates by 3 bolts through the spherical ball bearings, with 1 plate above the spider legs and the other plate an equal distance below the spider legs. The planet idlers are positioned at alternate locations between the spider legs, also 120° apart, and mounted on the planet shafts which are rigidly attached to the carrier plates (See Figure 22).

Gear loads are transmitted from the planet idlers to the carrier plates, which in turn transmit the loads through the attaching bolts to the spherical ball bearings in the spider
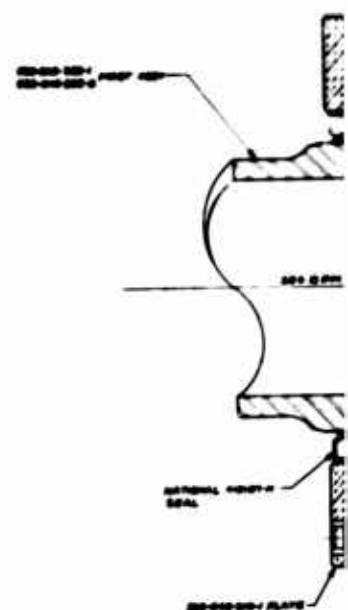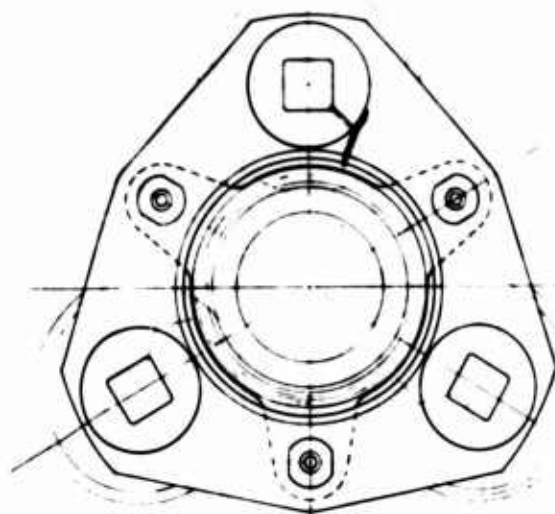
Figure 22.   Three-Stage Planetary Transmission.
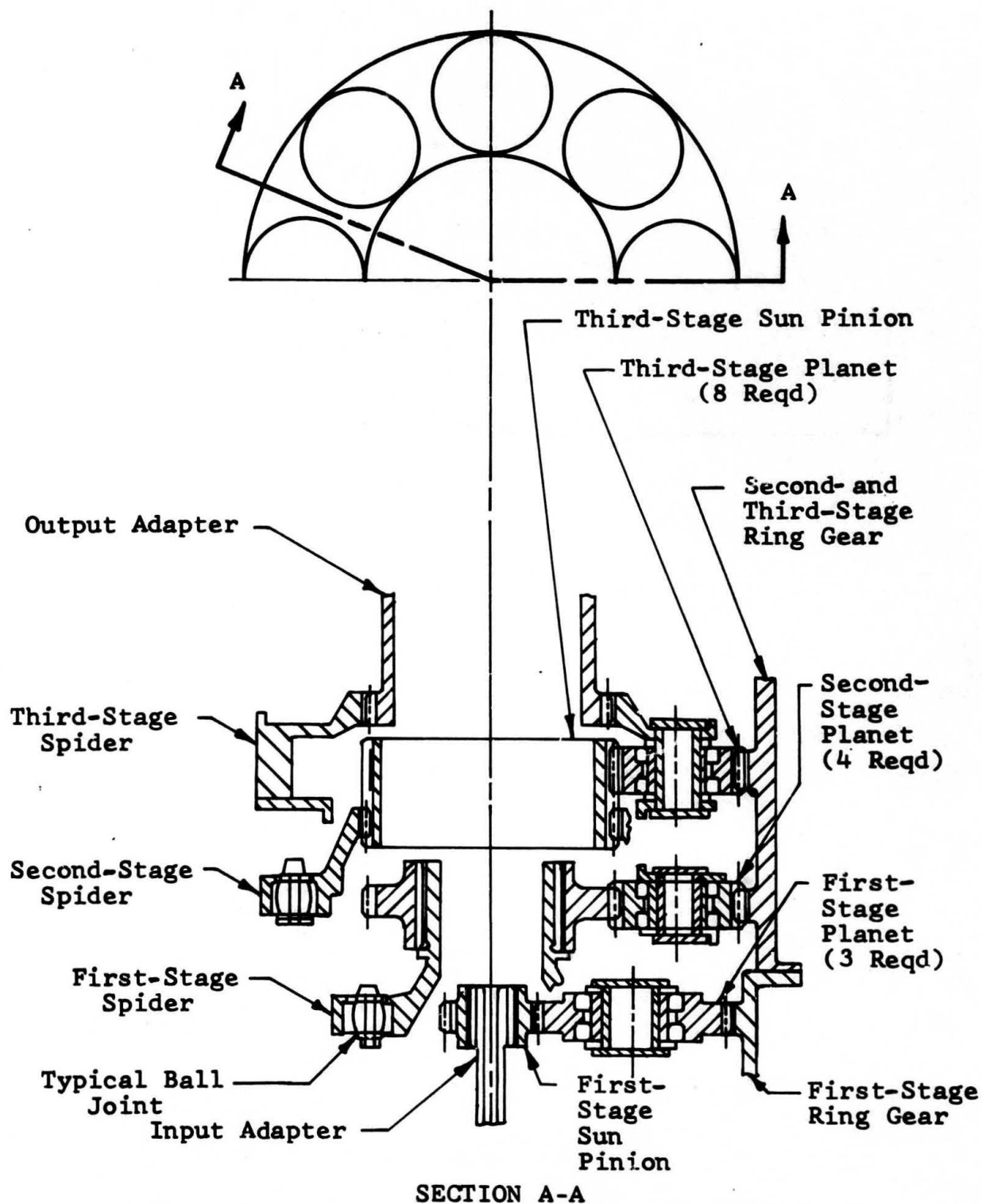
Figure 23.   Schematic of a Three-Stage
Planetary Reduction Drive.

95
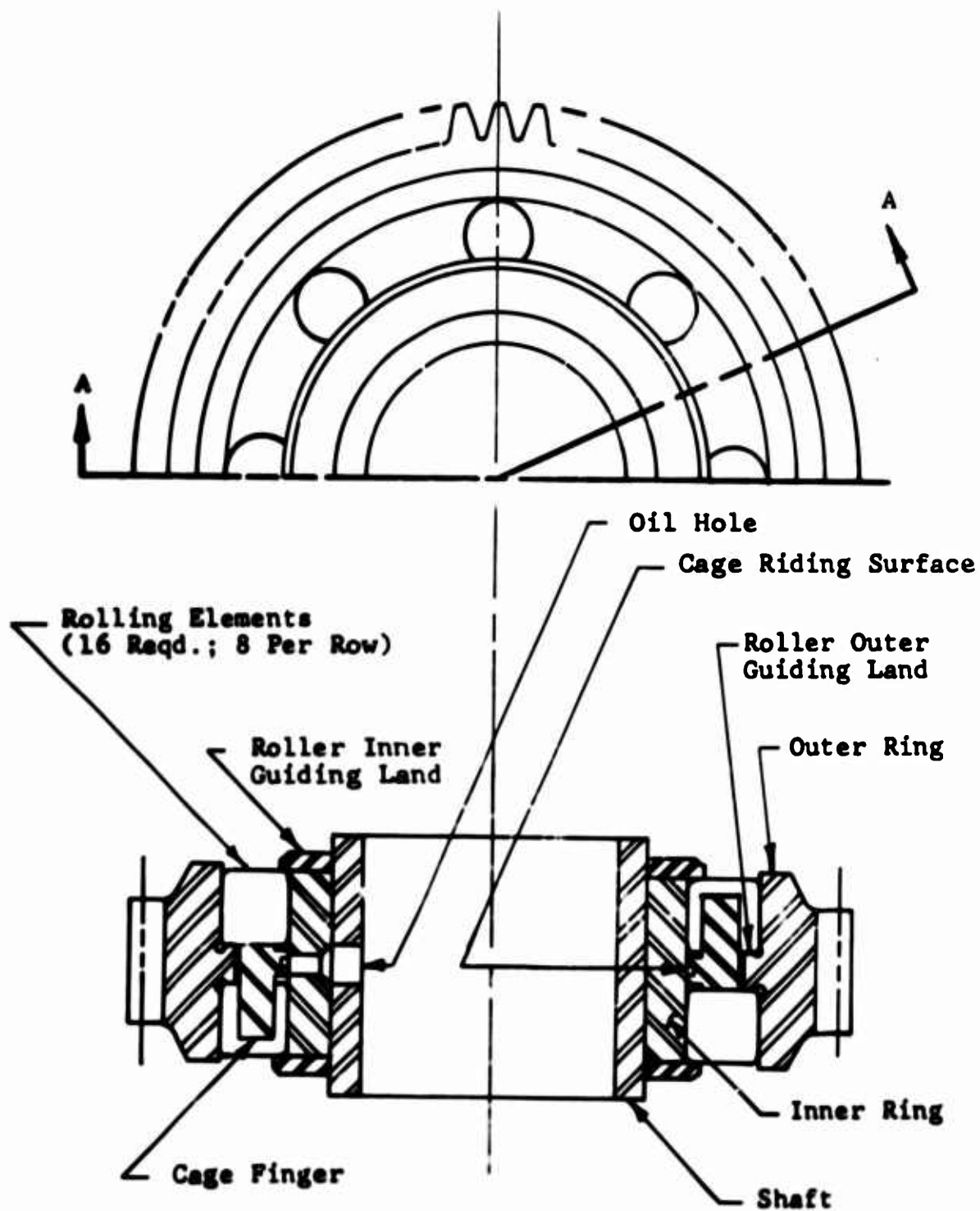
SECTION A-A

Figure 24. High-Speed Planet Idler Assembly.

legs. The spider legs are cantilevered from the hub which contains the internal drive spline. As torque is applied to the system, the spider legs deflect tangentially and twist forward, due to the load point location below the drive spline. The twist in the spider legs is isolated from the carrier plates by the spherical balls, thus permitting the plates to remain parallel. Therefore, the planet idler gear teeth are maintained in a plane perpendicular to the carrier plates and parallel to the sun and ring gear teeth. The ball joint spider thus achieves its purpose, viz., maintaining gear tooth contact in parallel planes, thus preventing high-pressure end-loading characteristics of conventional carrier designs independent of driving torque magnitude.

Equal load sharing in the three sun-planet meshes and three ring-planet meshes is attained by the inherent stability of three-point contact, the high compliance of lightweight carrier plates, and the loosely splined ring gear. The dynamic over-loads due to minor tooth spacing and profile errors and the mal-load sharing, introduced by planet location position errors in manufacture, are alleviated by the ability of the planet idlers to seek unrestrained equilibrium. This concept has been well established by the BHC Model 206 (LOH) planetary transmission. See Reference 6 for a complete discussion of the 206 system.

The high-speed planetary reduction ratio (4.5:1) in conjunction with the two existent UH-1 planetary stages provides the same overall reduction as that of the RGT design (ref. page 23). The input bevel ratio is 1.518:1 (identical to the RGT), the first-stage planetary ratio is 4.5:1, and the second- and third-stage planetary ratios are 3.087:1 each, resulting in an overall ratio of 64.970:1 (compared to 64.864:1 for the RGT).

A hunting tooth ratio was preferred in order to minimize oper-ating distress propogation due to production anomalies in the machined elements. The initially chosen tooth numbers for sun, planet, and ring were 36, 45, and 126. Since each number is divisible by 3, a single mesh distress would rapidly propogate to every third tooth of every meshing gear element. The hunt-ing tooth system used was accomplished by dropping two teeth from the planet idlers (spread center gearing), i.e., from 45 teeth to the prime number 43. Appendix V gives the addendum adjustments required.

By dropping two teeth from the idlers, definite strength and efficiency advantages were gained, in addition to the advan-tages inherent in the hunting tooth ratio. The method used in this adjustment is described in Appendix V. The sun-planet mesh operates at a relatively high-pressure angle, and the

97

ring-planet mesh operates in the arc of recess of the tooth action line, both conditions being conducive to maximum power transmission efficiency. The high pressure angle of the sun gear reduces the scoring tendency (over lower angles) and increases the bending strength. The ring gear recess action results in a lower scoring tendency (scoring generally occurs in the arc of approach), and the inherent superior bending strength of the internal tooth form permits operation at lower pressure angles, without compromise to the bending endurance limit.

The high-speed low-torque aspect of the planetary design permitted usage of relatively fine pitch gearing. The dynamic impact load conditions existing in a highly loaded involute gear set can be minimized by increasing pitch (and number of teeth) within safe strength limits.

This increased contact ratio (combined with proper tooth profile modification to compensate for loaded tooth deflections) increases power transmission efficiency and reduces gear noise propagation, as well as reduces dynamic tooth impact loads at high pitch line velocities. The predicted dynamic factors are shown in Appendix V.

PLANETARY SUPPORT BEARING

The lower planetary support bearing is used to maintain position of the three planetary stages and is subjected to the weight of all three assemblies. The bearing is an angular contact, deep-grooved ball bearing of 7108 basic size, made from SAE 52100 steel. It contains 15-5/16 in. diameter balls and operates at a 30° contact angle. The total load applied to the bearing at 1.0-g loading is 101 pounds, and the individual ball loads amount to 16.15 pounds each, with a 4.93-pound contribution due to centrifugal effects. With the outer ring rotating relative to the inner ring at 10,806 rpm, the calculated B_{10} life is 87,749 hours.

Lubrication is supplied to the bearing by a high-pressure jet that impinges on the sun gear inside a centrifugal dam. The sun gear has a series of holes drilled through the web, through which the lubricating oil flows and egresses onto the inner ring of the bearing. Hence, a continuous supply of oil is supplied to the bearing.

TSPT PLANET IDLER BEARING DESIGN

The major item of concern in the design of a high-speed planetary assembly employing a rotating carrier is the increased

planet idler bearing load due to centrifugal acceleration of the planet idler gear.

Ordinary type AFBMA bearing life calculations are inadequate to define the true loading conditions existent in most low-speed idler bearing applications, and far less adequate in high-speed applications.

It should be emphasized that the basic assumption, used in the AFBMA analysis, consider Hertzian deflections only and ignore the elastic deformation of the rings in defining the internal load distribution. Since the bearing outer ring is also an externally toothed gear (see Figure 24 for cross-sectional view of the planet idler bearing assembly) operating in diametrically opposed contact with the sun and ring gears, whose meshing forces are of sufficient magnitude to markedly affect its shape, the assumed internal rolling element load distribution may be greatly in error. The combined effects of internal clearance, ring section modulus, and gear tooth geometric form must be considered in proper definition of the load distribution and, in turn, predicted life calculations. A complete discussion of proper treatment of the fully elastic analysis may be found in Reference 8.

In the case of the high-speed planetary, a proper design analysis must also consider the load imposed by the mass of the idler gear-outer ring component operating in the attendent centrifugal field, as defined by its orbiting velocity. The magnitude of this load may easily exceed that engendered by the transmitted torque.

Additionally, second-order load effects are to be found in the increased rolling element-outer race load due to the rolling element mass operating in the centrifugal field defined by the bearing cage angular velocity about the inner ring axis, as well as in the previously defined field.

A graphic representation of the forces at work may be seen in Figure 25. While development of a computer program capable of the simultaneous treatment of all these variables is not impossible, such a task is beyond the scope of this study effort. However, as will be subsequently shown, a sufficiently rigorous and conservative analysis method has been used in the design of the high-speed planetary. Data are also included to show that the same order of force magnitudes exist in a similar high-speed planetary design of well demonstrated capability.

It is, therefore, understandable that most high-speed planetaries of this type have never passed the design board stage. Review of all present-day aerospace gearing hardware known to

Figure 25. Planet Idler Bearing Loads.
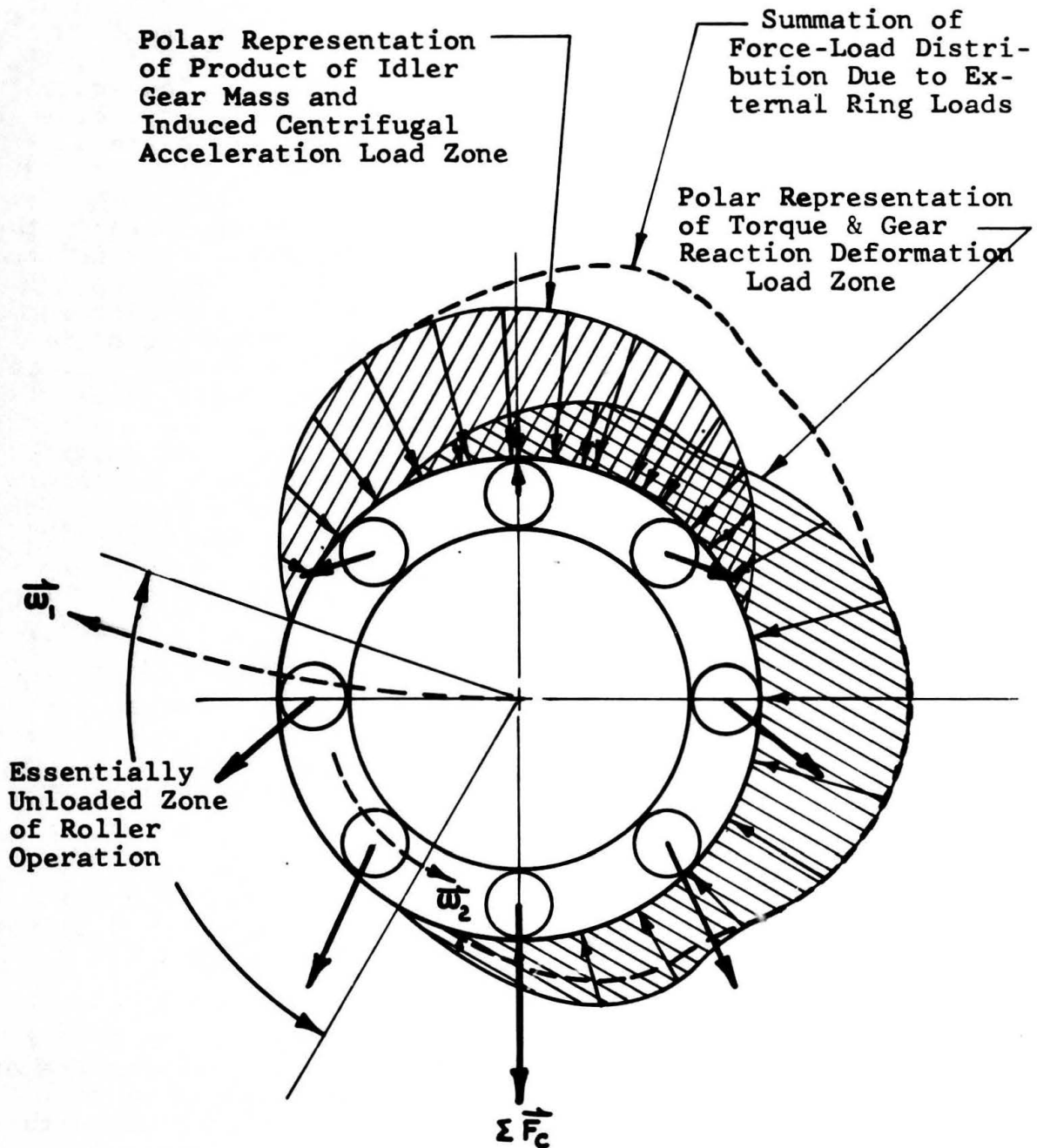
$\overrightarrow{\omega_1}$ = Angular Velocity - Idler Gear Orbit

$\overrightarrow{\omega_2}$ = Angular Velocity - Roller Element Orbit

$\Sigma \overrightarrow{F_c}$ = Summation of Product of $\omega_1 + \omega_2$ Centrifugal Field Accelerations and Roller Element Mass Load Vector

the authors reveals no such applications in existence. However, with the clearer understanding of the physical phenomena interacting in such applications, in part made possible by recent work in the field of elastohydrodynamics (Reference 9) and the recognition of certain fundamental axioms for avoiding known areas of hazard, successful applications are entirely feasible. The singularly known successful application now in existence (a speed increasing high-speed planetary in operation at BHC in a test stand) is discussed in length in a subsequent portion of this section. See page 116.

The above mentioned combination of speed and centrifugal loads and their attendent lubrication and cooling problems require a radical departure from the accepted norm in the design philosophy of the planetary idler rolling element bearings and cages. Only double-row cylindrical roller bearings with their spin axis parallel to their orbiting axis (contact angle of zero) are considered to be suitable for the application.

Self-aligning spherical or barrel-shaped roller types with a non-zero contact angle are precluded because of the large gyroscopic moment acting on each rolling element as a result of the cross axis orientation of their spin and orbit vectors.

At the design speed of this unit, these moments are sufficient to cause severe skidding in the unloaded zone. As explained previously in the discussion of the ball-joint carrier suspension system, excellent parallel gear tooth contacts can be maintained regardless of transmitted load level without recourse to self-aligning roller bearings, and the higher capacity cylindrical roller bearing may be advantageously employed.

The detail design of the cage is perhaps the most singularly critical factor in achieving success or failure in this application. A finger-type cage similar to those used in the UH-1 planetaries has been chosen for the high-speed stage of the TSPT. The fingers, or separators, are cantilevered and staggered one side to the other from a solid central ring (fixed between the 2 rows of rollers) of the rectangular cross section. These fingers function to maintain relative azimuth location of the roller complement and offer no roller guiding. (Roller guiding is accomplished by close clearance integral shoulders on both inner and outer raceways.) This type cage is simple, lightweight, and relatively inexpensive to fabricate. The cage design is shown in Figure 26.

The stresses to which these fingers are subjected are primarily bending and shear at the root fillet area where the fingers blend to the rim section. The finger loads producing these stresses are created by the rollers as they lead and lag the cage fixed azimuth locations when they enter and depart the
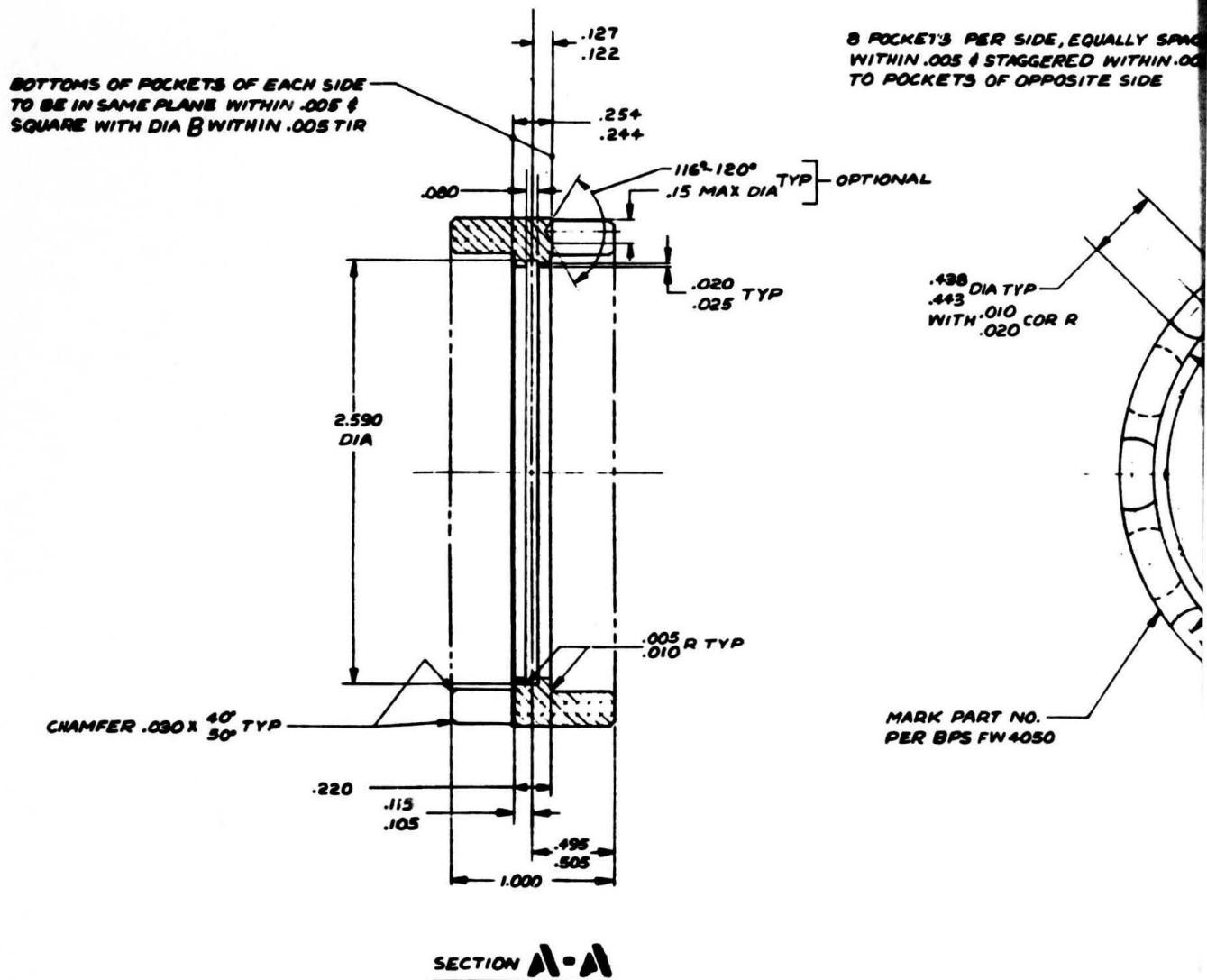
Figure 26. High-Speed Planetary Idler Bearing Cage

103

A.

8 POCKETS PER SIDE, EQUALLY SPACED
WITHIN .005 & STAGGERED WITHIN .005
TO POCKETS OF OPPOSITE SIDE

TYP — OPTIONAL

8 PORTS PER SIDE, EACH ¢
TO COINCIDE WITH CORRESPONDING
POCKET ¢ WITHIN .015

.438 DIA TYP
.443
WITH .010 COR R
     .020

.062
TYP

2.690

2.958
2.952
PITCH DIA

3.110

2.520 DIA
2.521

MARK PART NO.
PER BPS FW 4050

Cage

B.

externally loaded sector of the bearing. The bending and
shear stresses are produced when the cage restrains the rollers
to their proper geometric spacing. In highly loaded flexible
ring applications (characterized by all planet idlers in TSPT),
the roller emerging from the external load zone is accelerated
to a large degree by the elastic hysteresis or "pumpkin seed"
effect. (An attempt to hold a wet pumpkin seed tightly between
the thumb and forefinger yields graphic demonstration of this
phenomenon.) In the case of the high-speed planetary, the
large centrifugal force acting upon the emergent roller serves
to increase its acceleration to yet greater values. The
ability of the separator fingers to withstand these lead-lag
and impact loads is directly a function of the bending section
modulus of the finger-ring junction and the impact strength or
ductillity of the cage material and/or geometry. In order to
operate below the material endurance limit, adequate cross
section in the circumferential length direction must be pro-
vided. This in turn requires utilization of a reduced roller
complement. The reduced complement (or less than maximum
capacity design) serves the additional and most important
function of reducing the bearing heat generation. In practice,
a satisfactory roller center spacing has been demonstrated as
2 to 3 roller diameters. Adequate circumferential roller
clearance must be utilized in the finger spacing to minimize
loading caused by the roller angular velocity change in the
externally loaded zone, and to permit the cage to move off
center (to the limit of its land clearance) due to the centri-
fugal cage load without binding on the roller pitch line.
Excessive clearance on the other hand increases the impact
loading which occurs as the rollers depart the externally
loaded zone. Experience has shown that a 5 to 10 percent
roller diameter pocket clearance is best for roller diameter/
pitch ratios in the range of .1 to .15. As will be subsequently
shown, the sacrifice in theoretical bearing capacity necessi-
tated by the increased cage finger section is relatively un-
important.

The cage material should have a high strength-to-weight ratio,
a minimum density, an excellent thermal conductivity, a reason-
ably low coefficient of sliding friction against steel, and
should be relatively simple to fabricate. Of all the materials
evaluated in the existing high-speed design (which included a
wide range of metallics and plastics), wrought aluminum in the
T3 or T4 tensile range has proven to be most satisfactory. The
TSPT high-speed stage will use 2024-T4 aluminum alloy with a
.0005-inch to .001-inch thick silver plating to increase run-
ning time in the event of loss of oil lubrication.

Although many high-speed aerospace bearings operate well with
outer land riding surfaces, such a choice is incorrect for
this application. The outer land riding cage contributes its

105

centrifugal weight directly to the planet idler and, in turn, it shows up as an additional externally applied load to the rolling elements. However, the inner land riding cage centrifugal weight is carried by the inner ring and concentric planet carrier shaft without increase in bearing load. In the TSPT high-speed stage, the inner land riding cage exhibits about an 11 percent higher land rubbing speed than would be the case with an outer land riding cage. However, this loss is offset by an approximate 5 percent weight reduction afforded by the smaller cage mean diameter and by the superior surface finish obtained on the inner ring. Excellent lubrication of this rubbing interface is provided by conventional hydrodynamic lubrication. In this instance, the velocity is high enough to build an adequate film. Oil is introduced on the high clearance side (outboard) of the interface by centrifugal feed through the inner ring oiling holes. The hydrodynamic wedge or taper is inherent in the eccentric displacement of the centrifugally loaded cage. This same eccentric cage displacement is in the proper direction to partially compensate for the angular velocity increase in the roller elements in the outboard zone.

The calculated life by standard AFBMA prediction methods for this reduced complement bearing is far short of the experienced life in high-speed applications. This method does not account for the thick lubricant film regime as predicted by elastohydrodynamic phenomenon calculations nor is there realistic representation of the roller-race osculation at the high imposed loads. High osculation is assured by excellent end guidance of the rollers by both inner and outer lands, as well as by high load intensity, which results in true modified line contact for the double crowned rollers.

Elastohydrodynamic calculations, Reference 9, predict a lubricant film thickness of 22 microinches under the highest roller-race load intensity. Since the planetary races are finished to a nominal 3-microinch roughness and black oxided, and the rollers are finished to a 2-microinch roughness, the average relative roughness for mean asperity contact is 3.6 microinches.

This ratio of film thickness to mean composite roughness of greater than 5 assures operation in the regime of greatly increased fatigue life. A conservative life factor for such applications may be taken as 2. (See Reference 10.)

The planet idlers in the high-speed planetary stage of TSPT operate in a centrifugal field of 1045 G's at an engine N_{II} speed of 21,016 rpm. The idler bearings comprise two rows of eight 11x11 mm rollers each. The calculated B_{10} (see Appendix V for method of handling centrifugal forces) is 336 hours at 1138 hp, which is equivalent to the 1250 hp engine takeoff

106

rating. This life is based upon the AFBMA material factor for
electric furnace 52100 bearing steel. The utilization of
clean, consumable electrode vacuum remelted high-temperature
steels (either 52CB or M-50) of course yields material capacity
factors several times greater than air-melt 52100.

Combining the thick film life factor with the material factors,
a conservative number of $4 \times 336 = 1,344$ hours B_{10} may be taken
for reliability calculations; these bearings are expected to
exceed the overhaul lives of the existent UH-1 planet idler
bearings.

DIAMETRAL PITCH, PRESSURE ANGLE, AND OPERATING STRESS CHARACTERISTICS

The TSPT utilizes the RGT input bevel gears and the two UH-1
planetary assemblies, which established the design specifica-
tions for the high-speed planetary assembly.

The basic design specifications for the high-speed planetary
stage were the input speed (13,886 rpm), the reduction ratio
(approx. 4.5:1), the transmitted power (1138 hp), and the
axial envelope (not to exceed the RGT dimension). Within
these basic specifications, the optimization criteria were
reliability, efficiency, weight, manufacturability, and cost.

The available axial envelope normally limits the gear face
width and bearing spread of the planet idlers. Therefore,
power limitations are set by the combination of maximum number
of planets and maximum face width that can be installed within
the radial envelope, which is determined by the reduction
ratio. In order to adequately transmit the imposed power
(1138 hp) from the input bevel gear shaft to the UH-1 lower
planetary, a maximum of 5 planets is available (reference
Figure 27) for the TSPT. However, it was deemed necessary to
incorporate the ball joint spider design (reference page 93)
in the high-speed planetary assembly in an effort to minimize
gear distress due to nonparallel gear axes. This last re-
quirement restricted the number of planets to 4.

By observation of the operating requirements and comparison to
the UH-1 lower planetary assembly, it was apparent that the
high-speed planetary assembly could function satisfactorily
with 3 planets instead of 4. The latter decision was suggested
by the fact that the 4 planets in the UH-1 lower planetary
assembly were capable of transmitting in excess of 1138 horse-
power at less than 25 percent of the speed. The actual torque
transmitted in the high-speed planetary assembly is thus less
than 25 percent of UH-1 lower planetary and can, therefore, be
adequately transmitted with fewer idlers. Also, because of the
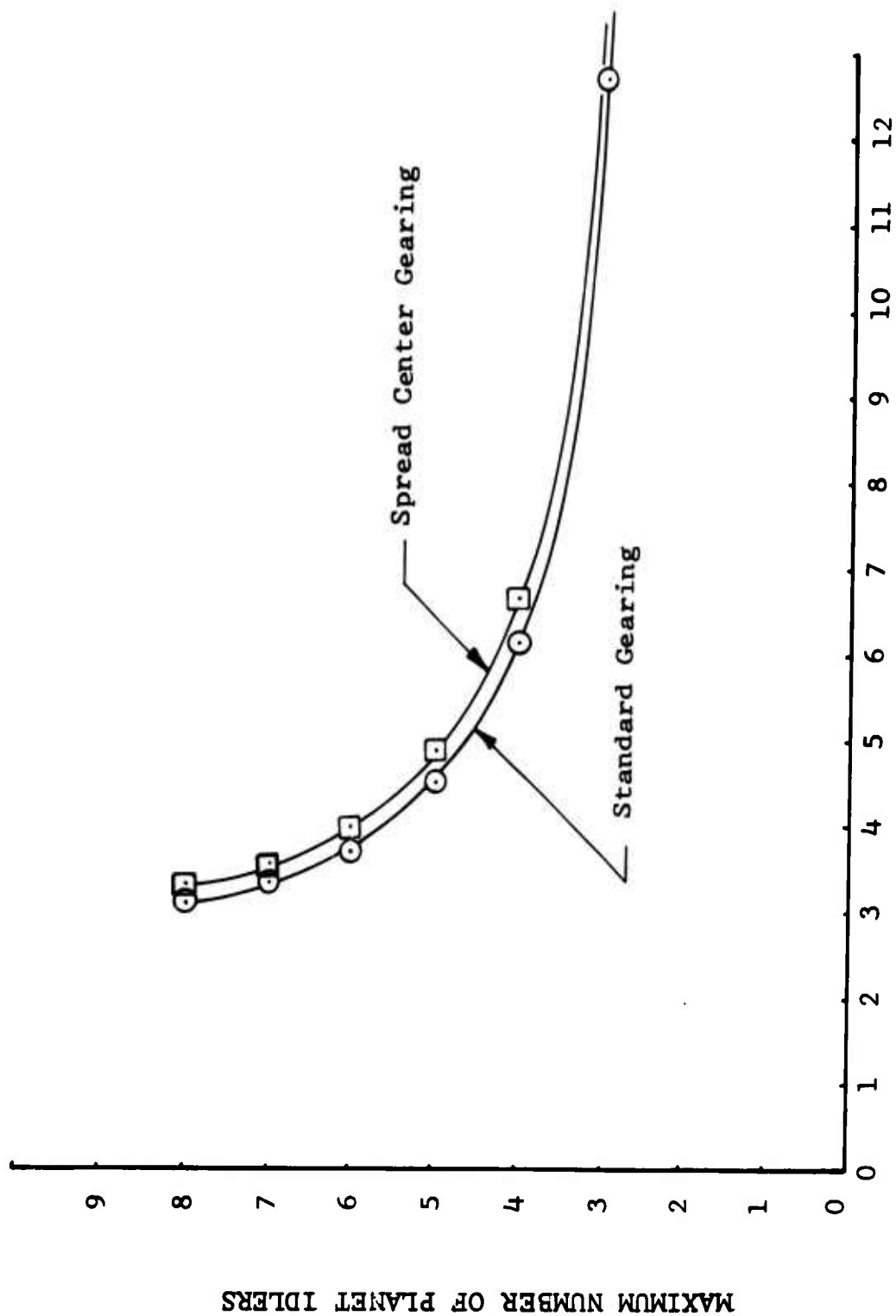
REDUCTION RATIO - (SUN INPUT - FIXED RING - CARRIER OUTPUT)

Figure 27. Maximum Number of Planet Idlers Versus Reduction Ratio.

relatively large housing diameter available for the ring gear, and in order to further increase reliability and reduce windage loss, weight, and cost, the choice of 3 idlers was preferable. Basic load sharing of the 3-planet idler gear design was discussed in the introduction to this section and in greater depth in Reference 6.

The high input speed, coupled with a probable 3- to 4-in. diameter sun gear, yielded approximately a 10,000-fpm pitch line velocity. The estimated minimum EHD film thickness is on the order of 33 microinches. Figure 36 predicts an adequate mean pitting life for the 1000 K-factor (approximately 180,000 psi Hertz stress). The expected dynamic load factor from Reference 13 is about 1.15, suggesting a reduction in the target design K-factor to about 925, when considering torque loading only.

Initial selection of pitch for adequate bending strength may usually be determined by the use of 20,000-unit load as a maximum value. Since the preferred tooth numbers for the sun, planet, and ring were 36-45(43)-126 (see page 97), selection of 12 D.P. teeth yielded a face width of only .40 in. at 20,000 U.L. This would normally lead the designer to try a larger D.P. number (smaller tooth) in the quest of increased efficiency and reduced weight. However, as noted previously, the design of a high-speed planetary requires some departure from the norm.

An additional check of the 12 D.P. sizing shows that the limit K-factor is achieved at a face width of .63 inch, which still suggests the use of a smaller pitch.

However, further investigation reveals that the size of the idler gear (3.58 in. P.D.) is restrictive with respect to the selection of a roller bearing complement and size (see bearing design discussion page 98) of adequate capacity. Consideration of the planet mass, the G-field, and the transmitted torque, yielded a C/P ratio for the bearing of approximately 4.1, which is inadequate for the desired application life at the outer ring speed of 9000 rpm. As mentioned previously, recourse to the use of 4 planet idler gears was not desirable. An increase of the tooth numbers to the next available optimum set of tooth numbers, i.e., 48-60(57)-168, for the sun, planet, ring, respectively, yields an excessively large sun gear at 4.0 inches P.D. In addition, the reduction of three teeth in the idler (from 60 to 57) to obtain a hunting tooth design produces an excessive recess action planet-ring mesh.

It may now be understood that the limiting design factor in the high-speed planetary is generally the planet idler bearing.

This factor suggests that the proper compromise solution may be found by reducing the diametral pitch number, providing flash temper rise or scoring indexes do not become prohibitive.

The final selection of a 10-D.P. basic tooth size provided an adequate idler bearing capacity, and the increase of the face width to .75 inch limited the calculated flash temperature rise to 143°F, which is considered to be satisfactory for this application. The resultant 3-planet idler 10-D.P. design remains lighter in weight than a 4-idler 12-D.P. design. Review of the design layout cross section, Figure 22, shows that the final 10-D.P. design fits well in the necessary envelope dimensions. The ring gear diameter is well suited for adaptation to the conical transition section in the main case between the bevel gear output and the first existent UH-1 planetary stage. The final weight calculation for this reduction stage of 28 lbs further reveals how small the penalties of this compromise design remain after obtaining adequate bearing life.

Development testing of such a planetary may reveal the ultimate power transmission capability to be 50 percent higher than the prescribed specification values. However, the increased reliability attendent with the more conservative gear stress levels obtained in the final design suggest rapid attainment of the T.B.O. goal for this system.

Table XIII summarizes the gear data applicable to the proposed high-speed planetary, and the idler bearing design is discussed on page 98.

TSPT LUBRICATION SYSTEM

The TSPT lubrication system is identical to that of the RGT except for the planetary gear and bearing oiling system. The oil flow requirements of the TSPT are approximately 3.3 GPM less than the RGT, due to the fewer number of jets required to lubricate and cool the orbiting planet idler assemblies. The RGT lubrication system discussion, page 80, has a detailed explanation of the increased oil flow requirements. Figure 28 shows a schematic of the TSPT lube system, and Table XII identifies the various lube system components.

As in the existent UH-1 system, the lubrication fluid chosen is MIL-L-7808, synthetic turbine engine oil, which has a kinematic viscosity of 3-3.5 centistokes at 210°F. This fluid is supplied to the gear meshes and bearings through high velocity jets, pressurized feed annuli around the bearing stationary rings, and by simple splash and mist. The oil system components include a 2-1/2-gallon capacity gravity return wet

To Lube
Cooler

From Lube
Cooler
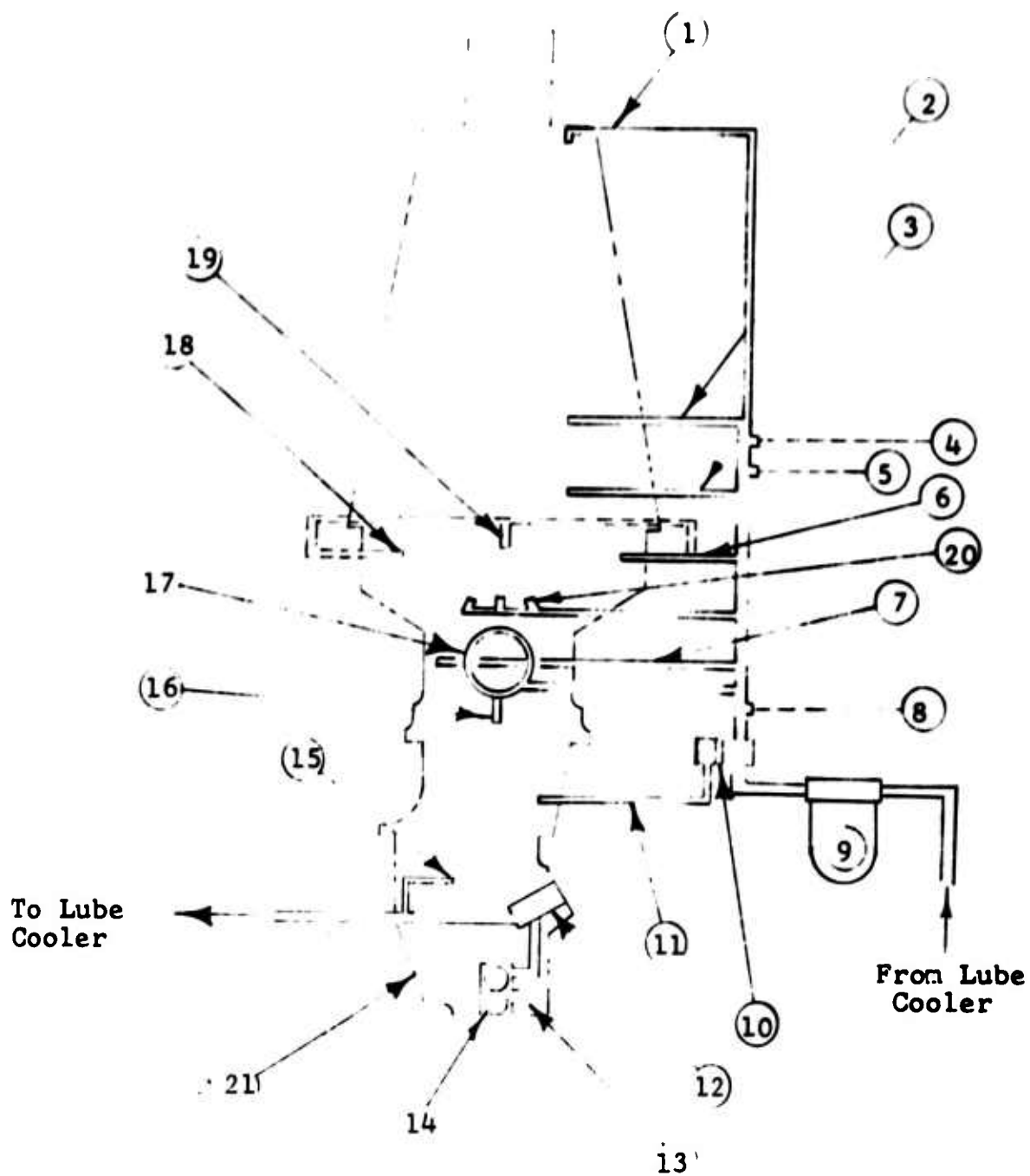
Figure 28.   Lubrication System Schematic, Three-
Stage Planetary Transmission.

111

TABLE XII. IDENTIFICATION OF LUBE SYSTEM COMPONENTS
(REFERENCE FIGURE 28)

Item No.	Nomenclature	Function	Pressure (PSI)	Flow Rate (GPM)
1	Lube Jet	Lubricates: Main Rotor Drive Shaft Roller Bearing	47	.28
2	Lube Jet	Lubricates: Main Rotor Drive Shaft Thrust Bearing	50	.54
3	Lube Jet	Same as Item No. 2		
4	Thermoswitch, High Lube Temp. (230°F)			
5	Lube Temp. Bulb			
6	Lube Jet (Ring of Three Jets with Items 18 and 19)	Lubricates: Second and Third Stage Sun Gears, Planet Idler Roller Bearings, and Planetary Support Bearings - One Jet, Three Streams	50	.38
7	Lube Jet, Main Case	Lubricates: a) Generator Drive Quill - One Stream b) Main Bevel Set - Two Streams c) Gear Shaft Roller Bearing - One Stream d) Input Pinion Roller Bearing - One Stream e) Freewheeling Unit - One Stream	50	1.70 (Total)
8	Pressure Gage			
9	Filter, Paper Element, Ten Micron			

TABLE XII (continued)

Item No.	Nomenclature	Function	Pressure (PSI)	Flow Rate (GPM)
10	Valve, Pressure Regulator, 60 psi			
11	Over-Pressure Discharge Duct from Item 10			
12	Filter, Wire Screen Cascade, 40-Micron			
13	Screen, Pump Inlet, 16x16 Wire Mesh			
14	Lube Pump, 15-GPM Gerotor			
15	Lube Jet, Sump Case	Lubricates: Tail Rotor and Hyd. Pump - Bevel Gear Drive - Three Streams	100	1.16 (Total)
16	Lube Jet (Supplied by Item 17)	Lubricates: Accessory Drive Spur Gear Ball Bearing	58	.30
17	Lube Gallery	Lubricates: a) Main Input Triplex Bearing b) Supplies Lube to Item No. 16	58	1.00 (To Brg.)
18	Lube Jet	Lubricates: Part of Second and Third Stage Planetary - One Jet, Three Streams	50	.38
19	Lube Jet	Lubricates: Part of Second and Third Stage Planetary - One Jet, Three Streams	47	.38

113

TABLE XII (continued)

Item No.	Nomenclature	Function	Pressure (PSI)	Flow Rate (GPM)
20	Lube Gallery	Lubricates: a) Gear Shaft Duplex Bearing b) Lower Planet Support Bearing, Three Jets c) High-Speed Sun Gear, Three Jets d) Planet Idler Roller Bearings, Three Jets	53	3.93 (Total)
21	Lubricant Sump - 2-1/2-Gallon Capacity MIL-L-7808 Synthetic Lubricant			

114

sump, a 15-GPM immersed positive displacement transmission driven pump, a three-phase filter system consisting of a 16-gage wire mesh coarse filter screen, a 40-micron metallic wafer type stacked element filter, a 10-micron paper element filter, a thermostatically controlled bypass oil-air heat exchanger, a spring compensated adjustable oil pressure regulator, externally removable oil jets, and associated tubing fittings and monitoring devices.

The oil is drawn into the pump through the coarse filter screen directly from the sump, and delivered under approximately 100 psi pressure to the 40-micron metallic wafer filter and then to the externally located heat exchanger. The thermostatically operated bypass valve begins to open at 165°F (below this temperature, the oil bypasses the cooler) and is fully opened at 180°F. Oil exiting the heat exchanger returns through a 10-micron paper element filter to the transmission mounted manifold and regulator assembly. Both the metallic screen wafer and the paper element filters are equipped with automatic 20 psi differential pressure actuated bypass valves and the paper element unit is additionally fitted with an impending bypass indicator which operates at 18 psi differential pressure. The pressure regulator assembly is set to maintain a 60-psi discharge pressure at the jets and bearing feed annuli; excess oil is discharged from the regulator directly inside the transmission casing where it returns to the sump by gravity feed. Distribution from the manifold to the various lubrication points is by internal and external passages and lines. The oil delivered at these lubrication points of course serves the dual function of lubricating and cooling. Sump return from these bearings and gears of the heated oil is by gravity flow. Transparent sight glasses are provided in the sump wall for rapid exterior inspection of oil level with suitable markings for "full" and "add". The transmission oil filler and breather vents are located in the top case.

HIGH-SPEED PLANETARY ASSEMBLY BALANCING INVESTIGATION

Due to the high operating speed of the high-speed stage carrier, an investigation was made to determine the operating effect of radial unbalance on the transmission. All elements that would directly affect the planet carrier unbalance were critically analyzed from a weight variation standpoint due to tolerance extremes. The critical dimensions on contributory parts were determined to be the lengths. For example, the planet idler has very closely controlled diameters for bearing journals, gear O.D., gear root diameters, etc.; thus, the maximum variation in weight from one planet idler to another is due primarily to the length differences of the gears.

The planet centers in the carrier plates are usually maintained within .003 in. of true position, and the weight variation attributed to the length tolerance on the planet idler is .0006 pound per .001 in., or .624 lb/.001 in. in a 1045 G-field. If the tolerance is held to ±.003 in., then the maximum idler unbalance contribution would be 3.844 lbs, assuming that the other two planets have equal weight at the minimum length. The weight distribution in the carrier is concentrated at three points 120° apart and, hence, the maximum centrifugal unbalance is produced when two of the three concentration points are of equal weight, while the weight of the third point is either more or less. Any weight difference that results in the three concentration points varying in weight (within the blueprint tolerance limits) tends to minimize the unbalance moment. Since the machined parts in the TSPT high-speed planetary assembly are manufactured primarily by turning operations, the weight distribution is centrally concentrated at the turning axis and the unbalance forces are minimal.

In deference to the expense and time involved in producing a dynamically balanced planetary assembly, and based on the successful operation of the bench test high-speed planetary assembly, which does not have any balancing requirements, no further consideration will be given to the TSPT with regards to centrifugal unbalance. However, should any unbalance problem occur during development testing, a reduction in unbalance moment could be readily attained by reducing the length tolerances of the detail parts and statically balancing the carrier assembly by removing material from the required area at the periphery adjacent to the idlers. Therefore, initial development testing would be accomplished without expectation of excessive centrifugal unbalanced forces, but momentary balancing could be acquired if the need should arise.

TEST AND DEVELOPMENT EXPERIENCE

Extensive development testing and operating experience has been obtained from a Bell-designed high-speed planetary system that has been operating on a bench test rig wherein UH-1 transmissions are tested.

This high-speed planetary assembly was developed from a Bell Model 61 transmission and normally operates at 6400 rpm of the sun gear and 2218 rpm of the carrier; for rotor overspeed simulation, the sun gear and carrier rotate at 6700 rpm and 2330 rpm, respectively. The planet gear centers are 6.111 in. from the center of the carrier and operate under a normal 852 G-field and an overspeed G-field of 893 G's, at which speed many hours have been run.

116

The bearings have fewer rollers than conventional planet bearing assemblies and, hence, have comparatively stronger cage fingers than the conventional counterpart. The gearbox elements have operated successfully at powers exceeding 1700 hp without distress.

The high degree of reliability of this gearbox is attested to by the infrequent overhaul requirement. Since final development testing was completed in 1954, the original gearbox has been overhauled 4 times - twice from high elapsed time (2000 hours operation above 800 hp) and twice due to inadvertent operation without benefit of lubricating oil. Over the life of the test stand, this gearbox has attained several thousand hours of operation at powers up to 1738 hp. The operating characteristics of this planetary assembly are shown in Table XIII and may be compared to the high-speed planetary designed for this report, also summarized in Table XIII.

This planetary assembly is fabricated from conventional gear materials machined to standard tolerances representative of Bell transmission designs. There are no static or dynamic balance requirements for any of the planetary details. The gearbox is fabricated from parts machined per blueprint requirements and assembled without benefit of "matching" or balancing.

The carrier is fabricated by either broaching or milling the space between the carrier plates for insertion of the idler assemblies. This method of machining results in a greater variation in weight distribution than would be experienced on a comparable part that is fabricated primarily by turning operations. In order to determine the residual unbalance moment in the high-speed bench test planetary, the actual assembly was removed from the gearbox, mounted on a specially made arbor, and checked on knife edges. Weights were added to the "light" side until no rotation occurred when supported on the knife edges. The weights were removed, and their radial location was noted. The resulting unbalance moment was .072 in.oz. At an operating speed of 6400 rpm, this amounts to 24.66 lbs centrifugal force. As described above, no balance requirements other than those attained through blueprint dimensional tolerances are levied on this unit (See Figure 29).

117

	Model 61 (1800 HP)	TSPT (1138 HP)
TABLE XIII. SUMMARY OF OPERATING CHARACTERISTICS FOR BELL MODEL 61 HIGH-SPEED PLANETARY AND TSPT HIGH-SPEED PLANETARY		
Sun-Planet Tooth Load (Lb)	1045	934
Ring-Planet Tooth Load (Lb)	1045	982
Sun-Planet K-Factor	566	640
Planet RPM	9445	9035
Ratio	3.09	4.50
G-Field	852	1045
Center Distance (In.)	6.111	4.05
Planet Weight (Lb)	1.9	1.73
Centrifugal Force (Lb)	1620	1895
Total Bearing Load (Lb)	2644	2835
Bearing Life (Hr) (Based on total load and SAE 52100 Steel)	541	336

Figure 29. High-Speed Planetary Assembly UH-1 Bench
Test (Modified Model 61 Planetary)

HIGH-SPEED ACCESSORY STUDY

A search of the accessory industry was conducted for the purpose of locating or developing lightweight, high-speed accessories that could be adapted to either the RGT or the TSPT in an additional effort to reduce the weight of the UH-1 reduction system.

The accessories involved in this study are an electrical generator, a hydraulic pump, an oil pump, and a tachometer.

The following discussion shows that the weight savings of 11 pounds on the generator was all that was realized from this study.

GENERATOR (300-Amp, 28V DC System)

Two sources were contacted: Red Bank Division of the Bendix Corporation and Power Equipment Division of Lear Siegler, Inc. Since an optimum design would have the generator drive pinion driven by the main bevel gear with the resulting speed of ?1,016 rpm (engine speed), the first effort was directed toward this speed range. Neither source, however, had anything to offer in the 21,000-rpm range. They agreed that it was within the state of the art; however, weight reduction (if any) would not be worthwhile when traded off with the decreased reliability, high cost, and long development time. Lear Siegler posed the following problem areas that would have to be investigated and resolved in order to obtain a 21,000 rpm brushless system:

- bearings, their lubrication and life
- ripple voltage
- radio noise.

A second effort was directed toward the highest speed range at which existing generators could operate satisfactorily.

Both sources had something to offer in the 12,000-rpm range and below. Bendix offered a shortened modified version of the 20/30 KVA, 400-cycle generator that they are fabricating for the Lockheed AAFSS. The modifications would include a voltage regulator and a transformer which would give a brushless 300-amp 30V DC system at a weight of 35 pounds. The current 300-amp 28V DC system on the UH-1 helicopter operates at 6600 rpm and weighs 46 pounds.

Lier Siegler offered a shortened modified version of one of their production generators. Its weight also would be in the neighborhood of 35 pounds.

The generator drive on the RGT and the TSPT operates at 12,059 rpm.

HYDRAULIC PUMP (12 GPM, 1500 PSI)

Since the hydraulic pressure range on the UH-1 helicopter is restricted to 1400 - 1500 psi (100 psi maximum variation) for quick and consistent responses to the movements of the control systems, either a variable-displacement pump must be used or a constant-delivery pump in conjunction with a large accumulator may be used.

No effort was directed toward obtaining a constant-delivery pump because of the overall weight increase due to the necessary accumulator.

Vickers, Inc., was contacted for this phase of the study. They report that V.D. (variable-displacement) pumps capable of attaining a speed of 15,000 rpm have been built; however, their applications were for missiles with a short life requirement. Overheating is the primary problem confronting high-speed V.D. pumps. Some V.D. pumps have been used at 8,000 rpm, but they tend to overheat at that rpm. About 5,000 rpm is the limit for continuous trouble-free operation.

The hydraulic pump drive on the RGT and the TSPT is the same as that on the UH-1 transmission. Two 6-gpm pumps operating at 4307 rpm are employed.

OIL PUMP (10 GPM, 50 PSI, MIL-L-7808 Oil)

W. H. Nichols Co. was contacted relative to an oil pump operating at 21,000 rpm and at 14,000 rpm. They have fabricated and operated a single-element pump at 14,500 rpm that produced a maximum flow of 5.5 gpm. The maximum flow rate was obtained at 12,000 rpm and then leveled off to a constant 5.5 gpm.

Their comment on a 10-gpm, 21,000-rpm pump was that it is not practical at this time; 14,000-rpm pump is considered to be marginal. Most of their high-speed pumps are under 5-gpm capacity.

The inquiry concerning the 10-gpm, 50-psi, 14,000-rpm pump was made during the investigation of the possibility that the oil pump could be driven directly by the bevel gear shaft. The W. H. Nichols Company offered the following information in response to the inquiry:

121

- Nothing is available as an off-the-shelf item.

- Such a pump would have to be designed and developed.

- High altitude operation would be marginal.

- It would take from 4 to 6 months to design and produce a pump to meet the above needs.

- Because of the additional parts, including the scavenge pump, the cost would be slightly greater than the GC 1669 pump currently used on the UH-1 transmission.

- No weight savings could be expected. To improve the high-speed performance, they would want to increase the size of the inlet port of the pump.

On the RGT and the TSPT, the oil pump will be operating at 4148 rpm, which is the same rpm at which the GC 1669 pump on the UH-1 transmission operates. Since its flow rate is only 12.5 gpm at 50 psi, and since both drive systems need 15 gpm at 80 psi, the GC 1669 pump will be modified for these applications by lengthening the pump element.

TACHOMETER GENERATOR (Electrical Type)

Tachometer generators weigh only about 13 ounces, so no effort was expended to investigate if one could be made lighter.

SUPERCRITICAL TAIL ROTOR SHAFTING

Two systems were analyzed in the SCTRS study: (1) design new shafting, sump assembly, and 90° gearbox to accommodate high rpm installation; (2) remove two bearing hanger assemblies and use the same shafting and gearbox system as used in the present UH-1, with the addition of one long shaft (reference Figure 30).

The first system considered was to operate the tail rotor drive shafting from main transmission output to the 90° tail rotor box at 8159 rpm. This would involve the design and fabrication of a new sump case and accessory drive system on the main transmission to operate at the required 8159 rpm output. This would also involve a major redesign of the 90° gearbox to reduce the input speed back to the 1654 output rpm required by the tail rotor (reference Figure 31). The drive shafts themselves would be smaller in diameter with a thicker wall than those on the UH-1, and two bearing hanger assemblies would be eliminated. The 8159 rpm system would be required to operate with a minimum of three vibration dampers (considering no redundancy) for the three shaft sections shown in Figure 30. The first section, 56 inches long, with flexible couplings, is required to absorb the motion between pylon and airframe inherent in the elastomerically mounted main transmission pylon system. The system would then consist of three dampers, three shafts (two sections 56 inches long and one section 183 inches long), a 42° gearbox, and a 90° gearbox; the 42° gearbox being the only component common to the UH-1. The elimination of the two bearing hangers and attendent coupling assemblies would reduce the system weight by 6.96 pounds, but the addition of the three vibration dampers at 3 pounds each would add 2.04 pounds net to the system. The SCTRS shafting weight is 1.15 pounds less than the UH-1. The new 90° gearbox weight is 38 pounds compared to 23.5 for the UH-1. The total weight change would indicate a 15.39-pound increase over the present UH-1 system. This does not account for airframe changes to accommodate damper mounting brackets, support structure, and ballast. Ballast is required in the nose of the helicopter to offset the added moment induced by increasing the weight of the 90° gearbox. The 90° gearbox is located 322.025 inches aft of the C.G. of the ship and, hence, would require ballast amounting to 2.98 times each additional pound of weight due to the larger 90° gearbox, assuming that the ballast can be installed as far forward as 108 inches from the C.G. (the nose is located 131.225 forward).

The fact that the SCTRS system is heavier, coupled with the major change of the 90° gearbox (which would be 16.2 percent
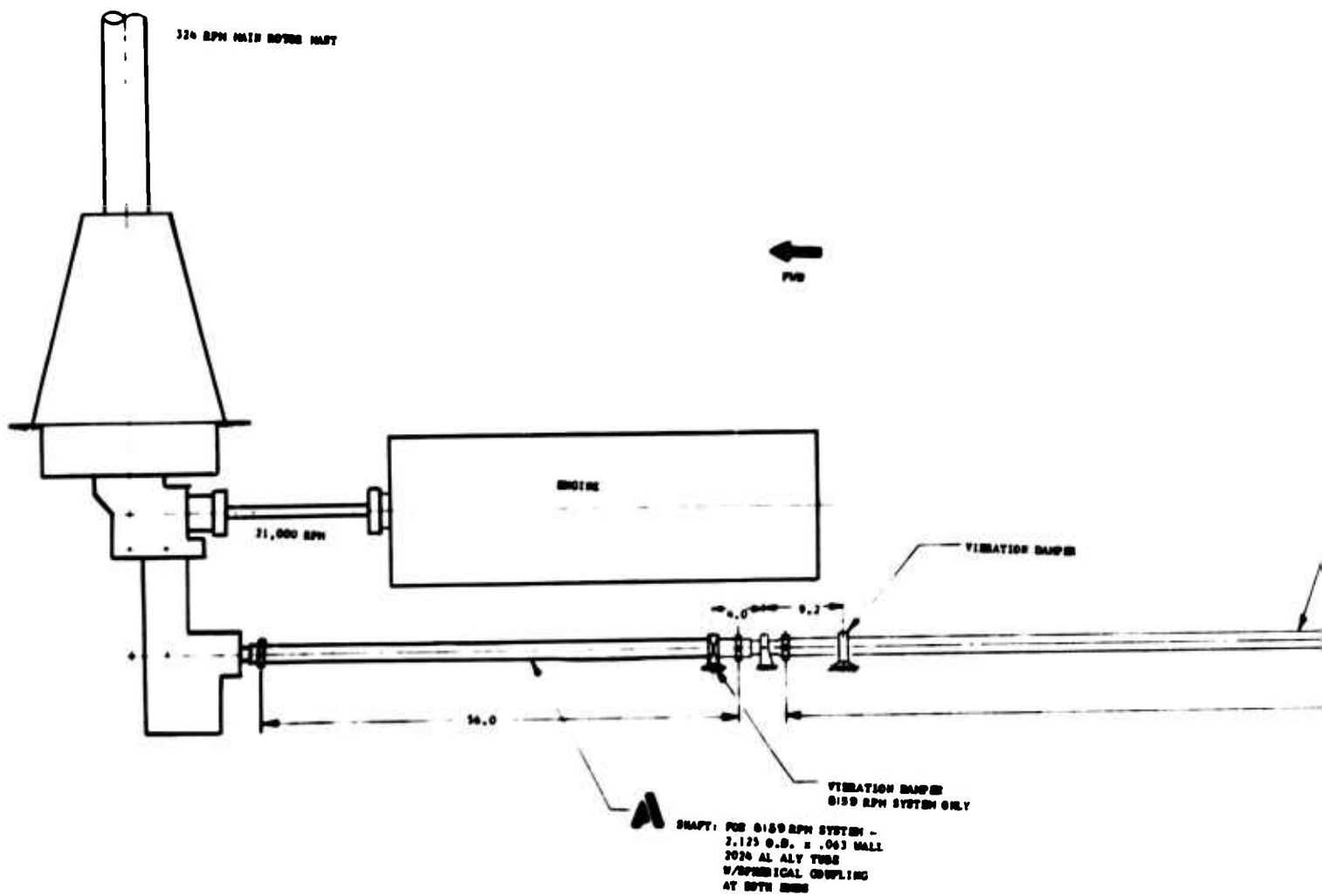
Figure 30. RGT Supercritical Shaft Schematic

13

SHAFT: FOR 8150 RPM SYSTEM
2.125 O.D. x .063 WALL
2024 AL ALY TUBE
W/SPHERICAL COUPLING
AT BOTH ENDS
FOR GG-1 SYSTEM
4200 RPM
3.00 O.D. x .049 WALL
2024 AL ALY TUBE
W/SPHERICAL COUPLING
AT BOTH ENDS

183.0

B.

56.0

C SHAFT: SAME AS "A"

VIBRATION DAMPER
8150 RPM SYSTEM ONLY

C.

1654 RPM
OUTPUT
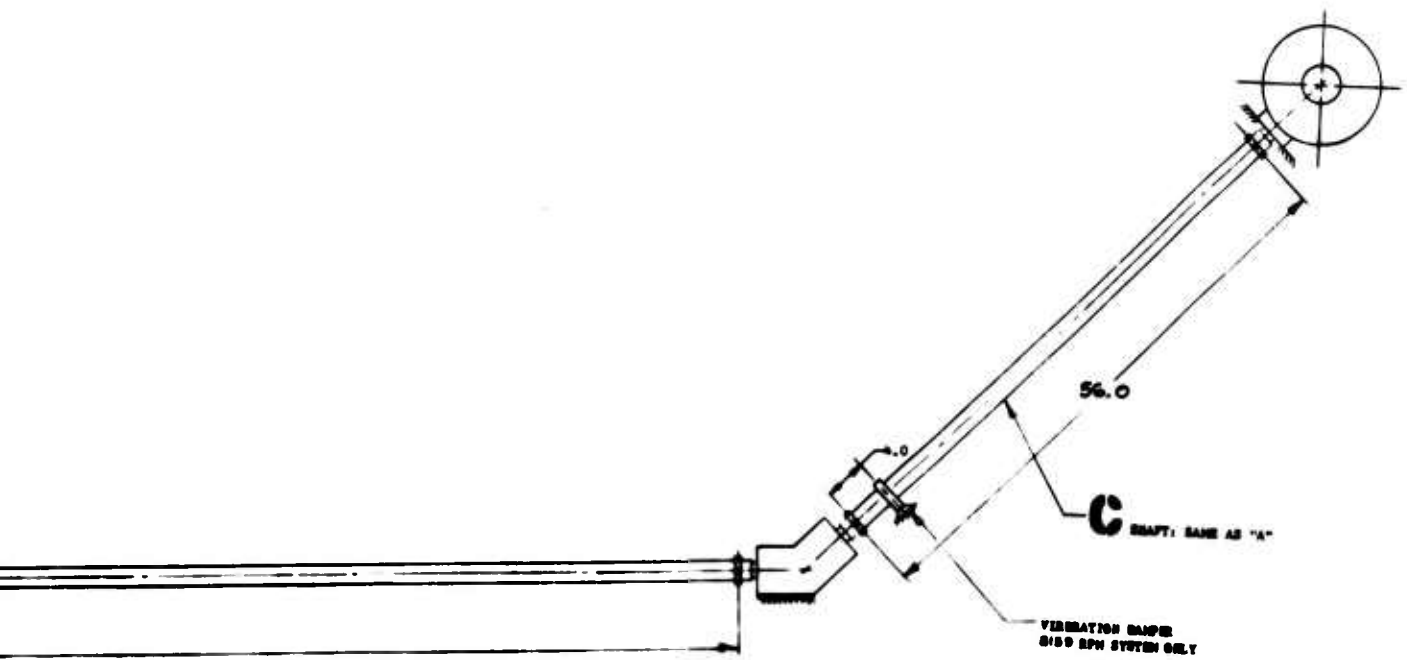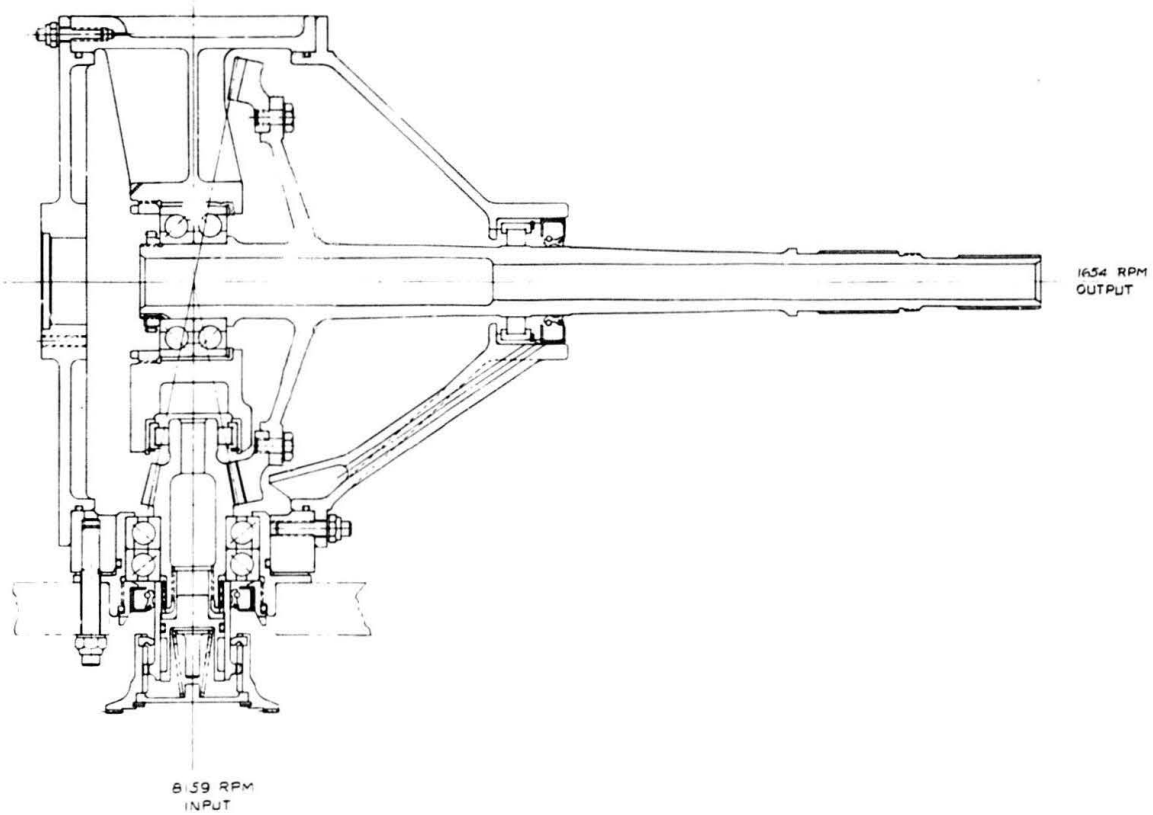
8159 RPM
INPUT

Figure 31.   90° Gearbox - Supercritical -
Antitorque Drive System

heavier due to the larger reduction for the SCTRS), makes the
8159 rpm configuration unattractive.

The second system consists of all standard UH-1 components ex-
cept for a long shaft (183 inches) replacing three standard
sections. The operating requirements are identical to the
present UH-1. Two bearing hanger assemblies would be elimi-
nated and one vibration damper would be required. The sections
between the 42° and 90° gearboxes would require no dampers
since they operate below the first critical speed. The ad-
vantage to this system would be the removal of the two hanger
assemblies and the replacement with one damper, wherein approxi-
mately 1.64 pounds of weight could be saved. The system is
otherwise the same as the standard UH-1.

However, in the single damper installation, the lack of redun-
dancy could well result in catastrophic failure of the drive
system. Since there is only one damper on the long super-
critical shaft, there is no margin of safety in the event of
damper failure. Although the shaft could be rotating at a
speed well removed from the critical rotational frequency, a
resonant condition with the vibrating tail boom could easily
be attained if the damper became ineffective. This would re-
sult in an immediate loss of the drive shaft, with possible
explosive results.

In the interest of flight safety and reliability, it would be
necessary to install either two dampers or a double bladder
version of the damper shown in Figure 32. The resultant weight
increase would be no less than 2 pounds.

Notwithstanding the weight differences between the subcritical
and supercritical systems, there exists a further problem of
logistics. The impact of utilizing the longer shafts (183
inches) and dampers would be felt through additional storage
requirements in military inventory, handling, transportation,
and special containers. Also, the damage limits would be more
stringent on the long shafts due to the critical nature of
stress concentrations or unbalance than on the shorter UH-1
shafts, and any scrappage due to handling damage would result
in a more costly replacement.

In conclusion, no advantage is indicated to support the adapta-
tion of a supercritical tail rotor drive shaft system to the
UH-1 helicopter. Projected weight differences are in favor of
the subcritical UH-1 drive assembly. Storage, handling, and
transportation of the longer shafts are unjustifiably greater
with the longer supercritical shafts.
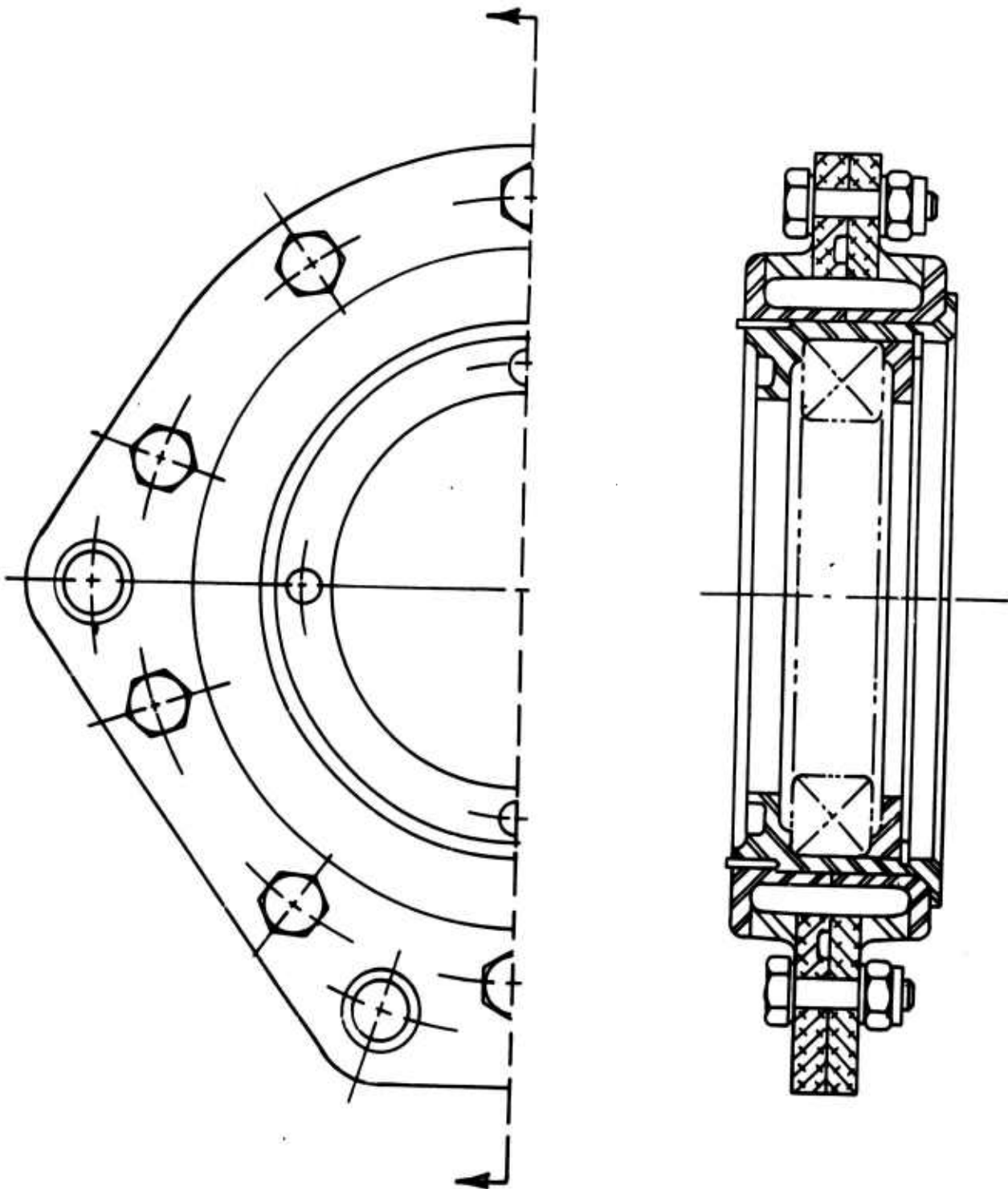
Figure 32. Vibration Damper J-13354.

130

WEIGHT COMPARISON

The estimated weights of the proposed RGT and TSPT are shown in the following comparison of the weights of the RGT, the TSPT, and the UH-1 total reduction systems.

	TOTAL REDUCTION SYSTEMS		
	UH-1	RGT	TSPT
Total Weight, Lb	681	598	547
Percentage of UH-1 Wt	100%	88%	80%
Weight Savings Relative to UH-1 Weight, Lb	-	83	134
Weight Savings Relative to RGT Weight, Lb	-	-	51

Figure 33 summarizes the weight comparison of the three systems in terms of their major components; Figure 34 identifies these components with their respective systems.

The 83-pound estimated weight savings of the RGT over the UH-1 total reduction system is primarily the result of removing the reduction components and torquemeter hardware from the engine nose box, additional engine rework, and utilizing a lightweight high-speed bevel gear set; whereas, the 51-pound estimated weight savings of the TSPT over the RGT is due solely to the weight differences of their final drives (and surrounding housings), since the remainder of the RGT and the TSPT systems are identical.

No fuselage structure is included in this analysis, as the advantage will lie alternately with various vehicle configurations which adapt themselves to each distinctive type of mounting system. The various factors that are analyzed in this weight comparison are individually discussed below.

SUPPORT CASE AND MAST ASSEMBLY

It is estimated that a support case and a mast assembly for both the RGT and the TSPT will weigh approximately the same as the 160-pound combined weight of the mounting component part of the UH-1 transmission support case and the UH-1 mast assembly. However, it should be noted that the combined weight of the support case and the mast assembly (shown in Figures 7 and 22 and schematized in Figure 34) for the RGT and the TSPT respectively, is 218 pounds. These large components were

UH-1
Total Wt = 681 LB

| Eng. Nose Box and Other Eng. Rework | 74 |

| Two-Stage Planetary Reduction Drive | 111 |

| Main Bevel Gear Drive | 124 |

| Generator and Quill | 52 |

| Drive Shaft | 18 |

| Offset Spur Box | 16 |

| Sump Assy | 46 |

| Lube System | 80 |

| Support Case and Mast Assy | 160 |

UH-1 Weight   (LB)

83 LB

RGT
Total Wt = 598 LB

| Roller Gear Reduction Drive | 191 |

| Main Bevel Gear Drive | 52 |

| Generator and Quill | 39 |

| Drive Shaft | 14 |

| Offset Spur Box | 16 |

| Sump Assy | 46 |

| Lube System | 80 |

| Support Case and Mast Assy | 160 |

RGT Weight   (LB)

134 LB

TSPT
Total Wt = 547 LB

| Three-Stage Planetary Reduction Drive | 140 |

| Main Bevel Gear Drive | 52 |

| Generator and Quill | 39 |

| Drive Shaft | 14 |

| Offset Spur Box | 16 |

| Sump Assy | 46 |

| Lube System | 80 |

| Support Case and Mast Assy | 160 |

TSPT Weight   (LB)

Figure 33. Weight Comparison of the Total Reduction Systems.

132
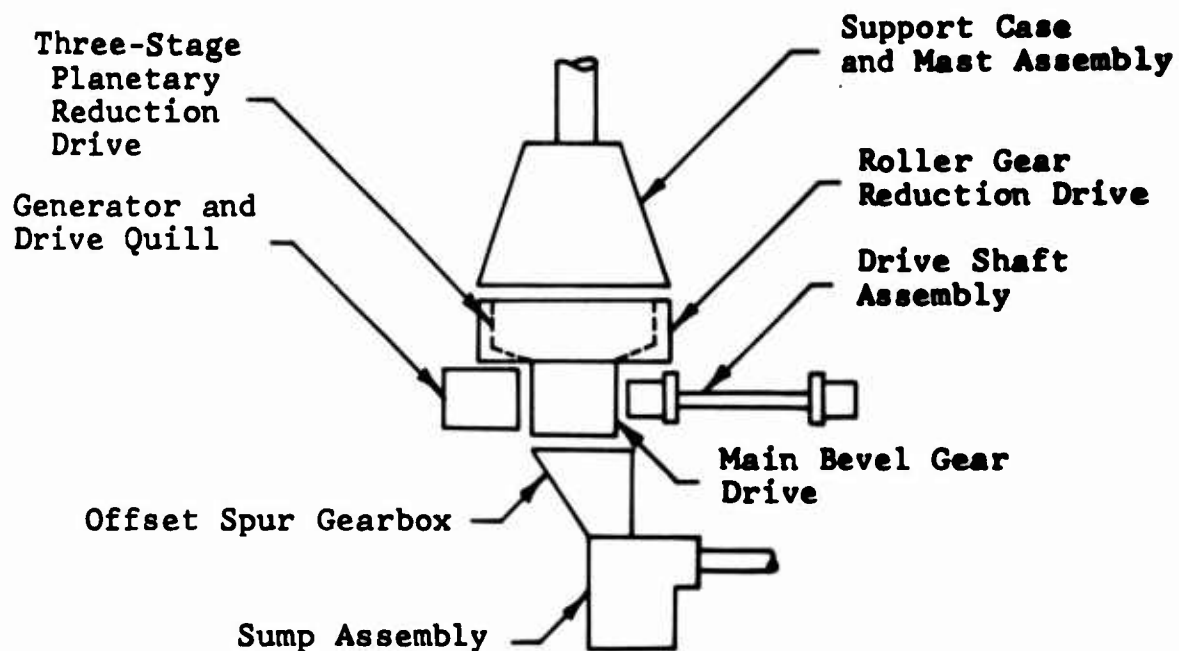
RGT AND TSPT SYSTEMS
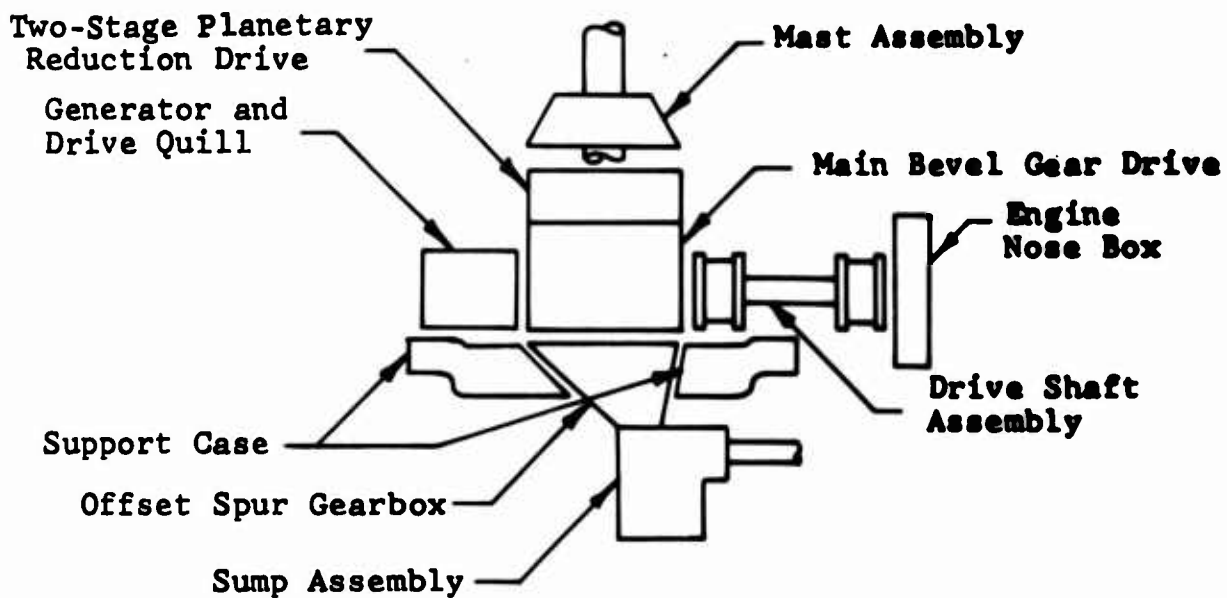
UH-1 SYSTEM

Figure 34. Schematic of RGT, TSPT, and UH-1
Systems for Weight Analysis.

originally designed for a heavier helicopter utilizing 1800 hp (versus the 1250 hp in this study). They are adapted to the proposed RGT and TSPT because they are existent components, and because the stubbed mast does not protrude downward into the reduction hardware area. The design of a new support case and a new stubbed mast specifically for the 1250-hp capacity RGT and TSPT was not accomplished for the same reason given in the preceding paragraph for not including any fuselage structure design in this report. However, it is assumed that a new 1250-hp capacity support case and stubbed mast would be similar to the existent components shown except reduced in size to a combined weight of 160 pounds.

SUMP ASSEMBLY

The UH-1 transmission, the RGT, and the TSPT utilize the same sump assembly, which weighs 46 pounds (dry). The sump assembly consists of an input bevel gear quill, a tail rotor output bevel gear quill, a combination hydraulic and tachometer bevel gear quill, an oil pump, a wire-screen element oil filter, and a 2.5-gallon capacity lubricant sump.

A brief design study was accomplished concerning a new tail rotor and accessory drive system in which the tail rotor and all the accessories (a generator, a tachometer, and two hydraulic pumps) would be driven by a spur gear train extending downward from the engine-to-transmission input bevel gear quill. The lubricant sump and the oil pump would be incorporated in the lower portion of the main bevel gear housing. This brief study indicated that the spur gear train system would probably have a slight advantage over the proposed sump assembly and the offset spur gearbox (discussed in the next section) in the areas of weight, efficiency, reliability, and cost; however, the particular system utilized would depend primarily upon which system would fit better in the vehicle for which the total reduction system is designed. For example, if the transmission designer designed a spur gear train system 5 pounds lighter than the proposed system, and if the airframe designer had to use an additional 10 pounds of structure to accommodate the spur gear train system, then the 5-pound weight saving would revert to a 5-pound weight increase.

OFFSET SPUR GEARBOX

The offset spur gearbox which is schematized in Figure 34 for the RGT and the TSPT (shown in Figure 7 for the RGT and Figure 22 for the TSPT) is estimated to weigh 16 pounds. That portion of the UH-1 transmission support case required to house the sump system drive spur gears is included with the weight of the spur gears and the associated hardware in the 16-pound

total. Thus, there is estimated to be no weight differential between the offset spur gearbox on both the RGT and the TSPT and the weight allocated to the offset spur gearbox on both the RGT and the TSPT and the weight allocated to the offset spur gearbox on the UH-1 transmission.

LUBE SYSTEM

For the purposes of the weight comparison section of this report, the lube system is defined to include oil coolers, filters (except the wire-screen element oil filter in the transmission sump assembly), jets, oil lines, pressure regulators, bypass valves, etc., i.e., everything pertaining to a lubrication system except the oil pumps, the lubricant, and the method by which the heat is transferred from the oil coolers. The latter is discussed later in the Engine Nose Box and Other Engine Rework discussion.

The estimated weight of the lube system for the UH-1 total reduction system and the engine is 80 pounds, 25 pounds of which is attributed to the UH-1 transmission, and 55 pounds of which is attributed to the engine and the engine nose box.

The estimated weight of the lube system for the engine with the RGT or the TSPT is also 80 pounds, 29 pounds of which is attributed to the RGT or the TSPT, and 51 pounds of which is attributed to the engine. The 4-pound reduction in the engine oil cooler was offset by a required 4-pound increase in the size of the transmission oil cooler. A detailed analysis of this condition may be found in the Lubrication System Analysis for this report. It should be mentioned here that an additional weight reduction of the engine oil cooler will be discussed later in the Engine Nose Box and Other Engine Rework section and dealt with numerically in that section rather than this section.

DRIVE SHAFT

The net reduction of 4 pounds (from 18 pounds to 14 pounds) for the drive shaft assembly (due primarily to decreased transmitted torque) on the RGT and the TSPT as compared to the drive shaft assembly on the UH-1 system was limited by the increase in shaft length necessitated by the reduction in size of the bevel gear drive assembly. Engine induction filter system restrictions prevent moving the engine further forward.

GENERATOR AND GENERATOR DRIVE QUILL

The 12,000-rpm 300-amp generator used on the RGT and the TSPT weighs 11 pounds less than the 6600-rpm 300-amp generator used

135

on the UH-1 transmission. The 12,000-rpm drive quill weighs 2 pounds less than the 6600-rpm quill. Thus, the total weight savings attributed to the high-speed generator on the RGT and the TSPT is 13 pounds.

MAIN BEVEL GEAR DRIVE

Table XIV gives a partial weight component breakdown for the main bevel gear drives on the RGT, the TSPT, and the UH-1 system. The 72-pound weight saving attributed to the high-speed bevel gear set points out the significance of "turning the corner" with a high-speed low-torque bevel gear drive such as that designed for the RGT and the TSPT rather than the relatively low-speed high-torque bevel gear drive used in the UH-1 transmission.

FINAL REDUCTION DRIVE

The final reduction drive on the RGT is the 42.857-ratio roller gear reduction drive. It weighs 191.24 pounds. Table XV contains a complete breakdown of the weight analysis.

The final reduction drive on the TSPT is the 42.903-ratio three-stage planetary reduction drive. It weighs 140.69 pounds. Table XVI contains a complete breakdown of the weight analysis of the first stage (high-speed stage) and Table XVII contains a partial breakdown of the weight analysis of the existing second and third stages.

The final reduction drive on the UH-1 transmission is the 9.534-ratio two-stage planetary reduction drive; it weighs 110.74 pounds. Table XVII contains a partial breakdown of its weight analysis.

The 50.55-pound weight advantage of the three-stage planetary drive in the TSPT over the roller gear drive in the RGT is due primarily to the different enveloping diameters of the two drives, since the axial space requirements are approximately the same.

ENGINE NOSE BOX AND OTHER ENGINE REWORK

The estimated total weight reduction, in the area of the engine nose box and due to additional engine rework, from the UH-1 system to the system using the RGT or the TSPT is approximately 74.2 pounds. The component breakdown is shown in the tabulation on page 141, with the discussion following.

136

TABLE XIV. WEIGHT ANALYSIS OF THE MAIN BEVEL GEAR DRIVES

	RGT	TSPT	UH-1
Input Pinion Quill, Lb	26.0	26.0	41.5
Output Gear Quill, Lb	17.0	17.0	49.5
Housing, Lb*	9.42	9.42	33.0
Total Weight, Lb	52.42	52.42	124.0

* The housing on the RGT and the TSPT is that area between the gear shaft quill attachment point and the offset spur gear housing attachment point.

* The housing weight for the UH-1 of 33.0 lb is the actual weight of the 204-040-353 main case assembly with the two roller bearings installed.

Name	Unit Wt (Lb)	Quantity	Total Wt (Lb)
TABLE XV. WEIGHT ANALYSIS OF THE ROLLER GEAR REDUCTION DRIVE			
Sun Pinion	1.98	1	1.98
First-Row Cluster	3.80	6	22.80
Second-Row Cluster	6.98	6	41.88
Ring Gear	12.40	2	24.80
Spider Base Plate	16.58	1	16.58
Spider Upper Plate	10.73	1	10.73
Input Adaptor	1.04	1	1.04
Output Adaptor	24.10	1	24.10
Spider Spherical Brg.	.27	6	1.62
Cylindrical Roller Brg.	1.56	6	9.36
Support Bearing	.63	1	.63
Support Bearing Sleeve	.60	1	.60
Oil Manifold	.66	1	.66
Housing	-	*	34.46

Roller Gear Reduction Drive Total Weight = 191.24 Lb

* The housing includes that area between the top support case attachment point and the junction of the flat plate section with the cylindrical section of the bevel gear housing, and a plate for adapting the large diameter housing to a smaller top case designed for 1250 hp.

138

TABLE XVI. WEIGHT ANALYSIS OF THE HIGH-SPEED PLANETARY STAGE

Name	Unit Wt (Lb)	Quantity	Total Wt (Lb)
Spider	3.56	1	3.56
Carrier Plate	.97	2	1.94
Bearing Pins, Bolts, and Nuts	-	3 ea.	3.03
Inner Race and Washers	-	3 sets	2.12
Roller	-	48	.88
Planet Idler	1.73	3	5.19
Sun Gear	1.63	1	1.63
Ring Gear	4.45	1	4.45
Roller Cage	.13	3	.39
Spherical Bearing	.13	3	.39
Spherical Bearing Spacer	.04	6	.24
Carrier Bolts and Nuts	-	3 ea.	.42
Support Bearing	.45	1	.45
Support Sleeve	.26	1	.26
Housing	-	*	5.00

High-Speed Planetary Stage Total Weight = 29.95 Lb

* The housing includes only that area between the retaining ring which retains the ring gear and the junction of the conical section with the cylindrical section of the bevel gear housing.

TABLE XVII. WEIGHT ANALYSIS OF THE TWO-STAGE PLANETARY DRIVE

Name	Unit Wt (Lb)	Quantity	Total Wt (Lb)
Upper Planetary Assy	40.0	1	40.0
Lower Planetary Assy	26.5	1	26.5
Upper Sun Gear	4.1	1	4.1
Lower Sun Gear	4.0	1	4.0
Output Adaptor	5.0	1	5.0
Support Liners and Oil Deflector	-	4	1.5
Dual Ring Gear	24.0	1	24.0
Support Bearing	1.0	2	2.0
Housing	-	*	3.64

Two-Stage Planetary Total Weight = 110.74 Lb

* The housing includes that area between the lower flange of the dual ring gear case and the retaining ring which retains the high-speed stage ring gear plus the hardware required for the lower flange attachment to the housing.

140

SOURCE	WEIGHT REDUCTION (LB)
Engine nose box hardware	54.0
Engine nose box heat absorption by the engine, in terms of fuel saved	2.5
Bleed air hardware	3.8
Engine oil cooler	4.7
Bleed air elimination, in terms of fuel saved	9.2
TOTAL	74.2

This 74.2-pound weight reduction does not include the estimated 108-pound increase in the effective hot-day hover capabilities of the UH-1 helicopter as the result of removing the engine nose box and reworking other areas of the engine. This aspect of the weight reduction is discussed at the end of this section.

The net weight reduction, in the area of the engine nose box, is approximately 54 pounds. This removes from the UH-1 system an estimated 5 pounds of engine nose box casting, 51 pounds of gear reduction and torquemeter hardware, and adds 2 pounds for installation of an electronic torquemeter device. (The information on the latter two items was furnished by Lycoming Division of AVCO.) Figure 35 shows the engine nose box in the UH-1 system and a general redesign of it for the RGT and the TSPT systems.

The removal of the engine reduction drive gears and bearings afforded an additional effective 2.5-pound weight saving through the elimination of heat transfer from the nose box into the engine's air induction system. In the Gearbox Efficiency discussion later in this report, it is shown that the convective heat drawn into the engine's air induction system from the nose box was equivalent to 3.45 hp. This injested heat by the engine air flow results in a 0.93°F increase in compressor inlet temperature. This in turn results in a 0.16-percent increase in specific fuel consumption, and when considering a helicopter mission consuming 1600 pounds of fuel, this necessitates an increase of 2.5 pounds in the fuel load for the same range of mission.

Thus the total weight decrease of the engine attributed only to removing the engine reduction drive is 56.5 pounds.

141
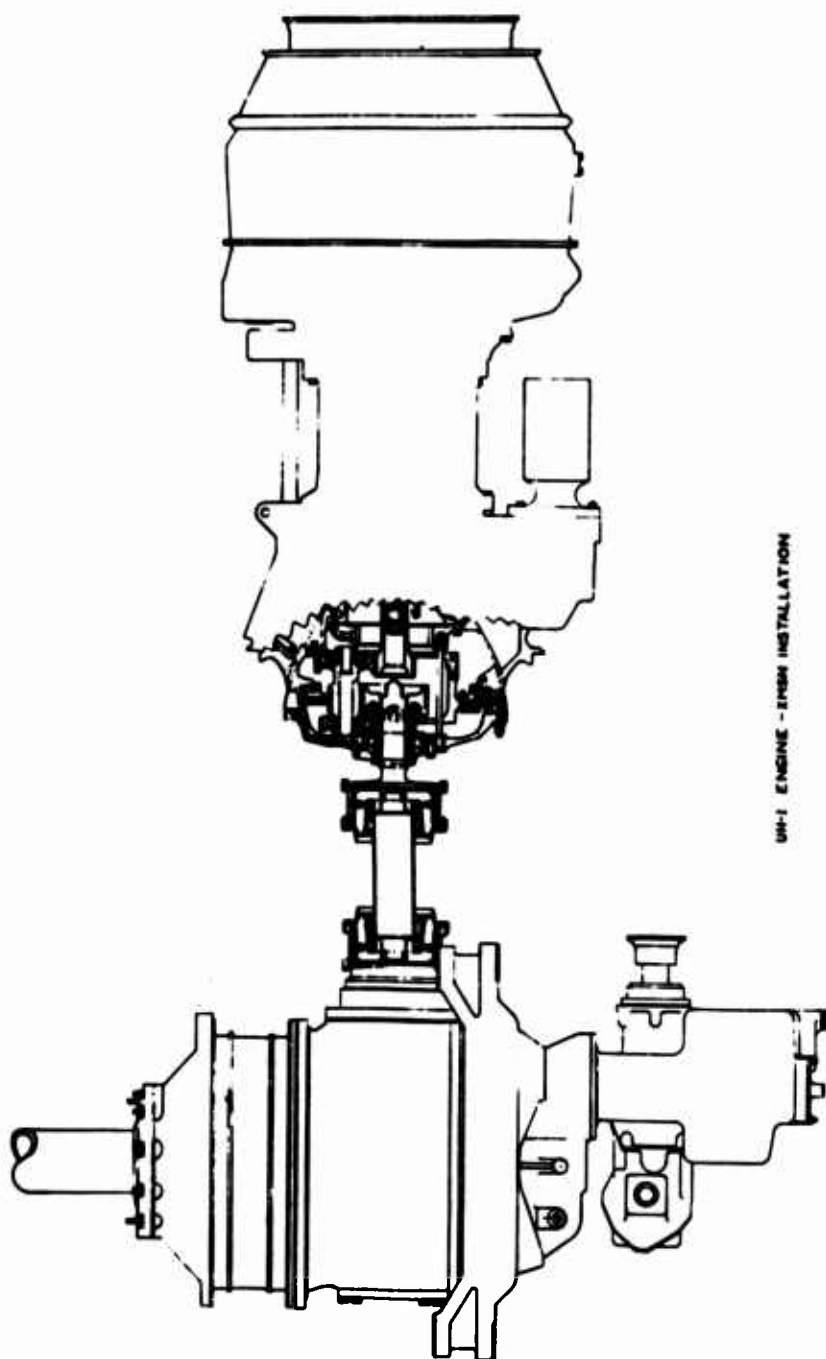
UH-1 ENGINE - EPRM INSTALLATION

Figure 35. Engine and Transmission Installation

143

A.

UH-1 ENGINE - XMSN INSTALLATION
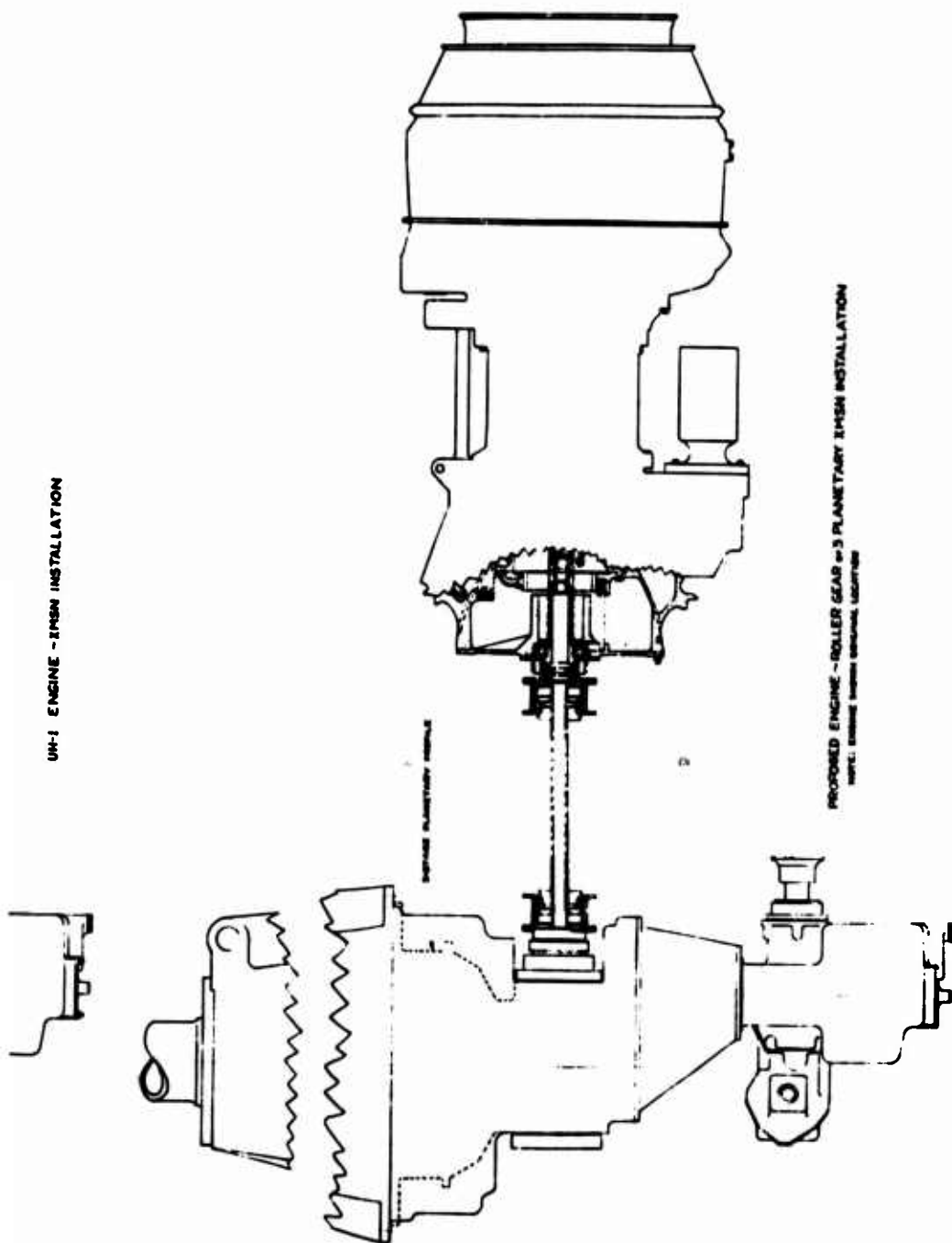
PROPOSED ENGINE - ROLLER GEAR or 5 PLANETARY XMSN INSTALLATION

NOTE: ENGINE SHOWN IN ORIGINAL LOCATION

5 STAGE PLANETARY XMSN

.ation

B.

The weight study was expanded at this point to search for additional weight-saving areas relative to the UH-1 power plant and reduction system, and the following data are reported.

On the current UH-1 system, the transmission oil cooler and the engine oil cooler are placed side by side, with both coolers utilizing a common blower source. This blower is powered by a small turbine wheel using engine compressor bleed air for its motive force. Since the weight of the engine oil cooler was reduced 4 pounds by virtue of removing the engine nose box reduction drive (see Lube System of this section), it is proposed that the smaller oil cooler be replaced by a fuel-oil liquid heat exchanger for an additional weight reduction of an estimated 4.7 pounds.

This leaves only the transmission oil cooler to be cooled by the compressor bleed air. Thus, it is proposed that a squirrel-cage fan, mounted concentrically with and driven by the tail rotor shafting, be used as a blower for cooling the transmission oil cooler, thereby eliminating the necessity for the bleed air hardware. The resulting net weight reduction is estimated to be 3.8 pounds.

Since the cooling requirement for the compressor bleed air has been eliminated, the fuel expended for that purpose is no longer required. This amount of fuel, less the amount calculated to power the squirrel-cage fan, is estimated to be 0.575 percent of the specific fuel consumption. Thus, when considering a helicopter mission consuming 1600 pounds of fuel, the 9.2 pounds of fuel that would not be used for the same range of mission represents a 9.2-pound weight saving.

Though not a specific task of this study, it is interesting to note that there is a 108-pound gain in the effective hot-day hover capabilities of the UH-1 helicopter as the result of removing the engine nose box from the engine air inlet area and eliminating the compressor bleed air requirements for cooling the oil coolers.

As discussed earlier in this section, the convective heat (equivalent to 3.45 hp) drawn into the engine's air induction system from the nose box results in a 0.93°F increase in compressor air inlet temperature. Assuming the ratio of 6 for the lifting and hovering capabilities of the UH-1 helicopter for each horsepower available (lb/hp = 6), then during the hot-day hover operation where the horsepower available from the engine is turbine-inlet temperature limited, the 0.93°F increase in temperature reduces the available sea-level horsepower by 4.95 hp (based on a nominal 1100 hp available).

145

Multiplying the 4.95 hp by 6 gives a 29.7-pound reduction in the takeoff gross weight capabilities of the helicopter.

It is estimated that the compressor bleed air used to cool the oil coolers, less the power required to drive the squirrel-cage fan, represents 13.10 engine hp. Multiplying this 13.10 hp by 6, gives a 78.6-pound increase in the takeoff gross weight during a hot-day hover operation.

Thus, by removing the engine nose box and eliminating the bleed air requirements, the takeoff gross weight during a hot-day operation may be increased by a total of 108.3 pounds without increasing the compressor red-line temperature limit.

RELIABILITY ANALYSIS

This analysis has been prepared to determine the relative re-
liabilities of the existent UH-1, the proposed RGT, and the
proposed TSPT main drive systems. The scope of these indi-
vidual analyses is limited to the main rotor reduction drive,
which includes the T-53 integral speed decreaser gearbox (SDG)
in the UH-1 system.

A reliability analysis is only an estimation, hopefully de-
termined by use of the best information and tools available,
of the probability of successful operation of the system for
a specified period of time and use environment. The RGT
analysis assumes that the system design is initially capable
of successful operation. In this study, the best tools avail-
able are considered to include the proper mathematical summa-
tion of individual component lives with respect to their
characteristic failure modes and dispersion, as supported by
extensive test experience. For component lives which appear
incalculable or calculable but insufficiently correlated with
test experience for adequate confidence, the use of adjusted
failure rates extracted from the best information available,
i.e., overhaul experience on service units, was adopted. It
is believed that this approach yields the most accurate com-
parison possible at this time.

The predicted reliability values presented in USAAVLABS Tech-
nical Report 64-29 (Reference 1), appear to be inadequate and
misleading when tested against observations of mechanical
transmission test and service experience. The failure rates
advanced in the referenced study are identical to the mean
generic failure rates for electronic servo-mechanism bearing
and gear experience as tabulated in Reference 12. These
failure rates were advanced without multiplication factors or
adjustments for such considerations as load, speed, aircraft
environment, size, or type. No distinction was made between
ball and roller bearings or type gear (spiral bevel, straight
spur, helical, etc.) involved, or the several possible lubri-
cation environmental effects present. These mean generic
failure rates simply imply the bearing failure frequency to
be five times greater than that of a gear. The obvious con-
clusion for comparative study purposes is that the replacement
of one bearing by five gears is an equitable trade. As will
be subsequently shown, such assumptions cannot be supported
by experience in mechanical power transmission systems.

While the use of adjusted failure rates from UH-1 overhaul
experience may at first glance seem arbitrarily parochial,
such is not the case. In a recently published study

(Reference 13), conducted on helicopters in the U. S. Navy inventory supplied by four different manufacturers (including BHC), the characteristic problem areas were shown to be universal.

The calculation of gear pitting endurance lives used in this analysis is based upon information contained in a paper presented to the American Gear Manufacturers Association (Reference 14) in 1967. This information on characteristic gear life data was extracted from the analysis of over 200 spur gear failures in extended planetary testing at BHC and is summarized in Figure 36, page 149. The calculation of bearing lives is in accord with accepted AFBMA practices, the statistical methods of Weibull (Reference 15), Palmgren and Lundberg (References 16 and 17), as modified and correlated with the results of extensive test work at BHC. The determination of failure rates for all other components was based exclusively upon data extracted from the statistical history of helicopter components obtained through the UH-1 Maintainability and Reliability (M & R) Program (Reference 18) and the BHC dynamic component overhaul activity records. In general, the overhaul parts replacement statistics cannot be directly used to generate meaningful information with respect to the gears and bearings in the planetary drive system, because of the very large incidence of secondary debris damage emanating from a first or characteristic failure. This is commonly the case; a simple characteristic failure rate may easily generate a tenfold overhaul part replacement rate.

To facilitate a meaningful analysis, the drive train is divided into five stages or groupings. Either the failure rates for each component in that stage are summed directly, or the 90-percent survival life of the cumulative bearing subsystem (95 percent for gears) is established, converted into a failure rate, and summed. The failure rates for the five groupings are then combined and reduced to an effective reliability for equal time intervals. See page 152.

In this study, the term failure, as used in establishing failure rates, is defined as the inability of the equipment to satisfy performance or design specifications (once the equipment has experienced successful operation) without adjustment, unscheduled maintenance, or replacement at overhaul. The final failure rates given represent an effective index of comparison for the most probable reliabilities of three systems in service operation, after comparable initial development periods wherein the customary de-bugging is accomplished.

All three drive systems are studied at 1250 horsepower. It should be realized that the RGT and the high-speed stage of

148

CASE CARBURIZED VACUUM MELT
AMS 6260 GEARS OPERATING IN
MIL-L-7808E. FINISH GROUND CLA-17
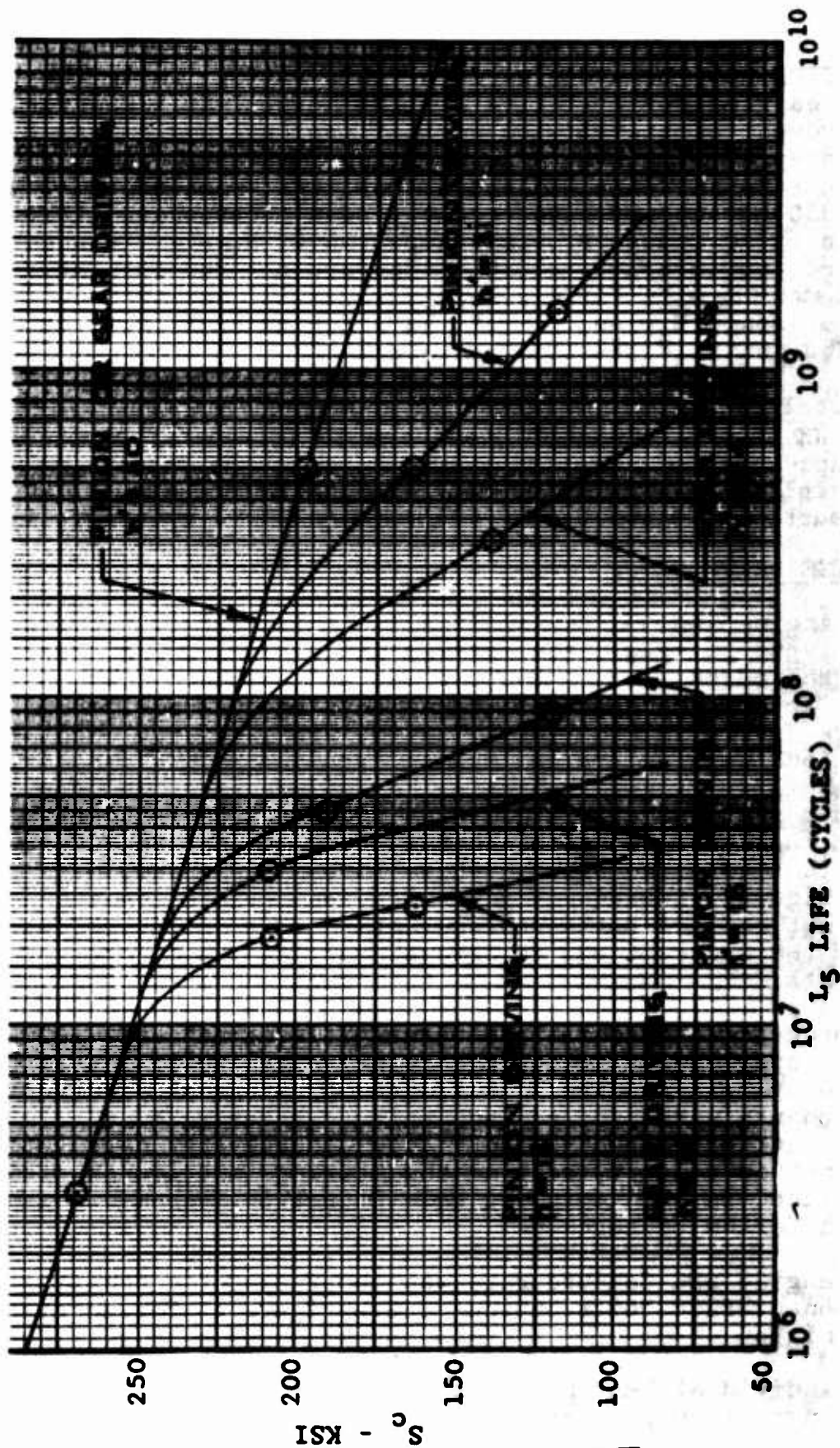
Figure 36. Gear Pitting Endurance.

149

the TSPT have been designed for this rating, while the UH-1 was designed for operation at 1100 horsepower. However, since the advent of the T53-L13 engine, the UH-1 system has been operated at a 1250-horsepower rating. Significant engineering changes to increase the actual reliability of the UH-1 system at 1250 horsepower have recently been incorporated through Engineering Change Proposal acceptance; however, since their respective forecast reliabilities are not representative of equipment now in field service, they will not be used in this comparison. Explanation of the affected areas will be included in the discussion, however.

The relative failure rates are enumerated in Tables XVIII, XIX, and XX for the UH-1, RGT, and the TSPT respectively. Table XXI presents a comparative summation of the total system rates. The following discussion concerns the method of determination of each.

ENGINE DRIVE GROUP

The engine SDG unit was initially considered in three sections: the input sun gear, the carrier and layshaft gear assemblies, and the output seal. The carrier and layshaft gear assemblies were not broken down into components because of lack of complete detail information. The failure rates for the first two sections were determined from a Lycoming Maintainability and Reliability Program report. The failure rate used for the SDG output seal was determined from the Model UH-1 M & R Program data; however, the combined failure rates for the first two sections totalled only .0362 failures/1000 hours, a remarkably low figure. Subsequent investigation revealed that these rates did not reflect parts replacements during premature overhaul when the cause of engine removal was failure of other components.

In order to secure failure rates yielding a better comparison for proper evaluation of the relative reliabilities of the three systems studied, detail gear drawings of the Lycoming components were procured and failure rates were calculated by the identical methods used in the other system calculations. The method used in treating the bearings and gear systems is explained in detail in the Main Reduction System discussions which follow on page 161.

The engine SDG failure rate was comprised of seven distinct component rate contributions. See Figure 37 for schematic definition.

The individual bearing lives for the torque loaded layshaft bearings at 60 percent full power are estimated in Appendix
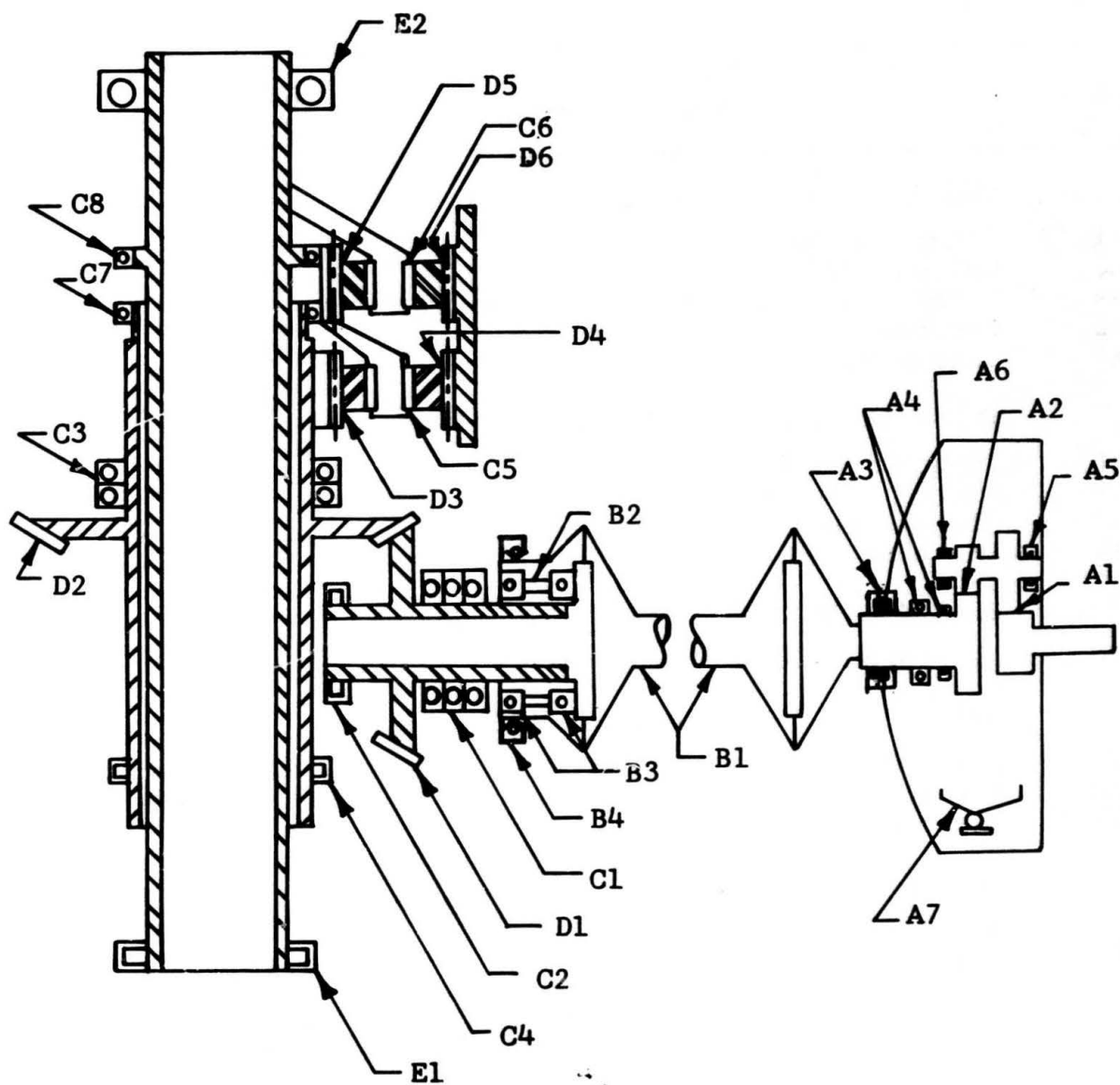
Figure 37. Components Schematic - UH-1 System.

151

Part	Nomenclature	Est. Part Due to All Failures
	TABLE XVIII. 1250 HP UH-1 MAIN DRIVE TRAIN FAILURE RATES (λ) (λ = Failures/1000 Hours)	
	ENGINE SPEED DECREASER GEARBOX	
A1,A2	Reduction Gears	.2131
A3	Output Seal	.0460
A4	Output Shaft and Support Bearings	.0100
A5,A6	Layshaft Roller Bearings	.1804
A7	Torque Meter	.0110
	INPUT SHAFT AND FREEWHEELING ASSEMBLY	
B1	Input Drive Shaft	.5780
B2	Clutch - One Way	.0260
B3	Clutch Bearing (2 each)	.0692(Total)
B4	Input Seal	.9090
	BEARINGS IN MAIN POWER TRAIN ASSEMBLY	
C1-C8	All Torque-Loaded Bearings	.5861
	GEARS IN MAIN POWER TRAIN ASSEMBLY	
D1	Bevel Pinion	.0198
D2	Bevel Gear	.0168
D3-D6	Planetary Gears	1.5384
	MAST BEARINGS	
E1	Mast Roller Bearing	.0112
E2	Mast Ball Thrust Bearing	.1950

TABLE XIX. 1250 HP RGT DRIVE TRAIN PART FAILURE RATES (λ)		
(λ = Failures/1000 Hours)		

Part	Nomenclature	Est. Part Due to All Failures
	ENGINE OUTPUT	
F1	Output Ball Bearing	.0075
F2	Engine Output Shaft	.0025
F3	Output Seal	.0230
F4	Electric Torque Meter	.0110
	INPUT SHAFT AND FREEWHEELING ASSEMBLY	
G1	Input Drive Shaft	.5780
G2	Clutch	.0300
G3	Clutch Bearing (2 each)	.1038 (Total)
G4	Input Seal	.9090
	BEARINGS IN RGT ASSEMBLY	
H1-H9	All Torque-Loaded Bearings	.3895
	GEARS IN RGT ASSEMBLY	
I1	Bevel Pinion	.0198
I2	Bevel Gear	.0168
I3-I5	Roller Gears	1.2679
	MAST BEARINGS	
E1	Mast Roller Bearing	.0112
E2	Mast Ball Thrust Bearing	.1950

TABLE XX.	1250 HP TSPT DRIVE TRAIN PART FAILURE RATES (λ)
	(λ = Failure/1000 Hours)

Part	Nomenclature	Est. Part Due to All Failures
	ENGINE OUTPUT	
F1	Output Ball Bearing	.0075
F2	Engine Output Shaft	.0025
F3	Output Seal	.0230
F4	Electric Torque Meter	.0110
	INPUT SHAFT AND FREEWHEELING ASSEMBLY	
G1	Input Drive Shaft	.5780
G2	Clutch - One Way	.0300
C3	Clutch Bearing (2 each)	.1038 (Total)
G4	Input Seal	.9090
	BEARINGS IN TSPT ASSEMBLY	
J1,J2, H1-H4, C5-C8	All Torque-Loaded Bearings	.4124
	GEARS IN TSPT ASSEMBLY	
I1	Bevel Pinion	.0198
I2	Bevel Gear	.0168
K1,K2, D3-D6	All Torque Loaded Gears	1.5386
	MAST BEARINGS	
E1	Mast Roller Bearing	.0112
E2	Mast Ball Thrust Bearing	.1950

154

TABLE XXI. MAIN POWER TRAIN FAILURE RATE (λ) COMPARISON
(λ IN FAILURES/1000 HOURS)

UH-1	RGT	TSPT
A. ENGINE SPEED REDUCER GEARBOX $\lambda = .4605$	F. ENGINE OUTPUT $\lambda = .0440$	F. ENGINE OUTPUT $\lambda = .0440$
B. INPUT SHAFT AND FREEWHEELING ASSEMBLY $\lambda = 1.5822$	G. INPUT DRIVE SHAFT AND FREE-WHEELING ASSY $\lambda = 1.6208$	G. INPUT DRIVE SHAFT AND FREE-WHEELING ASSY $\lambda = 1.6208$
C. TORQUE LOADED BEARINGS $\lambda = .5861$	H. TORQUE LOADED BEARINGS $\lambda = .3895$	C. TORQUE LOADED H. BEARINGS J. $\lambda = .4124$
D. POWER LOADED GEARS $\lambda = 1.5750$	I. POWER LOADED GEARS $\lambda = 1.3045$	I. POWER LOADED K. GEARS $\lambda = 1.5752$
E. MAST BEARINGS $\lambda = .2062$	E. MAST BEARINGS $\lambda = .2062$	E. MAST BEARINGS $\lambda = .2062$
TOTAL UH-1 MAIN DRIVE TRAIN $\lambda = 4.4100$	TOTAL RGT MAIN DRIVE TRAIN $\lambda = 3.5650$	TOTAL TSPT MAIN DRIVE TRAIN $\lambda = 3.8586$

VIII as 7922 hours for (A5) and 4660 hours for (A6) using the applicable dispersion exponent of 4 (see page 161), and recalling that there are three each of (A5) and (A6) bearings, the cumulative life is:

$$L_{10_A} = \frac{1}{\left[3\left(\frac{1}{7922}\right)^{4.0} + 3\left(\frac{1}{4660}\right)^{4.0}\right]^{\frac{1}{4.0}}} = 3442.13 \text{ hours}$$

Correcting for the mean or 50 percentile life for a dispersion exponent of 4, we have

$$L_{50_A} = 1.61 \ L_{10_A} = 5541.83 \text{ hours}$$

The failure rate, λ, may then be effectively expressed as

$$\lambda = \frac{1000}{L_{50_A}} = .1804 \text{ (A5, A6)}$$

The individual gear mesh (A1 and A2) lives for the characteristic pinion driver pitting failure mode may be found from Figure 36, as a function of the Hertz stress and EHD lubricant film thicknesses given in Appendix VIII. These lives are functionally reduced in the following tabulation:

Gear Mesh	$h'(10^{-6} \text{ in.})^*$	Sc KPSI**	L_5(cycles)	CYC/Hr x 10^{-6}	L_5(Hrs)
A1	40	90	2×10^{10}	3.78	5300
A2	30	100	2.8×10^{9}	.78	3600

* $h' = 1.29h$ Where h = Film thickness number at full power @ LPSTC and 1.29 = correction factor for 70 percent power $(.7W_t)$

$$h \propto \left(\frac{1}{W_t}\right)^{0.7}$$

**$Sc' = .83C$, Where Sc = Hertz Stress (LPSTC) at full power from Appendix VIII. .83 = correction factor for 70 percent power $(.7W_t)$

$$Sc \propto (W_t)^{0.5}$$

Using the applicable dispersion exponent of 5.5, and noting that there exists 1 (A1) mesh and 3 (A2) meshes, the cumulative life is

$$L_5 = \frac{1}{\left[\left(\frac{1}{5300}\right)^{5.5} + 3\left(\frac{1}{3600}\right)^{5.5}\right]^{\frac{1}{5.5}}} = \underline{2927.35} \text{ hours}$$

Correcting for the mean or 50 percentile life for a dispersion exponent of 5.5: $L_{50_A} = 1.603 L_{5_A} = \underline{4692.54}$ hours

The failure rate, λ (failure/1000 hours), is then given as

$$\lambda = \frac{1000}{L_{50_A}} = .2131 \text{ (A1, A2)}$$

The extremely lightly loaded bearings and splined output shaft (A4) are assigned a combined failure rate of $\lambda = .0100$.

The mechanical torquemeter (A7) is assigned a failure rate $\lambda = .011$ as determined from the UH-1 M & R program data.

The output seal (A3) is assigned a failure rate of .0460 as determined from the UH-1 M & R program data.

In the case of the RGT and TSPT engines (see schematics in Figures 38 and 39), the SDG is assumed to be replaced with an output ball bearing (F1), a splined output shaft (F2), and an output shaft seal (F3).

The failure rate assigned to (F3) is arbitrarily chosen as one-half of (A3). Even though the shaft seal rubbing velocity will be approximately three times greater, it is considered that the reduction in oiling rate from 5 gpm in the SDG to an estimated 1/2 gpm for the bearing (F1) and the increase in available seal envelope space will enable the design of a significantly more reliable seal.

The extremely lightly loaded bearing (F1) and splined output shot (F2) are assigned the same total failure rate as (A4) above.

The electronic torquemeter (F4) is assumed to consist of an adaptation of the Lycoming magneto-st.iction torque sensing system used in the T-55-L11 engine. It is assigned the same failure rate as (A7).
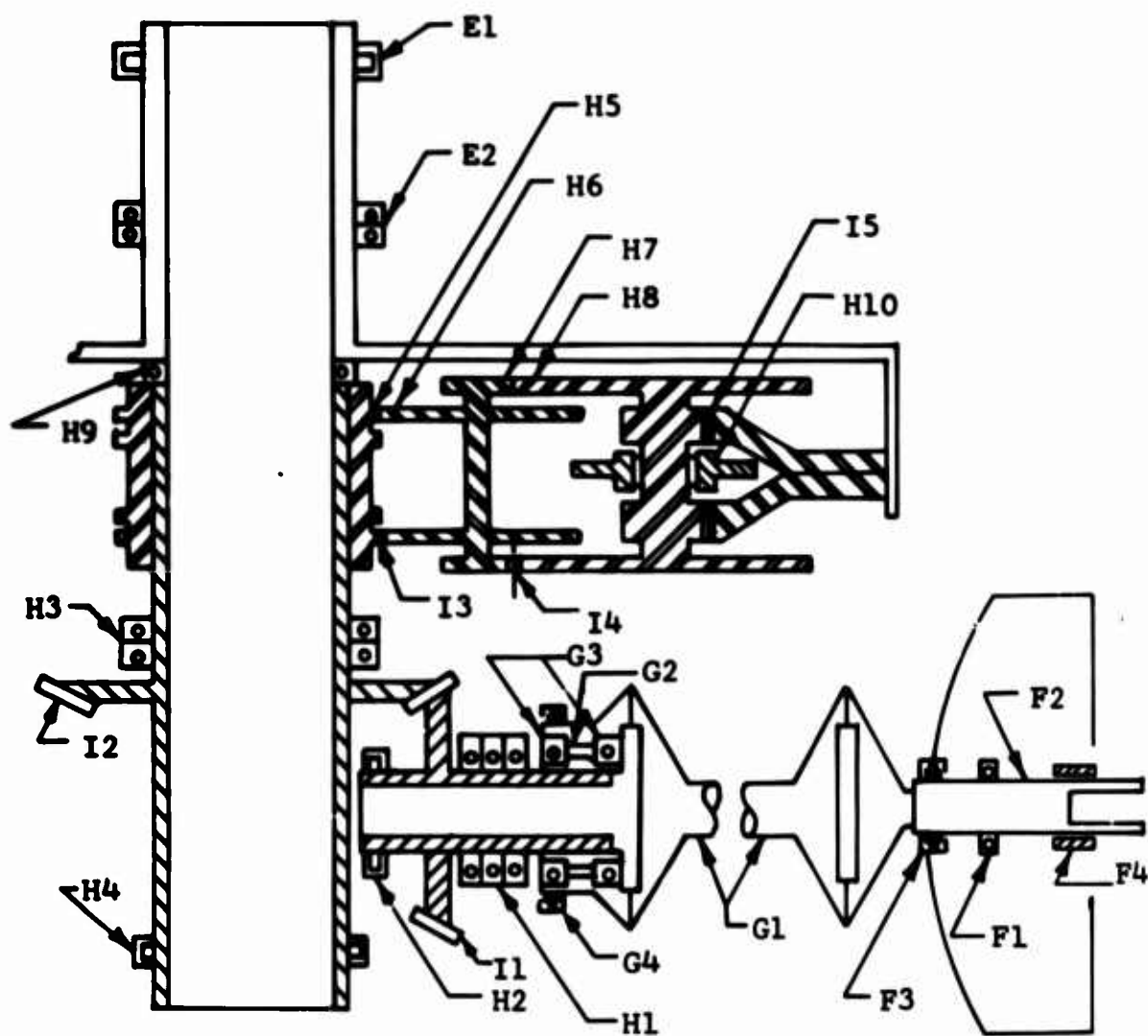
Figure 38. Components Schematic - RGT System.

158
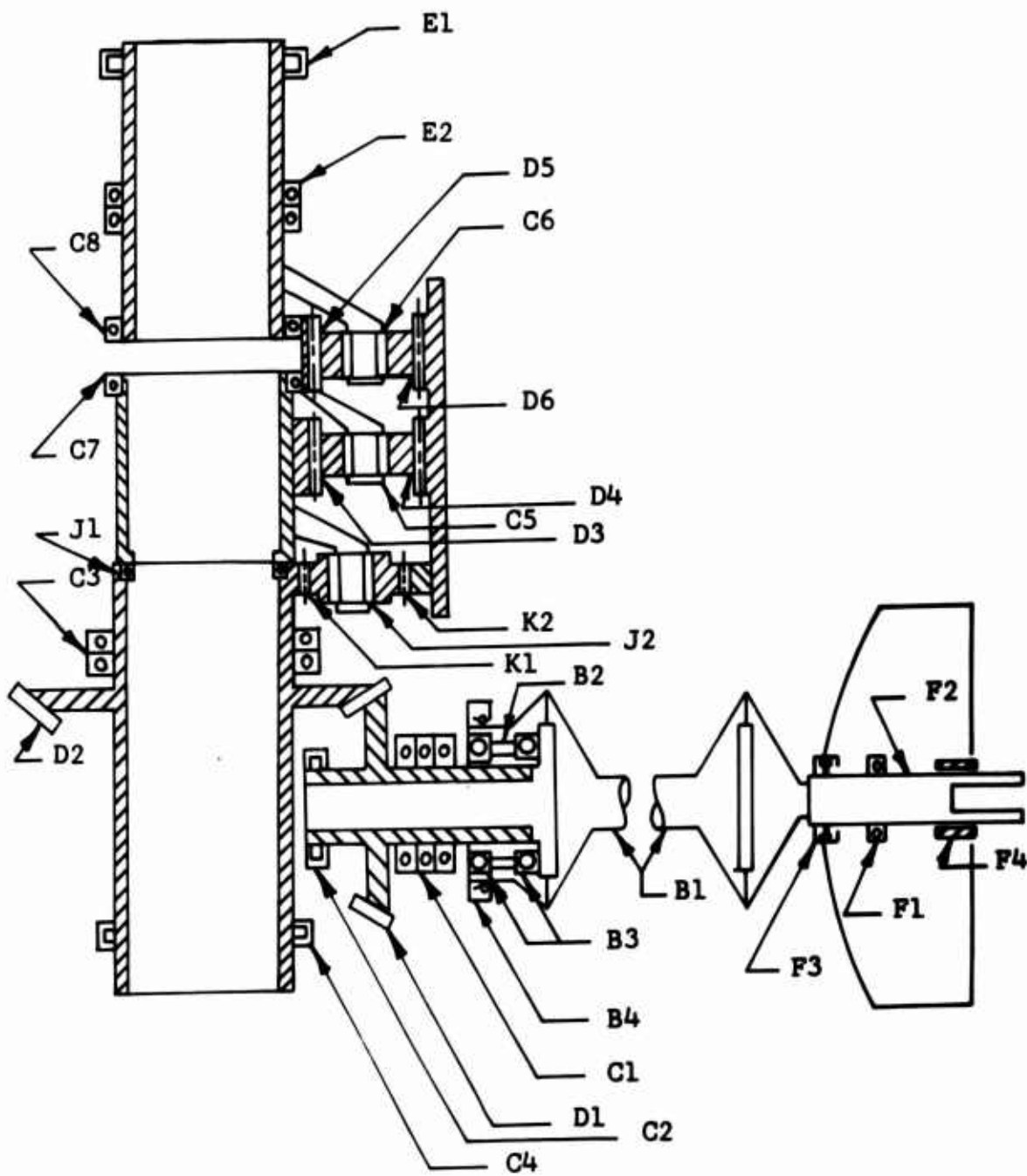
Figure 39. Components Schematic Triple-
Stage Planetary System.

159

INPUT DRIVE SHAFT AND FREEWHEELING ASSEMBLY

This section is comprised of the main input drive shafts (B1) and (G1), UH-1 and RGT/TSPT, respectively; the one-way clutches (B2) and (G2); the clutch bearings (B3) and (G3); and the input seals (B4) and (G4).

The UH-1 drive shaft (B1) failure rate is established from Reference 18 and reflects service experience with the 204-040-010 main input drive shaft, and represents 13 percent of the listed total failure rate. Difficulties here are lubricant sealing, lubrication degradation, too frequent maintenance (the failure rate here would vary inversely with inspection interval), and low-angle (engine end) tooth welding. Although a new shaft assembly (205-040-004 super shaft) has been introduced into the field and appears to exhibit a failure rate of one-fifth the older model, there exists less confidence in this value; the older M & R data will be shown in this report. As will be subsequently explained, no loss of comparative value will be incurred by this failure rate selection.

The complexities involved in the high-speed shaft (G1), even though its increased length will reduce mean angular coupling misalignments, would suggest a failure rate equal to the low-speed shaft (B1). The centrifugal field (C_f) the lubricant and seals must operate in decreases with the coupling diameter reduction but increases as the square of the speed changes, hence

$$C_f = \left(\frac{3.1}{5.0}\right)\left(\frac{21,000}{6,600}\right)^2 (B_1) = 6.2 \ (B_1)$$

The six-fold increase additionally imposes a critical requirement for dynamic balancing on this external and, hence, easily damaged component. Consequently, neither drive system incurs undue penalty from the inclusion of the higher service experience dictated failure rate.

The one-way clutch (G2) has been assigned a failure rate of 1.15 (B2). The virtually doubled over running speed will reduce inner race drag spring life, even though adoption of silver plating on the beryllium copper springs will reduce the wear rate significantly.

The (G3) clutch bearing shows an increased rate of 50 percent above the (B3). The failure here consists of frequent replacement at overhaul and is due to excessive bearing roughness. This roughness is primarily due to the centrifuging of wear particle debris from the oil system. Since the force field

160

is greatly increased, the frequency of bearing roughness will increase. However, the assigned factor of 1.5 is thought to be conservative. The failure rates of (B2) and (B3) were determined from analysis of records on 54 transmissions selected at random from normally scheduled 1100-hour overhauls.

The input seal failure rate for (G4) was equated to the rate of (B4), which was obtained from Reference 18. Although the sealing surface speed has more than doubled in the RGT, incorporation of the more expensive carbon face seal is expected to hold the failure rate down. A more lengthy discussion of this seal design may be found in the design discussion on page 82.

MAIN REDUCTION SYSTEM ANTIFRICTION BEARINGS

Due to the extreme problem of secondary damage, mentioned earlier with regard to treating overhaul statistics, the far more accurate reliability prediction lies with the proper analysis of the respective calculated fatigue spalling or flaking. It is assumed that the bearing application is sufficiently well designed, manufactured, and inspected, and that distress modes such as cage failure are effectively eliminated. This assumption is well borne out by the UH-1 experience.

The individual lives in Table XXII have been found by digital computer treatment of all the significant loading, deflection, speed, and geometric variables. See Appendix IV for a complete discussion of these factors. The lives (which are based upon 60 percent full power, since the life varies approximately inversely as the cube of the power) may be combined in the following manner to yield a cumulative L_{10} for the entire bearing system (Reference 16).

$$\frac{1}{L} = \left[\sum_{i = 1}^{i = x} N_i \left(\frac{1}{L_i} \right)^e \right]^{\frac{1}{e}}$$

where x = total number of different bearings
N = the total number of like bearings of kind i
e = the dispersion exponent

The dispersion exponent e is given the mean value of 4, since extensive testing with aircraft quality antifriction bearings lubricated with MIL-L-7808 has shown that the characteristic Weibull slopes range from 2 to 6. The letter C designates the UH-1 bearings; the letter H, the RGT bearings; and the

letter J, the bearings peculiar to the TSPT. Refer to Figures 37, 38, and 39 for location of the relative bearings.

The cumulative lives are

$$L_{10_C} = \cfrac{1}{\left[\left(\frac{1}{1450}\right)^4 + \left(\frac{1}{2500}\right)^4 + \left(\frac{1}{1300}\right)^4 + \left(\frac{1}{7000}\right)^4 + \left(\frac{1}{4000}\right)^4 + 8\left(\frac{1}{2600}\right)^4 + \left(\frac{1}{150,000}\right)^4 + \left(\frac{1}{900,000}\right)^4\right]^{\frac{1}{4}}}$$

$$L_{10_C} = 1059.67 \text{ hours}$$

Note:

L_{10_C} = 1500 hours for the improved reliability components (ECP) mentioned earlier in this discussion. Bearings C1, C2, C3, and C4 are made from the same improved materials used in bearings H_1, H_2, H_3, and H_4.

$$L_{10_H} = \cfrac{1}{\left[\begin{array}{c}\left(\frac{1}{13,920}\right)^4 + \left(\frac{1}{115,000}\right)^4 + \left(\frac{1}{46,700}\right)^4 + \left(\frac{1}{1,210,000}\right)^4 \\ + 4\left(\frac{1}{4,440}\right)^4 + 12\left(\frac{1}{29,600}\right)^4 + 12\left(\frac{1}{18,150}\right)^4 \\ + 12\left(\frac{1}{51,800}\right)^4 + \left(\frac{1}{13,600}\right)^4 + 6\left(\frac{1}{2,540}\right)^4\end{array}\right]^{\frac{1}{4}}}$$

$$L_{10_H} = 1594.7 \text{ hours}$$

$$L_{10_J} = \cfrac{1}{\left[\begin{array}{c}\left(\frac{1}{13,920}\right)^4 + \left(\frac{1}{115,000}\right)^4 + \left(\frac{1}{46,700}\right)^4 + \left(\frac{1}{1,210,000}\right)^4 \\ + \left(\frac{1}{87,700}\right)^4 + 3\left(\frac{1}{5,376}\right)^4 + 4\left(\frac{1}{4,000}\right)^4 + 8\left(\frac{1}{2,600}\right)^4 \\ + \left(\frac{1}{150,000}\right)^4 + \left(\frac{1}{900,000}\right)^4\end{array}\right]^{\frac{1}{4}}}$$

162

Brg	L_{10}	N	Brg	L_{10}	N	Brg	L_{10}	N
				TABLE XXII. INDIVIDUAL BEARING LIVES				
C1	1,450	1	H1	13,920*	1	J1	87,700	1
C2	2,500	1	H2	115,000*	1	J2	5,376**	3
C3	1,300	1	H3	46,700*	1	H1-H4	(See RGT)	
C4	7,000	1	H4	$1.21 \times 10^{6*}$	1	C5-C8	(See UH-1)	
C5	4,000	4	H5	4,440	4			
C6	2,600	8	H6	29,600	12			
C7	150,000	1	H7	18,150	12			
C8	900,000	1	H8	51,800	12			
			H9	13,160	1			
			H10	2,540	6			

* See bearing design discussion, Appendix IV, for the significance of the adjusted lives shown here for use of improved materials. The very high speed bevel gear application, with its sensitivity to destructive vibration resulting from an initial flaking and hence relatively rapid failure propagation, requires use of an extremely reliable bearing system to preclude catastropic failure occurrences.

** See Appendix V for the significance of this adjusted life.

$$L_{10_J} = 1506.18 \text{ hours}$$

Since, by definition, the cumulative failure rate is 10 percent for the listed hours, we shall correct for the proper failure rate for 1000 hours to enter the rate summation tables. The mean life for cumulative bearing failure shall be used in setting the 1000 hr rate, i.e.,

$L_{50} = 1.61 L_{10}$ (for the dispersion exponent, e = 4.0)

$$\lambda = \frac{1000}{L_{50}}$$

For the UH-1 system

$$\lambda = \frac{1000}{(1.61)(1059.67)} = .5861$$

For the RGT system

$$\lambda = \frac{1000}{(1.61)(1594.7)} = .3895$$

For the TSPT system

$$\lambda = \frac{1000}{(1.61)(1506.18)} = .4124$$

MAIN REDUCTION SYSTEM GEAR MESHES

The input bevel pinion and gear members (D1, D2) and (I1, I2) are considered as separate gear elements quite apart from the remaining spur gears, since their characteristic mode of failure involves shaft wear and debris damage rather than tooth failure per se. As described under "Gear Design Philosophy" in Appendix VII, bevel gear teeth at endurance power limit will characteristically exhibit the tooth breakage failure mode. In the entire UH-1 service experience to date (envoling some 5,500 helicopters, 9,000 transmission, and 5 million flight hours), we are cognizant of this mode occurrence but three times, once on the member (D1) and twice on the member (D2). Consequently, the failure rates given were extracted from the analysis of 56 transmissions selected at random from normally scheduled 1100-hour-overhaul maintenance records and reflect parts replacements for the above noted causes. This method of course yields a conservative failure rate estimate since many parts are replaced on the judgement that they are inadequate for an additional 1100 hours of service, rather than for inadequate performance at the 1100-hour level.

The increased dynamic loads attendant in the (I1) and (I2) bevel meshes have been accounted for in the torque load stress levels selected for the high-speed set employed in the RGT and TSPT transmissions. Therefore, the failure rates assigned to (I1) and (I2) are equal to (D1) and (D2).

The spur gear meshes in all three systems are treated in the following manner: as discussed at length in Appendix VII, the dominant or characteristic failure mode is pitting of the active involute profile. The 5-percentile life can be read directly in cycles as a function of the calculated Hertz stress and elastohydrodynamic lubricant film thickness at the lowest point of single tooth contact, on Figure 36, for both pinion and gear driving. Each set of meshing gears shall be considered as a singular event (although two elements exist in contact), since the driver dedendum is at least 50 times more likely to fail in the thin film regime of lubrication. The individual dispersion exponents are of such large magnitude that the 98-percentile rank of the driver pitting occurs at fewer cycles than the 2-percentile rank of the driven member on Weibull plots of test sample sizes of N = 30. The referenced figure of life cycles to pitting is produced from extensive data, collected from a 3-year program on UH-1 gears in a planetary regenerative test stand at BHC (Reference 20), supported by AVCOM under Product Improvement Task 2E4. The failure probabilities represented in this figure represent the occurrence of a single pit or spall of approximately 3/32 in. diameter on a single tooth of the driver.

Since the individual lives vary as $(1/LOAD)^{1/3}$, 70 percent of full power rating has been chosen to fix the individual L_5 lives of the gear meshes, rather than the 60 percent used in the bearing analysis. The cumulative wear life shall be summed as before.

$$\frac{1}{L} = \left[\sum_{i=1}^{i=x} N_1 \left(\frac{1}{L_i}\right)^e \right]^{\frac{1}{e}}$$

Where: x = total number of different meshes

N = total number of like meshes of kind i

e = the characteristic dispersion exponent

e is chosen as 5.5 for a mean value since the test gear pittings gave Weibull slopes ranging from 3 to 8. Each separate load carrying mesh (whether a multiple or redundant configuration or not) must be treated as an individual event with

165

its own intrinsic failure rate tendencies. Each mesh is sub-
ject to the above dispersion for summation since it exists as
an entity with its own errors, metallurgical characteristics,
surface finishes, and other signatory irregularities. Even
in multiple row antifriction bearings, produced to tolerance
values expressed in units of millionths of an inch, $(N)^{0.7}$ is
the relative capacity rating given for the number of rows N.
The argument has been advanced in some quarters that the four
separate sun driving meshes in the RGT cluster should be
treated as the equivalent of one gear. Considering that each
is individually manufactured and subsequently welded together
to form a cluster that must transmit equal power through each
of the four gears (if they are to operate at the calculated
stress levels), little can be found to support such a conten-
tion. However, the value of e used in this gear analysis
implies that multiple row gears are far more consistent and
predictable than multiple row bearings.

The predicted individual mesh lives are summarized below.
Refer to Figures 37, 38, and 39 for the location of these
meshes. The conversion of life cycles given in Figure 36 to
the hours listed below may be found in Table XXIII.

	UH-1			RGT			TSPT		
	Gear Mesh	L_5	N	Gear Mesh	L_5	N	Gear Mesh	L_5	N
First Stage	D3	1,000	1	I3	3,200	4	K1	153,000	1
	D4	21,739	4				K2	1.5×10^6	3
Second Stage	D5	406	1	I4	783	12	D3	1,000	1
	D6	2,702	8				D4	21,739	4
Third Stage				I5	1,260	12	D5	406	1
							D6	2,702	8

The cumulative lives are

$$
L_{5_{UH-1}} = \frac{1}{\left[\left(\frac{1}{1000}\right)^{5.5} + 4\left(\frac{1}{21,739}\right)^{5.5} + \left(\frac{1}{406}\right)^{5.5} + 8\left(\frac{1}{2,702}\right)^{5.5}\right]^{\frac{1}{5.5}}}
$$

$$
L_{5_{UH-1}} = 405.5 \text{ hours}
$$

$$L_{5_{RGT}} = \cfrac{1}{\left[4\left(\cfrac{1}{3,200}\right)^{5.5} + 12\left(\cfrac{1}{783}\right)^{5.5} + 12\left(\cfrac{1}{1,260}\right)^{5.5}\right]^{\frac{1}{5.5}}}$$

$$L_{5_{RGT}} = 492.00 \text{ hours}$$

and

$$L_{5_{TSPT}} = \cfrac{1}{\left[\left(\cfrac{1}{153,000}\right) + 3\left(\cfrac{1}{1.5\times10^6}\right)^{5.5} + \left(\cfrac{1}{1000}\right)^{5.5} + 4\left(\cfrac{1}{21,739}\right)^{5.5} + \left(\cfrac{1}{406}\right)^{5.5} + 8\left(\cfrac{1}{2,702}\right)^{5.5}\right]^{\frac{1}{5.5}}}$$

$$L_{5_{TSPT}} = 405.46 \text{ hours}$$

Since, by definition, the cumulative failure rate is 5 percent for the listed hours, we shall correct for the proper failure rate for 1000 hours to enter the rate summation tables. The mean or 50 percentile life for cumulative gear failure shall be used in setting the 1000 hour rate, i.e.,

$$L_{50} = 1.603 \, L_5 \quad \text{(for the dispersion exponent, } e = 5.5\text{)}$$

$$\lambda = \frac{1000}{L_{50}}$$

For the UH-1 system

$$\lambda = \frac{1000}{(1.603)(405.5)} = 1.5384$$

For the RGT system

$$\lambda = \frac{1000}{(1.603)(492.0)} = 1.2679$$

and for the TSPT system

$$\lambda = \frac{1000}{(1.603)(405.46)} = 1.5386$$

167

TABLE XXIII. GEAR LIFE CALCULATIONS
(Reference Figure 36)

Gear Mesh	*h' $(10^{-6}$in.)	**Sc' (KPSI)	L_5(Cycles)	CYC/Hr x 10^{-6}	L_5(Hours)
D3	27	129	5×10^8	.50	1,000
D4	38	129	5×10^9	.23	21,739
D5	18+	135	1.3×10^8	.32	406
D6	22	134	2×10^8	.074	2,702
I3	41	116	2×10^9	2.5	3,200
I4	28	145	6.5×10^8	.83	783
I5	22	139***	1.9×10^8	.15	1,260
K1	77	106	$3.0 \times 10"$	1.96	153,000
K2	63	89.5	$8.0 \times 10"$	.53	1,500,000

*h' = 1.29h   Where h = EHD lube film thickness @LPSTC at full power and 1.29 = corrective factor for 70% power $(.7W_t)$

$$h \propto \left(\frac{1}{W_t}\right)^{0.7}$$

**Sc' = .83 Sc   Where Sc = Hertz stress (LPSTC) at full power from Table XXIV, and .83 = correction factor for 70% power $(.7W_t)$

$$h \propto \left(\frac{1}{W_t}\right)^{0.5}$$

***Sc' = .70Sc   Same as above except additional $.7W_t$ correction used for 30° = ♥ (Helix Angle)

$$Sc \propto (.49W_t)^{0.5} = \quad Sc' = .70Sc$$

168

MAST BEARING AND SUPPORT SYSTEM

The failure rate used for the cylindrical roller bearing (E1) and the ball thrust bearings (E2) are extracted from the UH-1 M & R program (Reference 18). No adjustment has been made on the system redesign used with the RGT and TSPT, since it seems logical to conclude that suitable comparable life components could easily be employed. The rotor mast support bearings are not a significant factor in the study conclusions, and their design parameters are unaffected by the scheme chosen for the power reduction gearing system. The mast and pylon support systems shown for the RGT and TSPT are borrowed from an advanced rotor IR&D program and are overdesigned for a 1250 hp, 9500-lb gross weight helicopter. To include the slight overall reliability gain of these two greatly increased life bearings would force the obviously unjust penalty of including their greatly increased weight in the system weight comparisons.

COMPARATIVE SYSTEM RELIABILITIES

In the foregoing analysis, it has been shown that the predicted failure rates for the proposed RGT and TSPT designs are less than for the existing UH-1 system operated with a 1250-hp maximum takeoff rating. Reduced to reliability figures for a 1-hour operation, for the convenience of an illustrative value (although it should be understood that this is physically and hence mathematically incorrect), the corresponding values are

$$R_{RGT} = .9964$$

$$R_{TSPT} = .9961$$

$$R_{UH-1} = .9956$$

Therefore, it may be concluded that all systems have a reliability value of the same approximate order of magnitude, even though they differ widely in their design concepts. As designed, the RGT has the best value, although its confidence level is quite low until it is actually built, tested, and developed.

The overall impact of technology improvements and evolutionary development are difficult to assess in such comparisons. Both the RGT and the TSPT high-speed stage benefit greatly from the advances in knowledge gained in the past decade since the design and introduction of the UH-1 system.

The significance of evolutionary development may be seen in the fact that the current production UH-1 - through the incorporation of Engineering Change Proposal reliability improvements - has a predicted total λ of 3.733 and an anticipated 1-hour reliability of .9963.

In general, the reliability analysis does serve to pinpoint characteristic trouble items and weak spots in the design. To further illustrate the cause and effects of singularly important items, assume that the last stage planetary of the TSPT upper sun gear (common to the UH-1) was modified by conversion to honed profile nitrided AMS 6475 material. Prior tests (Reference 6) indicate the equivalent of a 50-percent EHD film thickness increase effect upon their failure time. The L_5 hours increased from 406 to 625, the total TSPT failure rate decreased to 3.3295, and the 1-hour reliability increased to .9967.

Applying a similar treatment to the 12 I4 gears of the RGT (albeit 12 times as costly in manufacturing time), we find their L_5 hours increase from 783 to 1808, the total λ decreases to 3.0931, and the 1-hour reliability increased to .9969, again moving slightly into the lead.

However, since these types of improvements may go on ad infinitum (with ever decreasing returns once the singular worst risk is removed), it is concluded that the reliability rankings given on the preceding page for the three systems do represent a fair and comparative demonstration of their intrinsic capabilities.

GEARBOX EFFICIENCY COMPARISON

The calculated efficiencies of the RGT, the TSPT, and the
UH-1 total reduction system are tabulated below and followed
by a discussion of the methods used and the comparisons made
in determining the efficiencies shown.

TOTAL REDUCTION SYSTEM

	UH-1	RGT	TSPT
Percent efficient	97.36	97.73	97.59

The gears in the respective drive systems were analyzed for
load sharing, scoring, bending stress, surface compressive
stress, subsurface shear stress, power loss, and elasto-
hydrodynamic lubricant film thickness at the maximum design
power limit, as shown in Table XXIV. These stresses and
operating conditions were predictable by a computerized
analysis that was tailored to investigate instantaneous load-
ing and lubrication phenomena as the gear teeth progress
through mesh from the first to the last point of contact under
operating load and rotational speed. The rise in instantaneous
contact temperature and the reduced radius were calculated for
21 points of contact on the operating profiles by the AGMA
scoring formula. These values were used in subsequent calcu-
lations to predict instantaneous contact temperatures, associ-
ated coefficient of friction, lubricant viscosity, and film
thickness. The coefficient of friction, normal load, and
relative sliding velocity were then combined to calculate in-
stantaneous power loss. The average power loss was finally
calculated by integrating the instantaneous power loss across
the active tooth profiles.

Windage losses are calculated for the RGT, TSPT, and UH-1
transmissions by a modification of the formula

$$P_w = \frac{(n^3)(D^5)(\ell^{.7})}{10^{17}} \quad \text{(Reference Appendix I)}$$

$$10^{17} = f(\rho)$$

which corrects the value of ρ to consider the mean density of
an oily atmosphere. The shafts and discs are assumed to be
relatively smooth, and the analysis, including the adjusted
ρ, has been shown to correlate well with observations. The
losses that are calculated do not account for the effect of
any centrifugal "pumping" action of the gear teeth. This

TABLE XXIV.   FUNCT

PART NUMBER	HP	AVG PWR LOSS PER MESH (FT-LB/SEC)	TANG LOAD (LBS)	RELATIVE RPM OF DRIVER	MAX TEMP RISE (°F)	SLIDING VEL (FT/SEC)
204-040-329 204-040-108	1138	242.9	1732	2090	194.5	13.9
204-040-330 204-040-108	1138	196.4	2674	676	117.0	4.5
204-040-331L 204-040-108	1138	161.1	1732	3840	26.9	11.4
204-040-331U 204-040-108	1138	139.8	2674	1242	19.8	3.7
High-Speed Sun Planet	1138	175.9	934	10792	143.2	50.4
High-Speed Ring Planet	1138	151.3	981.4	9035	27.3	49.6
6x6C Sun X_1	1138	102.5	358.5	13886	172.7	41.2
6x6C Y_1 X_2	1138	81.09	461	6943	161.7	19.6
6x6C Y_2 Ring	1138	180.38	2562	2430	73.9	5.8

	TSPT	RGT	UH-1
Total HP Loss in Planetary	9.89	10.04	8.1
Planetary Efficiency %	99.2	99.11	99.29

* Lowest point of single tooth contact

A

LE XXIV. FUNCTIONAL GEAR DATA

SLIDING VEL (FT/SEC)	MAX HERTZ STRESS (PSI)	TOTAL PWR LOSS (HP)	DIAMETRAL PITCH	ROOT STRESS BENDING (PSI)	EHD FILM THICKNESS AT LPSTC* (MICROINCHES)
13.9	155998	1.76	8.5	34,657 29,589	20.975
4.5	162598	2.96	8.5	33,338 41,104	14.429
11.4	155782	1.28	8.5	39,256 31,898	29.483
3.7	161934	2.10	8.5	42,418 41,161	17.244
50.4	128080	.96	9.753	26,387 Planet 19,174 Sun	60.298
49.6	108663	.827	10.247	25,125 Planet 23,764 Ring	48.934
41.2	139308	2.3	10.0	23,900 25,519	32.692
19.6	175486	3.91	11.25	37,562 37,141	22.280
5.8	199410	3.84	10.424	48,507 66,315	16.995

B.

pumping action, though not included, can represent a considerable amount of power absorption.

The windage losses in the UH-1 transmission are much lower than the RGT or TSPT under any circumstances because the higher operating speed and large number of rotating elements in the RGT and TSPT. However, the overall power loss situation in the RGT can be minimized by judiciously shrouding gear elements baffling passages and eliminating trapped or vortexing oil. This aspect of the RGT design is basically a problem to be investigated in a test and development phase since the complexity of the lubricant/rotation situation seldom leads to an acceptable solution in the initial design, even when major difficulties are recognized.

In spite of the limitations imposed by the assumptions in the empirical windage calculations, close correlation between calculation and design may be achieved, but often only after a thorough test and development program.

The accuracy of the heat loss predictions have been verified by test results obtained from bench testing of the UH-1 transmission, wherein the heat losses were determined by measurement at various transmitted powers. Close correlation between test results and predicted results has been obtained.

A tabulated comparison of the operating conditions of stress, efficiency, and lubrication of the 6x6C RGT, TSPT, and UH-1 transmissions at 1138 hp are shown in Table XXIV.

The overall efficiencies of the roller gear transmission, triple planetary, and UH-1 transmission are shown in Table XXV. These efficiencies include bearing losses, bevel gear losses (reference page 198), windage losses (reference page 199), and planetary gear losses (reference end of Table XXIV).

The efficiency figure shown for the UH-1 transmission system includes the losses attributed to the approximately 3:1 ratio speed decreaser gearbox on the Lycoming T-53 engine. An engine gearbox efficiency figure of 99.3 percent was furnished by Lycoming, based on the heat rejection in the oil cooler, isolated to the gearbox. No correction was made for the amount of heat rejected to the inlet air flowing over the gearbox.

In order to more closely approximate the actual heat loss of the T53-L13 engine SDG, an analogy is made with a cooling study conducted on a 2:1 ratio SDG unit on a T-55 SDG which was designed, manufactured, and tested by Bell Helicopter.

175

TABLE XXV. POWER LOSS AND EFFICIENCY			
	UH-1 (HP)	RGT (HP)	TSPT (HP)
Planet Gears	8.09	10.05	9.89
Planet Cages	.12	-	1.34
Windage	2.274	7.236	7.575
Bevel Gears	4.560	4.720	4.72
Bearings	2.837	3.870	3.87
Engine SDG	12.20	-	-
Power Loss	30.081	25.876	27.395
Efficiency, %	97.36	97.73	97.59

For initial operation in an engine test cell, a bellmouth inlet for the engine induction air was employed. All inlet air passed over the SDG outer casing. At operation up to 1800 hp (limit tested), no auxiliary oil cooling was required. Inlet air temperature was 65°F and oil stabilization temperature was 165°F. The air mass flow was on the order of 20 lbs/sec.

During a subsequent operation of the identical gearbox on the helicopter, the induction system was so arranged that no inlet air flow passed over the SDG. Under this condition, the heat rejected to the oil cooler was 12 hp, for a stabilized oil inlet temperature of 183°F, giving a calculated efficiency of 99.3 percent.

However, in the T53-L13 engine, the SDG system is housed within the engine front frame which forms the inner surface of the air inlet section. While the heat transfer to the inlet air in this instance is not expected to be as efficient as in the T-55 bellmouth example cited above, it would certainly not be represented by the baffled T-55 configuration used in the helicopter installation.

A reasonable heat transfer figure of merit of .5 for the T-53, with respect to the T-55 bellmouth example, is suggested. Considering that the comparable mass flow for the T-53 at 1250 hp is 11.5 lb/sec, the following correction is employed:

$$\text{HP} = (.5) \left(\frac{11.5}{20}\right)(12 \text{ HP}) = 3.45 \text{ HP}$$

Adding this value to the furnished T-53 cooler loss of 8.75 hp yields a corrected total loss value of 12.20 hp and a corrected efficiency of 99 percent.

The efficiency of the RGT as determined by analytical methods is somewhat lower than would be expected, based on data that have been previously reported on a comparable reduction unit (Reference 2). In the referenced report, the RGT transmission exhibited approximately 98.5 percent efficiency. The method used in determining the efficiency figures (Reference 2) was by direct measurement of inlet temperature and outlet temperature of the lubrication oil. Then, based on oil flow and power input, the efficiency was determined. However, this accounts only for the heat transferred to the oil and omits the necessary determination of the heat removed by convective air over the transmission cases. The efficiency figure thus calculated is erroneous in that the total heat loss has not been directly measured or otherwise determined. In order to accurately ascertain the total heat loss by direct measurement, it is necessary to measure shaft input power and shaft output power

with accuracies approaching 0.05 percent or to monitor oil temperature at inlet and outlet with the further restriction that all heat generated be removed via the lubricating/cooling oil. This latter method can be implemented only through complete insulation of the exterior surface of the reduction unit. A suitable procedure is presented in Reference 21, page 14-56.

In an effort to determine a realistic value of convective heat loss from the exterior surfaces of a transmission, the results of efficiency determination by testing three Bell designed gearboxes have been reduced and are presented in Table XXVI. The figures presented for the Models 204, 206, and 563 gearboxes are from measured data wherein input and output horsepower, input and output oil temperature oil flow rate, and external wetted area were measured. The data shown for the Model 563 embody the effect of slight air flow forced across the gearbox. It should be noted that the USAAVLABS RGT was also tested with forced air flow present. The Bell RGT and USAAVLABS RGT losses reflect calculated data based on wetted external casing area.

As can be seen from Table XXVI, the major factors involved in ascertaining the percentage heat loss by convection are the external wetted area of the gearbox and the disturbance of air around the gearbox.

The specific convective heat rejection (Table XXVI) is the index by which ready comparison of convective heat loss for various gearboxes can be made. While the specific heat rejection for the 206 and 204 are very close, the values are only about half the values for the 563. This is due to the airflow forced across the gearbox as noted above. This is also reflected in the percent of heat rejected to the oil cooler.

Since the USAAVLABS RGT has in excess of 3000 square inches of surface area, and since forced air was flowing past the gearbox during the efficiency determination (by monitoring oil temperature), it is expected that a high percentage of heat was lost by the convection route. The actual efficiency figure would necessarily be diminished a commensurate amount.

As mentioned on page 80, the low predicted heat loss (or transfer) for the USAAVLABS RGT is due to the relatively low oil flow rate used in the lubrication system. The oil flow rate directly affects the amount of heat carried away by the oil, with low oil flow yielding low heat transfer via the oil.

It should be noted that the oil flow requirements for the Bell RGT are in excess of the requirements of the USAAVLABS RGT.

TABLE XXVI. COMPARATIVE HEAT REJECTION DATA FOR VARIOUS TRANSMISSIONS

	BHC 206	BHC 204	BHC 563	BHC RGT	USAAVLABS RGT
Horsepower	300	1100	1400	1138	1100
Effective Wetted Area, in.^{2}	600	1856	2131	1856	3000+
Convection Cooling, Btu/min/°F	.797	2.50	5.7	2.50	-
Convection Cooling, HP/°F	.019	.059	.137	.059	-
Specific Heat Rejection, Btu/min/°F/in.^{2}	.00133	.00135	.0027	.00135	-
Total Horsepower Loss	6.30	17.88	19.60	25.88	-
HP Loss to Convection	2.14	5.90	8.04	5.90	9.5-18
HP Loss to Cooler	4.16	11.98	11.56	19.98	-
Percentage of Total Loss	66	67	59	77	-
Efficiency, percent	97.9	98.4	98.6	97.73	-
Efficiency, Neglecting Convection Loss, percent	98.6	98.9	99.2	98.24	-

The Bell RGT was designed for a helicopter drive system and, as such, embodies the major design features normally required for a helicopter, viz, lightweight gear elements with attendant high operating stresses in a relatively small package. It is because of the high operating stresses and small size that greater lubricant cooling requirements are manifest. The heat generating points (gear meshes and bearings) will necessarily produce larger heat flux density than a heavier (wider face width) mesh which is subjected to a lower unit operating load. Since the heavily loaded mesh produces more heat (per unit time), it must have more oil flowing by to remove this heat. Since the gearbox in which the highly loaded meshes are housed has a relatively smaller surface area for convective cooling, the oil flow requirements are further increased. Hence, the Bell RGT being designed for a helicopter is light and highly stressed while the USAAVLABS RGT was designed to test the roller gear concept and is perforce large with low gear unit loads. The oil flow rate then must be commensurate with the cooling requirements as well as the lubricating requirements.

In summary, the apparent disparity in the calculated efficiency of the BHC RGT and that reported for the USAAVLABS RGT is primarily explained by the exclusion of convective heat losses from the efficiency determination employed on the latter unit.

COMPARATIVE MAINTAINABILITY

Maintainability of the various support systems (drive system, electrical system, fuel system, etc.) is directly responsible for the flight status of the operational helicopter. After a reliable T.B.O. is established, it becomes a problem of maintenance in keeping the vehicle operational. Component configuration and accessibility are design features that should be given primary consideration in the initial design stages in order to facilitate rapid inspection and service and component change. The requirements for special tools and work aids should be minimized.

The UH-1 airframe is designed with integral work platforms and the major drive system components are attached to the airframe with standard wrenching hardware or quick disconnects. Ease of preflight maintenance, service, and component change are built-in features. The installation of a new transmission into the UH-1 basic airframe would enjoy the advantages now available to the standard UH-1 transmission.

The regular required maintenance of the RGT, TSPT, and UH-1 transmissions should be essentially identical, assuming an equal service introductory and field experience basis for each. Regular preflight maintenance includes visual inspection of transmission lube quantity and inspection for visible signs of component damage and lube leakage. Preflight maintenance can be performed with equal ease on all three transmission systems.

Table XXVII compares the relative maintainability of UH-1 transmission and RGT and TSPT components that are likely to be involved in maintenance activities.

In bringing the maintainability of the T-53 engine output reduction box (nose box) into the analysis, regular maintenance includes visual inspection of the unit for output shaft seal leakage with occasional replacement of a defective seal. Seal replacement requires removal of transmission input drive shaft, numerous airframe baffles and engine air inlet screens, and several reduction box components.

The RGT and TSPT systems require no engine speed decreaser gearbox.

181

TABLE XXVII. MAINTENANCE COMPARISON

Item	UH-1 Transmission	RGT AND TSPT
1. Oil Filler Port	On transmission support case - accessible from transmission work deck.	In top case, also accessible from work deck.
2. Sump and Accessory Drive Unit (contains magnetic chip detector, lube pump inlet screen, air maze oil filter) inspected at 100-hr intervals and lube level sight glass inspected before each flight.	Sight glasses visible from side of helicopter, other components of limited accessibility from within hell hole.	Same basic sump assembly in same relative helicopter location.
3. Lube Filter (paper element) 100 hr periodic replacement.	Filter easily changed from transmission deck.	Same as UH-1
4. Generator	Generator and drive quill readily accessible at transmission work deck.	Generator and quill have same relative accessibility as that of UH-1.
5. Input Drive Quill	Limited accessibility - Maintenance requires input driveshaft removal and removal of various airframe baffles, etc.	Same relative accessibility but improved quill oil seal should eliminate the majority of maintenance required on this unit.

TABLE XXVII - Continued

Item	UH-1 Transmission	RGT AND TSPT
6. Mast (removal)	Easily accomplished - mast with thrust bearing and bearing retention assembly can be withdrawn from transmission with crane. Majority of work performed from transmission work deck.	Difficult - requires complete removal of top case assembly.
7. Transmission	Requires removing bolts of limited accessibility from five mounts, and life link. Various lube lines, hydraulic lines and electrical connections must be broken.	Focused transmission mount will retain transmission with 32 readily accessible bolts. Removal will also require breaking lube, hydraulic, and electrical connections.

183

DIMENSIONAL TOLERANCE AND MANUFACTURING COST
STUDY AND COMPARISON

The estimated fabrication costs of the proposed RGT and TSPT at production rates comparable to that of the UH-1 transmission are shown in the following comparison of the RGT, TSPT, and UH-1 transmission fabrication costs with the current cost of the latter being approximately $10,000 each.

	UH-1 Transmission	RGT	TSPT
Fabrication Cost	$10,000	$15,000	$11,500

Lycoming has estimated a $2,500 reduction in engine costs in adapting their T53-L13 engine to the RGT system or the TSPT system. (This reduction in cost is the result of (1) replacing the speed decreasing hardware such as gears, bearings, spider, etc., in the engine nose box with a single extension driveshaft and (2) relocating and changing the torque metering system.)

Combining the UH-1 transmission cost of $10,000 and the reduction in engine cost of $2,500 gives a $12,500 comparative cost for the UH-1 total reduction system. Thus the following comparison of the RGT, TSPT, and UH-1 total reduction system can be made.

	TOTAL REDUCTION SYSTEMS		
	UH-1	RGT	TSPT
Fabrication Cost	$12,500	$15,000	$11,500
Percentage of UH-1 Cost	100%	120%	92%

Figure 40 shows the cost trends of the UH-1 transmission from the year 1957 through 1966, with the estimated cost trends of the RGT, the TSPT, and the UH-1 total reduction system overlayed. The significance of the cost trend curves in Figure 40 lies in the difference between the estimated fabrication costs of the RGT and TSPT during the early stages of manufacture.

This significant difference is attributed to the fact that all components in the TSPT are either identical or so similar to the UH-1 components that existing and proven high-production rates of manufacturing and inspection methods can be utilized. It is estimated that the manufacture of the RGT, because of the gear teeth alignment, E. B. welding, and roller manufacturing requirements, will require a manufacturing and
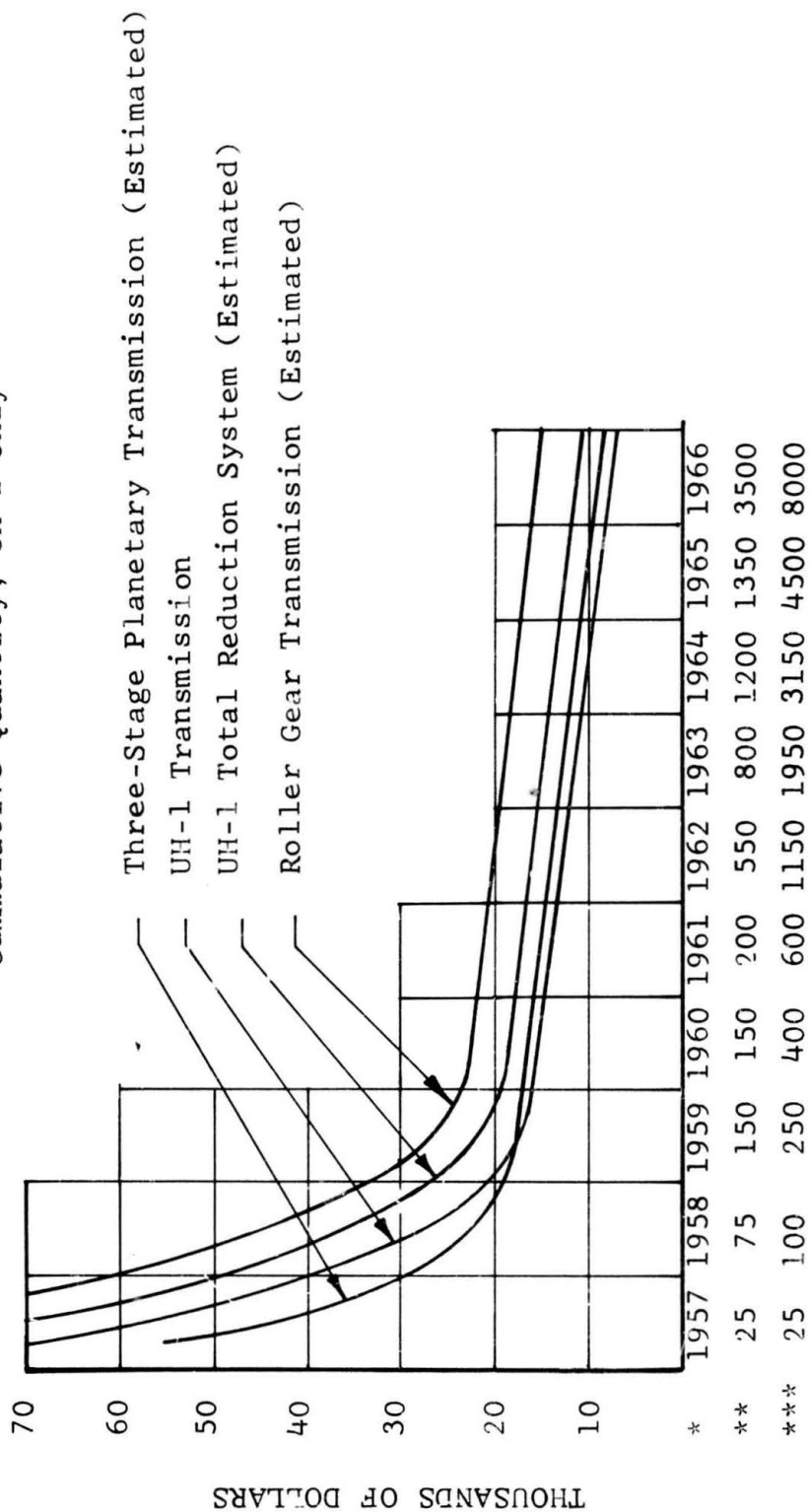
Figure 40. Cost Trends for UH-1 Transmission, Roller Gear Transmission, Three-Stage Planetary Transmission, and UH-1 Total Reduction System.

185

inspection development period similar to that required for the UH-1 transmission in its early production stages. Thus the cost trend curves for the RGT and the UH-1 transmission are shown parallel throughout the production ranges shown in Figure 40, whereas the cost trend curve for the TSPT reflects a distinct advantage during the early stage of manufacture.

In the discussion that follows, a comparison of the RGT and the UH-1 reduction systems only will be made since the manufacturing methods utilized for the TSPT and the UH-1 systems are so similar.

The 20-percent increase in cost of the RGT as compared to the UH-1 total reduction system is dictated primarily by the differences in dimensional tolerances and manufacturing methods between the two systems.

The following discussion describes these differences in light of their effects on the total cost of the RGT. The discussion also elaborates on the problems involved in estimating an accurate production-rate fabrication cost on such a system as the RGT.

The significant dimensional tolerancing and manufacturing method differences between the RGT and the UH-1 systems which affect cost are in the areas of gear teeth alignment, E.B. welding, and roller manufacturing.

The UH-1 transmission has no gear teeth alignment requirements; none are necessary in a single bevel gear set and simple planetary reduction system. Also, the UH-1 transmission contains no E.B. welded parts and no rollers.

The T-53 engine nose box reduction unit has three gear teeth alignment requirements: three clusters of two gears, each which has master teeth required to be in line. The nose box contains no E.B. welded parts and no rollers.

The RGT has a total of 54 gear teeth alignment requirements: four on each of the second-row clusters, four on each of the first-row clusters, one on each of the two ring gears and four on the sun gear. The RGT contains a total of 66 E.B. welded joints and 40 rollers.

The above three areas of significant difference are summarized as follows:

	UH-1 Transmission	Nose Box	RGT
Number of teeth alignment requirements	0	3	54
Number of E.B. welded joints	0	0	66
Number of rollers	0	0	40

The tooth alignment requirements and the E.B. welded joints are closely related, since the high degree of accuracy required on the teeth alignment must be obtained during the E.B. weld process.

The additional processes required on each cluster and the sun gear shaft, because of the above requirements, are as follows:

- The alignment of the gear teeth on the welding arbor.

- The actual E.B. welding process.

- A finish machine cut on both sides of each weld.

- A penetrant inspection (Zyglo) on both sides of each weld.

- A radiographic inspection (X-ray) of each weld.

- A magnetic particle inspection on each side of each weld.

- A final check on the gear teeth alignments.

- The complete manufacturing and inspection of all the rollers.

Also, two teeth alignment requirements must be obtained during the finish grinding process:

- Each Y_2 gear with its curvic coupling teeth

- Each X_2 gear with its adjacent Y_2 gear (after curvic grinding).

Each gear will require two complete inspections: one prior to E.B. welding, to make certain that an entire cluster will not be scrapped due to the use of one or more defective gears, and the second during final inspection, to check for any distortion that may have resulted from E.B. welding or subsequent machining.

Manufacturing errors in finishing the rollers can result in scrapping an entire cluster or sun gear shaft, since the rollers necessarily have to be ground and super-finished in the final phase of the processing. The two major causes for final rejection will be size control and grinding burns. Intensive efforts will have to be directed toward establishing suitable size control and grinding techniques in the early development stages, since no roller diameter outside the ±.0001-inch tolerance band can be tolerated and since no grinding burn indications revealed by the nital etch inspection per BPS FW-4092 can be allowed.

The estimated cost of the RGT and the actual cost of the UH-1 total reduction system (UH-1 transmission and engine nose box) at the production rate of 100 units per month would be approximately equal if the RGT had no teeth alighment requirements, no E.B. welded joints, and no rollers to be manufactured and inspected.

This is to say that if the proposed RGT had all the rollers removed, had no alignment requirements on the gear teeth, and had all the gears on each cluster and sun gear shaft joined together (after manufacturing) at no cost, then the estimated cost of the RGT system would be $12,500.

Thus, a cost comparison of the two reduction systems can be simply reduced to assigning a $2,500 value to the requirements for gear teeth alignment, E.B. weld joints, and rollers. Unfortunately, this is not an easy task.

Since E.B. welding on a production basis is relatively new, and since the proper alignment of the gear teeth and the sizing of the rollers demand extremely close tolerances, this estimate of the actual cost of the proposed RGT assumes the successful development of new and efficient production methods.

A reasonable indication of a projected production cost of the RGT could be obtained by actually fabricating from three to five units, using production-type tooling; however, manufacture of at least 250 units would be necessary before cost trends could be established that would accurately compare with the production cost trends of the combined UH-1 transmission and T53-L13 engine nose box reduction systems. Figure 23 shows the cost trends of the UH-1 transmission from the year 1957 through 1966, with the estimated cost trend of the RGT overlayed. It is assumed that the cost trend of the engine nose box would simulate that of the UH-1 transmission.

The large number of items considered - 66 E.B. welds, 54 teeth alignment requirements, and 40 rollers - implies that

a small error in process cost evaluation could compound into
a large dollar error. The problem gets further involved when
a realistic scrap rate is to be attached to a cluster, since
there are so many elements that require inspection on the
finished cluster. Effort must certainly be directed toward
developing salvage procedures such as machining-off a defective
roller, E.B. welding another one on, and then finish-grinding
without adversely affecting the other characteristics on the
finished cluster.

CONCLUSIONS

Extensive detail design studies for the proposed RGT and TSPT systems revealed the following general conclusions.

1. Of the various RGT systems studied, the 6x6 nonpreloaded configuration, incorporating opposed helical final stages, ball-joint carrier retention, and electron beam welded cluster gear assemblies is superior for adaptation to a UH-1 type helicopter.

    (a) The high-speed pinion gear tooth requirements tend to size the entire RGT.

2. Use of a three-planet idler, ball-joint carrier, cylindrical idler roller bearing, spread center conventional planetary stage in the high-speed section of the TSPT proposed for adaptation to the UH-1 type helicopter is entirely feasible.

    (a) The idler bearing life requirements tend to size the entire stage.

3. Neither system must be restricted by a coaxial main rotor mast location if size and weight advantages are to be obtained.

Comparative evaluations of the UH-1, RGT, and TSPT drive systems within the study objective criteria suggest the following rankings:

4. Adaptation of high-speed drives through elimination of the engine SDG offers significant weight savings in both the hardware and effective regimes in the UH-1 type helicopter.

    (a) The TSPT ranks first with a potential hardware weight reduction of 134 lbs.

    (b) The RGT ranks second with a similar figure of 83 lbs.

5. Both high-speed drives offer an increased reliability above the existent UH-1 level. The calculated 1-hour reliabilities are:

    (a) RGT - .9964

    (b) TSPT - .9961

    (c) UH-1 - .9956

6. Both high-speed drives exhibit increased drive train efficiency above the existent UH-1 system. Their rankings are:

   (a) RGT - 97.73%

   (b) TSPT - 97.59%

   (c) UH-1 - 97.36%

7. The maintainability of the RGT, the TSPT, and the UH-1 systems are essentially identical. There is no significant difference in the assembly techniques or work aid expense involved in overhaul.

8. The manufacturing cost study analysis predicts the following relative rankings:

   (a) TSPT - .92

   (b) UH-1 - 1.00

   (c) RGT - 1.20

Additional related system studies indicated the following:

9. The high-speed accessory study reveals significant weight savings (13 lbs net) can be achieved through the use of a 12,000 rpm generator for the electrical system. No other weight savings were currently attainable in the remaining accessory systems.

10. The use of supercritical shafting in the antitorque rotor drive offers no advantages in the adaptation of a high reduction drive system to the UH-1 helicopter.

11. Further engine system modification (beyond simple removal of the SDG) to replace the bleed air driven cooling fan with a direct shaft drive fan yields additional weight and efficiency advantages.

Demonstration of the above conclusions requires the implementation of a fully integrated design, manufacture, bench test, ground run, and flight test program.

BIBLIOGRAPHY

1. Nasvytis, A. L., and Bauer, J. E., <u>Parametric Study on the Roller Gear Reduction Drive</u>, USAAVLABS Technical Report 64-29, U. S. Army Aviation Materiel Laboratories, Fort Eustis, Virginia.

2. Thompson Ramo Wooldridge Engineering Report 6371, <u>Endurance Test of AN-1 Roller Gear Drive</u>, USAAVLABS Technical Report 65-31, U. S. Army Aviation Material Laboratories, Fort Eustis, Virginia.

3. <u>High Speed Drive Train</u>, U. S. Army Aviation Materiel Laboratories Contract DA44-177-AMC-411(T), 28 June 1966.

4. <u>Modification Agreement No. 3</u>, Supplemental Agreement to Contract No. DA 44-177-AMC-411(T), 1967.

5. <u>Analysis, Design, and Feasibility Study for Installation of a High Speed Roller Gear Transmission in the UH-1 Helicopter</u>, Bell Helicopter Company, Report No. 25)-099-314, 13 May 1966.

6. Braddock, C. E., and Hopfensperger, L. J., <u>Designing Planetary Gears to Operate with Low Viscosity Synthetic Lubricants</u>, Society of Automotive Engineers, 1968.

7. McIntire, W. L., and Malott, R. C., <u>Advancement of Spur Gear Design Technology</u>, USAAVLABS Technical Report 66-85, U. S. Army Aviation Materiel Laboratories, Fort Eustis, Virginia, December 1966.

8. Jones, A. B., and Harris, T. A., <u>Analysis of a Rolling-Element Idler Gear Bearing Having a Deformable Outer-Race Structure</u>, ASME, 1961.

9. Chiu, Y. P., and McCool, J. I., <u>Calculation of Minimum Lubricant Film Thickness in Rolling Bearings</u>, SKF Research Laboratory Report No. AL64L006, 1964.

10. Baile, G. H., et al, 1963 <u>Aero-Space Research</u>, SKF Research Laboratory Report No. AL63M003, 1963.

11. McIntire, W. L., et al, <u>Bending Strength of Spur and Helical Gear Teeth</u>, AGMA 229.11, 1967.

12. Earles, D. R., and Eddins, M. F., <u>Reliability Engineering Data Series Failure Rates</u>, AVCO Corporation, 1962.

13. Study of Helicopter Transmission Ground Test Requirements, Vitro Laboratories, SSL-AD-T-60(66), 27 December 1967.

14. Bowen, C. W., Pitting Endurance of Carburized Spur Gears in Synthetic Lubricants, presented at the AGMA Technical Meeting, Chicago, Illinois, November 1967.

15. Weibull, W., A Statistical Theory of the Strength of Materials, Royal Swedish Academy of Engineering Sciences (Stockholm), 1939.

16. Lundberg, G., Palmgren, A., Dynamic Capacity of Rolling Bearings, ACTA POLYTECHNICA, Royal Swedish Academy of Engineering Sciences, 1947.

17. Lundberg, G., Palmgren, A., Dynamic Capacity of Roller Bearings, ACTA POLYTECHNICA, Royal Swedish Academy of Engineering Sciences, 1952.

18. Model UH-1 Maintainability and Reliability Program, per Contract DA 23-204-AMC-03694(T).

19. U. S. Army T-53 Reliability and Maintainability Evaluation Program, Report 1753.5.1.

20. 1400 Horsepower UH-1 Planetary Test on Regenerative Planetary Test Machine, Bell Helicopter Company Report No. 204-099-783, 1966.

21. Dudley, Darle W., Gear Handbook, The Design, Manufacture and Application of Gears, McGraw-Hill Book Co., 1962.

22. Aerospace Structural Materials Handbook, Vol. 1, Ferrous Alloys, Syracuse Univ. Press, Rev. 3, March 1966.

23. Zaretsky, E. V., Anderson, W. J., Material Properties and Processing Variables and Their Effect on Rolling Element Fatigue, NASA Tech Memorandum, TMX-52227.

24. Palmgren, Arvid, Ball and Roller Bearing Engineering, S. H. Burbank & Company, Philadelphia, Pa., Copyright 1945, 1946, 1959, SKF Industries, Philadelphia, Pa.

25. Bowen, C. W., Low Speed Bearing Fatigue Problems and Their Possible Relation to Gear Problems, Presented at Aerospace Gearing Committee Meeting, Orlando, Florida, February 1964.

POWER LOSS

Power Loss in Input Bevel Gears

$$P_L = 50f \, (\cos \Gamma + \cos Y) \, \frac{\cos \Psi^2}{\cos \emptyset_n} \left(\frac{H_S^2 + H_t^2}{H_S + H_t} \right)$$

Γ = Pitch Cone Angle of Gear

Y = Pitch Cone Angle of Pinion

Ψ = Spiral Angle

$\emptyset_n$ = Normal Pressure Angle

f = Coefficient of Friction

$$H_S = \left(\frac{M_G + 1}{M_G} \right) \left[\sqrt{\left(\frac{r_o}{r} \right)^2 - \cos \emptyset^2} - \sin \emptyset \right]$$

$$H_t = (M_G + 1) \left[\sqrt{\left(\frac{R_o}{R} \right)^2 - \cos \emptyset^2} - \sin \emptyset \right]$$

M_G = Gear Ratio$_1$ $\gtrless$ 1

r_o = Outside Radius of Pinion

R_o = Outside Radius of Gear

r = Pitch Radius of Pinion

R = Pitch Radius of Gear

UH-1 Input Bevel Set

$$P_L = 50f \, (\cos \Gamma + \cos Y) \left(\frac{\cos \Psi^2}{\cos \emptyset_n} \right) \left(\frac{H_S^2 + H_t^2}{H_S + H_t} \right)$$

$\Psi = 35°$	$\cos \Gamma = .42367$
$\Gamma = 64°56'$	$\cos Y = .90582$
$Y = 25°4'$	$\cos \emptyset = .93969$
$\emptyset = 20°$	$\sin \emptyset = .34202$
$r_o = 5.775$	$\cos \Psi = .81915$

$$r = 5.380$$

$$R_o = 11.590$$

$$R = 11.501$$

$$H_S = \left(\frac{62}{29} + 1\right)\left[\sqrt{\left(\frac{11.59}{11.501}\right)^2 - \cos^2 20° - \sin 20°}\right]$$

$$= .06906$$

$$H_t = \left(\frac{62/29 + 1}{62/29}\right)\left[\sqrt{\left(\frac{5.775}{5.38}\right)^2 - \cos^2 20° - \sin 20°}\right]$$

$$= .2595$$

$$P_L = 50f\ (.2083)$$

$$f = .035$$

$$P_L = (.00365)(hp)$$

$$hp = 1250$$

$$P_L = (.00365)(1250) = 4.56 \text{ HP}$$

6x6C Input Bevel Set

$$P_L = 50f\ (\cos \Gamma + \cos Y)\left(\frac{\cos^2 \psi}{\cos \emptyset_n}\right)\left(\frac{H_S^2 + H_t^2}{H_S + H_t}\right)$$

$\psi = 30°$	$\cos \Gamma = .866$
$\Gamma = 56°33'$	$\cos Y = .55121$
$Y = 33°27'$	$\cos \emptyset = .83437$
$r_o = 2.229$	$\cos \emptyset_n = .93969$
$r = 2.125$	$\sin \psi = .34202$
$R_o = 3.257$	
$R = 3.217$	
$\emptyset = 20°$	

$$H_S = \left(\frac{56/37 + 1}{56/37}\right)\quad \left(\frac{2.229}{2.125}\right)^2 - (.93969)^2 - .34202$$

$$= .2061$$

195

$$H_t = \left(\frac{56}{37} + 1\right) \quad \left(\frac{3.257}{3.217}\right)^2 - (.93969)^2 - .34202$$

$$= .0875$$

$$P_L = 50f(.55121 + .83437)\left(\frac{.866^2}{.93969}\right)\left(\frac{.2061^2 + .0875^2}{.2061 + .0875}\right)$$

$$= (12.59f)(hp)$$

$$f = .03$$

$$P_L = (12.59)(.03)(hp) = (.00378)(hp)$$

$$hp = 1250$$

$$P_L = (.00378)(1250) = 4.72 \text{ hp}$$

Separator Loss, UH-1 Lower Planet Bearing

$$P_S = PfVN$$

P = Centrifugal Load
f = Coefficient of Friction
V = Sliding Velocity
N = Number of Planets
$P = (.0000284)(4.2765)(.169)(1000)^2$
$\quad = 25.3 \text{ lbs}$
$f = .05$
$V = 785 \text{ ft/min}$

$$P_S = \frac{(25.3)(.05)(785)(4)}{(550)(60)}$$

$$= .12 \text{ hp}$$

Separator Loss, TSPT First-Stage Planet Bearing

$$P_S = PfVN$$

$P = 145 \text{ lbs}$
$f = .03$
$V = 3380 \text{ ft/min}$
$N = 3$

$$P_S = \frac{(145)(.03)(3380)(3)}{(550)(60)} = 1.337 \text{ hp}$$

| | | Friction | |
		Torque (In.-Lb)	HP
UH-1 BEARING			
204-040-346	1	2.004	.210
Input Triplex	2	9.561	1.000
	3	3.498	.993
204-040-345	1	8.562	.420
Gear shaft Duplex	2	4.922	.214
ROLLER GEAR BEARING			
Input Triplex	1	2.250	.750
	2	2.451	.817
	3	2.707	.904
Gear shaft Duplex	1	3.474	.765
	2	2.870	.632

TABLE XXVIII. BALL BEARING FRICTION LOSS

Windage Losses

The method of calculating windage loss shown in Reference 21 is adjusted below to account for the dense, oily atmosphere inside the gearbox. A brief derivation of the reference equation is given from basic propeller theory.

For the power loss due to windage, P_w

$$P_w = \frac{(n^3)(D^5)(\ell^{.7})}{10^{17}} \qquad \text{(Ref. 21)}$$

Propeller Theory

$$P = C_p \rho n^3 D^5$$

C_p = power coefficient

ρ = air density

n = rps

D = diameter in ft

P = ft-lb/sec

Conversion constant K for in. and rpm units is

in., rpm, and hp

$$K = 3.38 \times 10^{-14}$$

The assumed C_p = .124

ρ = .00238 slug/ft^3

For in. and rpm units, the referenced equation becomes

$$P_w = (n^3)(D^5)(\ell^{.7}) \times 10^{-17}$$

where $\ell^{.7}$ is the width correction (propeller is an infinitely thin disc).

For dense, oily atmosphere, the approximate mixture is

34.25 parts air to 1.0 part oil

ρ air = .00238 slug/ft^3

ρ oil = 1.748 slugs/ft^3

Correction factor, f, is

$$f = \frac{\rho G.B.}{air} = \frac{(1.748) + (34.25)(.00238)}{(35.25)(.00238)}$$

$$f = 21.8$$

The corrected value for P_w is

$$P_w = \frac{(2.18)(n^3)(D^5)(\ell^{.7})}{10^{16}}$$

P_w = hp

n = rpm

D = diameter of rotating element - inches

ℓ = width of rotating element - inches

A. UH-1 Transmission

1. Lower Sun Gear

$$P_w = \frac{(2.18)(3090)^3(6.880)^5(.933)^{.7}}{10^{16}} = .0871 \text{ hp}$$

2. Lower Planetary Pinions

$$P_w = \left[\frac{(2.18)(3840)^3(3.881)^5(1.333)^{.7}}{10^{16}}\right]4 = .0514 \text{ hp}$$

3. **Lower Carrier Assembly**

$$P_w = \frac{(2.18)(1000)^3(12.86)^5(1.56)^{.7}}{10^{16}} = .1040 \text{ hp}$$

4. **Upper Sun Gear**

$$P_w = \frac{(2.18)(1000)^3(6.88)^5(1.38)^{.7}}{10^{16}} = .0042 \text{ hp}$$

5. **Upper Planet Pinions**

$$P_w = \left[\frac{(2.18)(1240)^3(3.881)^5(1.333)^{.7}}{10^{16}}\right]8 = .0036 \text{ hp}$$

6. **Upper Carrier Assembly**

$$P_w = \frac{(2.18)(324)^3(12.86)^5(1.56)^{.7}}{10^{16}} = .0035 \text{ hp}$$

7. **Input Bevel Pinion**

$$P_w = \frac{(2.18)(6600)^3(5.0)^5(1.5)^{.7}}{10^{16}} = .258 \text{ hp}$$

8. **Input Bevel Gear**

$$P_w = \frac{(2.18)(3090)^3(10.7)^5(1.5)^{.7}}{10^{16}} = 1.1040 \text{ hp}$$

9. **Input Bevel Gear Shaft**

$$P_w = \frac{(2.18)(3090)^3(4.5)^5(13)^{.7}}{10^{16}} = .6587 \text{ hp}$$

Total UH-1 windage loss = 2.274 hp

B. RGT

1. Input Bevel Pinion

$$P_w = \frac{(2.18)(21,016)^3(3.75)^5(1.0)^{.7}}{10^{16}} = 1.495 \text{ hp}$$

2. Input Bevel Gear

$$P_w = \frac{(2.18)(13,886)^3(5.74)^5(1.0)^{.7}}{10^{16}} = 3.5698 \text{ hp}$$

3. Input Bevel Gear Shaft

$$P_w = \frac{(2.18)(13,886)^3(1.87)^5(9.68)^{.7}}{10^{16}} = .064 \text{ hp}$$

4. Sun Gear

$$P_w = \frac{(2.18)(13,886)^3(2.4)^5(4.5)^{.7}}{10^{16}} = .1303 \text{ hp}$$

5. First-Row Cluster Teeth (X_1) and Rollers

$$P_w = \left[\frac{(2.18)(6943)^3(4.976)^5(.53)^{.7}}{10^{16}}\right]12 = 1.7134 \text{ hp}$$

6. First-Row Cluster Shafts

$$P_w = \left[\frac{(2.18)(6943)^3(1.22)^5(3.94)^{.7}}{10^{16}}\right]6 = .031 \text{ hp}$$

7. First-Row Cluster Teeth (Y_1) and Rollers

$$P_w = \left[\frac{(2.18)(6943)^3(2.08)^5(.63)^{.7}}{10^{16}}\right]12 = .0249 \text{ hp}$$

8. **Second-Row Cluster Teeth (X_2) and Rollers**

$$P_w = \left[\frac{(2.18)(2430)^3(5.4755)^5(.63)^{.7}}{10^{16}}\right]12 = .1336 \text{ hp}$$

9. **Second-Row Cluster Shaft**

$$P_w = \left[\frac{(2.18)(2430)^3(1.66)^5(1.4)^{.7}}{10^{16}}\right]6 = .0003 \text{ hp}$$

10. **Second-Row Cluster Teeth (Y_2)**

$$P_w = \left[\frac{(2.18)(2430)^3(2.1586)^5(1.158)^{.7}}{10^{16}}\right]12 = .0019 \text{ hp}$$

11. **Ring Gear Adapter**

$$P_w = \frac{(2.18)(324)^3(18.7)^5(3.7)^{.7}}{10^{16}} = .0416 \text{ hp}$$

12. **Ring Gear**

$$P_w = \frac{(2.18)(324)^3(18.0)^5(3.0)^{.7}}{10^{16}} = .0301 \text{ hp}$$

Total RGT windage loss = 7.236 hp

C. **TSPT**

1. **First-Stage Sun Gear**

$$P_w = \frac{(2.18)(13,886)^3(4.0)^5(.75)^{.7}}{10^{16}} = .4881 \text{ hp}$$

2. **First-Stage Carrier**

$$P_w = \frac{(2.18)(3090)^3(10.1)^5(1.38)^7}{10^{16}} = .8470 \text{ hp}$$

3. **First-Stage Planet Gears**

$$P_w = \left[\frac{(2.18)(9063)^3(4.6)^5(0.8)^{.7}}{10^{16}} \right] 3 = .8577 \text{ hp}$$

4. RGT Bevels = 5.288 hp

5. UH-1 Planetaries = .2538 hp

Total TSPT windage loss = 7.5754 hp

POWER LOSS IN PITCH LINE ROLLERS

1. **Sun-X_1 Mesh**
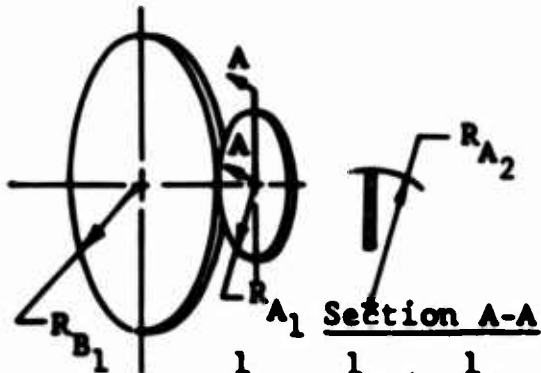
R_{A_1} = 1.20 in.

R_{A_2} = 4.50 in.

R_{B_1} = 2.40 in.

R_{B_2} = ∞

P = 511 lbs

$$\cos \tau = \frac{\dfrac{1}{R_{A_1}} - \dfrac{1}{R_{A_2}} + \dfrac{1}{R_{B_1}} - \dfrac{1}{R_{B_2}}}{\dfrac{1}{R_{A_1}} + \dfrac{1}{R_{A_2}} + \dfrac{1}{R_{B_1}} + \dfrac{1}{R_{B_2}}} = \frac{\dfrac{1}{1.2} - \dfrac{1}{4.5} + \dfrac{1}{2.4} - 0}{\dfrac{1}{1.2} + \dfrac{1}{4.5} + \dfrac{1}{2.4} + 0}$$

$$= \frac{.833 - .222 + .4166 - 0}{.833 + .222 + .4166 + 0} = \frac{1.0276}{1.4716}$$

$$= .698$$

$$\mu = 1.899 \quad ; \quad V = .609$$

$$g = \left[\frac{3P(\Theta_A + \Theta_B)}{8\left(\dfrac{1}{R_{A_1}} + \dfrac{1}{R_{B_1}} + \dfrac{1}{R_{A_2}} + \dfrac{1}{R_{B_2}}\right)} \right]^{1/3}$$

$$\Theta_A = \frac{4(1-.25^2)}{30 \times 10^6} \quad ; \quad \Theta_B = \frac{4(1-.25^2)}{30 \times 10^6}$$

$$g = \left[\frac{(3)(511)(2.5)(10^{-7})}{(8)(1.4716)} \right]^{1/3} = .0319$$

$$a = \mu g = (1.899)(.0319) = .0605 \text{ in.}$$

$$b = V g = (.609)(.0319) = .0194 \text{ in.}$$

204
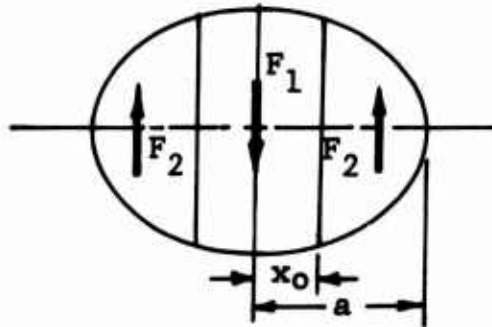
$$x_o = (.347)(a) = (.347)(.0605) = .021 \text{ in.}$$

Friction Forces

$$F_1 = \frac{3Pf}{2a}\left(\frac{x_o - x_o^3}{3a^2}\right) = \frac{(3)(511)(.0075)}{(2)(.0605)}\left(.021 - \frac{.021^3}{(3)(.0605)^2}\right)$$

$$= 1.915$$

$$F_2 = \frac{3Pf}{4a}\left(\frac{2a}{3} + \frac{x_o^3}{3a^2} - x_o\right)$$

$$= \frac{(3)(511)(.0075)}{(4)(.0605)}\left(\frac{(2)(.0605)}{3} + \frac{(.021)^3}{(3)(.0605)^2} - .02\right)$$

$$= .9585$$

Friction Force Resultant

$$F_f = 2F_2 - F_1$$

$$= (2)(.9585) - 1.915$$

$$= .0019 \text{ lbs}$$

Power Loss

$$P_f = \frac{(F_f)(V_S)(N)}{(550)(60)}$$

F_f = Friction Force, lbs
V_S = Pitch Line Velocity, ft/min
N = Number of Contacts

$$= \frac{(.0019)(8725)(12)}{(550)(60)} = .006 \text{ hp}$$

205

2. $\underline{Y_1 - X_2 \text{ Mesh}}$

R_{A_1} = .9333 in.

R_{A_2} = 2.666 in.

R_{B_1} = 15.0 in.

R_{B_2} = ∞

P = 947 lbs

$$\cos \tau = \frac{\dfrac{1}{R_{A_1}} - \dfrac{1}{R_{A_2}} + \dfrac{1}{R_{B_1}} - \dfrac{1}{R_{B_2}}}{\dfrac{1}{R_{A_1}} + \dfrac{1}{R_{A_2}} + \dfrac{1}{R_{B_1}} + \dfrac{1}{R_{B_2}}} = 0.7521$$

$\mu = 2.0696$; $\gamma = .5763$

$$g = \left[\left(\frac{3P(\theta_A + \theta_B)}{8} \right) \frac{1}{\dfrac{1}{R_{A_1}} + \dfrac{1}{R_{A_2}} + \dfrac{1}{R_{B_1}} + \dfrac{1}{R_{B_2}}} \right]^{1/3} = .0389$$

$a = \mu g = (2.0696)(.0389) = .0807$ in.

$b = \gamma g = (.5763)(.0389) = .0224$ in.

$x_o = (.347)a = (.347)(.0807) = .028$ in.

Friction Forces

$$F_1 = \frac{3Pf}{2a} \left(x_o - \frac{x_o^3}{3a^2} \right) = 3.548 \text{ lbs}$$

$$F_2 = \left(\frac{3Pf}{4a} \right) \left(\frac{2a}{3} + \frac{x_o^3}{3a^2} - x_o \right) = 1.777 \text{ lbs}$$

206

Friction Force Resultant

$$F_f = 2F_2 - F_1 = .00635 \text{ lb}$$

Power Loss

$$P_f = \frac{(F_f)(V_S)(N)}{(550)(60)} = \frac{(.00635)(3397)(24)}{(550)(60)}$$

$$= .0157 \text{ hp}$$
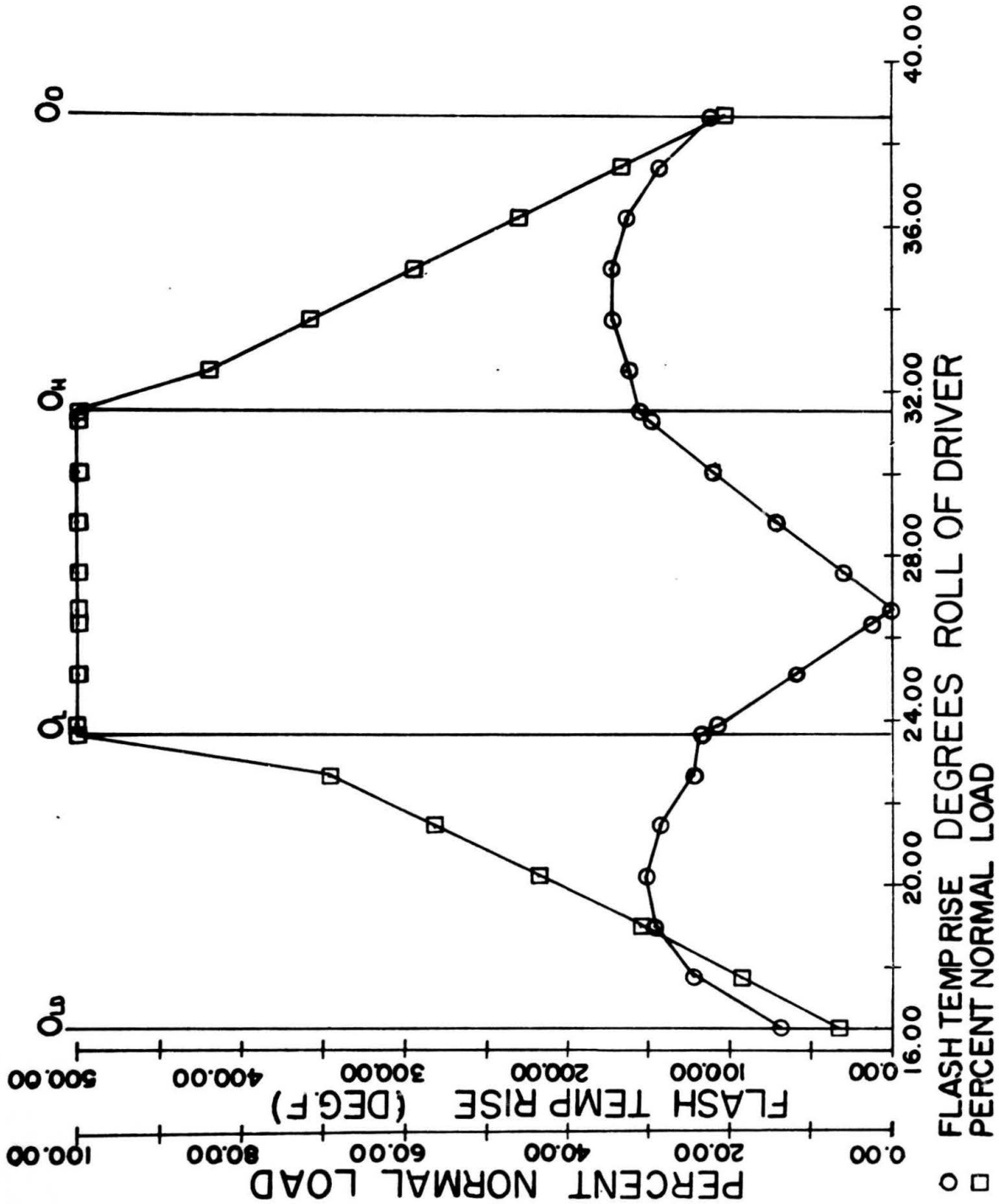
Figure 41. RGT Sun X_1 Mesh at 1138 HP - Load Diagram

Figure 42. RGT Sun X_1 Mesh at 1138 HP - Sub-Surface Shear Stress

209
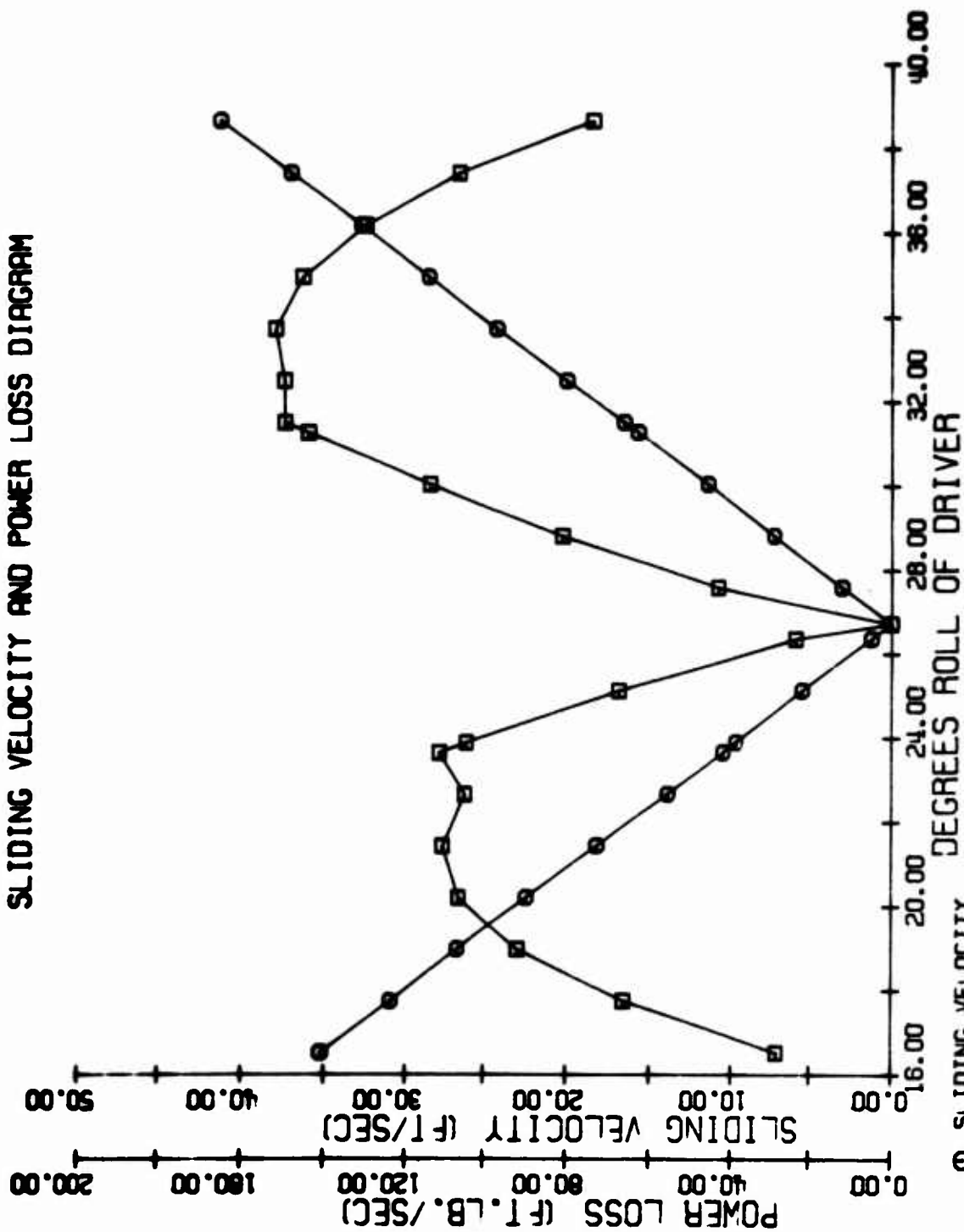
Figure 43. RGT Sun X_1 Mesh at 1138 HP - Power Loss Diagram

210
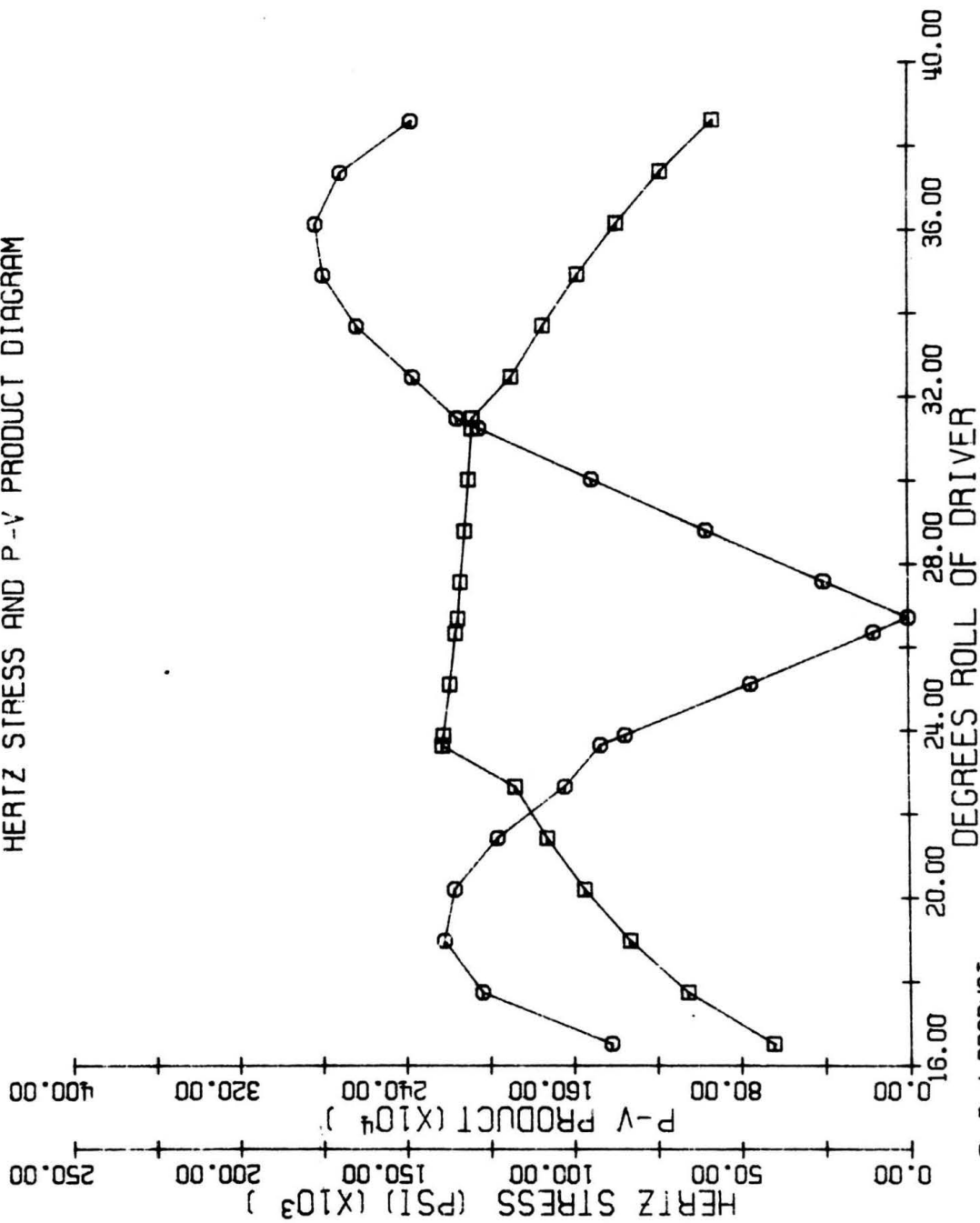
HERTZ STRESS AND P-V PRODUCT DIAGRAM

Figure 44. RGT Sun X_1 Mesh at 1138 HP - Hertz Stress Diagram

⊙ P-V PRODUCT
⊡ HERTZ STRESS

211

Figure 45. RGT Y_1-X_2 Mesh at 1138 HP - Load Diagram

212
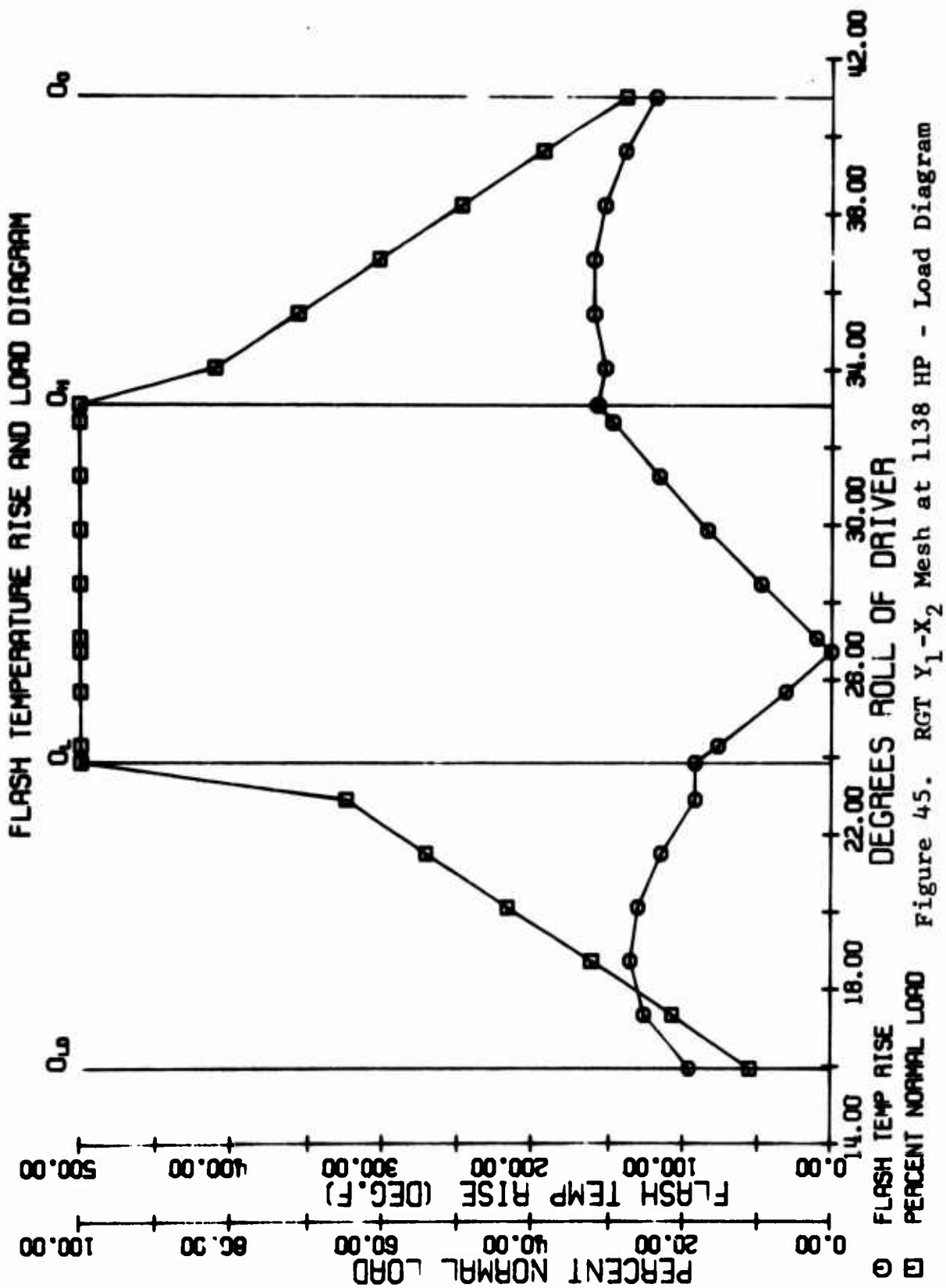
Figure 46. RGT Y_1-X_2 Mesh at 1138 HP – Shear Stress Diagram

213
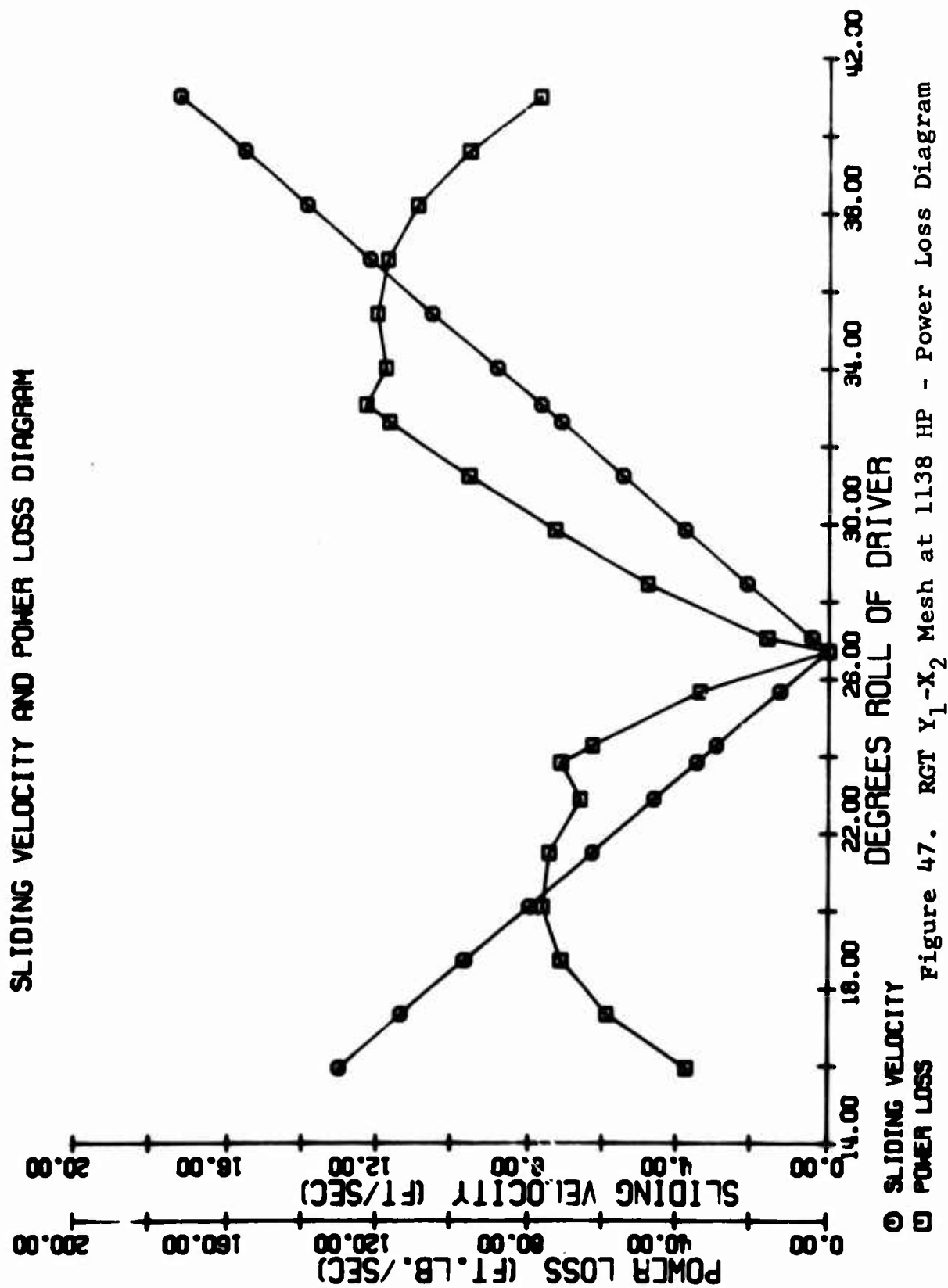
Figure 47. RGT Y_1-X_2 Mesh at 1138 HP - Power Loss Diagram

214
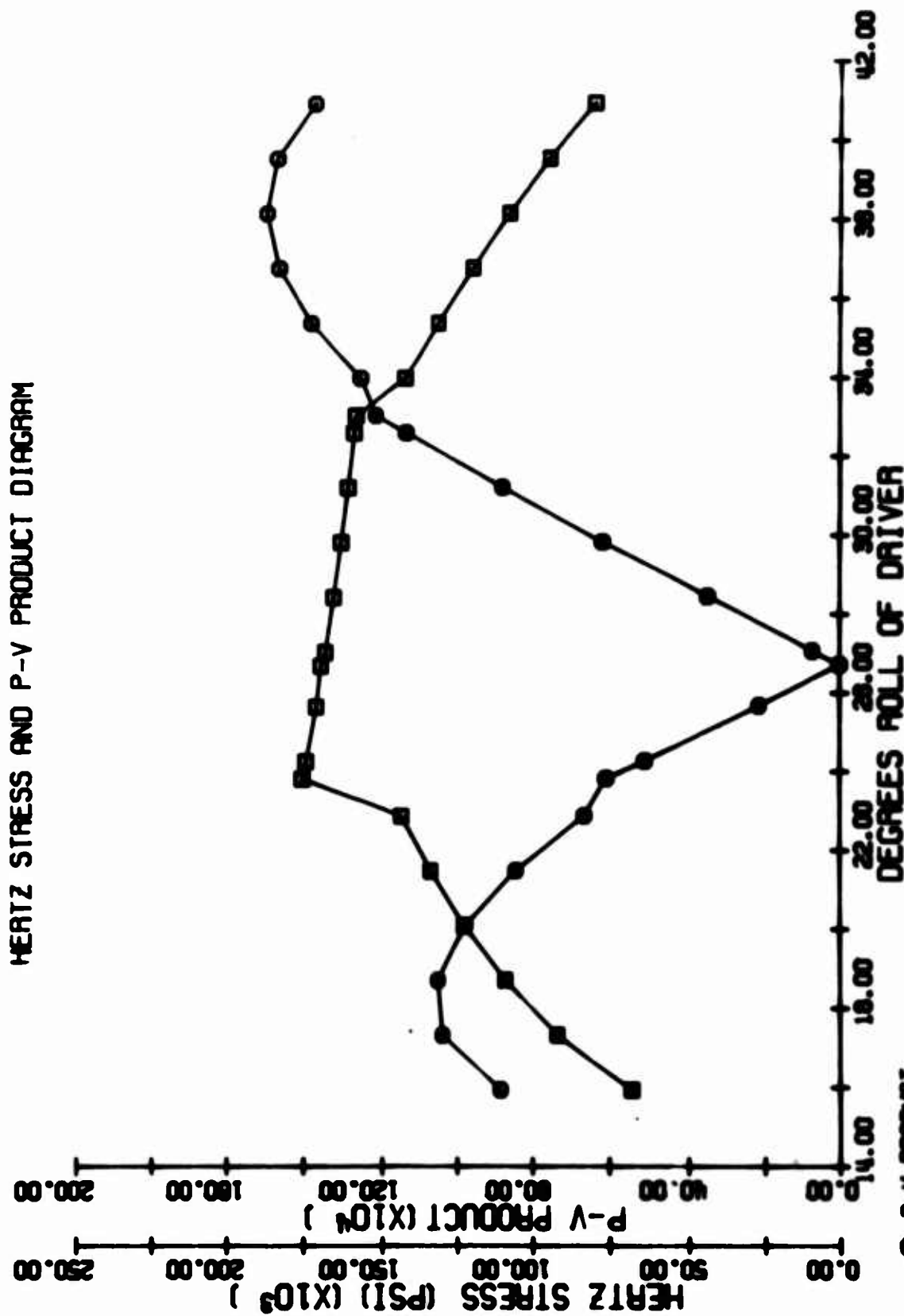
HERTZ STRESS AND P-V PRODUCT DIAGRAM

Figure 48. RGT Y_1-X_2 Mesh at 1138 HP - Hertz Stress Diagram

215
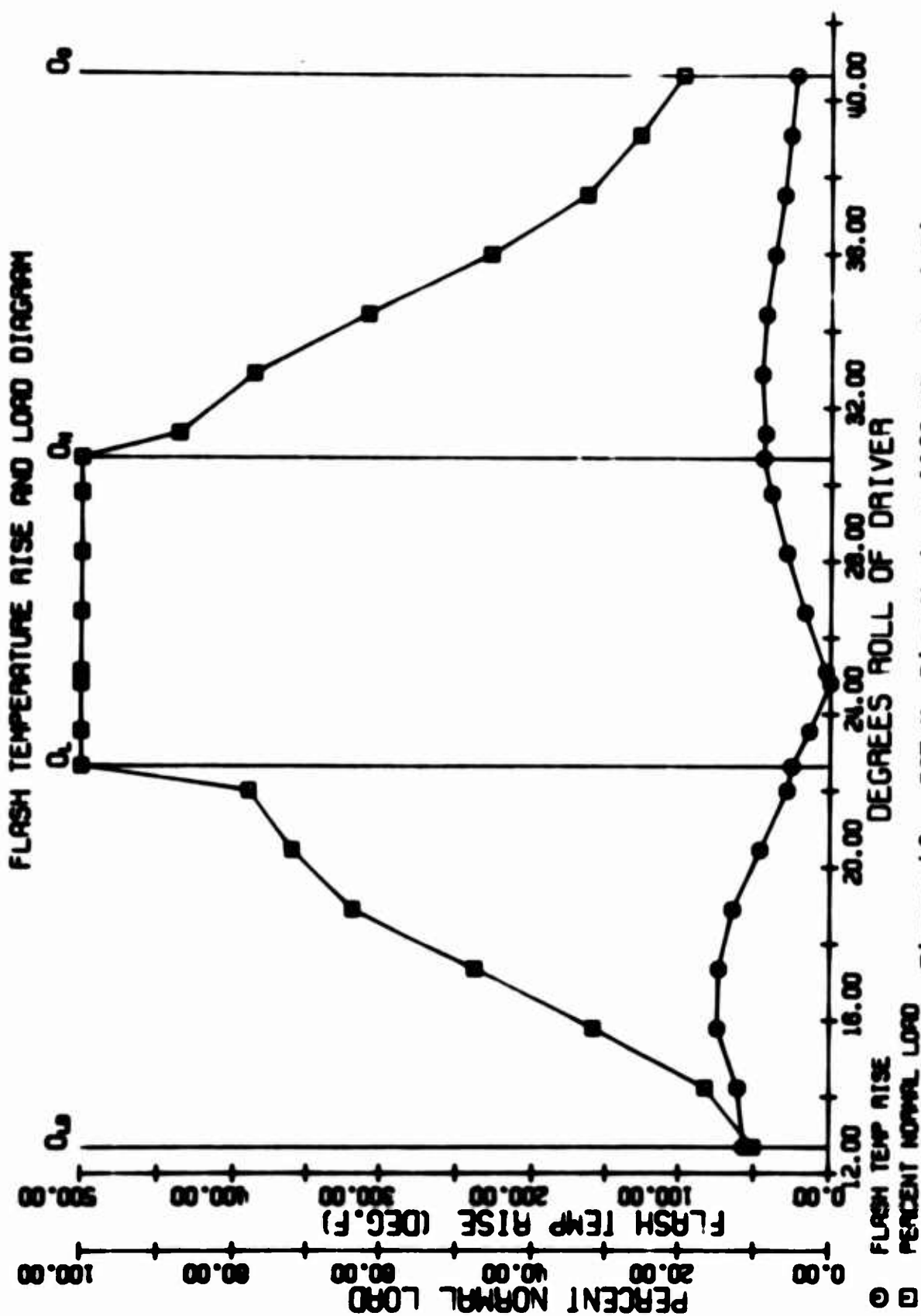
Figure 49.   RGT Y_2 Ring Mesh at 1138 HP - Load Diagram

216
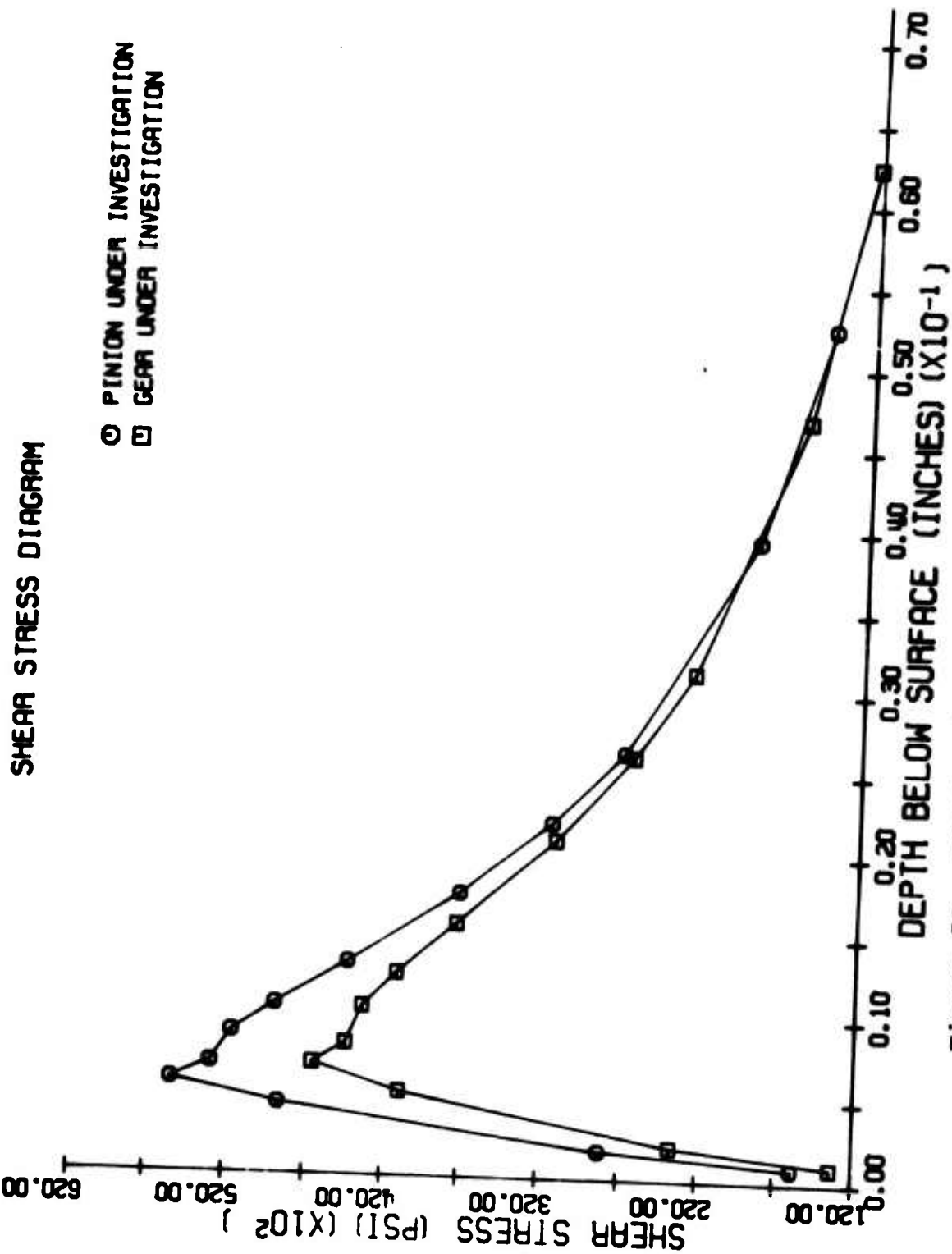
Figure 50. RGT Y_2 Ring Mesh at 1138 HP - Shear Stress Diagram

SLIDING VELOCITY AND POWER LOSS DIAGRAM

Figure 51. RGT Y₂ Ring Mesh at 1136 HP - Power Loss Diagram

210

Figure 52. RGT Y$_2$ Ring Mesh at 1138 HP – Hertz Stress Diagram
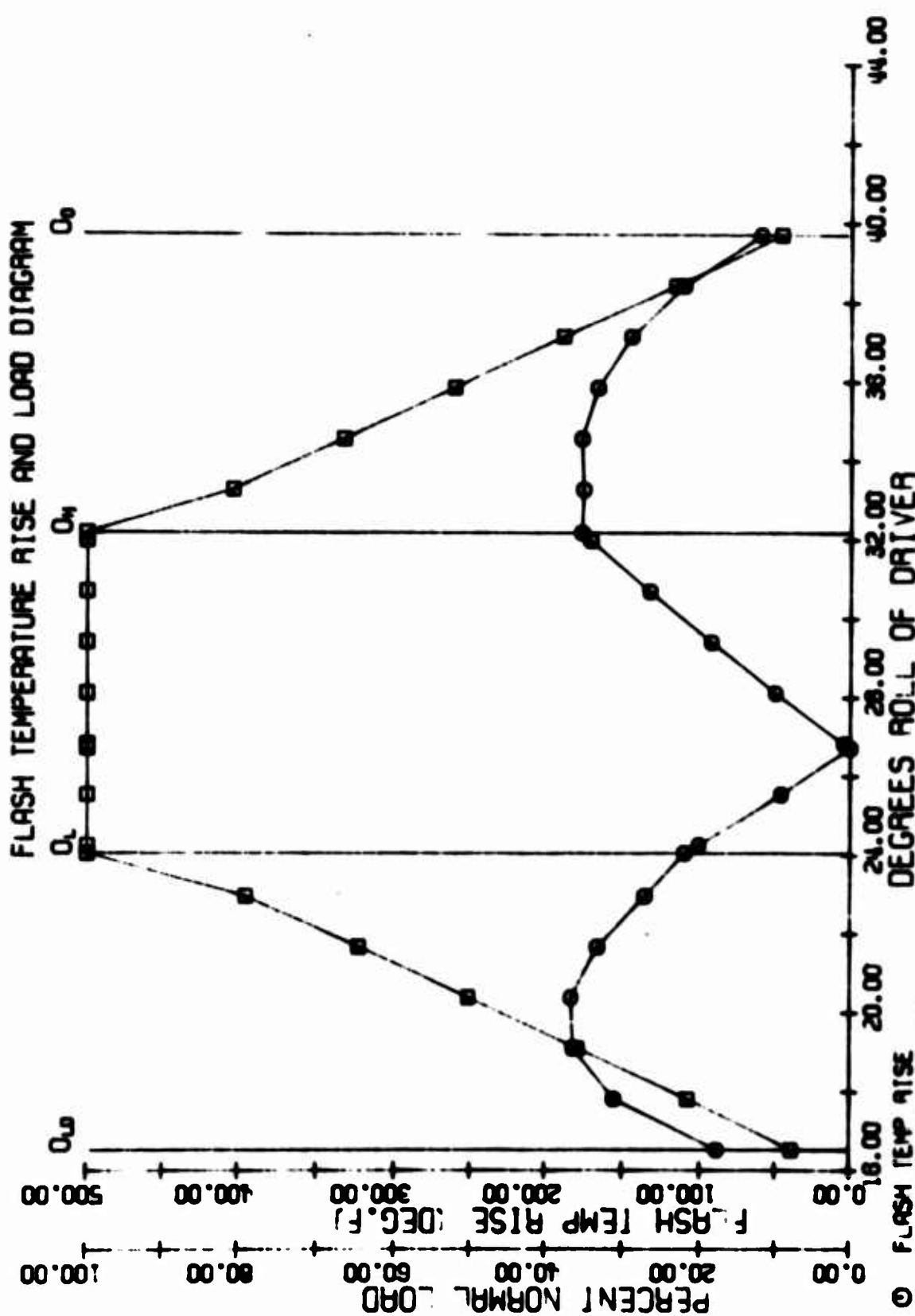
Figure 53. 6x6C Roller Gear Transmission Offset Spur Gears - Load Diagram

Figure 54. 6x6C Roller Gear Transmission Offset Spur Gears - Shear Stress Diagram
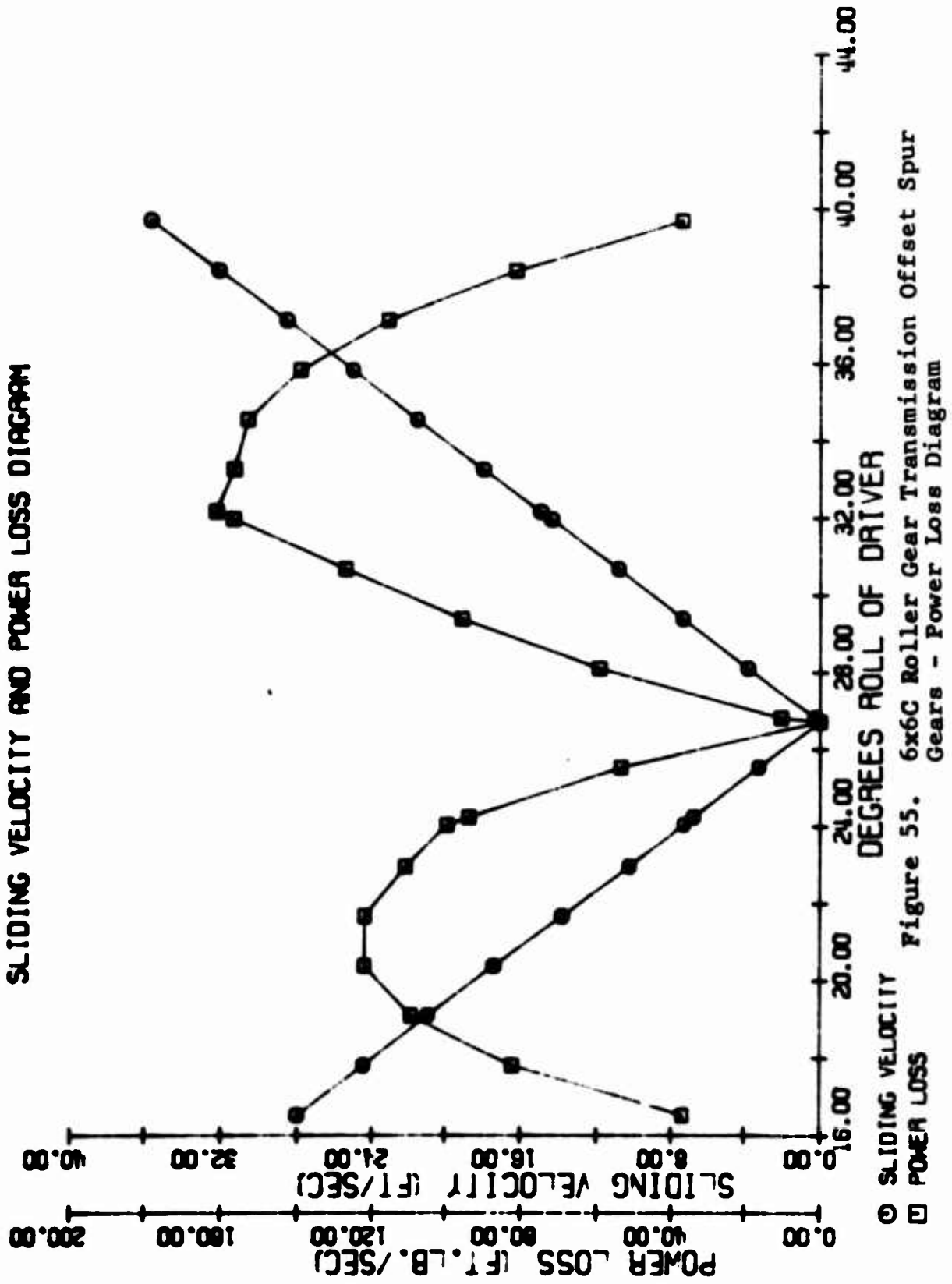
Figure 55. 6x6C Roller Gear Transmission Offset Spur Gears - Power Loss Diagram

HERTZ STRESS AND P-V PRODUCT DIAGRAM
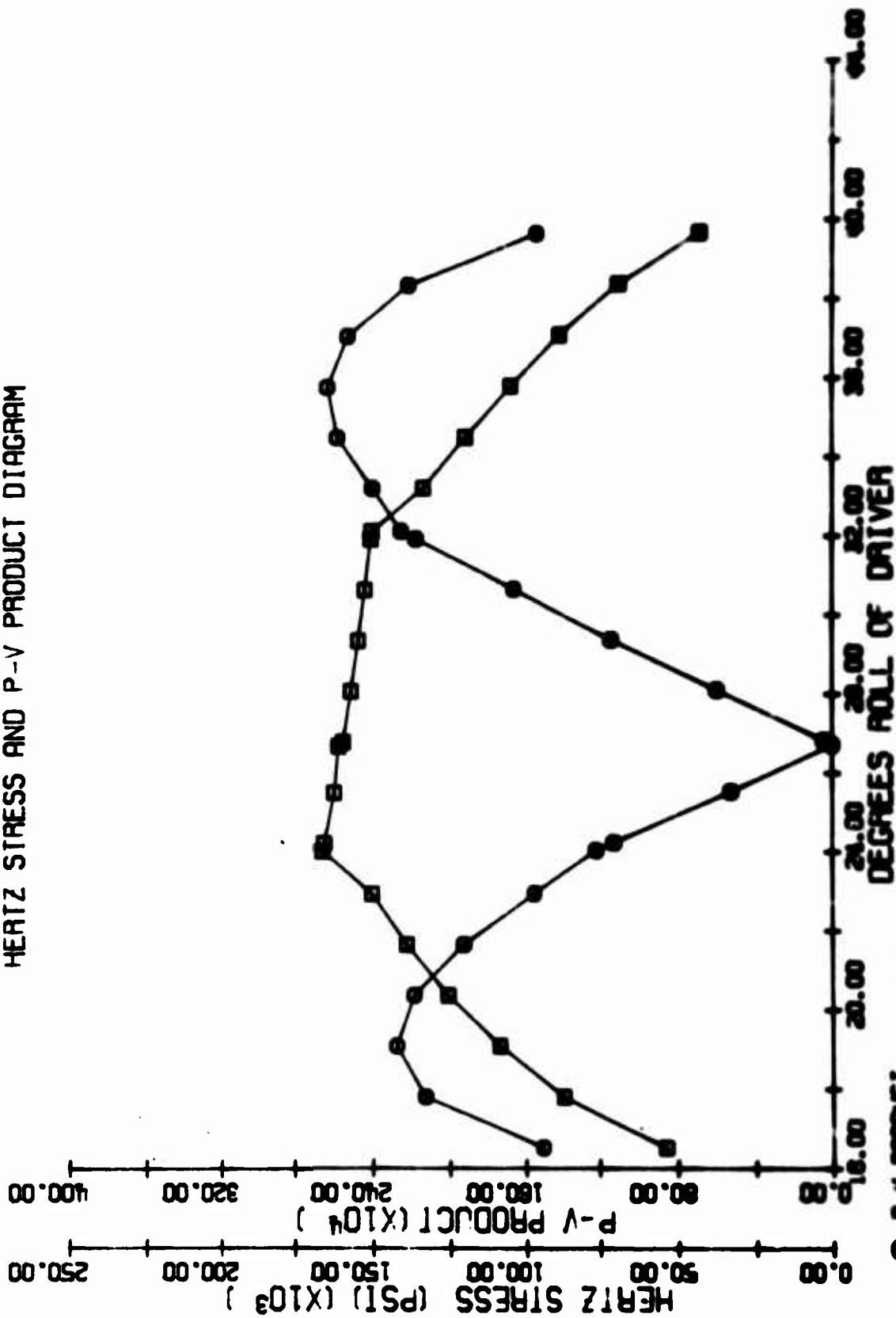
Figure 56. 6x6C Roller Gear Transmission Offset Spur
Gears - Hertz Stress Diagram

223
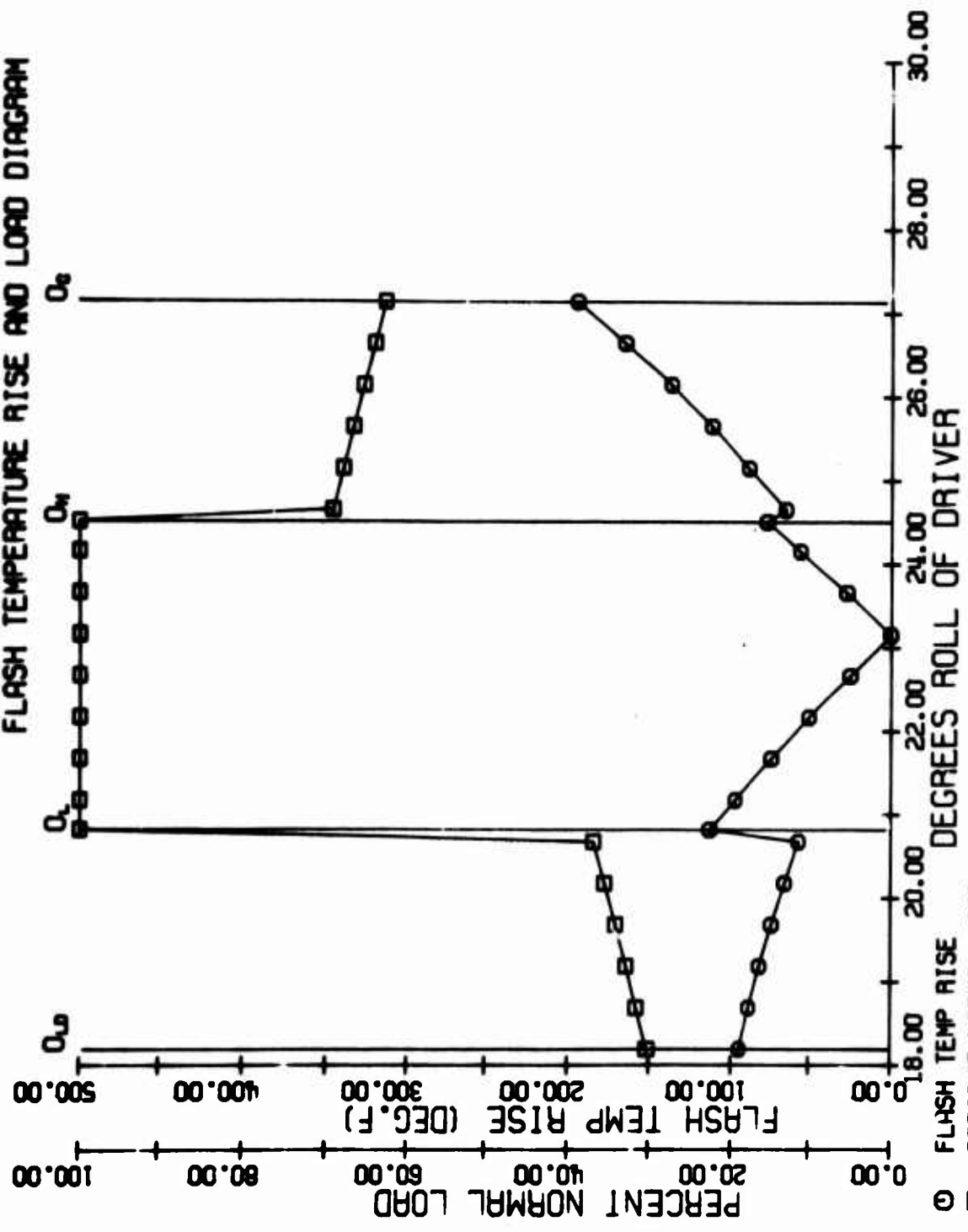
Figure 57. 204-040-108 and -329 Lower Sun Mesh 1138 HP Load Diagram

SHEAR STRESS DIAGRAM

⊙ PINION UNDER INVESTIGATION
⊡ GEAR UNDER INVESTIGATION
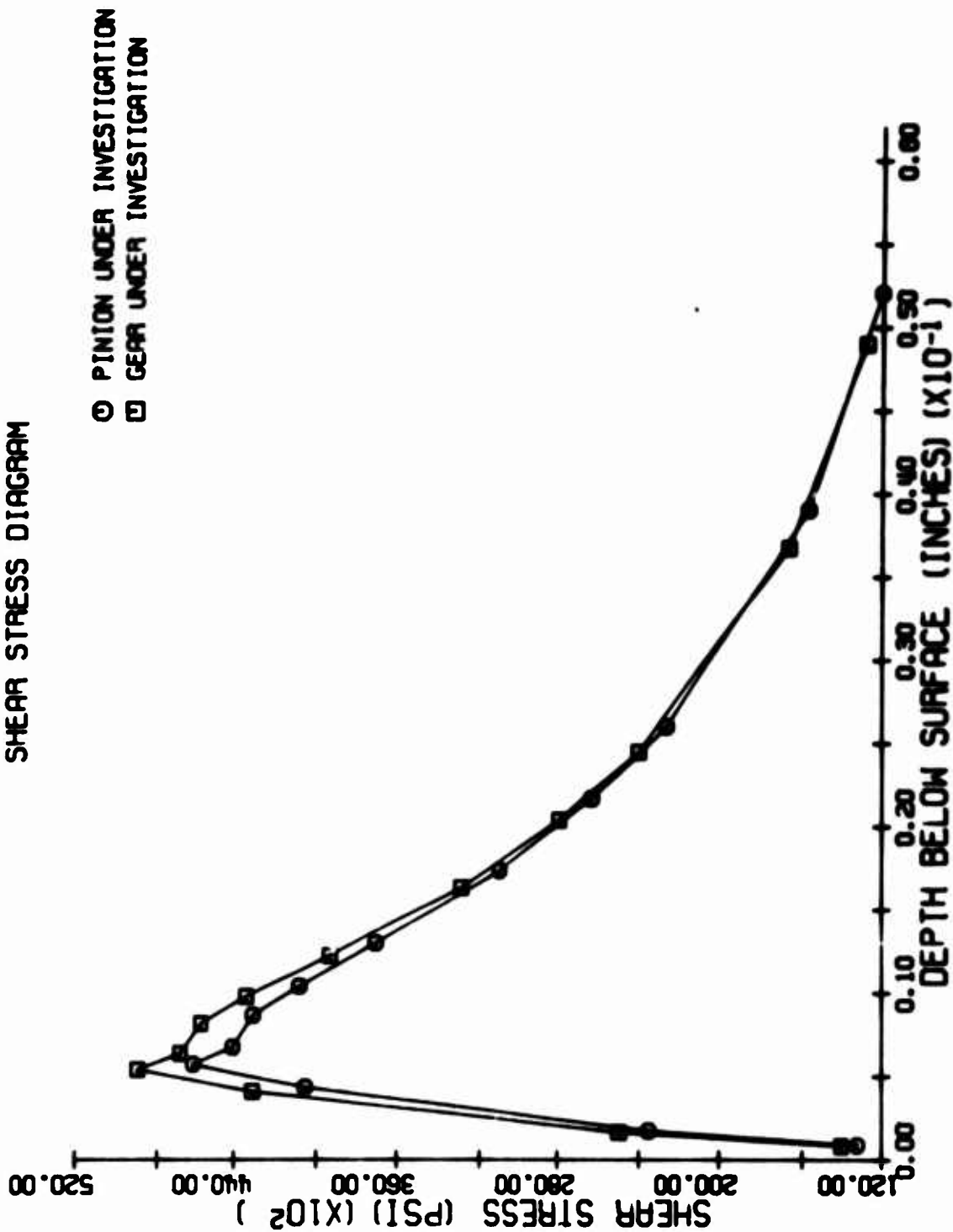
Figure 58. 204-040-108 and -329 Lower Sun Mesh 1138 HP
Sub-Surface Shear
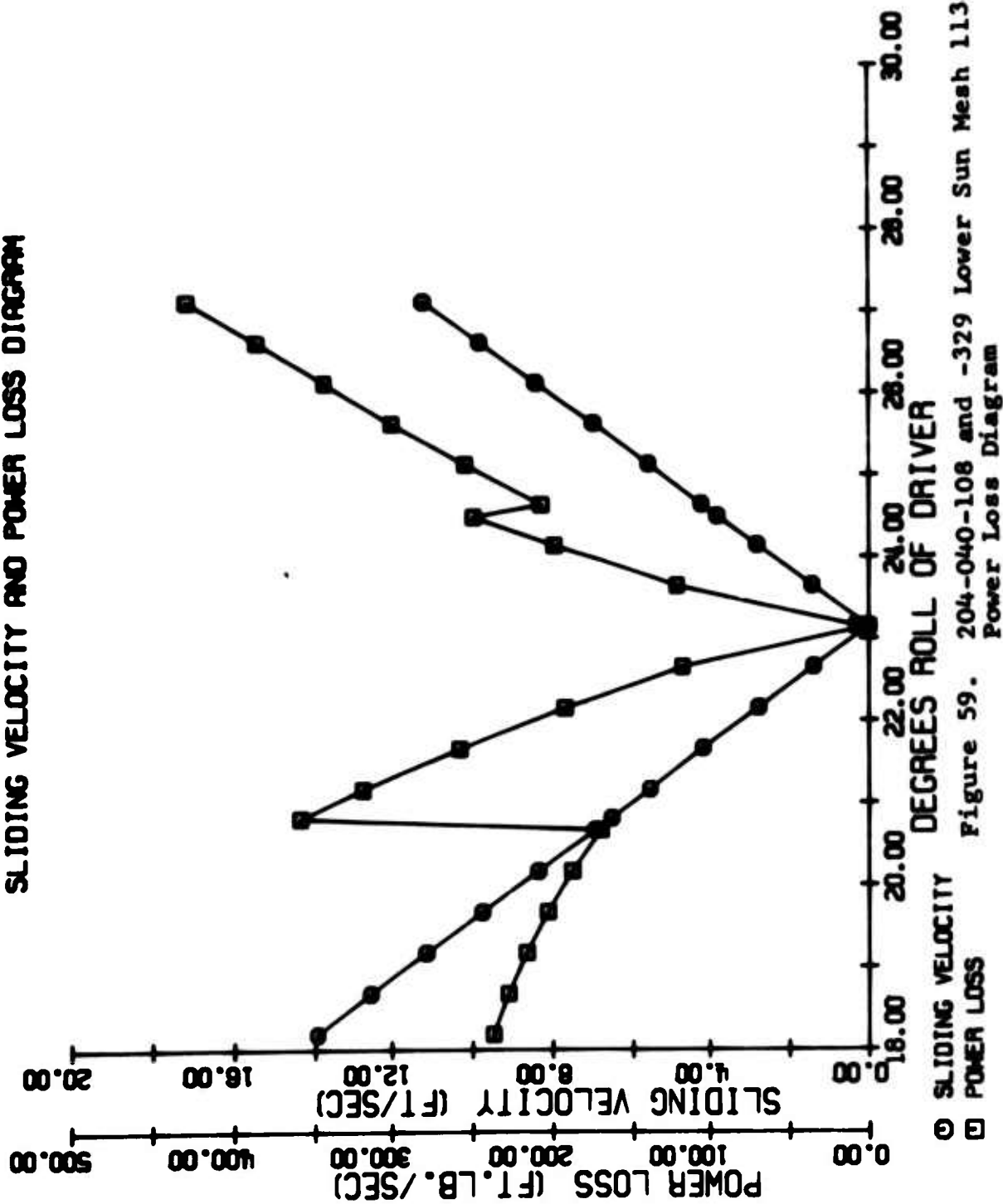
Figure 59.   204-040-108 and -329 Lower Sun Mesh
Power Loss Diagram

226

HERTZ STRESS AND P-V PRODUCT DIAGRAM

Figure 60.   204-040-108 and -329 Lower Sun Mesh 1138 HP
Hertz Stress Diagram

227
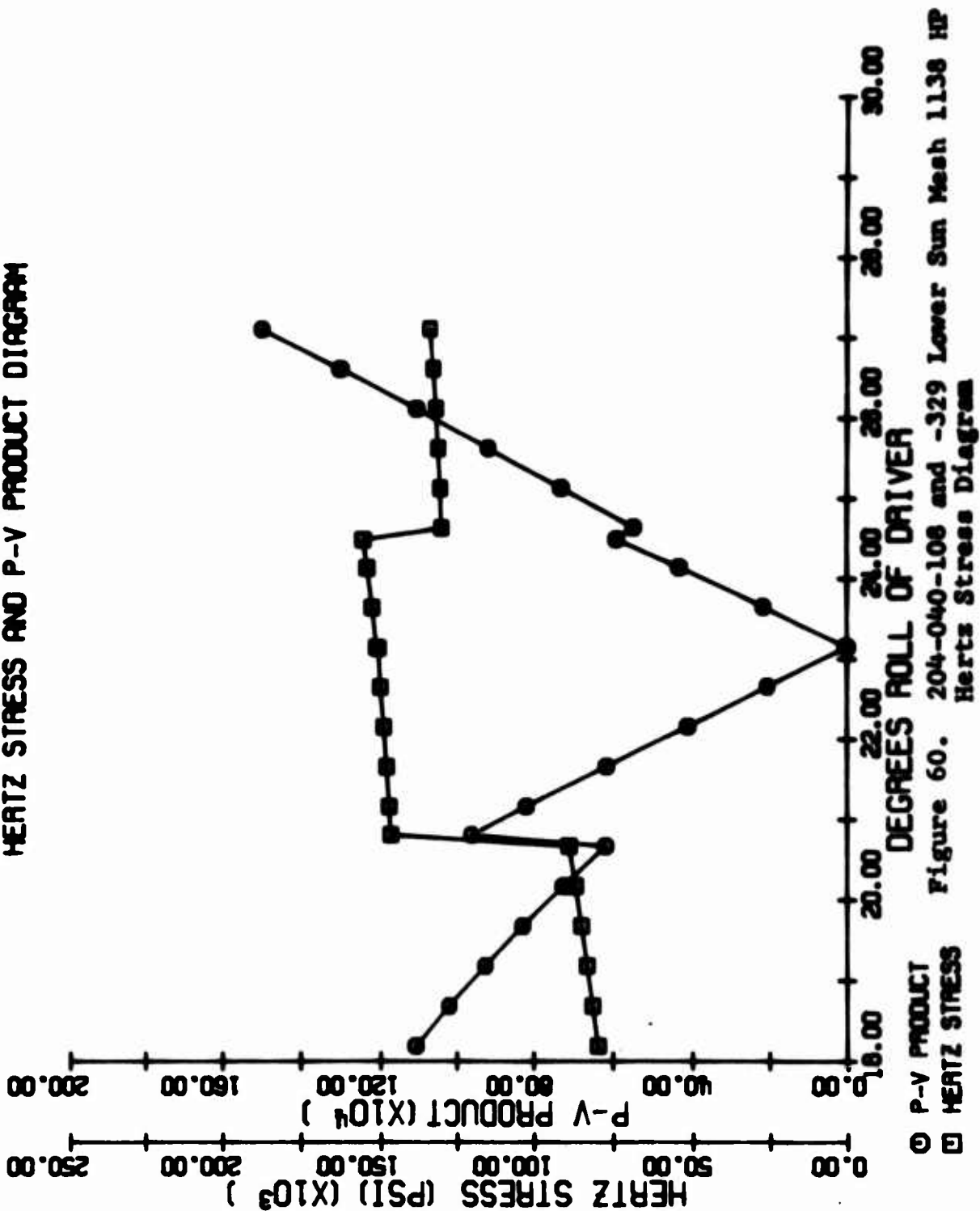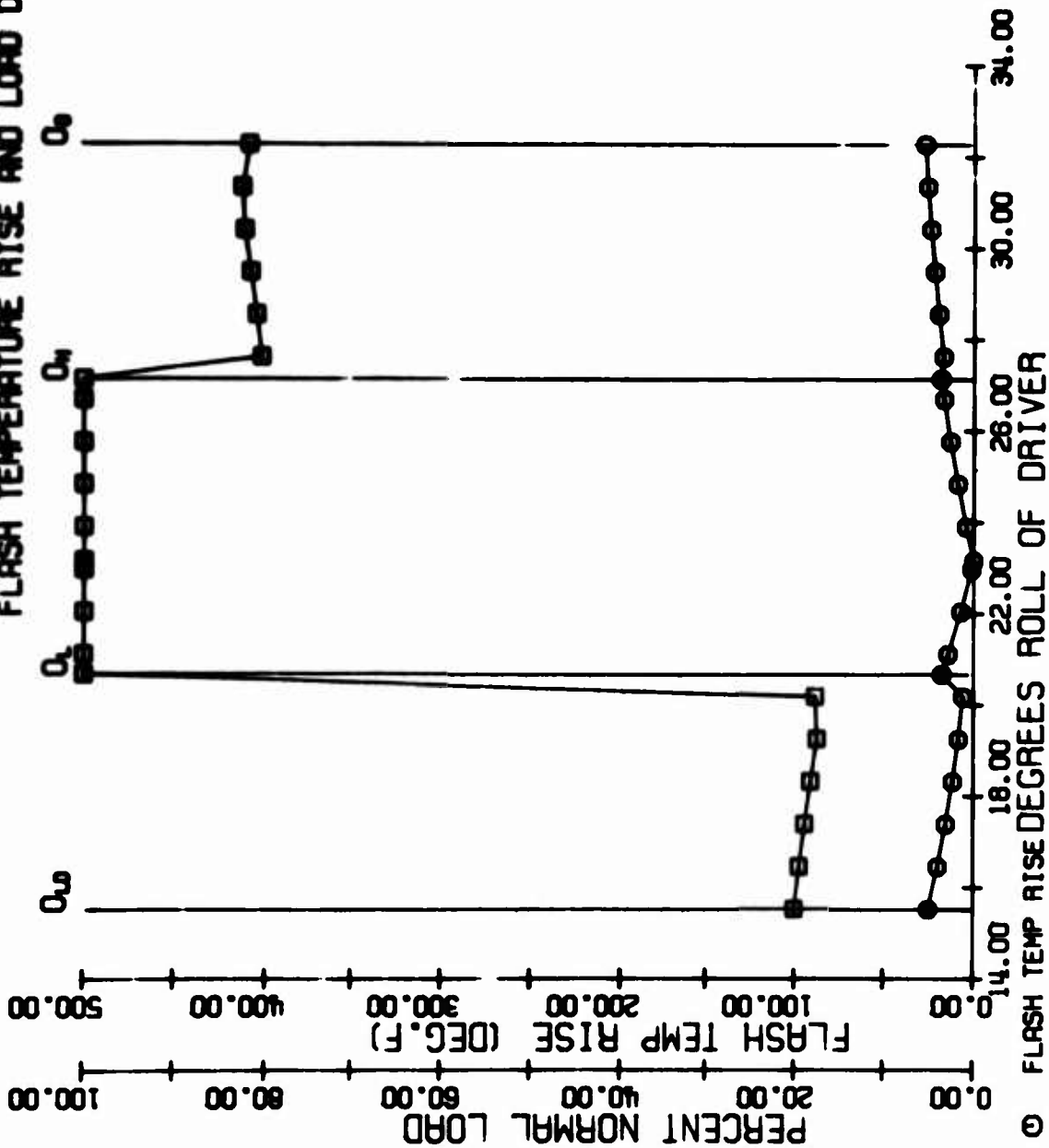
Figure 61. 204-040-108/204-040-331 Ring Planet Mesh Lower 1138 HP - Load Diagram

228
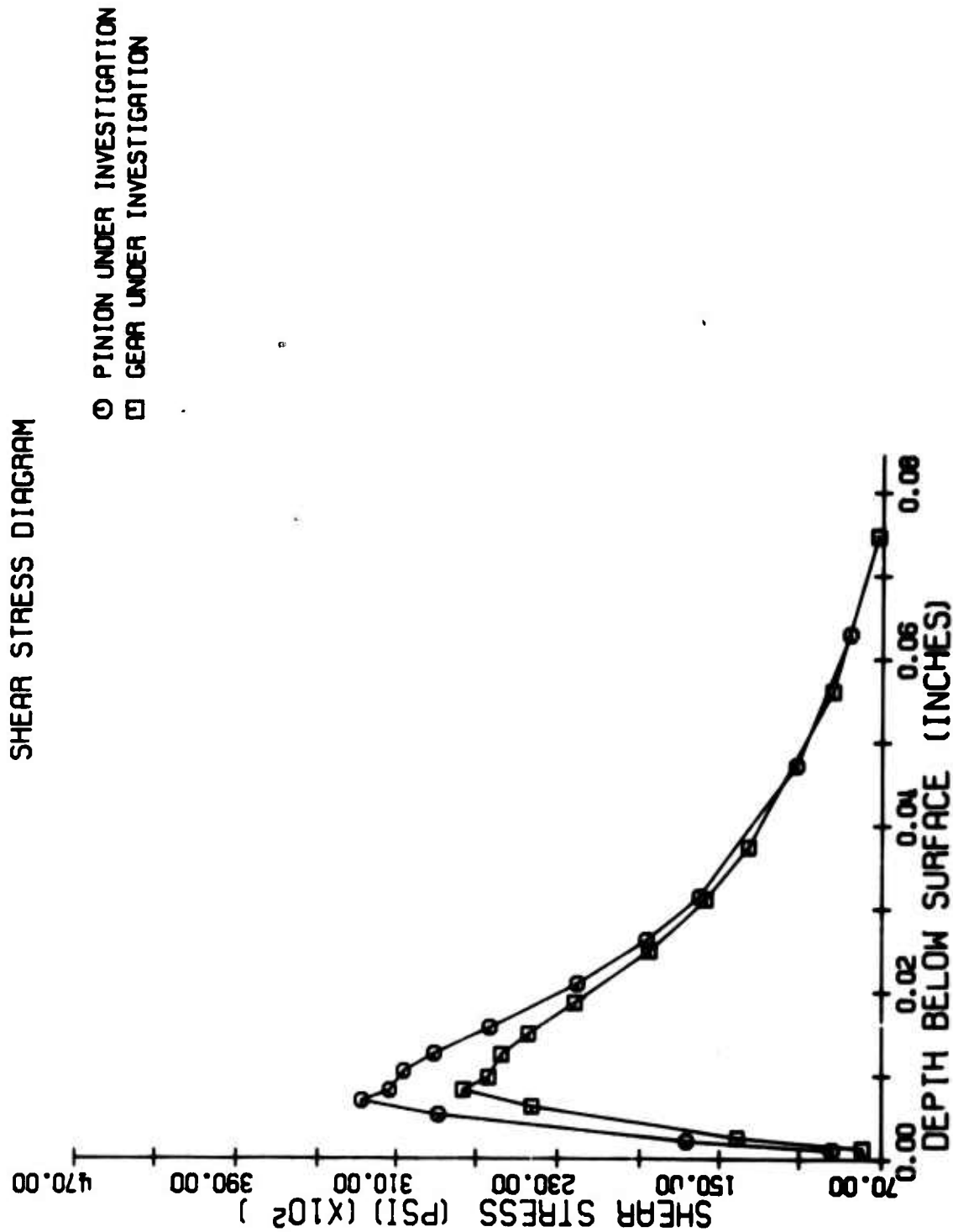
Figure 62.   204-040-108/204-040-331 Ring Planet Mesh
Lower 1138 HP - Shear Stress Diagram

229

SLIDING VELOCITY AND POWER LOSS DIAGRAM
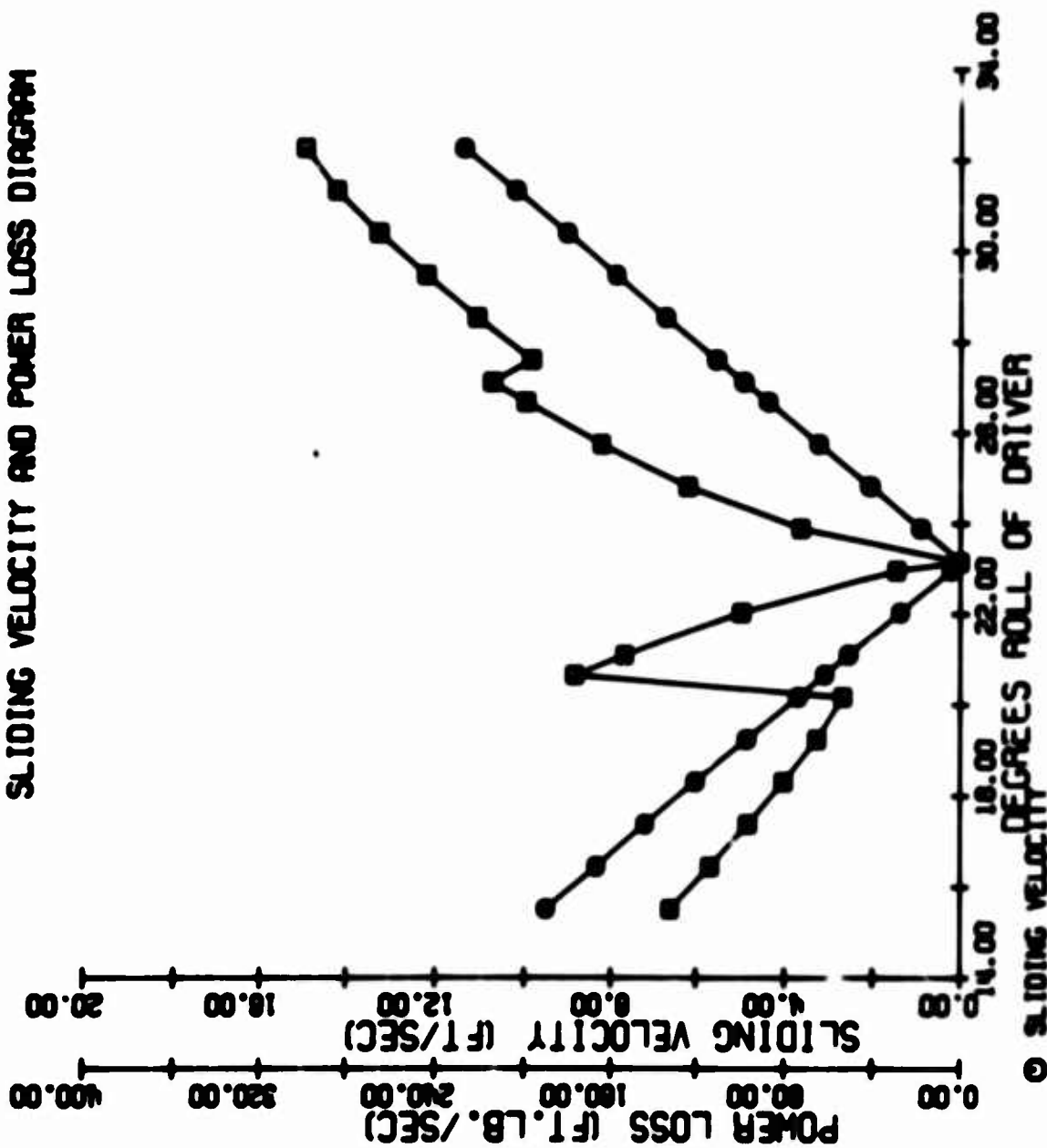
Figure 63.   204-040-108/204-040-331 Ring Planet Mesh
Lower 1138 HP - Power Loss Diagram
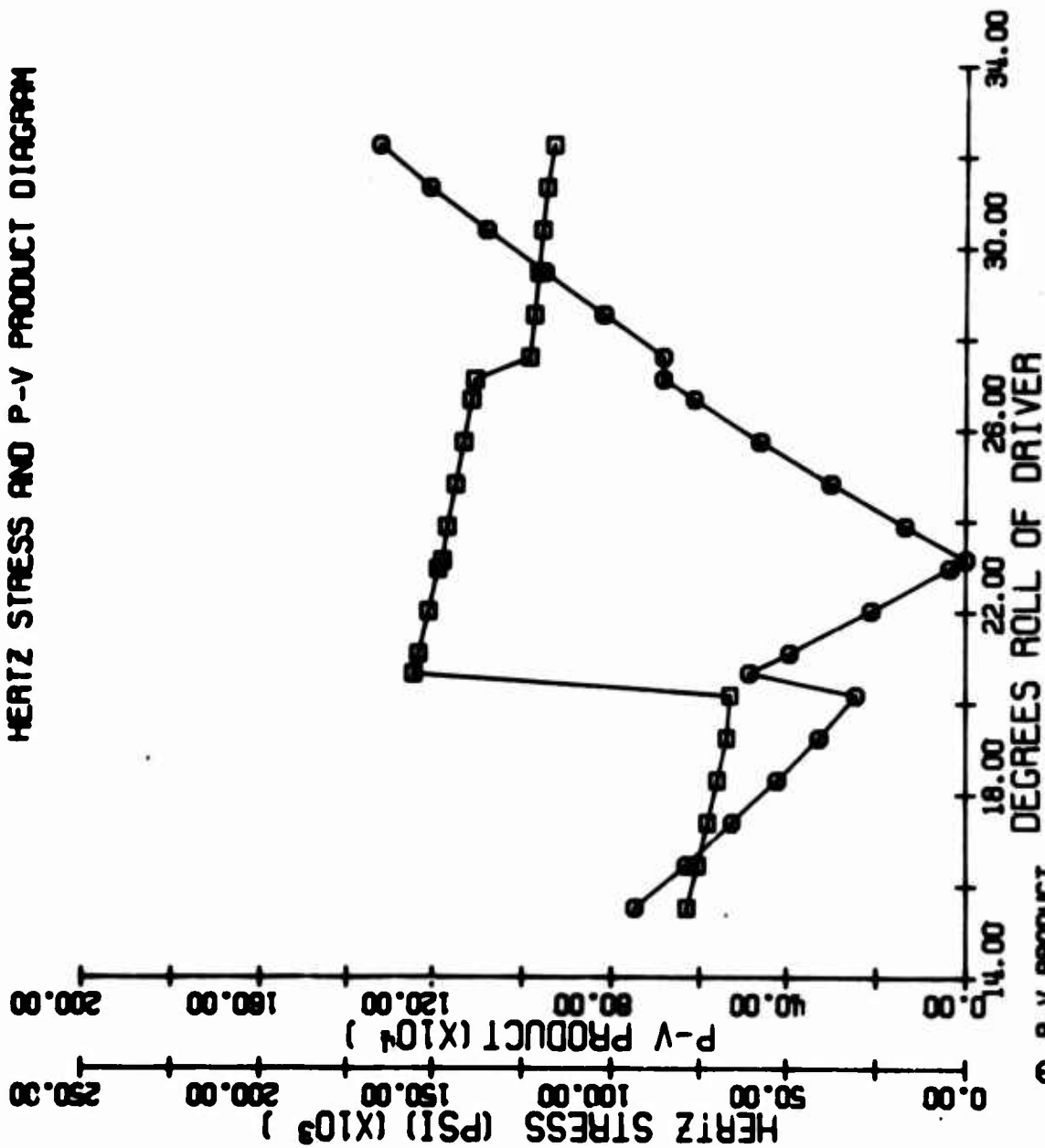
HERTZ STRESS AND P-V PRODUCT DIAGRAM

Figure 64.   204-040-108/204-040-331 Ring Planet Mesh
Lower 1138 HP - Hertz Stress Diagram

⊙ P-V PRODUCT
▣ HERTZ STRESS
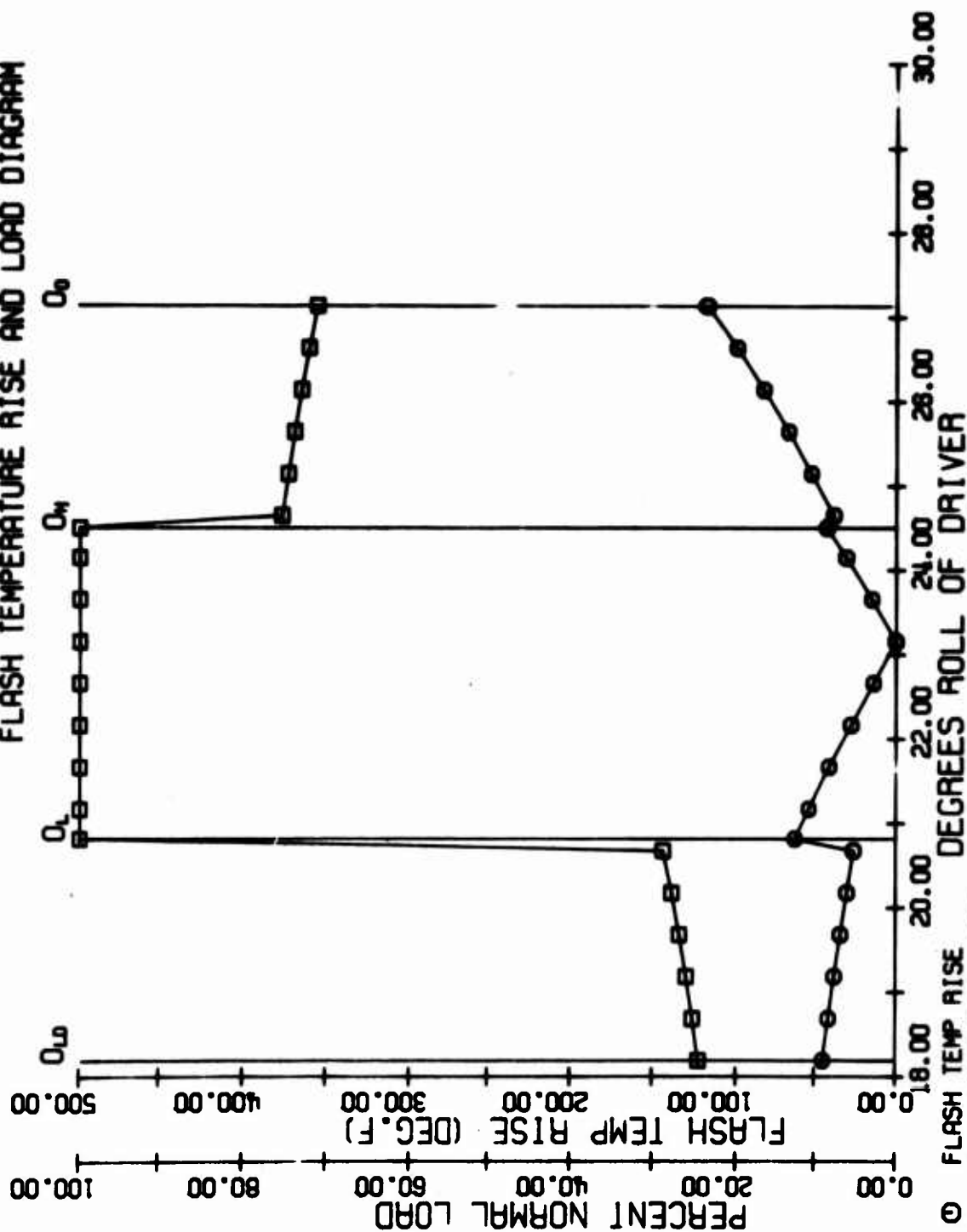
Figure 65. 204-040-108 and -330 Upper Sun Mesh 1138 HP Load Diagram

232

SHEAR STRESS DIAGRAM

⊙ PINION UNDER INVESTIGATION
⊟ GEAR UNDER INVESTIGATION
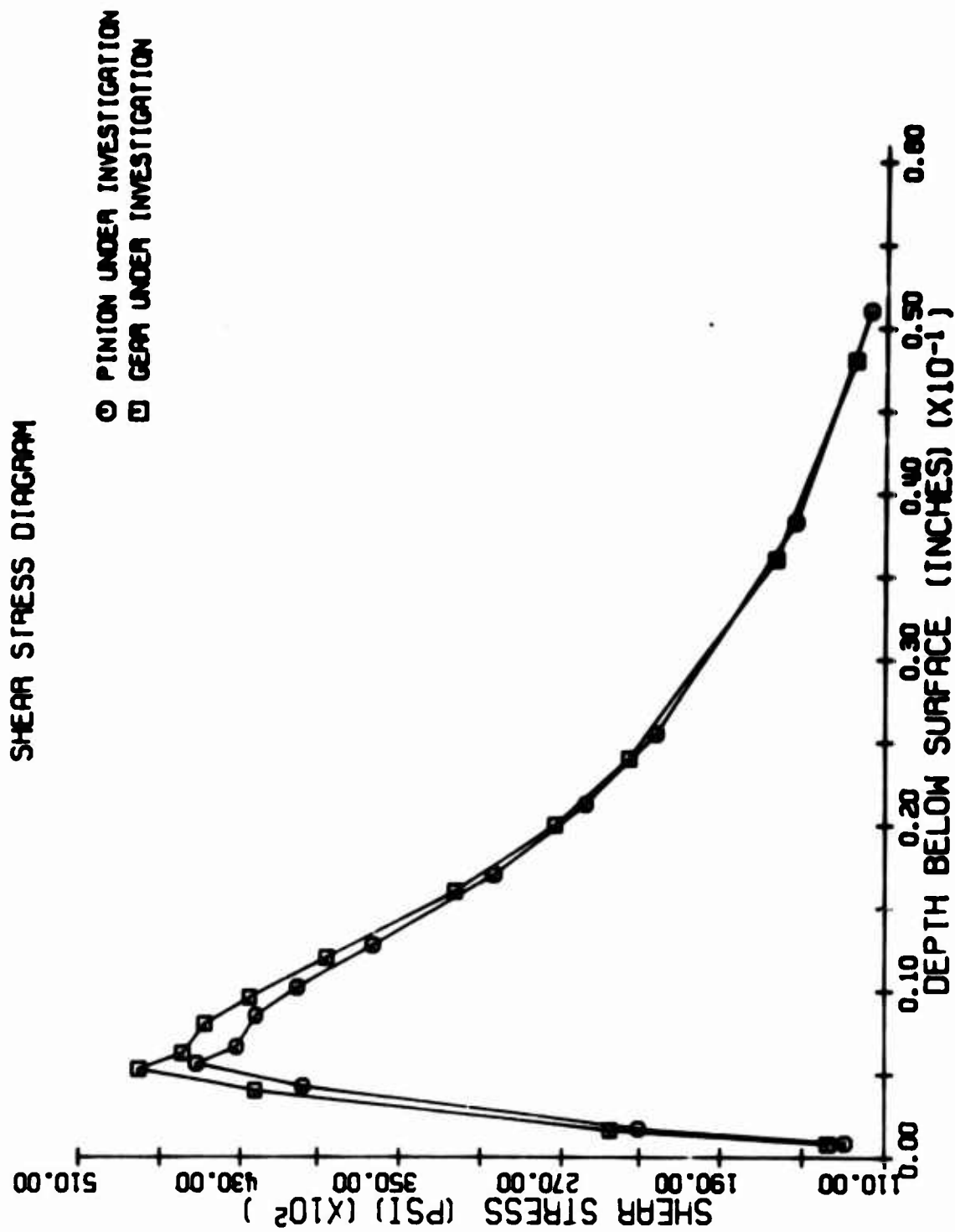
Figure 66. 204-040-108 and -330 Upper Sun Mesh 1138 HP
Shear Stress Diagram

SLIDING VELOCITY AND POWER LOSS DIAGRAM
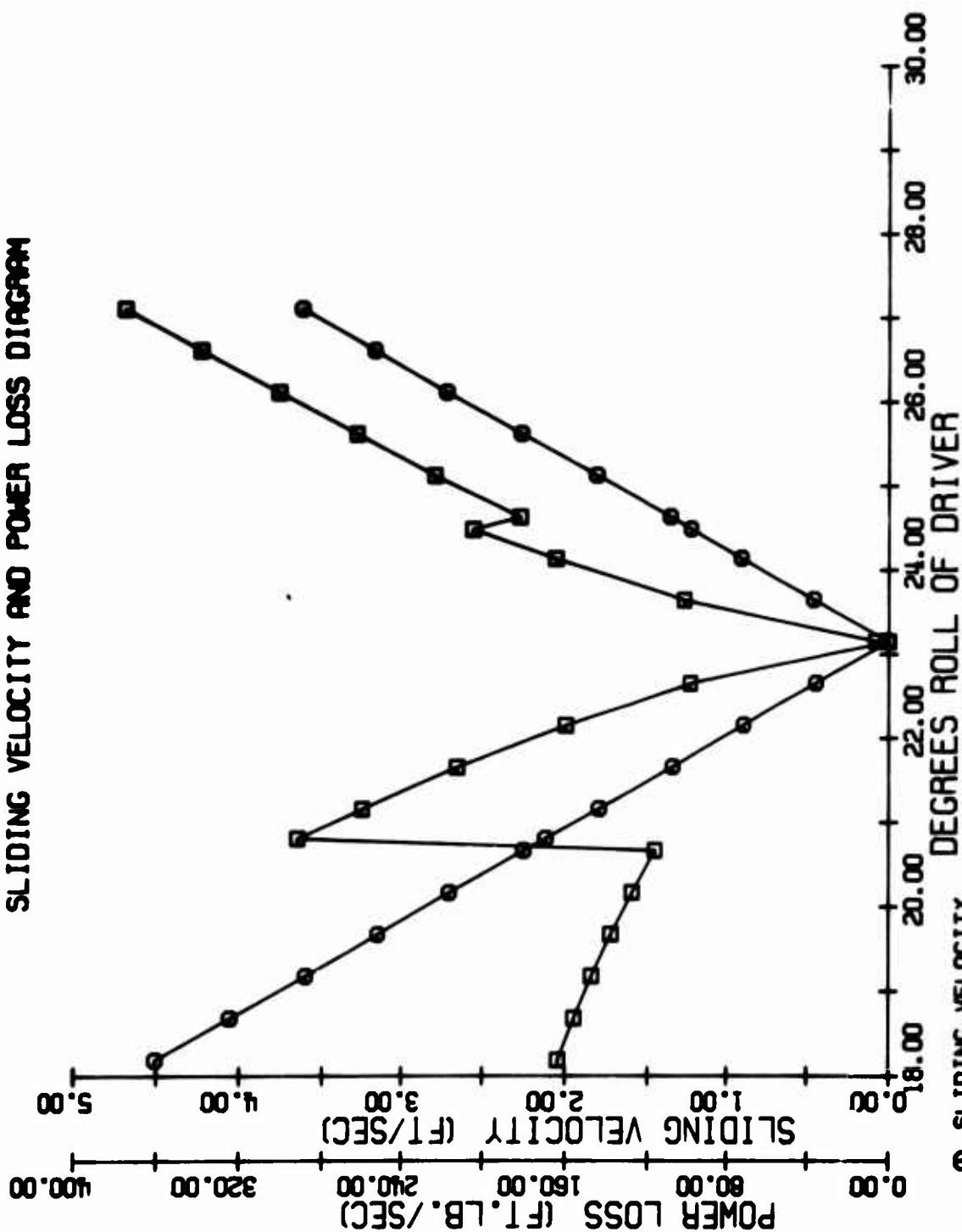
Figure 67. 204-040-108 and -330 Upper Sun Mesh 1138 HP
Power Loss Diagram

⊕ SLIDING VELOCITY
⊡ POWER LOSS

234
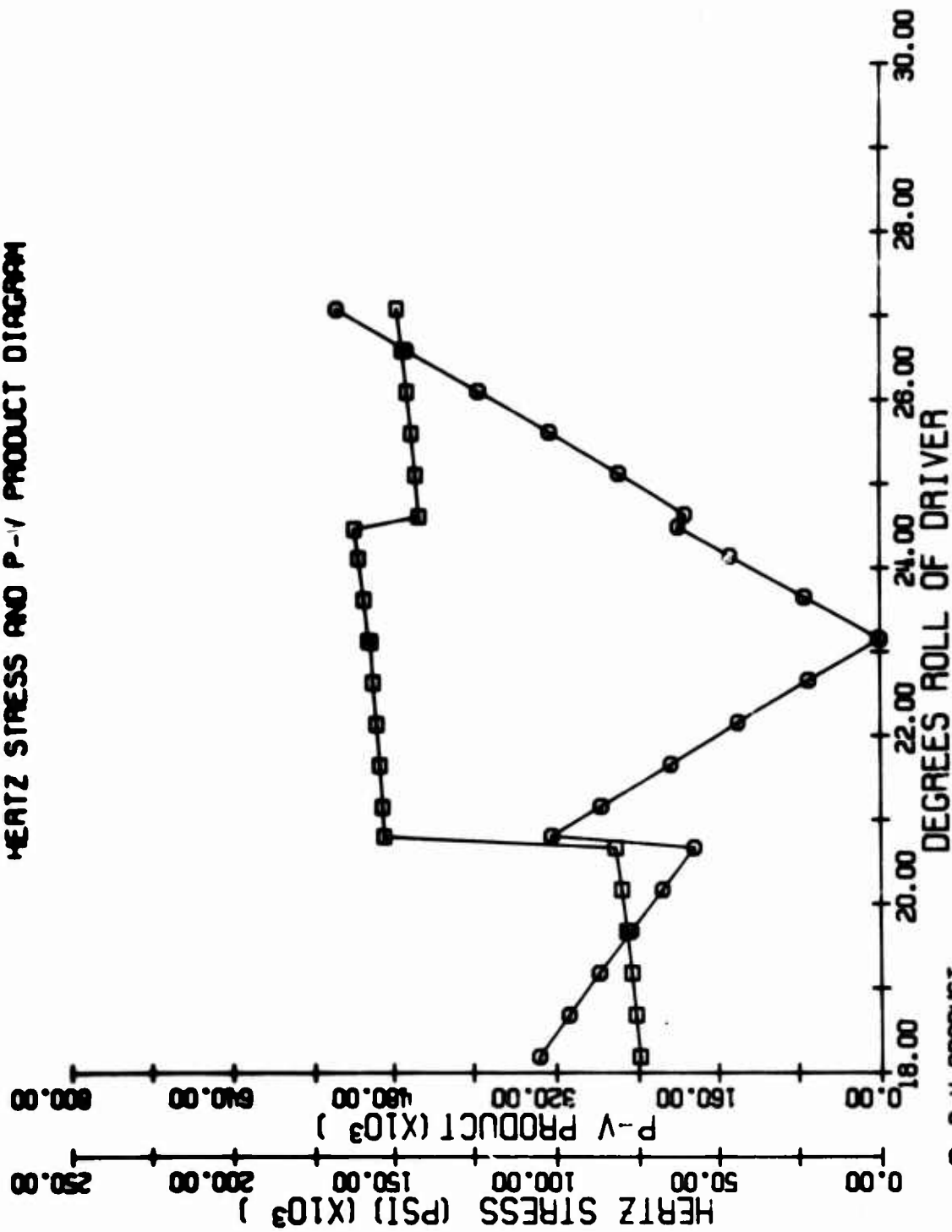
Figure 68. 204-040-108 and -330 Upper Sun Mesh 1138 HP
Hertz Stress Diagram

235
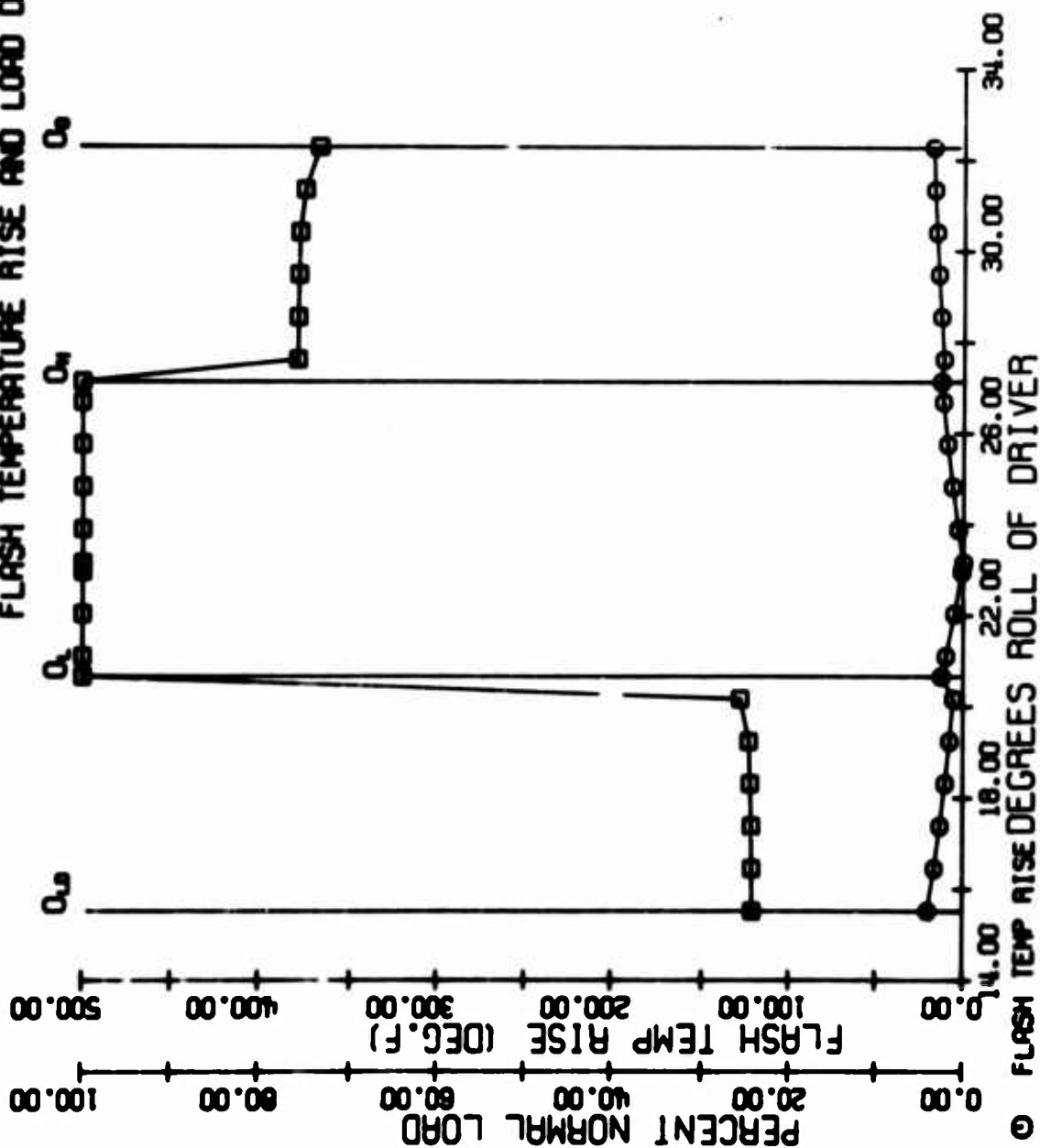
Figure 69. 204-040-108/204-040-331 Ring Planet Mesh Upper 1138 HP - Load Diagram

236

SHEAR STRESS DIAGRAM

⊙ PINION UNDER INVESTIGATION
⊟ GEAR UNDER INVESTIGATION

Figure 70. 204-040-108/204-040-331 Ring Planet Mesh
Upper 1138 HP - Shear Stress Diagram

237
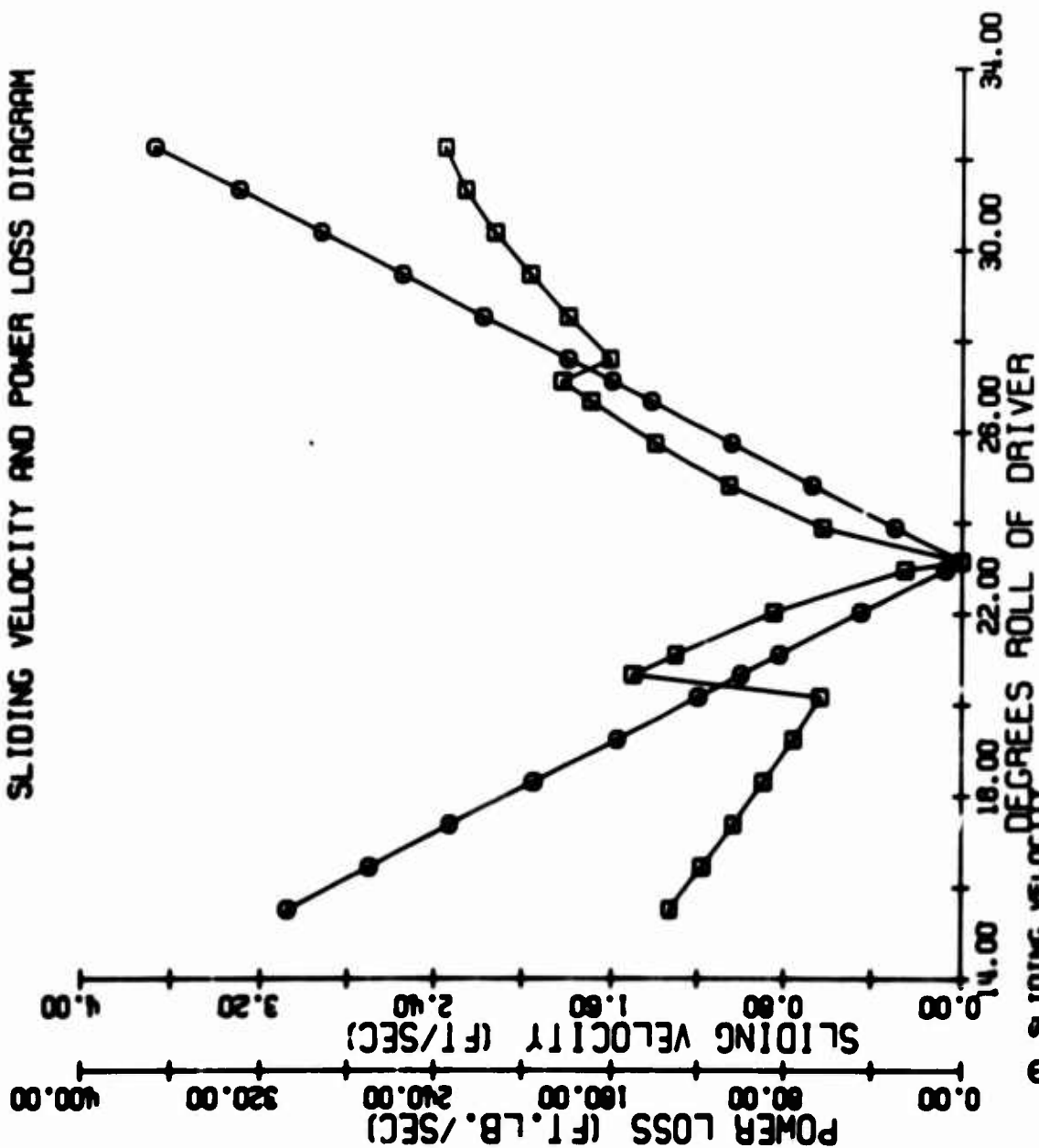
Figure 71. 204-040-108/204-040-040-331 Ring Planet Mesh
Upper 1138 HP – Power Loss Diagram

238
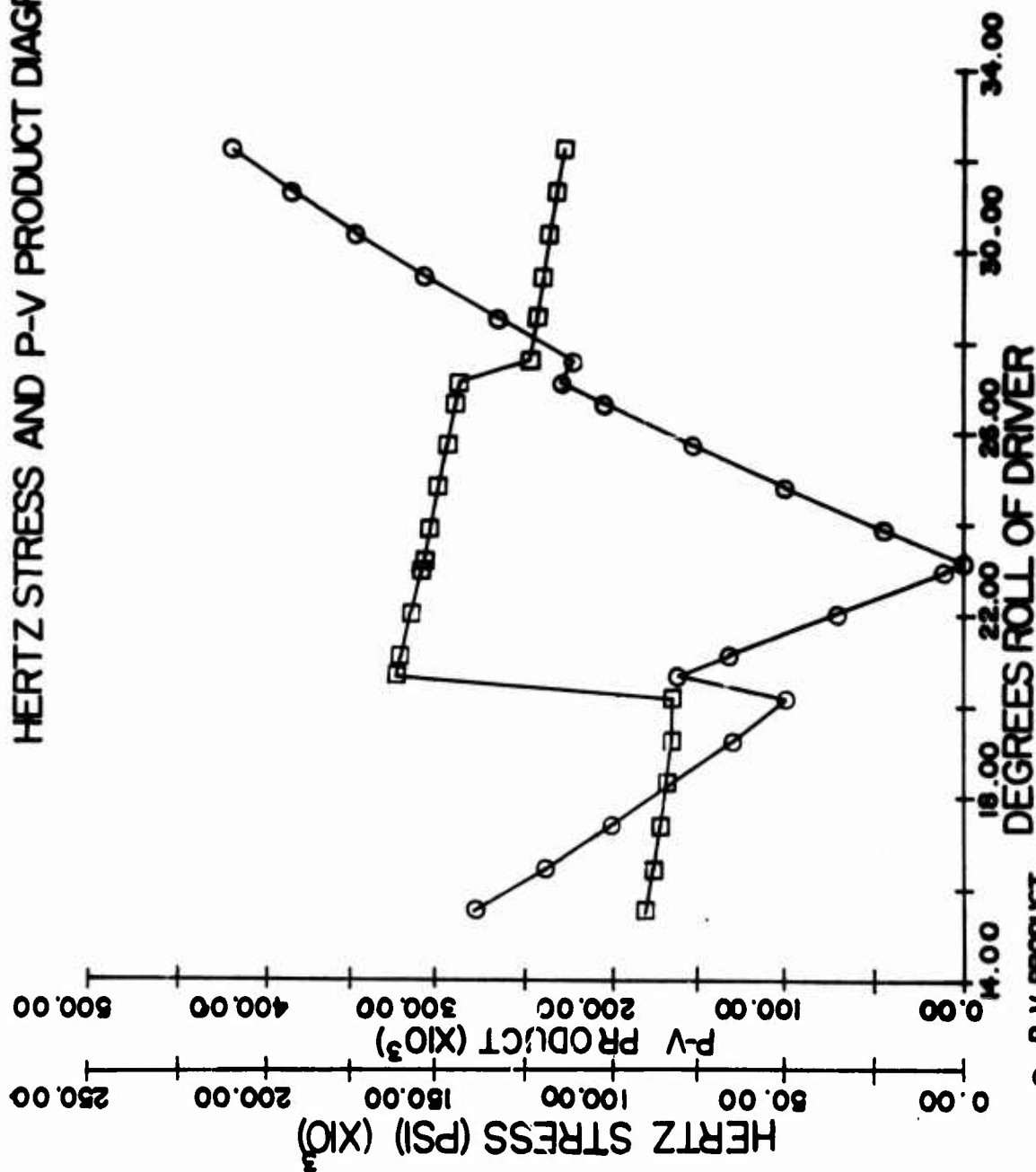
HERTZ STRESS AND P-V PRODUCT DIAGRAM

Figure 72. 204-040-108/204-040-331 Ring Planet Mesh
Upper 1138 HP - Hertz Stress Diagram

239

APPENDIX III

RGT STRESS ANALYSIS

Spider Post Stress
Material: H-11 Mod Tool Steel

F_{TU} = 260,000 psi

F_e = 130,000 psi (10^8 cycles)

Section A-A
(Rotated 90°)
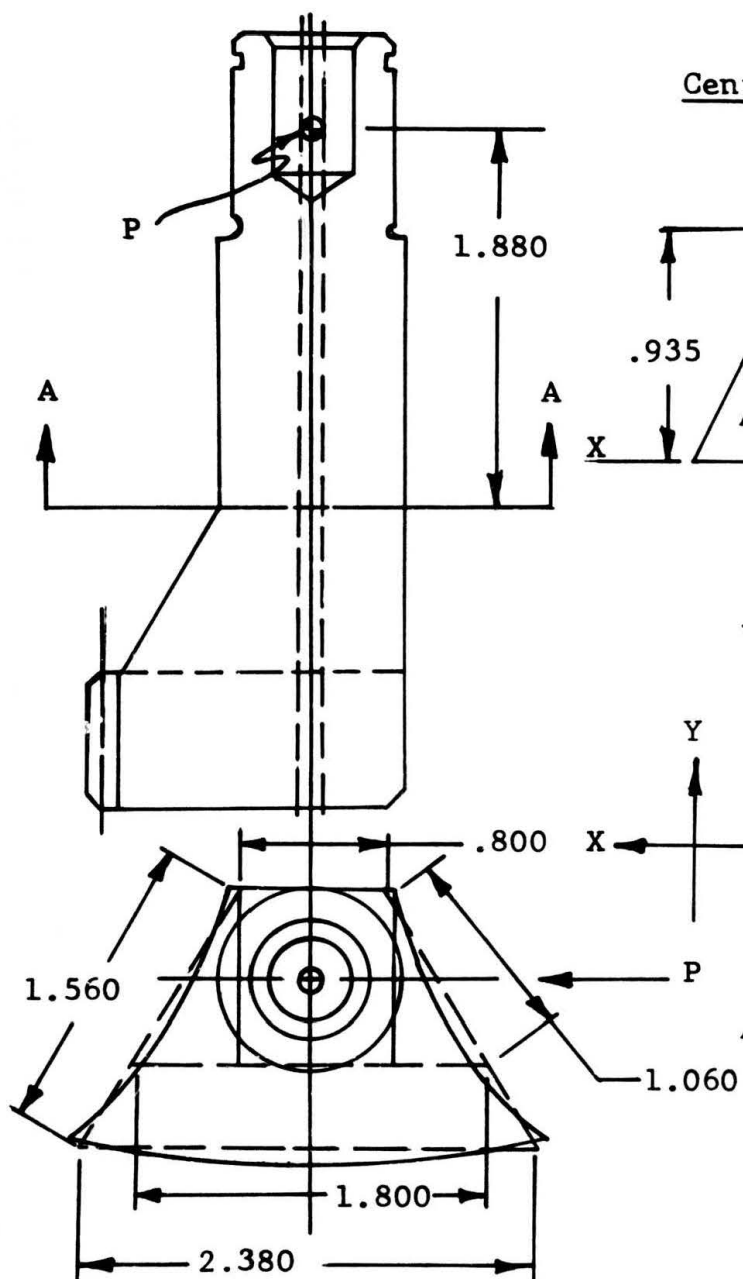
Centroid of Section A-A

$$\overline{Y} = \frac{A_1 Y_1 + A_2 Y_2 + A_3 Y_3}{\sum A}$$

$$= \frac{(.5)\left[(.935)(.5)\right]\left[\frac{.935}{3}\right]\left[2\right] + \left[(.8)(.935)\right]\left[(.935)(.5)\right]}{(.935)(.5) + (.935)(.8)}$$

$$= \frac{.495}{1.2144} = .4074$$

Area

$$A = A_1 + A_2 + A_3$$

$$= 2\left(\frac{bh}{2}\right)_{1,2} + b_2 h_2$$

$$= (.935)(.5 + .8)$$

$$= 1.2155 \ \text{In}^2$$

Moment of Inertia About Y-Y Axis

$$I_{yy} = 2(I_{y_1} + A_1 d_1^2) + I_{y_2}$$

$$= 2(\frac{bh^3}{36} + \frac{bh}{2} d^2) + \frac{b_1 h_2^3}{12}$$

$$= 2 \frac{(.935)(.5)^3}{36} + \frac{(.935)(.5)(.5667)^2}{2} + \frac{(.935)(.8)^3}{12}$$

$$= .1566 + .0399$$

$$= .1965 \text{ In.}^4$$

$$c = .4 + .5 = .90$$

Moment of Inertia About X-X Axis

$$I_{xx} = 2(I_{x_1} + A_1 d_1^2) + I_{x_2} + A_2 d_2^2$$

$$= 2(\frac{bh^3}{36} + \frac{bh}{2} d^2) + \frac{bh^3}{12} + bhd^2$$

$$= 2 \frac{(.5)(.935)^3}{36} + \frac{(.935)(.5)}{2} \frac{(.4074 - .935)^2}{3}$$

$$+ \frac{(.8)(.935)^3}{12} + (.8)(.935)(\frac{.935}{2} - .4074)^2$$

$$= .06746 + .05449 + .0027$$

$$= .1247 \text{ In.}^4$$

Bending Stress About Y-Y Axis

$$f_B = \frac{M_c}{I} \qquad M = (P)(1.880) = (5779)(1.88) = 10865$$

$$c = .90$$

$$I_{yy} = .1965$$

$$f_B = \frac{(10865)(.9)}{.1965}$$

$$= 49,761 \text{ psi}$$

Direct Shear Stress

$$f_{SD} = \frac{P}{A} \qquad P = 5779$$
$$A = 1.2155$$

$$f_{SD} = \frac{5779}{1.2155}$$

$$= 4754 \text{ psi}$$

Torsional Shear Stress

$$f_{ST} = \frac{Tc}{J} \qquad T = PR = 5779(.4074-.400) = 43 \text{ in.-lb}$$
$$c = (.4074^2 + .9^2)^{.5} = .988$$
$$J = I_{xx} + I_{yy} = .1965 + .1247 = .3212$$

$$f_{ST} = \frac{(43)(.988)}{.3212} = 132 \text{ psi}$$

Combined Stress on Section A-A

$$f_S = f_{ST} + f_{SD} = 4754 + 132 = 5886$$

$$f_{S(max)} = \left[\left(\frac{f_n}{2}\right)^2 + f_S^2\right]^{.5} = \left[\left(\frac{49761}{2}\right)^2 + 5886^2\right]^{.5}$$

$$= 25,493 \text{ psi}$$

$$f_{n(max)} = \frac{f_n}{2} + f_{S(max)} = \frac{49761}{2} + 29,493$$

$$= 50,374 \text{ psi}$$

The planetary spider will be fabricated from a forging made of CEVM H-11 Mod. steel. The machined part will be heat treated to 260,000 psi ultimate strength and shot peened.

The smooth specimen endurance limit for the H-11 Mod. steel heat treated to 260,000 psi is 130,000 psi, as determined by R. R. Moore Fatigue Test (Reference 14). Although the planetary spider does not compare in configuration to the R.R. Moore smooth specimen, it will have a comparable if not substantially higher endurance limit by virtue of the shot peening.

Considering each engine start as one stress cycle would then result in an operating range for the spider post that is considerably below the safe operating boundary.
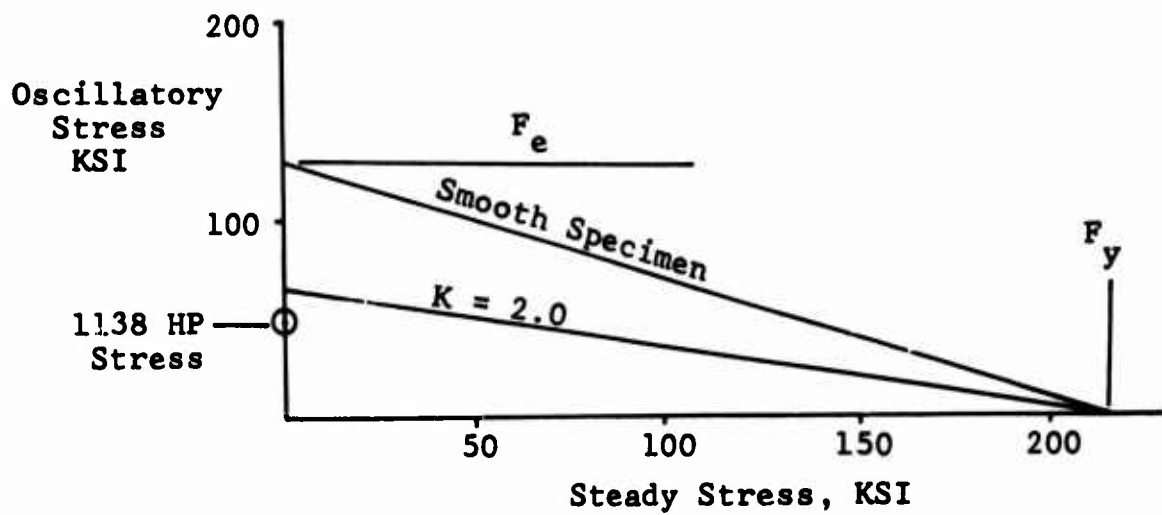
Figure 73. Modified Goodman Diagram for Spider Post.

6X6C TORSIONAL ANALYSIS

Bevel Gearshaft Torsional Shear Stress

A ↑   A ↑
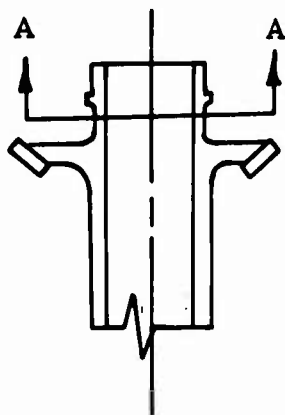
$D_o = 1.95$

$D_i = 1.40$

$J = .098(1.95^4 - 1.4^4) = 1.0405$

$$f_{ST} = \frac{T_c}{J} = \frac{(5671)(1.95)}{(2)(1.0405)} = 5314 \text{ psi}$$

Splined Adaptor, Sun Drive

$D_o = 1.25$

$D_i = 1.0$

$J = .098(1.25^4 - 1.0^4) = 0.1413$

$$f_{ST} = \frac{T_c}{J} = \frac{(5671)(1.25)}{(2)(.1413)} = 25,084 \text{ psi}$$

First-Row Cluster E.B. Joint

$D_o = 1.30$

$D_i = .88$

$J = .098(1.3^4 - .88^4) = .221$

$$f_{ST} = \frac{T_c}{J} = \frac{(860)(1.3)}{(2)(.221)} = 2529 \text{ psi}$$

244

INPUT BEVEL GEAR OPERATING STRESSES

The factors used to determine the operating stresses of the spiral bevel gears were calculated by a Gleason Company computer analysis. The bevel gear data are shown on page 69.

1. **Root Bending Stress**

    $f_B = (1.1)(3747(6.522) = 26{,}882$ psi (Pinion)

    $f_B = (1.1)(5671(4.323) = 26{,}967$ psi (Gear)

2. **Surface Compressive Stress**

    $f = 2801 \ (1.1)(3747) = 179{,}825$ psi (Pinion)

    $f = 2277 \ (1.1)(5671) = 179{,}841$ psi (Gear)

3. **Scoring Temperature Rise**

    $T = (.0166)(21000)^{.3125}(3747)^{.75} = 178^{\circ}F$

SPLINE STRESS CALCULATIONS

1. **Input Bevel Pinion**

$$P = 10/20$$

$$N = 18$$

$$d = 1.8$$

$$\mathcal{l}_{eff} = 1.4$$

$$2A_d = 1.8999 - 1.8 = 0.0999$$

$$2h_k = 1.8 - 1.7 + .0999 = .1999$$

$$T = 3747 \text{ In.Lb.}$$

Shear Stress

$$f = \frac{1.273 \, T}{d^2 \, \mathcal{l}_{eff}} = \frac{(1.273)(3747)}{(1.8)^2(1.4)}$$

$$= 1052 \text{ psi}$$

Bearing Stress

$$f_{BR} = \frac{2T}{dA} = \frac{(2)(3747)}{(1.8)(18)(.1999)(1.4)}$$

$$= 826 \text{ psi}$$

2. **Bevel Gear Shaft Spline**

$$P = 10/20$$

$$N = 15$$

$$d = 1.5$$

$$\mathcal{l}_{eff} = 0.90$$

$$2h_k = .19789$$

$$T = 5671$$

Shear Stress

$$f_S = \frac{1.273\ T}{d^2\ \ell_{eff}} = \frac{(1.273)(5671)}{(1.5)^2(.9)}$$

$$= 3565\ psi$$

Bearing Stress

$$f = \frac{2T}{dA} = \frac{(2)(5671)}{(1.5)(15)(.9)(.19789)}$$

$$= 3565\ psi$$

3. Sun Gear

Same as gear shaft

4. Mast Driving Adaptor

$$P = 10/20$$

$$N = 47$$

$$d = 4.7$$

$$2h_k = .1999$$

$$\ell_{eff} = 2.3$$

$$T = 221,222$$

Shear Stress

$$f_S = \frac{1.273\ T}{d^2\ \ell_{eff}} = \frac{(1.273)(221,222)}{(4.7)^2\ 2.3}$$

$$= 5543\ psi$$

Bearing Stress

$$f_{BR} = \frac{2T}{dA} = \frac{(2)(221,222)}{(4.7)(47)(.1999)(2.3)}$$

$$= 4356\ psi$$

$\underline{SUN - X_1}$

Sun-Roller Hertz Stress and Subsurface Shear Stress:

$$W_N = 511 \text{ lbs}$$
$$F = .069$$
$$D_S = 2.400$$
$$D_{X_1} = 4.8$$

A. **Calculate Width of Contact Band**

$$b = (.566)(10^{-3})\left(\frac{N}{F} \frac{\rho_1 \rho_2}{\rho_1 + \rho_2}\right).5$$

$$= (.566)(10^{-3})\left(\frac{511}{.069} \times \frac{(1.2)(2.4)}{1.2 + 2.4}\right).5$$

$$= .0436$$

B. **Calculate Surface Compressive Stress**

$$S_c = 2260 \left(\frac{W_N}{F} \frac{\rho_1 + \rho_2}{\rho_1 \rho_2}\right).5$$

$$= 2260 \left(\frac{551}{.069} \times \frac{1.2 + 2.4}{(1.2)(2.4)}\right).5$$

$$= 225,795 \text{ psi}$$

	TABLE XXIX.	SUBSURFACE SHEAR VS. DEPTH BELOW SURFACE SUN-X_1 ROLLERS		
K_B	d	KSC	S_C	Allowable
.05 x b	.0022	.090 S_c	20322	36.9
.10	.00436	.160	36127	65.7
.25	.0109	.276	62319	112.7
.3298	.0144	.314	70900	128.9
.39	.017	.300	67739	123.0
.50	.0218	.293	66158	120.2
.60	.0262	.278	62771	114.2
.75	.0327	.252	56900	108.4
1.00	.0436	.211	47643	86.5
1.25	.0545	.179	40417	73.5
1.60	.0698	.154	34772	63.3
2.25	.0981	.107	24160	44.0
3.00 x b	.1308	.082 S_c	18515	33.6
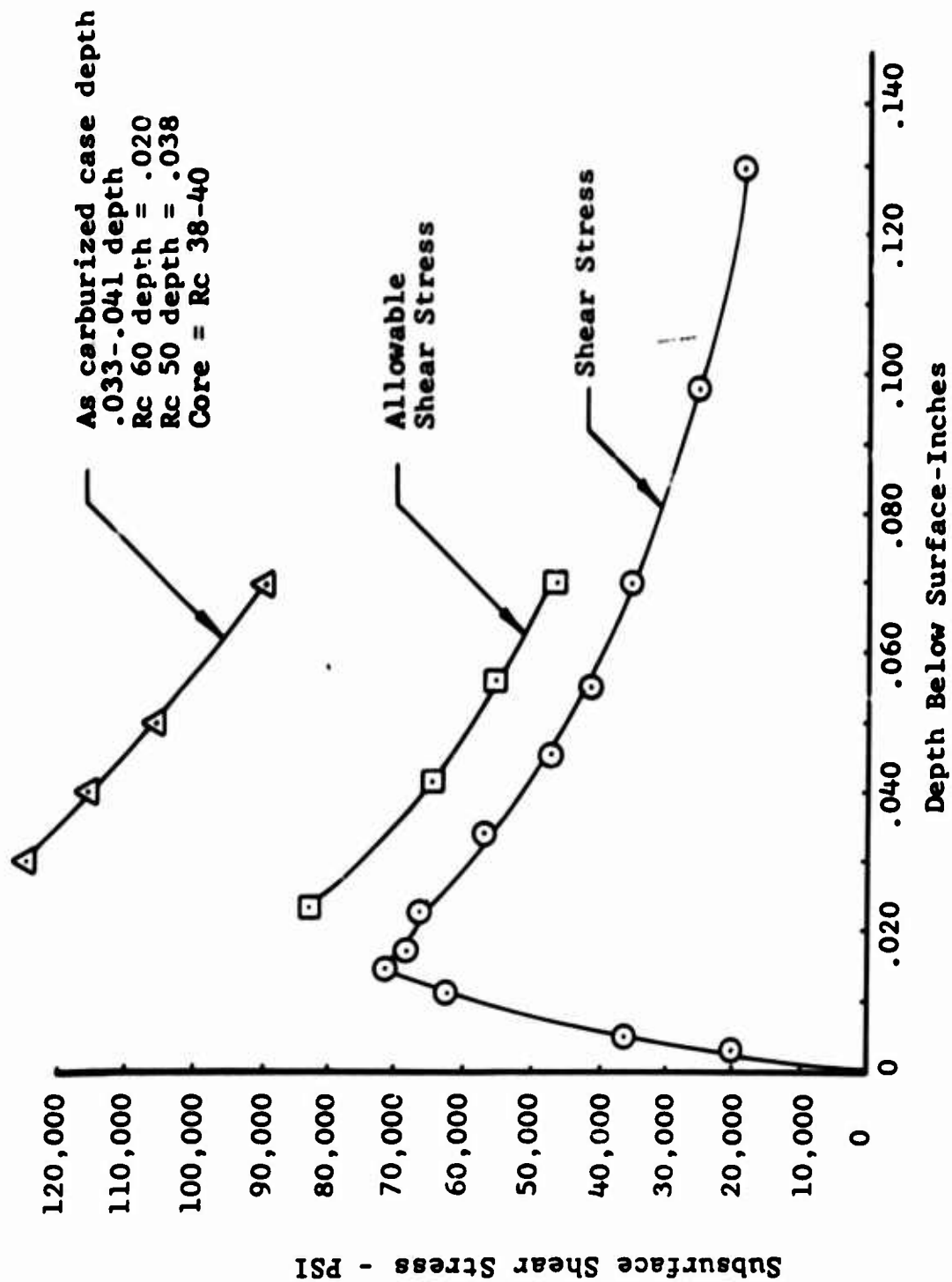
Figure 74. Plot of Subsurface Shear Stress on Sun-X$_1$ Mesh 6x6 Transmission.

250

$$\underline{Y_1 - X_2}$$

$Y_1 - X_2$ Hertz Stress and Subsurface Shear Stress on Rollers:

$$W_N = 947 \text{ lbs}$$
$$F = .1485$$
$$D_{Y_1} = 1.86667$$
$$D_{X_2} = 5.3333$$

A. **Calculate Width of Contact Band**

$$b = (.566 \times 10^{-3})\left(\frac{N}{F} \frac{\rho_1 \rho_2}{\rho_1 + \rho_2}\right).5$$

$$= (.566 \times 10^{-3}) \left(\frac{947}{.1485}\right)\left(\frac{1.86667 \times 5.333}{1.86667 \div 5.333}\right) \quad .5$$

$$= .0526 \text{ in.}$$

B. **Calculate Surface Compressive Stress**

$$S_c = 2260 \left(\frac{W_N}{F} \frac{\rho_1 + \rho_2}{\rho_1 \rho_2}\right).5$$

$$= 2260 \left(\frac{947}{.1485} \frac{5.333 + 1.86667}{\frac{5.333 + 1.8667}{2}}\right).5$$

$$= (153482 \text{ psi}) \sqrt{2}$$

$$= 217,056$$

K_B	d	K_{SC}	S_S
	.0526		217,056
.05 b	.0026	.090 S_c	14535
.10	.0053	.160	34729
.25	.0132	.276	59907
.3298	.0173	.314	68155
.39	.0205	.300	65117
.50	.0263	.293	65597
.60	.0316	.278	60342
.75	.0395	.252	54698
1.00	.0526	.211	45799
1.25	.0658	.179	38853
1.60	.0842	.154	33426
2.25	.1184	.107	23225
3.00 b	.1578	.082 S_c	17799

TABLE XXX. SUBSURFACE SHEAR STRESS VS. DEPTH BELOW SURFACE Y_1-X_2 ROLLERS
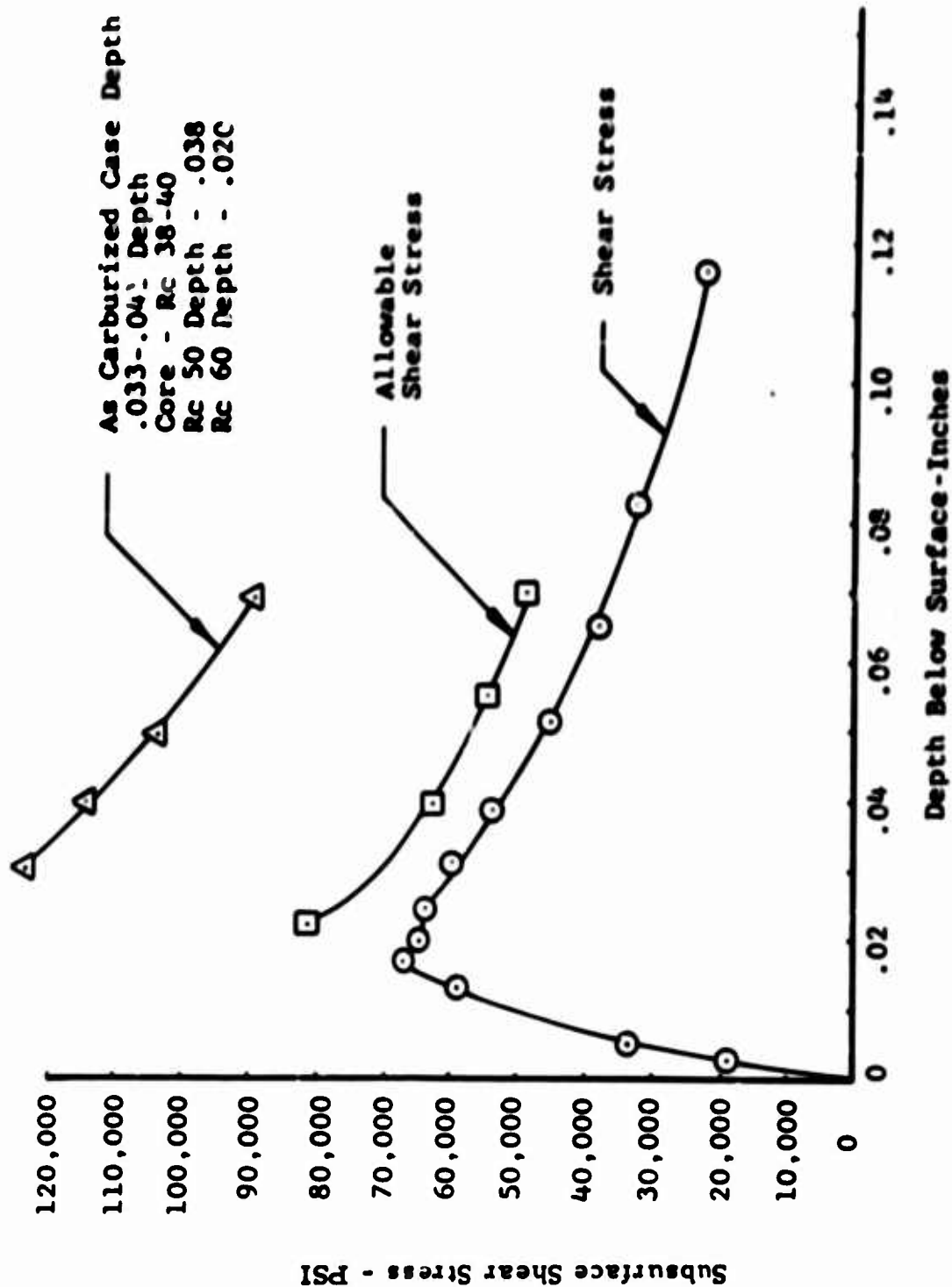
Figure 75. Plot of Subsurface Shear Stress on Rollers of Y_1-X_2 Meshes on 6x6 Transmission

SUBSURFACE SHEAR STRESS

SECOND-ROW CLUSTER ROLLER BEARING RACE

$W_N = 1829$ lbs

$F = .590$

$\rho_1 = (.5)(.551) = .2755$

$\rho_2 = (.5)(2.799) = 1.3995$

1. **Width of Contact Band**

$$b = (5.66)(10^{-4}) \sqrt{\left(\frac{W_N}{F}\right)\left(\frac{\rho_1 \rho_2}{\rho_1 + \rho_2}\right)}$$

$$= (5.66)(10^{-4}) \sqrt{\left(\frac{1829}{.59}\right)\left(\frac{.2755 \times 1.3995}{.2755 + 1.3995}\right)}$$

$$= .0151 \text{ in.}$$

2. **Maximum Compressive Stress**

$$S_c = 2260 \sqrt{\left(\frac{W_N}{F}\right)\left(\frac{\rho_1 + \rho_2}{\rho_1 \rho_2}\right)}$$

$$= 2260 \sqrt{\left(\frac{1829}{.59}\right)\left(\frac{.2755 + 1.3995}{.2755 \times 1.3995}\right)}$$

$$= 262,270 \text{ psi}$$
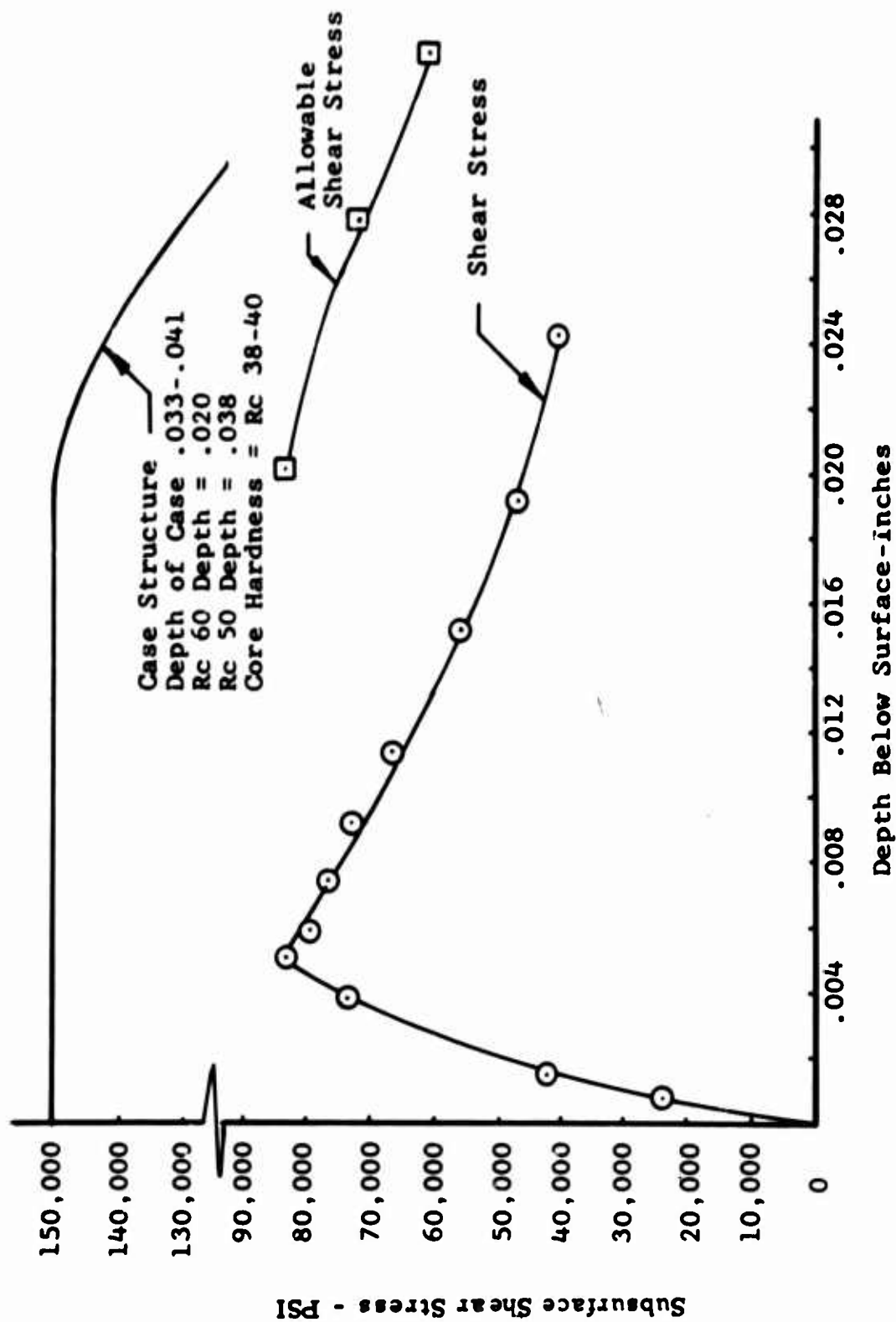
Figure 76. Plot of Subsurface Shear Stress
on Fixed Idler Roller Bearing

255

TABLE XXXI.	SUBSURFACE SHEAR STRESS VS. DEPTH BELOW SURFACE SECOND-ROW CLUSTER BEARING RACE		
K_b	d	K_{SC}	S_S
.05	.0007	.090	23600
.10	.0015	.160	41960
.25	.0038	.276	72387
.3298	.005	.314	82350
.39	.0059	.300	78680
.50	.0076	.293	76850
.60	.0091	.278	72900
.75	.0113	.252	66100
1.00	.0151	.211	55300
1.25	.0189	.179	46950
1.60	.0242	.154	40400
2.25	.034	.107	28000
3.00	.045	.082	21500

$b = .0151$ in.

$S_C = 262,270$ psi

APPENDIX IV

BEARING ANALYSIS

Analysis of the operation of the input triplex and roller
bearing on the input bevel pinion at 21,016 rpm requires a
significant departure from so-called classic antifriction
bearing life analyses as defined in AFBMA, Sections No. 9 and
No. 11. These works were, of course, based upon the pioneering
contributions of Lundberg and Palmgren in the Royal Swedish
Academy publications, Acta Polytechnica, 1947 and 1949.
Recent published research conducted by Talian, et al., SKF,
and Zaretsky of NASA in combination with much unpublished
research testing at Bell Helicopter Company, enables a much
more meaningful analysis. The actual fatigue life of these
bearings will approach a value 20 times greater than that
which the simple AFBMA prediction indicates, provided certain
fundamental requisites are achieved:

1. Adequate contact path retention within the raceways.
    (The computer program prepared by A. B. Jones for the
    high-speed analysis confirms this in its requirement of
    14% shoulder height versus the 25 percent employed.)

2. Common raceway ball spin axis control, i.e., spin axis
    control must not exchange from inner to outer (or vice
    versa) race during the balls' complete rotation about
    the shaft axis. This is similarly predicted by the
    above computer program.

3. The gyroscopic ball moment is to be less than the spin
    axis control moment. This is similarly verified by the
    program analysis.

4. Thick film lubrication from the E.H.D. effect of high-
    speed rolling elements effectively precludes asperity
    contacts under loaded operation. As the Hertzian con-
    tacts are entirely supported by an elastic film, the
    subsurface shear distribution is in reality less
    severe than Hertzian assumptions predict. The calculated
    film thickness for both bearings is 32 microinches to 40
    microinches, 4 times greater than the geometric
    average roughness of 8.2 microinches for conventional
    manufactured bearings. The conservative net life
    increase predicted is a = 2.

5. Consumable electrode vacuum remelt M-50 (AMS 6490) is
    well known to possess a significantly larger fatigue

stress endurance limit than conventional electric furnace air melt or vacuum degassed AISI 52100 steel.

A conservative material factor on capacity derived from published data from tests conducted under E.H.D. film thickness on the order of the geometric mean asperity heights is f = 1.59. This number appears far greater at very high Hertzian stresses, which may suggest a different mode of failure propagation. In particular, in the regime of harsh asperity contacts (no E.H.D. film), the superiority of M-50 is dramatic, with apparent material factors running as high as 3 to 4.

6. The further influence of grain orientation in the loaded raceways is of extreme importance. Tests conducted by Zaretsky (NASA) indicate an increase in material strength on the order of b = 2.15 for essentially race conformal grain orientation. Virtual absence of end grain in the loaded raceway may be achieved by employing proper forging techniques on the individual rings. These may be either ring rolling of the race groove or upsetting of the race shoulders.

The net life factor for the above individual variances may be combined as follows.

The accepted relationship of bearing capacity C, impressed equivalent load P, and life in millions of ring rotational cycles L is

$$L = (\frac{C}{P})^X$$

$X = 3$ for ball bearings
$X = 4$ for highly loaded roller bearings

The material factors, f and b, are associated with the basic capacity, while the E.H.D. factor, a, is used directly on life. Hence, the corrected relationship is:

$$L^1 = a (\frac{fbC}{P})^X$$

Therefore, the combined factors give

$$L^1 = a(fb)^X L$$

or,

$$L^1 = (2)(1.59 \times 2.15)^3 L = 80L$$

L^1 ranges conservatively from 20L to 30L, for this application for ball and roller bearings, respectively.

The B_{10} fatigue life of the pitch line rollers in the 6x6C is derived from the stress-cycle relationship exhibited by rolling contacts in the planet bearings in the UH-1 transmission. This analogy is used because of mechanical similarity and the well established material and lubrication system constants derived from extensive UH-1 planetary system testing. By high speed digital analysis, the stress pattern and stress cycle relationship has been shown to be

$$\frac{L_1}{L_2} \, \alpha \, \left(\frac{S_1}{S_2}\right)^{\eta}$$

where L_1 and S_1, L_2 and S_2 are hours of life and surface compressive stress at loads P_1 and P_2, respectively.

The exponent, η, was determined to be approximately 8.0 for the range of stresses involved. The life of the 6x6C roller elements was calculated by first considering the total number of cycles attained by the UH-1 inner race of the planet bearing (B_{10}) at its known stress level and calculating the proportional increase or decrease in life due to the variation in operating stress. Then, by calculating the number of stress cycles per hour attained by the 6x6 roller elements and dividing this into the total number of cycles, the B_{10} life of the 6x6C rolling element in hours was obtained.

L_1 = 266 hours, B_{10} life of 204-040-132 Inner Race at Stress S_1

L_2 = 1968 hours, B_{10} life of 204-040-132 Inner Race at Stress S_2

S_1 = 242,000 psi, mean surface compressive stress

S_2 = 189,000 psi, mean surface compressive stress

$$\left(\frac{L_1}{L_2}\right) = \left(\frac{S_1}{S_2}\right)^{\eta}$$

$$\eta = \ell n\left(\frac{L_1}{L_2}\right) \Big/ \ell n\left(\frac{S_1}{S_2}\right) = \ell n\left(\frac{266}{1968}\right) \Big/ \ell n\left(\frac{189,000}{244,000}\right)$$

$$= \ell n(1352) \Big/ \ell n(.781) = -2 \Big/ -.249 = 8.04$$

Number of Cycles of 204-040-132 = (No. Rollers)(Cage RPM)

$$= (13)(531)$$

$$= 6900/min$$

L_{B10}, In Number of Stress Cycles $= (6900/\text{min})(60)(L_{B10},\text{hrs})$

$$= (6900)(60)(1968)$$

$$= 8.15 \times 10^8 \text{ cycles}$$

1. **6x6C Sun Roller L_{B10} Life**

$S_c = 174,000$ psi

Cycles $= (3/\text{rev})(13886 \text{ rpm})$

$$= 41,658/\text{min}$$

$$L_S = (8.15 \times 10^8)\left(\frac{244,000}{174,000}\right)^{8.04}$$

$$= \frac{(110.8)(10^8)}{(60)(41,658)}$$

$$= 4440 \text{ hours}$$

2. **Life in Hours of X_1 Roller**

$$= (\text{Life}_{\text{Sun}}) \frac{\text{RPM Sun} \times \text{No. Cycles}}{\text{RPM } X_1}$$

$$= (4440)(3)\left(\frac{13886}{6943}\right) = 29,600 \text{ hours}$$

3. **Life of Y_1 (Mesh) Roller**

Life, Cycles $= \left(\frac{244,000}{168,000}\right)^{8.04} 8.15 \times 10^8 = 141 \times 10^8$

rpm $= 6943$
2 cycles/rev

Life, Hours $= \dfrac{141 \times 10^8}{(2)(6943)(60)} = 18,150 \text{ hours}$

4. **Life of X_2 Roller**

Life X_2, Hours $= (\text{Life } Y_1, \text{ hrs}) \dfrac{\text{rpm } Y_1}{\text{rpm } X_2}$

$$= (18,150(\frac{6943}{2430})$$

$$= 51,800 \text{ hours}$$

260

HIGH-SPEED PLANETARY STRESS ANALYSIS

The reduction ratio required for the high-speed planetary stage was predicated on the RGT bevel gear ratio (56/37) and the two UH-1 planetary assemblies $(176/57)^2$. At 21,016 rpm input and 324 rpm output to the main rotor mast, a 4.4951:1 ratio was required for the high-speed planetary stage (HSPS).

$$\text{Total reduction ratio} = \frac{21016}{324} = 64.864$$

$$64.864 = \text{Bevel ratio x HSPS x (UH-1 Planet)}^2$$

$$= 1.56 \text{ x HSPS x } (3.0877)(3.0877)$$

$$\text{HSPS} = \frac{64.864}{(3.0877)^2(1.5135)} = 4.4951$$

A basic 10P (10 diametral pitch) gear set consisting of sun gear with 36 teeth, planet gear with 45 teeth and ring gear with 126 teeth was finally chosen based on physical size and its approximate 4.4951:1 reduction ratio.

$$\text{HSPS Reduction Ratio} = \frac{N_S + N_R}{N_S} = \frac{126+36}{36} = 4.500$$

With this reduction, the overall ratio = 64.9343.

The tooth numbers thus chosen comprised a nonhunting tooth ratio. Two teeth were, therefore, removed from the planet gear, resulting in a 43-tooth planet. The following calculations were made to establish basic involute data:

NOTE

Primed values indicate operating data.

FOR SUN-PLANET MESH

1. Center distance, $C = \dfrac{N_S + N_R}{2P} = \dfrac{36+45}{2 \times 10} = 4.05$

2. $P' = \dfrac{36+43}{(2)(4.05)} = 9.753086$ (Operating diametral pitch)

3. $D_S' = \dfrac{36}{9.753086} = 3.691139$ in.

4. $D_P' = \dfrac{43}{9.753086} = 4.408861$ in.

FOR RING-PLANET MESH

5. $P_R' = \dfrac{126-43}{(2)(4.05)} = 10.246914$ (Operating diametral pitch)

6. $D_R' = \dfrac{126}{10.2469} = 12.296386$ in.

FOR 22° BASIC PRESSURE ANGLE

7. Sun base diameter, $D_{BS} = \dfrac{N}{P} \cos \phi = \dfrac{(36)}{(10)} \cos 22° = 3.337862$

8. $\cos \phi' = \dfrac{3.337862}{3.691139} = .904291$

9. ϕ' = Operating pressure angle of sun = $\cos^{-1} .904291$

$$= 25.272108°$$

10. Planet base diameter = $D_P' \cos \phi' = (4.408861)$

$$(\cos 25.272108) = 3.986893$$

11. Ring base diameter = $\dfrac{N}{P} \cos \phi = \dfrac{126}{10} \cos 22° = 11.682517$

12. $\cos \phi_R' = \dfrac{11.682517}{12.296386} = .950077$

13. $\phi_R' = 18.180738°$

14. Planet pitch diameter on ring, $D_P' = \dfrac{43}{10.246914} = 4.196385$ in.

The circular tooth thicknesses of the three-gear elements were determined, based on a minimum practical top land, on the planet gear of .040. Then, by setting a limit diameter for the planet gear at the ring I.D., a working depth for the planet was determined.

15. $Wd_p = \dfrac{2}{P} = \dfrac{2}{10} = .2$

16. $Do_p = D_{LIM} + (2)(.2) = 4.196385 - .020 + (2)(.2)$

   $= 4.576385$ in.

17. $D_{RLIM} = 12.631$ in.   (For $Do_p = 4.576385$)

18. $D_{IR} = 12.2837$ in.

19. Ring Mean Profile Diameter $= \dfrac{12.2837 + 12.631}{2}$

   $= 12.457$ in.

20. Set C.T.T. of Ring at .15, then C.T.T. at Ring ID = .0886

21. C.T.T. of Ring at Pitch Diameter = .0957

22. C.T.T. of Planet at Pitch Diameter (with ring) = p-.0957

   $= .300 - .0957 = .2043$

23. C.T.T. of Planet at O.D. = .041

Final calculations show the circular tooth thickness of the sun pinion to be .1900 at the operating pitch diameter and .041 at the sun outside diameter, which was determined to be 3.975 in. The remaining geometrical data are shown below.

	SUN	PLANET	RING
TABLE XXXII. DIMENSIONAL GEAR DATA FOR HSPS			
N	36	43	126
P'	9.753086	9.753086	10.246914
Φ', deg	25.272108	25.272108	18.180738
D', in.	3.691139	4.40886	12.296386
D_o, in.	3.975	4.5764	12.2837
C.T.T., in.	0.190	0.127	0.0907
D_{LIM}, in.	3.5315	4.1764	12.631
Ad, in.	0.142	0.0837	0.006
Dd, in.	0.079	0.1162	0.1675
W_d, in.	0.221	0.1999	0.1735
B.L., in.	0.005	0.005	0.005
MOD	tip	tip	tip
HPSTC, in.	3.7893	4.4088	12.3906
Profile Mod at			
O.D., in.	-.00035	-.00035	-.00035

HIGH-SPEED PLANETARY GEAR LOADS AT 1138 HP

Planetary Input Torque = $\frac{(1138\ HP)(63,000)}{13,886}$ = 5170 in.-lb

Sun Pinion, Tangential Load = $\frac{(2)(5170)}{(3)(3.691139)}$ = 934 lb

Sun Pinion rpm = 13886

Ring Gear, Tangential Load = $\frac{(126)}{(36)}\ \frac{(2)(5170)}{(3)(12.296386)}$ = 982 lb

Planet Gear, Total Gear Load = 934+982 = 1916 lb

HIGH-SPEED PLANET BEARING LOADS

Bearing Reaction to Gear Load = 1916 lb

Bearing Centrifugal Load = $(.0000284)(W_T)(R)(N^2)$

   W_T = Weight of Planet Gear and Partial Roller
      Compliment

   R = Radius to Center of Planet

   N = Carrier rpm

Roller W_T = .0192 lb

Planet W_T = 1.73 lb

5.52
5.41
5.09
4.62

Planet Center

Roller Normal Force

Roller Centrifugal Force
Cage Force

Alternate Row Rollers
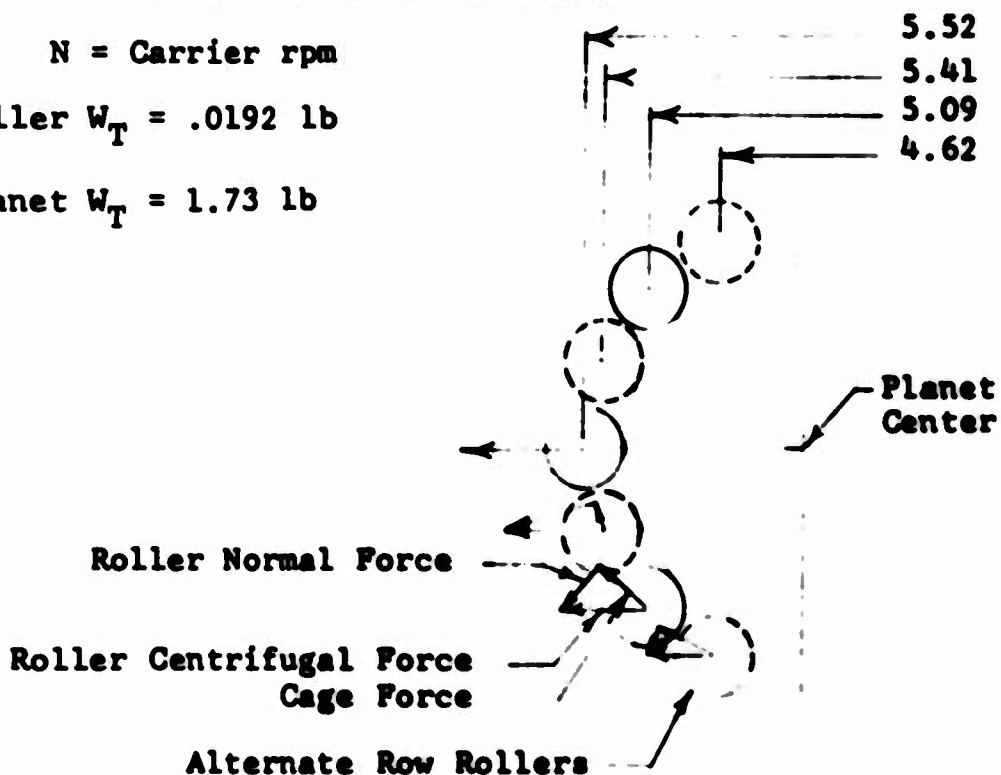
Centrifugal Planet Load $= (.0000284)(1.73)(4.05)(3083)^2$

$\qquad = 1895$ lb

Centrifugal Roller Load $= (.0000284)(.0192)(3083)^2$

$\qquad (2)(4.62+5.09+5.41)+5.52$

$\qquad = 186$ lb

Total Centrifugal Load $= 1895+186 = 2081$ lb

Resultant Bearing Load $= \sqrt{2081^2+1916^2} = 2835$ lb

HIGH-SPEED PLANET BEARING LIFE

Computed Bearing Life = 336 hours (based on 100% load, 2 Rows of 8-11x11MM rollers each, and 2.94 pitch diameter)

Reducing Load to 60%   (For ρ calculation):

$P_{100} = \sqrt{2081^2+1916^2} = 2835$ lbs   (Centrifugal 2081 lb)
$\qquad$ (Torque = 1916 lb)

$P_{60} = \sqrt{2081^2+1150^2} = 2378$ lbs   (60% of 1916 = 1149.6 lb)

P_{60} Factor $= \frac{2835}{2378} = .840$

$L \propto (\frac{1}{p})^4$ for roller bearings $\qquad (\frac{1}{.84})^4 = 2.003$

Load Factor = 2 (60%)

EHD Factor = 2 (Thick Film Lubrication)

Material Factor = 4 (CEVM M50)

$L_{10} = (2)(2)(4)(336) = 5376$ hours

SUN GEAR STRESS CALCULATIONS

The stresses to which the sun gear is subjected are produced by cyclic bending moment in the gear teeth, steady tensile stress due to centrifugal force of the teeth, and hoop tension at the teeth roots due to centrifugal effects of the gear rim. The combined stresses are then a steady tensile stress plus an oscillatory bending stress.

1. Hoop tension calculation for rotating gear rim

$$f_n = (.0000284)(P)(R_m^2)(N^2)$$

> P = density of gear material, lb/in^3
>
> R_m = mean radius of rim, in.
>
> N = rpm of gear
>
> .0000284 = units and gravitational constant

$$f_n = (.0000284)(.3)(1.52)^2 (13886)^2$$

$$= 3796 \text{ psi (in root of teeth)}$$

2. Centrifugal root stress

$$f_{CF} = \frac{P_{CF}}{AREA}$$

> $$AREA = (CTT_R)(F)$$
>
> $$= (.2532)(.875)$$
>
> $$= .2216 \text{ in}^2$$
>
> $$P_{CF} = (.0000284)(WT)(R)(N^2)$$
>
> $$WT = \frac{(D_o - D_r)(CTT_D)(1)(.3)}{2}$$
>
> $$= \frac{(3.975 - 3.486)(.19)(.875)(.3)}{2}$$
>
> $$= .0112 \text{ lb/tooth}$$

267

$$P_{CF} = (.0000284)(.0112)(3.691)(13886)^2$$

$$= 227 \text{ lb}$$

$$f_{CF} = \frac{227}{.2216}$$

$$= 1025 \text{ psi}$$

3. Tooth bending stress

$$f_{BR} = (K)(f_B)$$

$$K = \text{dynamic factor}$$

$$= 1.12 \text{ (ref. 6)}$$

$$f_B = 19,174 \quad \text{(calculated by computer, shown in Table XXIV)}$$

$$f_{BR} = (1.12)(19174)$$

$$= 21450 \text{ psi}$$

Steady Stress $= f_{CF} + f_n$

$$= 1025 + 3796$$

$$= 4821 \text{ psi}$$

Total stress condition $= 4821 \pm \dfrac{21450}{0}$

$$= 15,546 \pm 10,725 \text{ psi}$$

FLASH TEMPERATURE RISE AND LOAD DIAGRAM
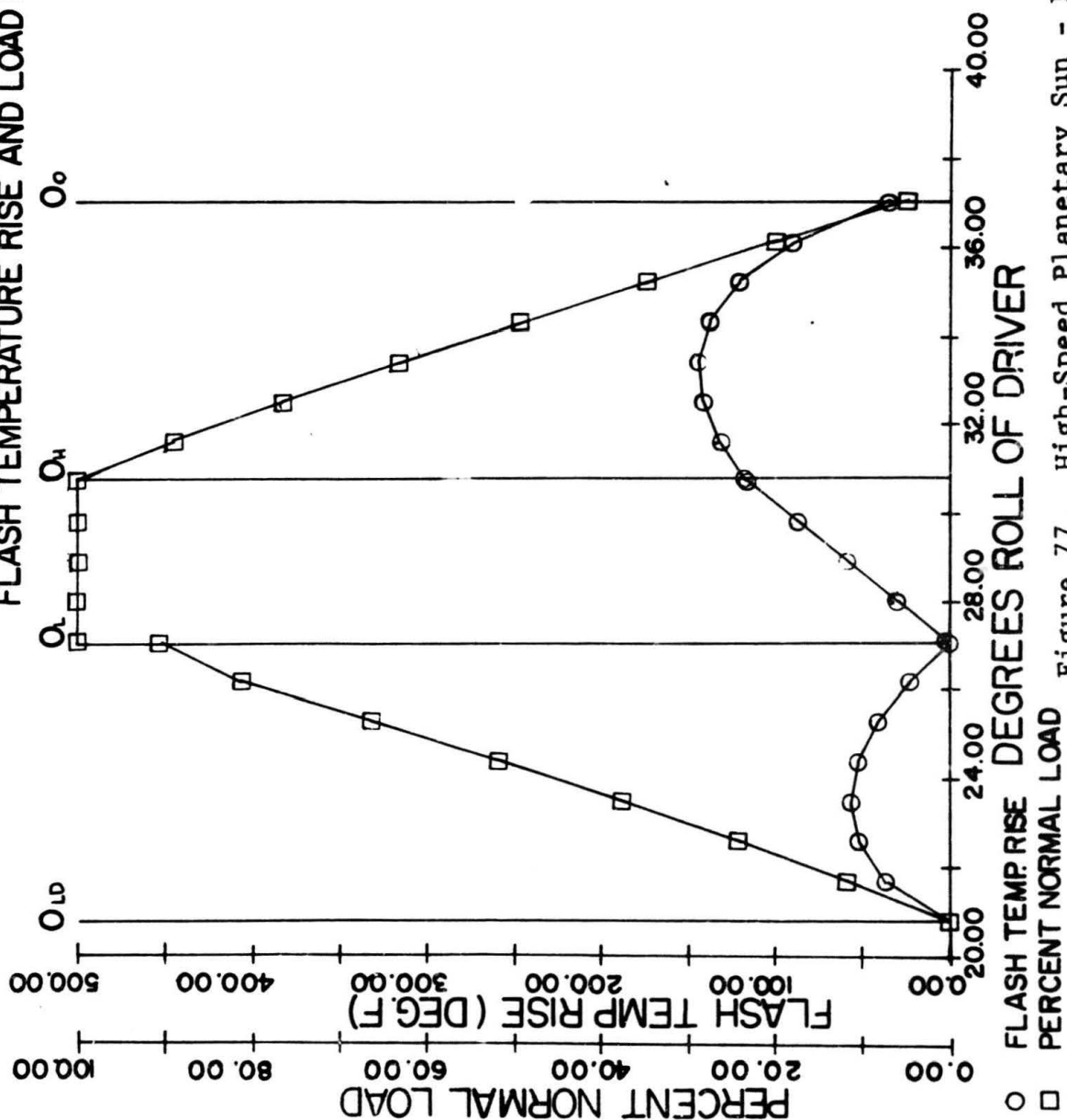
Figure 77. High-Speed Planetary Sun - Load Diagram

269
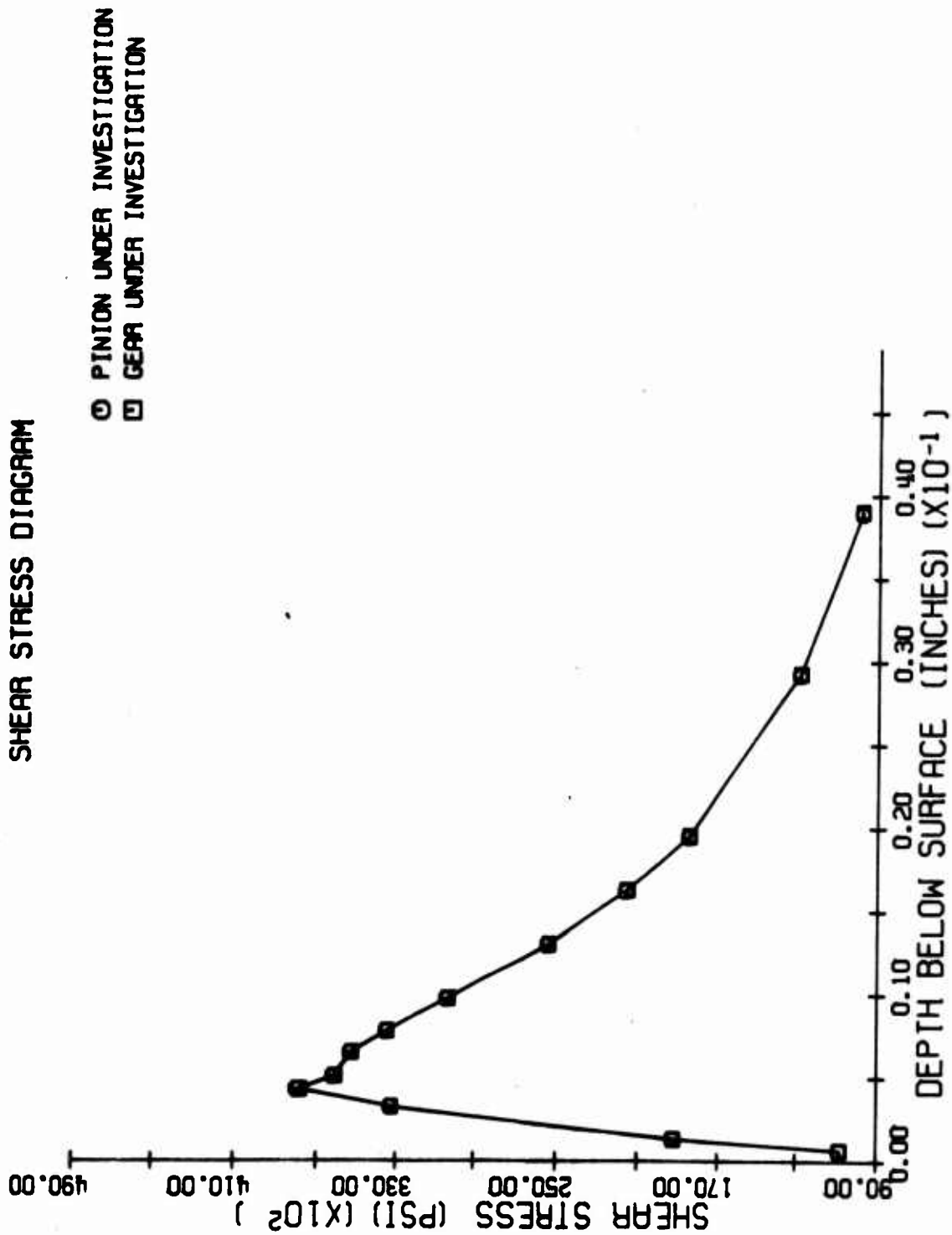
Figure 78. High-Speed Planetary Sun – Shear Stress Diagram
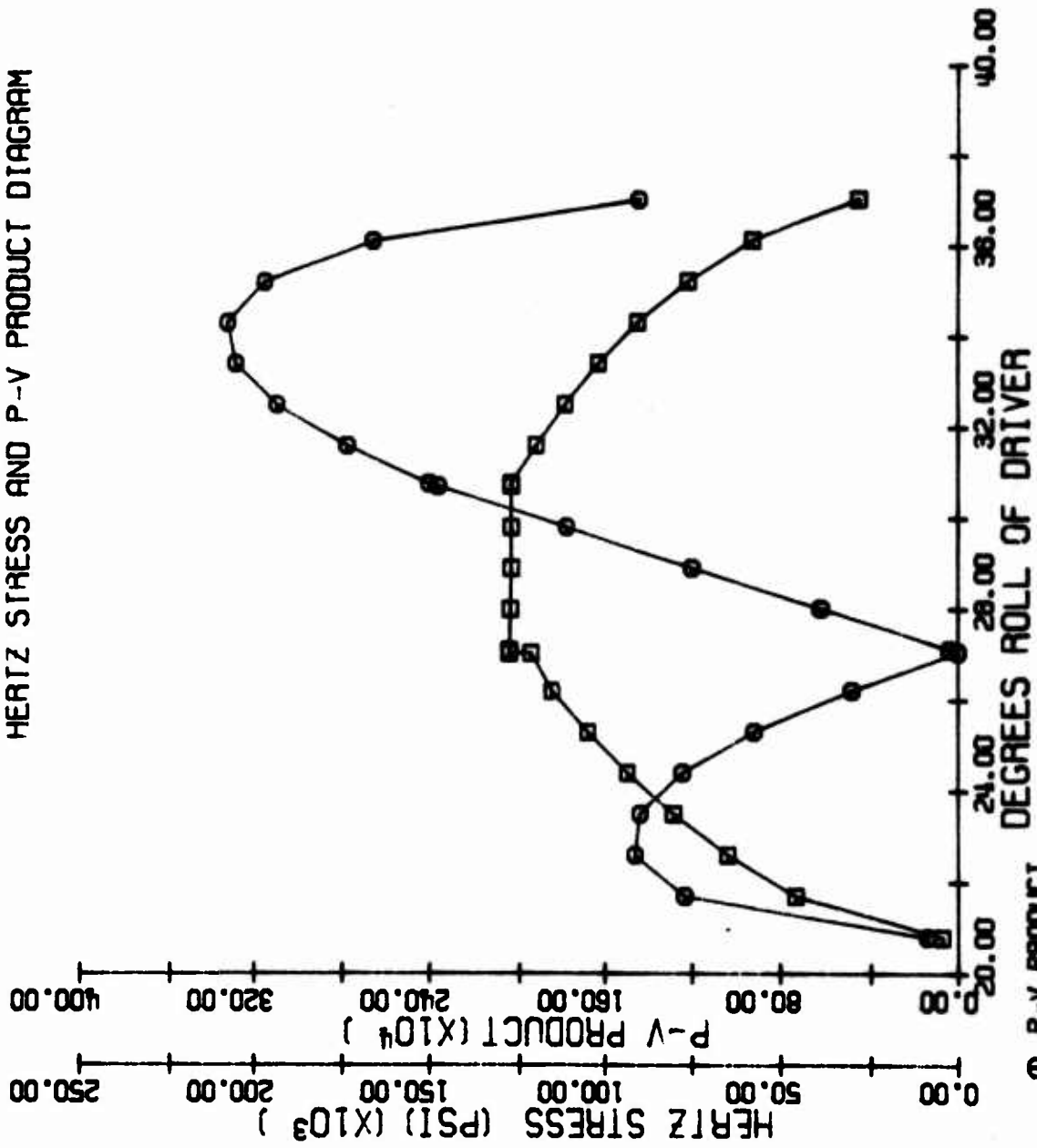
Figure 79. High-Speed Planetary Sun – Hertz Stress Diagram
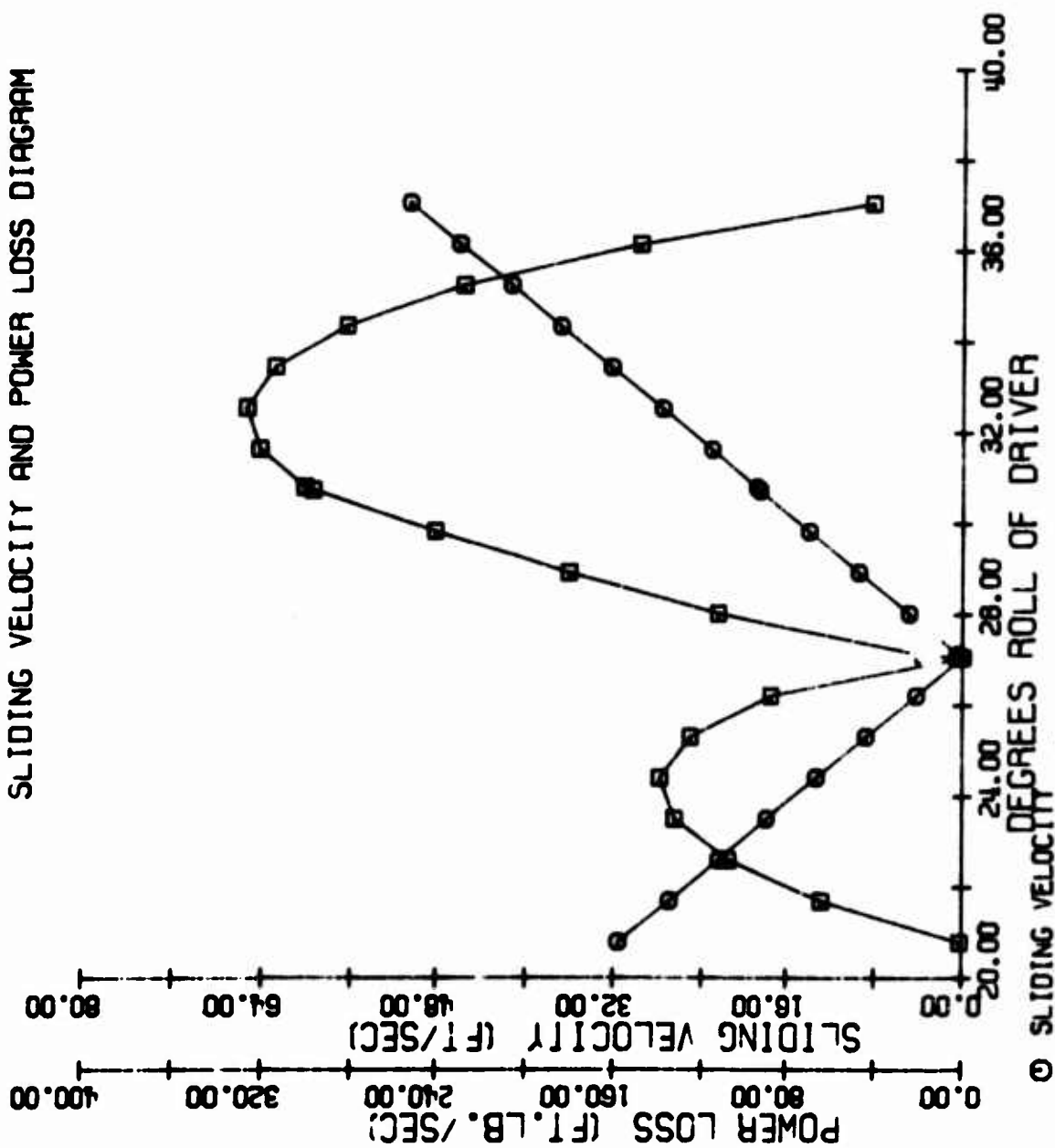
Figure 80. High-Speed Planetary Sun – Power Loss Diagram

272

FLASH TEMPERATURE RISE AND LOAD DIAGRAM
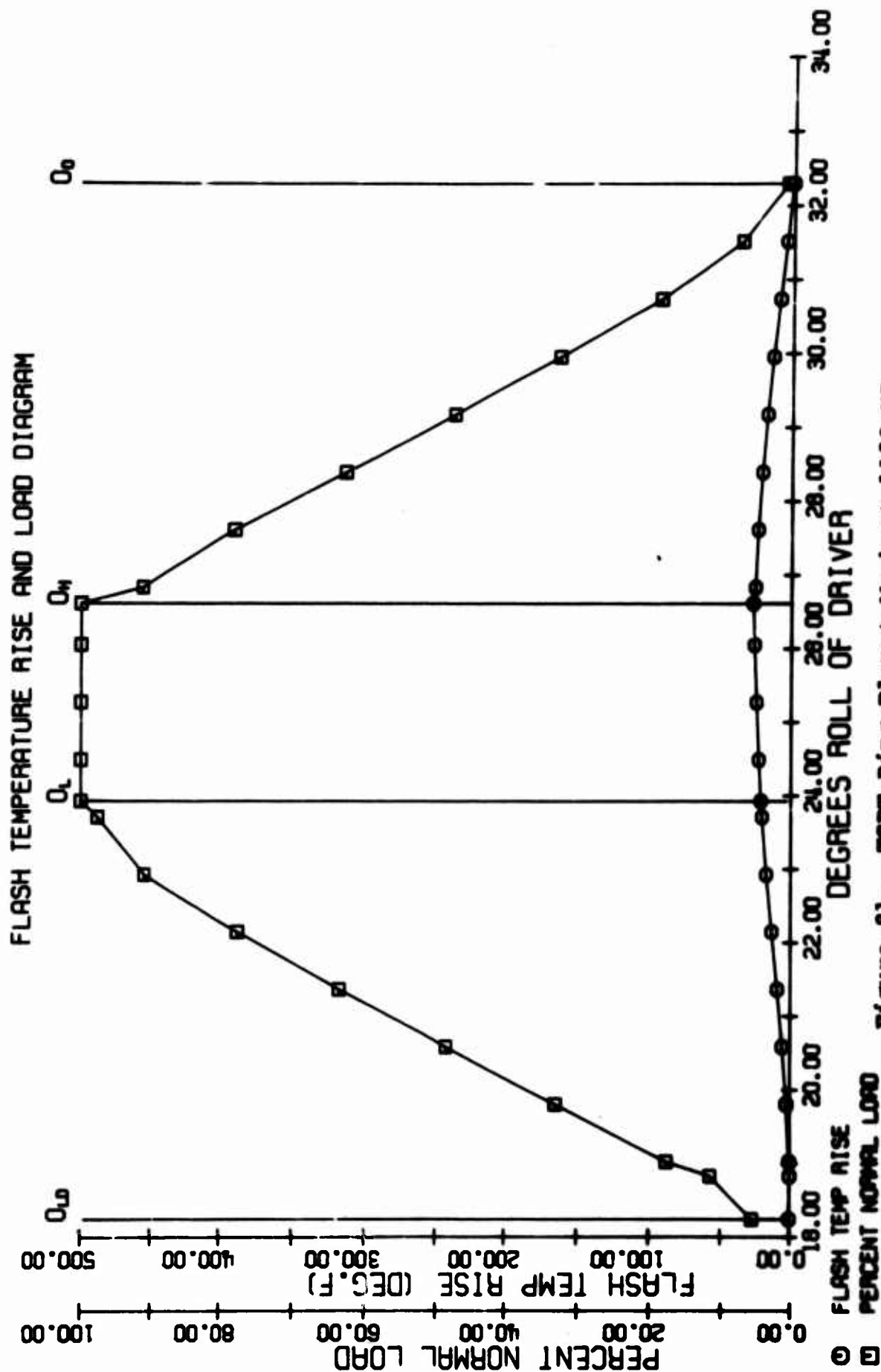
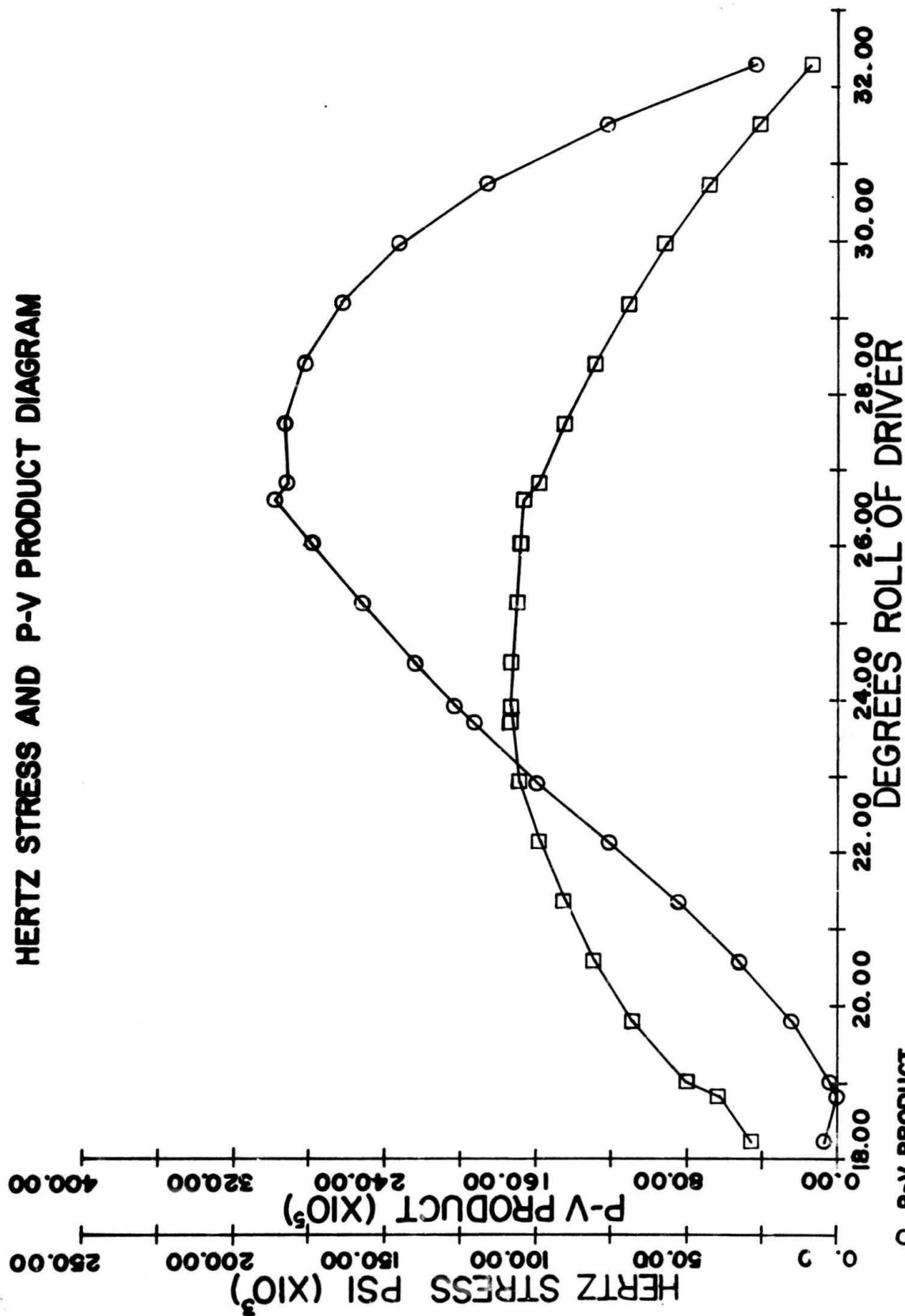Figure 81. TSPT Ring Planet Mesh at 1138 HP
9035 RPM of Pinion - Load Diagram

273

SHEAR STRESS DIAGRAM

○ PINION UNDER INVESTIGATION
□ GEAR UNDER INVESTIGATION
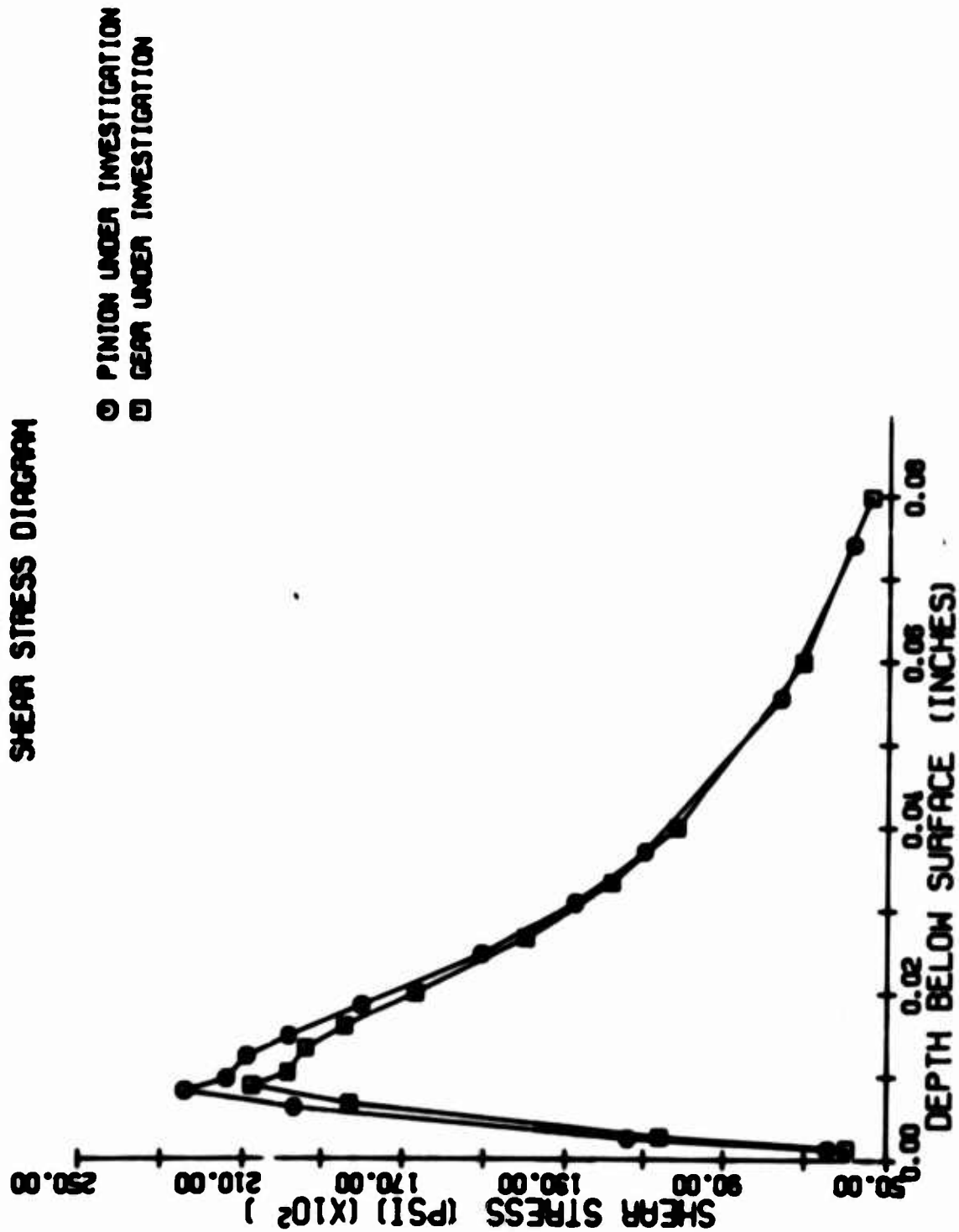
Figure 82. TSPT Ring Planet Mesh at 1138 HP
9035 RPM of Pinion - Shear Stress Diagram

Figure 83.   TSPT Ring Planet Mesh at 1138 HP
9035 RPM of Pinion - Power Loss Diagram

HERTZ STRESS AND P-V PRODUCT DIAGRAM

DEGREES ROLL OF DRIVER

P-V PRODUCT (X10⁵)

HERTZ STRESS PSI (X10³)
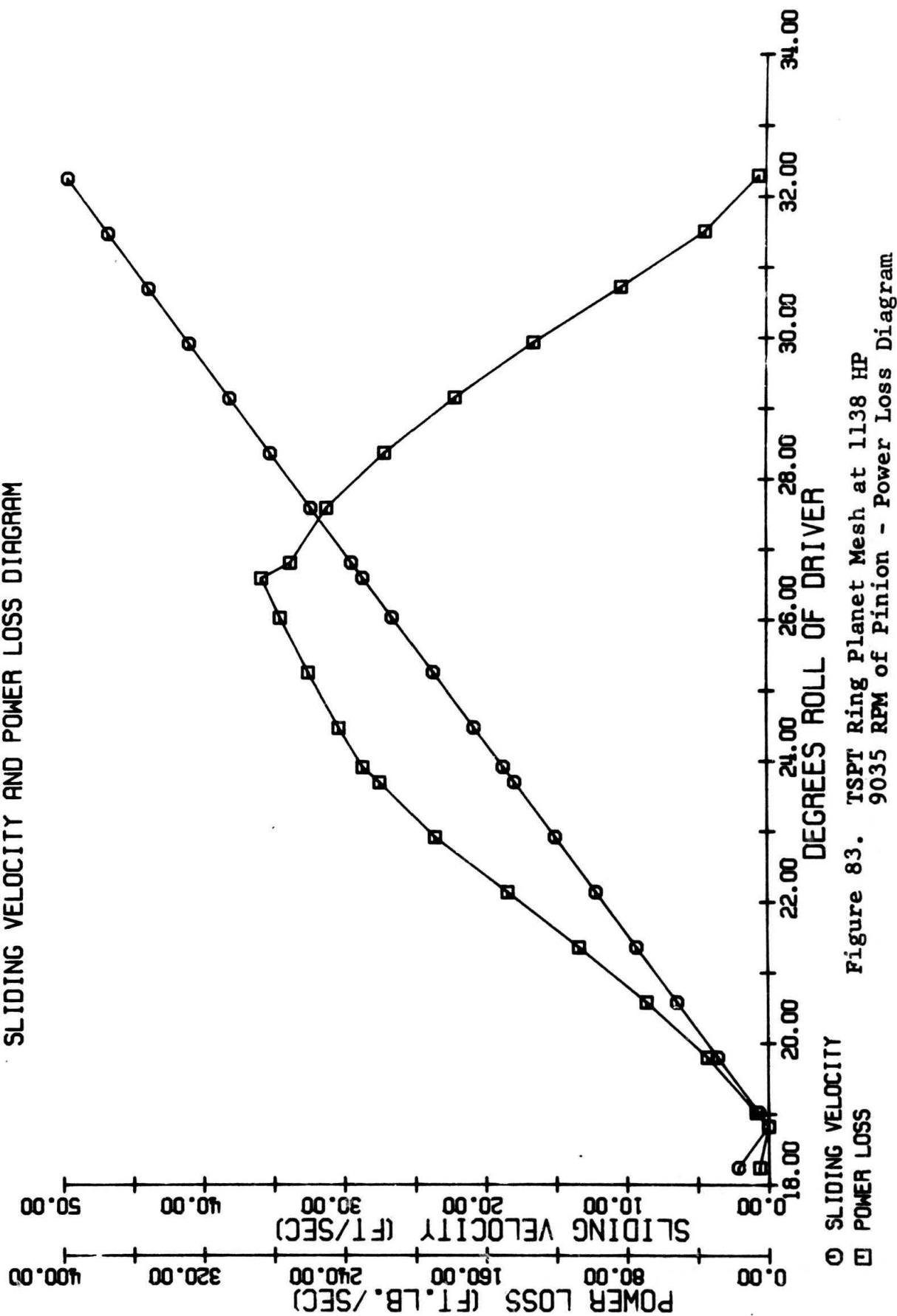
O P-V PRODUCT
□ HERTZ STRESS

Figure 84.   TSPT Ring Planet Mesh at 1138 HP
9035 RPM of Pinion - Hertz Stress Diagram

276

APPENDIX VI

ANALYSIS AND DISCUSSION OF 5x5 ROLLER GEAR SYSTEM

The 5x5 system was pursued until it became evident that a more suitable system could be derived. A concurrent and similar analysis was made of the 8x8 system (as described by TRW). Both systems were eliminated from consideration in favor of the 6x6 configuration.

I. Advantages

    A. Geometry

        1. Roller size is not restricted by interference with adjacent roller shafts for a given ratio reduction.

        2. Fewer gears are required to transmit load.

        3. Gears are loaded higher than in the comparable 6x6 system. This allows (or requires) larger face width, but the gear flanges are (or can be) the same thickness as for a 6x6, since a minimum flange thickness is desired from a rigidity standpoint; i.e., the 6x6 is designed by rigidity requirements rather than torque requirements and is thus a bit more "weighty" than 5x5.

        4. Toggle angle can be easily kept to a small value.

            a. A small toggle angle is (evidently) necessary for "self-preloading."

            b. Whether the floating idler can actually maintain a 3-point contact is highly questionable, but an inward component does exist in the proper design, and this might load the floating idlers.

        5. Only 5 bearings are required to restrain fixed idlers. Parts requirements are minimized.

            Note: A spherical roller bearing is a must for final stage idlers, or a carrier that is ball jointed to prevent roller edge loading.

        6. Helical gearing should be used throughout for the purpose of supporting the weight of the gear elements. Herringbone helices will serve to support the weight of the floating gears.

        7. A planetary support bearing should be incorporated to prevent end loading of the fixed idler roller bearings.

II. Disadvantages

    A. For a staggered system, it is necessary to have an even number of planets due to the "over-under" positioning of the alternate idlers.

1. An odd number of idlers requires five roller paths on the sun gear.
2. System becomes too heavy and too large due to increased size requirements for load-carrying capacity. 5x5 does not have enough load paths. Gear face widths become excessive.
3. Increasing size of gear (P.D.'s) immediately makes reduction ratio too low and spider post size is restricted.
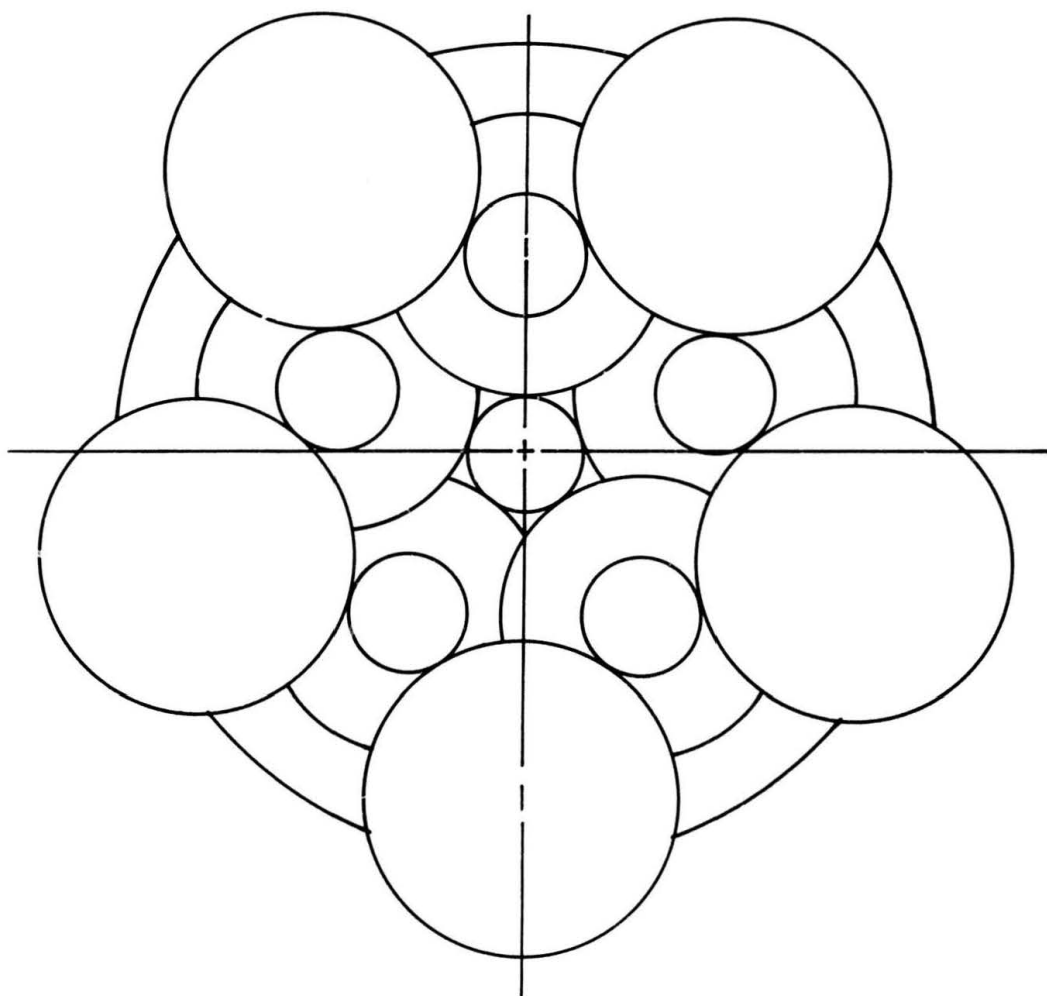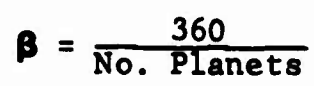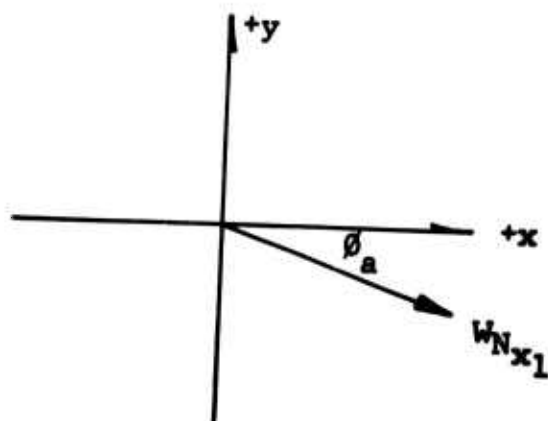
Figure 85. 5x5 Roller Gear Arrangement.

$$\beta = \frac{360}{\text{No. Planets}}$$

Figure 86. System Preloading Formulation.

Resultant Gear Load on Floating Idler

$$P_R = W_{N_{x1}} \ + \ W_{N_{y1}} \ + \ W_{N_{y1}}$$

$\underline{W_{N_{x1}}}$

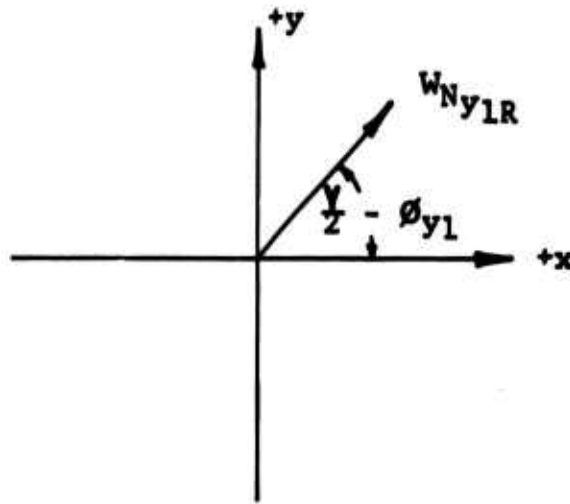$$F_x = W_{N_{x1}} \cos(-\phi_a) = W_{N_{x1}} \cos \phi_a$$

$$F_y = W_{N_{x1}} \sin(-\phi_a) = -W_{N_{x1}} \sin \phi_a$$
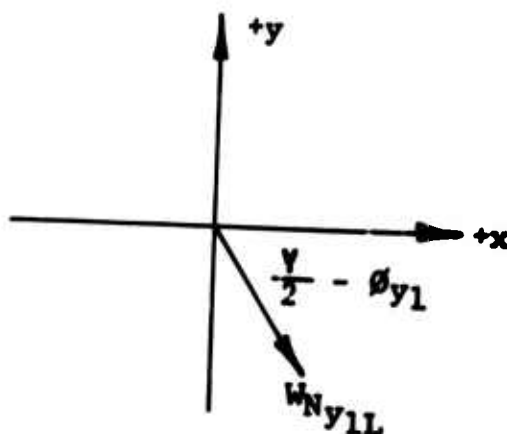
$\underline{W_{N_{y1L}}}$

$$F_x = W_{N_{y1L}} \cos -\left(\frac{\gamma}{2} - \phi_{y1}\right) = W_{N_{y1L}} \cos\left(\frac{\gamma}{2} - \phi_{y1}\right)$$

$$F_y = W_{N_{y1L}} \sin -\left(\frac{\gamma}{2} - \phi_{y1}\right) = -W_{N_{y1L}} \sin\left(\frac{\gamma}{2} - \phi_{y1}\right)$$

281

W_{Ny1R}

$$F_x = W_{Ny1R} \cos\left(\frac{\gamma}{2} - \emptyset_{y1}\right)$$

$$F_y = W_{Ny1R} \sin\left(\frac{\gamma}{2} - \emptyset_{y1}\right)$$

Σ Gear Forces

$$\Sigma F_x = W_{Nx1} \cos\emptyset_a + W_{Ny1R}\cos\left(\frac{\gamma}{2} - \emptyset_{y1}\right) + W_{Ny1L}\cos\left(\frac{\gamma}{2} - \emptyset_{y1}\right)$$

$$W_{Ny1L} = W_{Ny1R} = (.5)\left(W_{Nx1}\right)\left(\frac{N_{x1}}{N_{y1}}\right)$$

$$\Sigma F_x = W_{Nx1}\left[\cos\emptyset_a + \left(1 + \frac{N_{x1}}{N_{y1}}\right)\cos\left(\frac{\gamma}{2} - \emptyset_{y1}\right)\right]$$

$$\Sigma F_y = -W_{Nx1}\sin\emptyset_a - W_{Ny1L}\sin\left(\frac{\gamma}{2} - \emptyset_{y1}\right) + W_{Ny1R}\sin\left(\frac{\gamma}{2} - \emptyset_{y1}\right)$$
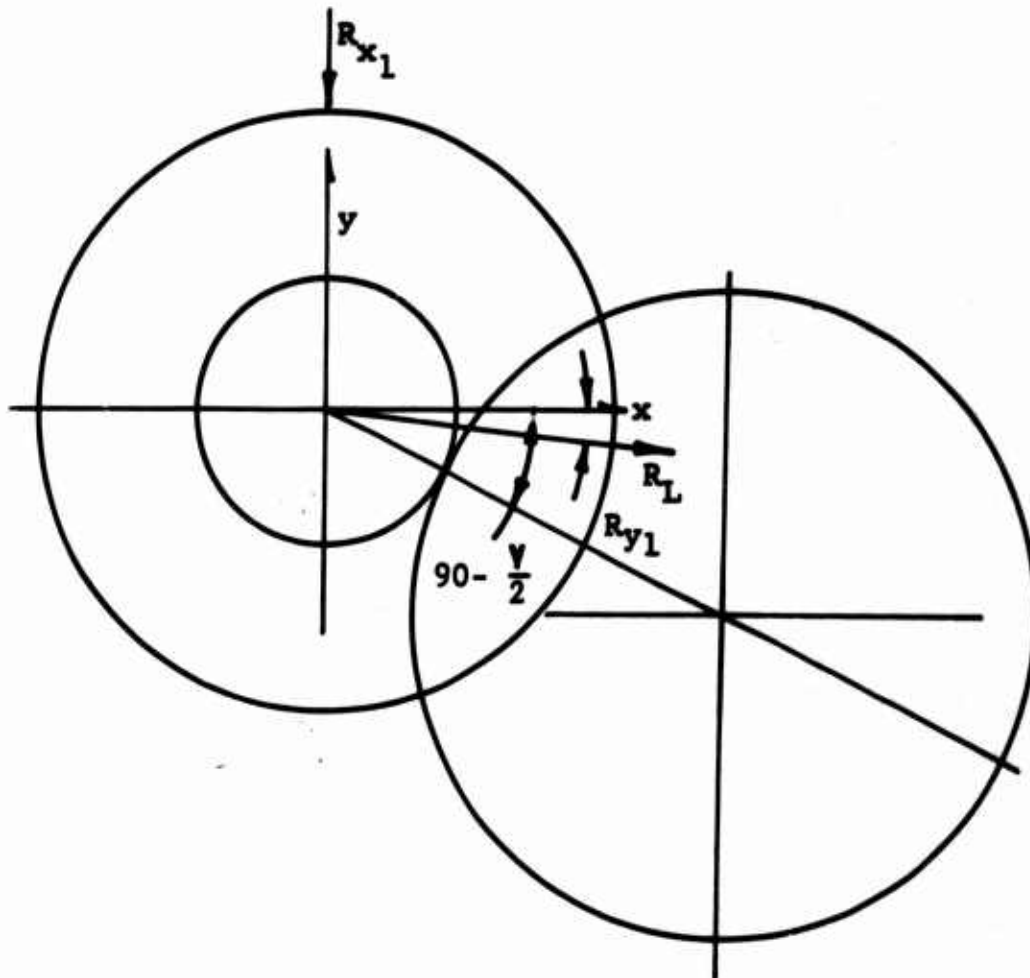
$$= -W_{Nx1}\sin\emptyset_a$$

$$R_L = \text{Resultant Load} = \left[(\Sigma F_x)^2 + (\Sigma F_y)^2\right]^{.5}$$

$$= W_{Nx1}\left\{\left[\cos\emptyset_a + \left(1 + \frac{N_{x1}}{N_{y1}}\right)\cos\left(\frac{\gamma}{2} - \emptyset_{y1}\right)\right]^2 - \left[\sin\emptyset_a\right]^2\right\}^{.5}$$

$$\text{Direction Angle} = \tan^{-1}(\Sigma F_x / \Sigma F_y)$$

Roller Contact Reactions

R_{x_1} = Roller Contact Load at
Sun - x_1 Mesh

R_{y_1} = Roller Contact Load at
y_1 - x_2 Mesh

$$R_{x_1} \leftrightarrow R_{y_1} = R_L$$

$$\Sigma F_y = 0 = R_{y_1} \sin\left(90 - \frac{v}{2}\right) - R_{x_1} - R_L \sin \sigma$$

$$R_{x_1} = R_{y_1} \cos \frac{v}{2} - R_L \sin \sigma = R_L\left(\frac{\cos \sigma}{\tan \frac{v}{2}} - \sin \sigma\right)$$

$$\Sigma F_x = 0 = R_L \cos \sigma - R_{y_1} \sin \frac{v}{2} ; \quad R_{y_1} = R_L \cos \sigma / \sin \frac{v}{2}$$

283

Observations

R_L = Resultant Load Produced by 3 Gear Meshes

    a. R_L is dependent upon only gear loads.

    b. Roller loads are dependent upon gear loads but the ring gear - y_2 tooth loads do not get back into first stage gear meshes. They do, however, load the rollers.

    c. R_{x_1} is read when σ <90 - Υ/2

    d. The forward side of the fixed idler is <u>not</u> loaded by the floating idler (due to gear loads).
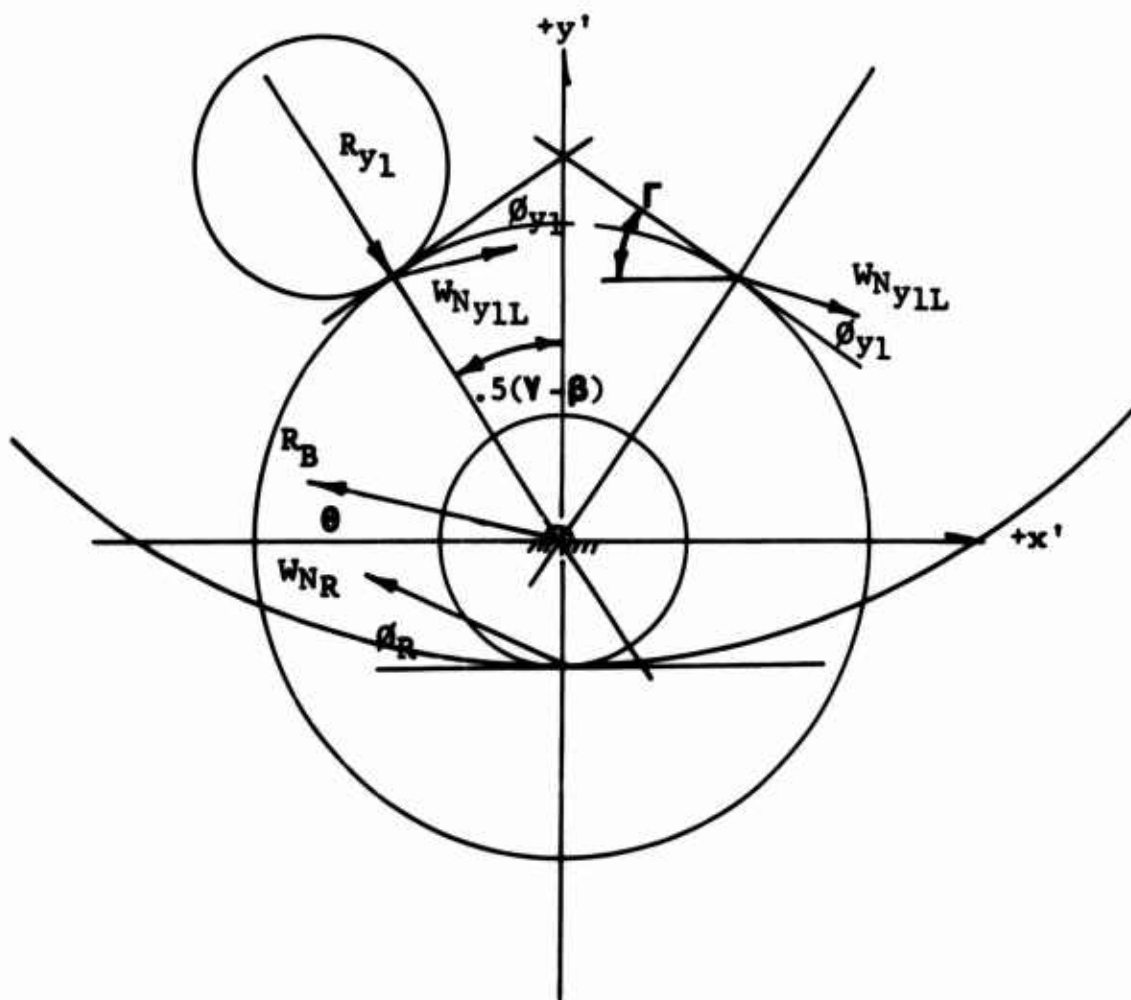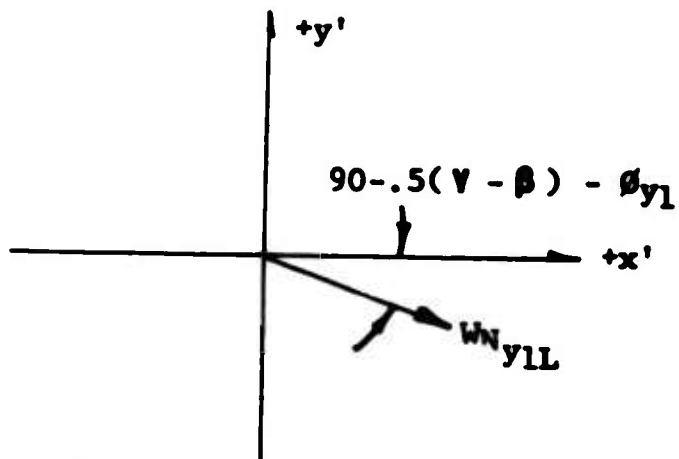

Figure 87. Fixed Idler Load System.
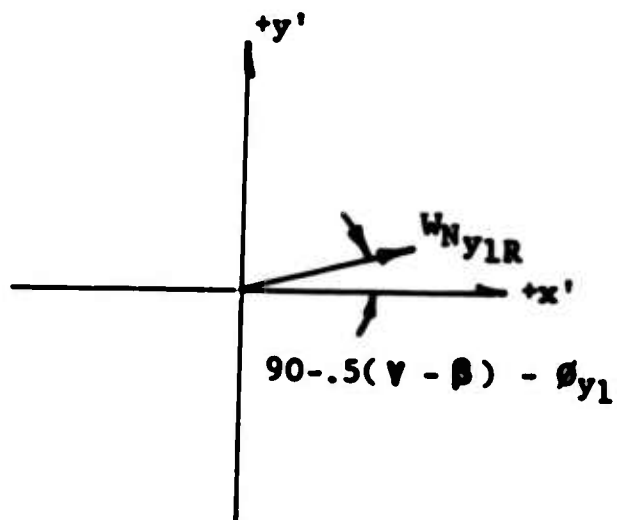
$^{W}N_{y1L}$

$$F_{x'} = W_{N_{y1L}} \sin \left[.5(V - \beta) - \phi_{y1} \right]$$

$$F_{y'} = -W_{N_{y1L}} \cos \left[.5(V - \beta) - \phi_{y1} \right]$$
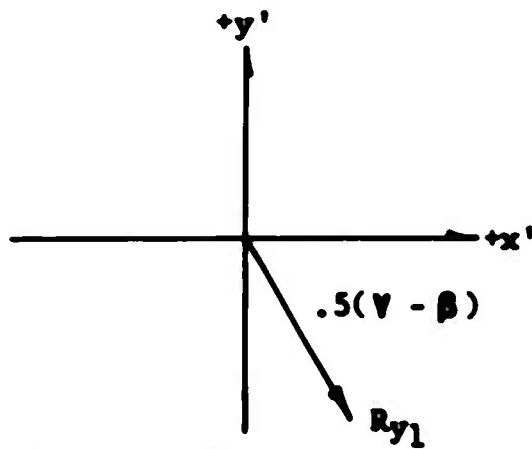
$^{W}N_{y1R}$

$$F_{x'} = W_{N_{y1R}} \sin \left[.5(V - \beta) - \phi_{y1} \right]$$

$$F_{y'} = W_{N_{y1R}} \cos \left[.5(V - \beta) - \phi_{y1} \right]$$

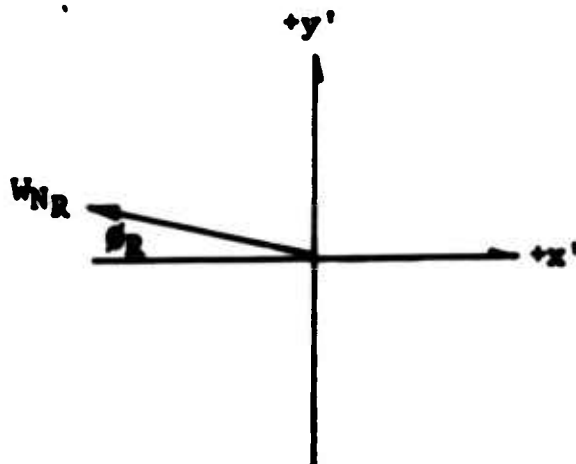$\underline{R_{y1}}$

$$F_{x'} = R_{y1} \sin \left[.5(V - \beta)\right]$$
$$F_{y'} = R_{y1} \cos \left[.5(V - \beta)\right]$$

$\underline{W_{N_R}}$

$$F_{x'} = -W_{N_R} \cos \phi_R$$

$$F_{y'} = W_{N_R} \sin \phi_R$$

$$\Sigma F_{x'} = 0 = (W_{N_{y_{1L}}} + W_{N_{y_{1R}}}) \sin \left[.5(\gamma - \beta) - \emptyset_{y_1} \right]$$

$$+ R_{y_1} \sin \left[.5(\gamma - \beta) \right] - W_{N_R} \cos \emptyset_R - R_{B_x}$$

$$R_{B_x} = W_{N_{x_1}} \sin \left[.5(\gamma - \beta) - \emptyset_{y_1} \right]$$

$$+ R_{y_1} \sin \left[.5(\gamma - \beta) \right] - W_{RN} \cos \emptyset_R$$

$$\Sigma F_{y'} = 0 = W_{N_R} \sin \emptyset_R - R_{y_1} \cos \left[.5(\gamma - \beta) \right] - R_{B_y}$$

$$R_{B_y} = W_{N_R} \sin \emptyset_R - R_{y_1} \cos \left[.5(\gamma - \beta) \right]$$

$$R_B = \text{Resultant Bearing Load} = \left[(R_{B_x})^2 + (R_{B_y})^2 \right]^{.5}$$

$$\theta = \text{Angle with Respect to x' axis} = \tan^{-1}(R_{B_x}/R_{B_y})$$

Observations

1. Fixed idler will move in the direction of R_B an amount equal to the bearing internal clearance.
2. If, and only if, the bearing clearance is sufficient to allow component movement in the direction of the center of the forward floating idler, there will be contact at that idler.
3. R_{y_1} is identically equal to the value calculated on page 283 unless there is positive 3-point idler contact.
4. The radial component of the fixed idler resultant must be large enough to allow contact with the leading floating idler, and it will be if δ is large enough

   δ = Movement of fixed idler normal to leading floating idler

   $$= (\Delta P_d) \sin \theta \cos \left[.5(\gamma - \beta) \right]$$

5. As an example of the magnitude of normal movement, δ, the 38.4 ratio 5x5 allows .0000535 inch/.001 inch internal clearance. Assuming that the bearing inner race is positioned to allow the full radial movement inward, then a .004 P_d results in .00021 normal travel.

6. The 5x5 is apparently the optimum self-preloading geometric system. For larger numbers of idlers, the angle θ decreases and $\gamma - \beta$ increases, resulting in progressively less inward movement (for same pressure angles).

7. The pure roller drive must be preloaded in order for torque
   to be transmitted through the system. This necessitates
   the use of some device to accomplish preloading, whether
   shrink fitting the ring or eccentric mounting the fixed
   idlers. However, for the roller gear drive there is no
   longer any dependency upon the roller friction to transmit
   the torque. The rollers are used merely to position the
   floating idlers and to maintain good alignment. Position
   can be maintained by two roller contacts rather than three,
   which requires preloading.

   In essence, since we do not depend upon roller friction
   for torque transmission, we do not require a normal load
   at the three "contact" points. Positive positioning is
   attained by two reaction points and one resultant load
   between them.

8. With a two-contact-point-positioning criterion established,
   we can further eliminate the requirement for an inward
   component of the fixed idler resultant load.

5x5 Load and Ratio Analysis

Sun Pinion	X_1	Y_1	X_2	Y_2	Ring
N = 25	62	27	64	26	170
P_d = 10.4	10.4	10.0	10.0	10.0	10.4
d_p = 2.4	5.95	2.7	6.4	2.6	17.0
p = .302	.302	.3142	.3142	.3142	.3142
F = .54	.54	.55	.55	2.6	2.6
$\emptyset$ = 20°	20°	20°	20°	20°	25°

1. Ratio = $\frac{17.0}{2.4} \cdot \frac{5.95}{2.7} \cdot \frac{6.4}{2.6}$ = 38.4365

2. Mast Torque = 221,222 in.-lb

3. Mast rpm = 324

4. Sun rpm = 12,453

5. Bevel Ratio = 1.6863

6. Engine rpm = 21,000

7. Sun Pinion Torque = 5564.74 in.-lb

8. Sun Pinion Normal Tooth Load = 986.98

9. X_1 Gear Normal Tooth Load = 986.98   (W_T = 927.46)

10. Y_1 Pinion Normal Tooth Load = 1021.93

11. X_2 Gear Normal Tooth Load = 1021.93   (W_T = 960.29)

12. Y_2 Pinion Normal Tooth Load = 5552.9

13. Ring Gear Normal Tooth Load = 5552.9 (W_T = 5031)

APPENDIX VII

GEAR DESIGN PHILOSOPHY

Speaking in the completely general sense, there are four fundamental failure modes for gear teeth. These are considered to be mechanical wear, breakage (impact or bending fatigue), pitting or spalling, and scoring or scuffing.

The first, simple wear, is generally abrasive in nature and, under conditions of proper protective environment, exists only in relatively soft materials and very low pitch line velocities. For helicopter transmission system design, the use of hardened (Rc 58 min) gears and pitch line velocities in excess of 1000 ft/min completely eliminates failure from simple mechanical wear.

Tooth breakage, the second mode of failure, is most generally related to the basic material endurance strength; impact sufficient to produce brittle failure is not generally found in relatively high-compliance mechanical drives such as found in helicopter systems. In practice, today's limiting design loads tend to be fixed by pitting and scoring phenomena. At such load levels, helicopter transmission spur and helical spur gears can be designed and manufactured with such accuracy and control that failure of this nature rarely, if ever, occurs. As an example of this fact, over 6000 UH-1 transmission systems have been built, containing well over 100,000 spur gears and in all units returned for overhaul, not one instance of tooth breakage has been observed. However, this is not entirely the case with regard to spiral bevel gears. These gears, when manufactured on Gleason machines, have an inherently inferior root fillet geometry, resulting in higher stress concentration and greater tolerance variation in root fillet radii when compared with conventional spur and helical gears.

For these reasons, coupled with the observation that spiral bevel gears will generally exhibit greater pitting life than spur gears under equal load intensity, design loads are more often than not limited by tooth breakage. The AGMA spur bending stress calculation method and the Gleason Works hypoid and bevel stress method (both computerized at BHC) are adequate design tools to obtain wholly reliable service operation.

Pitting failure phenomena cannot be discussed apart from the scoring and lubrication distress failure modes. In classical gear design practices, the pitting life of gears is related to the Hertzian contact stress by the inverse ninth power law much as in antifriction bearing life theory. In this

approach, the basic material endurance or capacity is proportional to its macroscopic hardness and further related to specific chemistry, nonmetallic inclusion size and frequency, grain orientation, and residual stress field.

In this sense, the pitting defined is essentially pitch line or rolling contact fatigue. More often than not, however, other pitting or spalling modes give more trouble in helicopter transmissions. Scoring, discussed in depth later, can lead directly to pitting if the severity is of sufficient magnitude. The scored areas are surrounded with untempered rehardened (mass quenched) martensite, while the primary scored area may be in a relatively soft tempered or annealed state. Repeated stressings will lead to progressive crack propagation from the rehardened interface until severe pitting occurs. The second alternate mode is generally termed case crushing. The gear face develops severe longitudinal and transverse cracks, which yield to formation of large pits or spalls. This is simply attributed to insufficient case depth to support the subsurface shear stress envelope beneath the Hertzian contact hand. The final pitting mode is usually the most frequent in spur gears operating in synthetic lubricants such as MIL-L-7808 at relatively modest pitch line velocities. It may be treated as an interrelation between elasto-hydro-dynamic lubricant film thickness and tooth surface roughness. The origin of such pits is on the surface, at severe asperity contact locations, generally on the driver dedendum at the location of the first point of single tooth contact. The exfoliation progresses in a fan-like shape, broadening and deepening in the direction of sliding (often undermining large sections with subsurface cracks) until large pitts or spalls are evidenced. A design chart, based upon the reduction in normal pitting life vs. relative film thickness, is shown in the Reliability Study discussion. This type of pitting accounts for 90 percent of the primary gear failures observed in closed-circuit overhaul of UH-1 transmission systems.

Successful operation of a properly designed set of gears is finally dependent upon the uniform axial and controlled profile distribution of normal tooth loads and the interdependent conditions of lubrication. Assuming that proper alignment is achieved at the design power deflection condition, the first point of contact occurs at the tip (O.D.) of the driven gear, and contact progresses down the profile until the tooth goes out of action at the driven gear flank. The driven gear tooth assumes a certain amount of the transmitted load immediately upon contact. This load can range from near zero to several times the single tooth transmitted load. Since the teeth are cantilevered beams acting under an elastic loading conditon, there is a calculable amount of deflection present. The pair of teeth just preceding the set that is about to

291

contact at the driven gear tip will be deflected such that the
net effect will be felt as an index error at the first point
of contact. If no attempt is made to relieve this index error,
a direct overload will occur. By proper analysis and design,
this "mis-indexing" can be eliminated. This generally is ac-
complished by modifying, or relieving, the tooth profile at the
driven gear tip an amount that will be equal to, or slightly
less than, the deflection of the pair of preceding teeth. A
similar condition of deflection and modification must also
exist at the last point of contact, to prevent an overload con-
dition as the teeth go out of action.

There are several types of distress that can occur as an ul-
timate result of improper tip and flank relief in a heavily
loaded set of gears. Generally, the initial distress is
scoring which may rapidly progress to destruction of the
critical profile shape, leading ultimately to premature pit-
ting, if the load, lubrication, and speed conditions are suf-
ficiently severe. Scoring may be evidenced as bright-polished
radial grooves at the tips and flanks of the teeth, caused by
direct metal-to-metal contact in conjunction with the swiping
action present at the gear tooth extremities.

Although the exact physics of definition remain the source of
much debate, scoring may certainly be attributed to a pro-
gressively increasing contact temperature generated by high
relative sliding, high unit load, gear tooth geometry, and
constant metallic contact of sufficient energy density to
reach the surface liquification temperature of approximately
2900°F. The ability to transmit high torque loads is con-
tingent upon maintenance of a film of lubricant within the
contact area that is of sufficient depth to prevent progres-
sive harsh asperity contact between the conjugate surfaces
and limit the surface energy density to less than critical
values. Providing there are no asperity contacts, or infre-
quent contacts, the lubricant temperature in the contact area
will stabilize and no distress will occur. However, if the
speed, lubricant type, and transmitted load are combined so
that incipient scoring occurs before temperature stability is
attained, then scoring distress is imminent. The design of a
successfully operable gear set would then dictate that an
adequate lubricant film relative to the surface roughness
values of the operating teeth be maintained under all con-
ditions of operation within the design power envelope.

Definition of adequate thickness film must, of course, con-
sider the total system of lubricant - gear metal reaction
in the so-called EP additives can grossly influence apparent
critical film thickness ratios. Lubricant film thickness is
interdependent with coefficient of friction; in the thick
film lubrication region, an increase in temperature decreases

292

coefficient of friction. Thus, the efficiency increases with lubricant temperature. However, an increase in temperature is accomplished by a decrease in lubricant viscosity and film thickness. If progressive asperity contacts occur, the coefficient of friction will increase and the temperature will not stabilize. Scoring will then result. Whether or not this metallic contact is an abrupt result of collapse of the lubricant film at some intrinsic "critical temperature" of the lubricant, is an unsettled question in today's gearing technology.

The analytical tools at hand, while not completely general in nature, are quite adequate for engineering design work when based upon extensive experience. For operation in mildly reactive lubricants, such as MIL-L-7808 with the case carburized and nitrided gear steel used in this design, such experience is available. The stress levels to which such gear teeth can be loaded and still successfully operate for requisite time intervals have been determined by extensive testing of the UH-1 transmission. Based on the test results and with an intimate knowledge of the operating loads and environment, a theoretical analysis has been devised that will satisfactorily predict the instantaneous stresses and loads of a given gear set. With the theoretical analysis as a design tool and with knowledge gained through experience as a guide, a highly reliable transmission system can be designed and manufactured, with a minimum development cycle. The 6x6C roller gear transmission has been designed to these known operating limits and represents a reasonable approach for the existent state of the art.

STRESS ANALYSIS - ENGINE SDG

For the purpose of a commensurate reliability study, the following rudimentary stress analysis of the engine speed decreaser gearbox was required.

The engine gearbox consists of a concentric input-output drive, a two-stage helical gear reduction unit, with three parallel axis idler cluster gears, equally spaced about the input sun pinion and output sun gear. Each cluster gear is supported by two cylindrical roller bearings mounted in a carrier assembly. The carrier assembly is retained in a mechanical-hydraulic torque reaction device which operates the cockpit torque meter via a pressure transducer system. A scale representation of this drive is shown on page 295.

For analysis purposes, consider 1300 hp input and 1270 hp output.

Necessary gear data are summarized below wherein DP - diametral pitch, N = number of teeth, PD = pitch diameter, Ψ = helix angle, Φ = pressure angle, R = ratio, and F = face width.

Gear	D_p	N	PD	Ψ	Φ	F	R
G_1	15.09	38	2.518	18°5'	20.9		
G_2	15.09	61	4.042	18°5'	20.9	.95	1.605:1
G_3	12.5	27	2.187	10°1'	20.8	1.61	3.21:1
G_4	12.5	54	4.373	10°1'	20.8		2.00:1

Let Q indicate torque

$$Q_{G_1} = \frac{63,000 \times 1300}{21,189} = 3,865 \text{ in.-lbs}$$

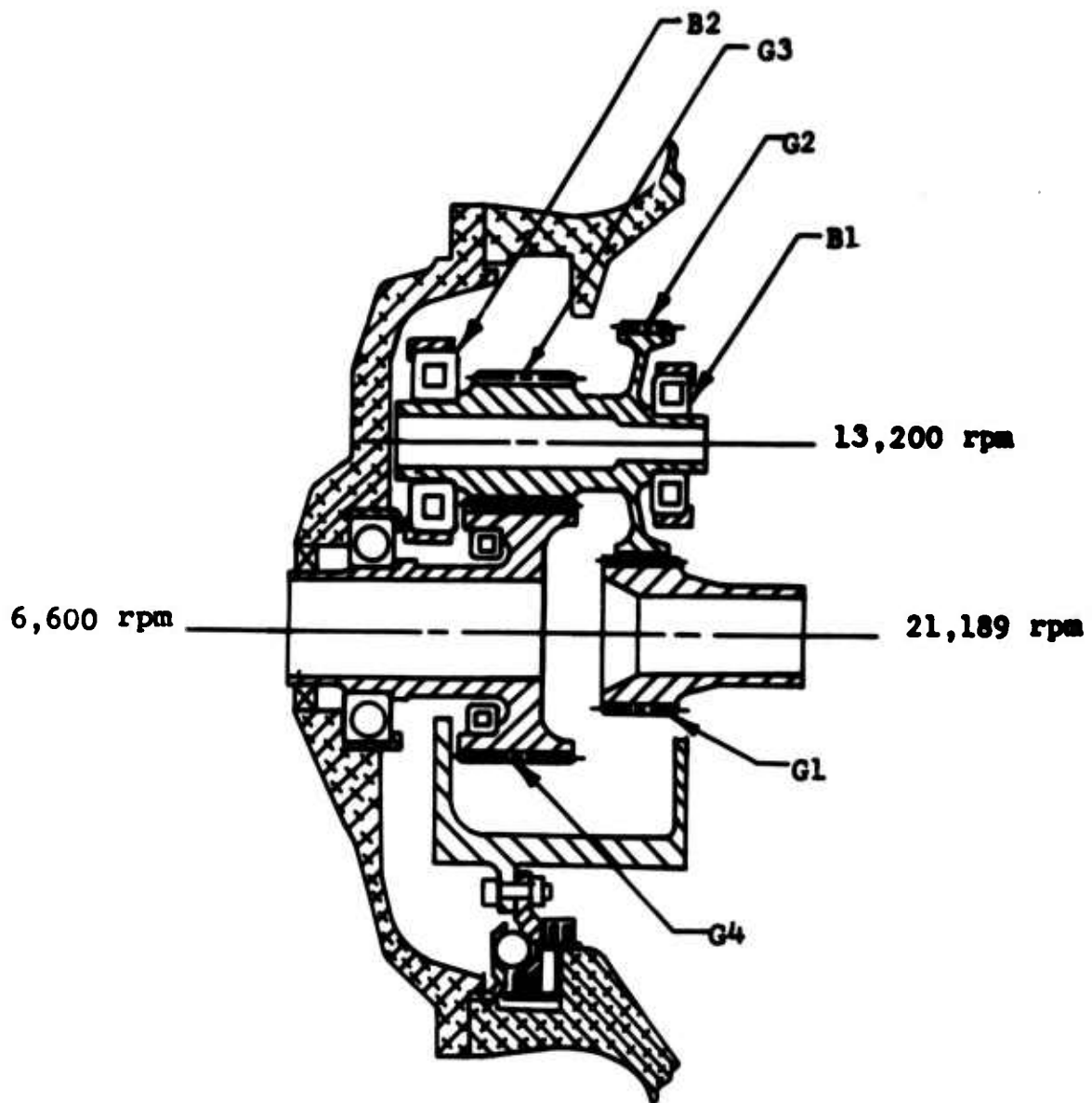$$Q_{G_4} = \frac{1.27}{1.30} \ (3.21) = 12,120 \text{ in.-lbs}$$

Figure 88. Engine Speed-Decreaser Gearbox.

Let W_t indicate tangential tooth load/single mesh

$$W_{t_{G_1}} = \frac{(3865)}{(3)(1.259)} = 1{,}023 \text{ lbs (assuming perfect load sharing between three layshafts)}$$

$$W_{T_{G_3}} = \frac{(12{,}120)}{(3)(2.186)} = 1{,}848 \text{ lbs}$$

The approximate Hertz stress may be calculated via the familiar K factor approach. If d is the pinion P.D.,

$$K = \frac{W_t}{Fd} \left(\frac{R+1}{R}\right), \quad \text{and}$$

$$K_{G_1} = \frac{1023}{(.95)(2.518)} \left(\frac{2.605}{1.605}\right) = 694, \quad \text{and}$$

$$K_{G_3} = \frac{1848}{(1.61)(2.187)} \left(\frac{3}{2}\right) = 787.$$

For helical gears, an acceptable expression for Hertz stress (Sc) is

$$S_C = \left[\frac{.7 \cos^2 \psi}{\left(\frac{1}{E_1} + \frac{1}{E_2}\right) \cos \phi \; \sin \phi \; M_p}\right]^{\frac{1}{2}} (K)^{\frac{1}{2}}$$

Where $E_{1,2}$ = Young's modulus for the respective gears in mesh, and M_p is the profile contact ratio.
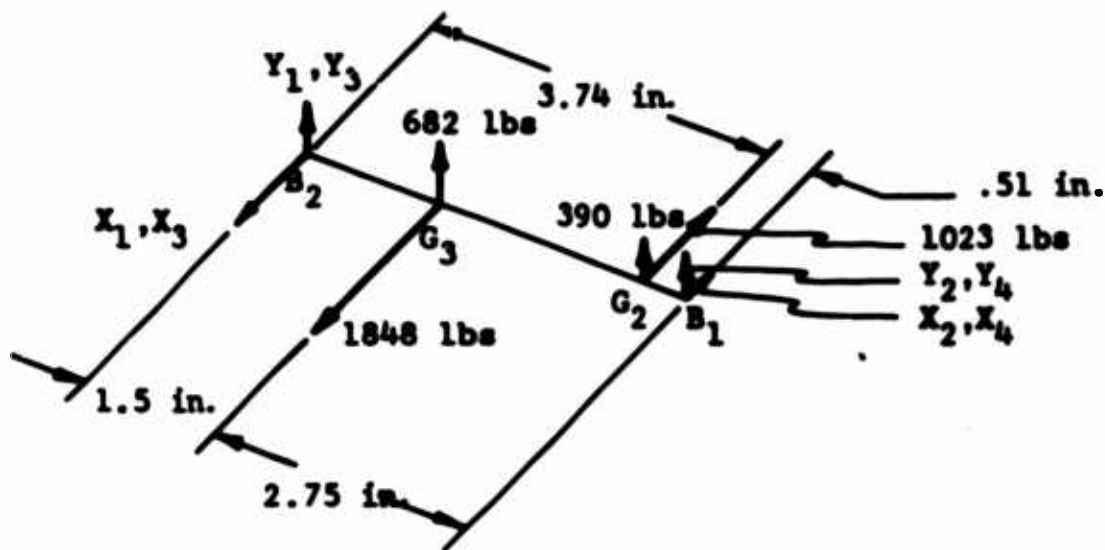
$$S_{C_{G_1}} = \left[\frac{(.7)(.903)\,10^6}{(.067)(.934)(.357)(1.74)}\right]^{\frac{1}{2}} (694)^{\frac{1}{2}}$$

$$= 10^2 (1627.4)^{\frac{1}{2}} (694)^{\frac{1}{2}} = 106{,}000 \text{ P.S.I.}$$

$$S_{C_{G_3}} = \left[\frac{(.7)(.969)\,10^6}{(.067)(.938)(3.47)(1.69)}\right]^{\frac{1}{2}} (787)^{\frac{1}{2}}$$

$$= 120{,}000 \text{ P.S.I.}$$

From EHD computor program runs the elasto-hydro-dynamic film thickness for the G_1 - G_2 mesh is 40×10^{-6} in., and for the

G_3 - G_4 mesh is 30×10^{-6} in.

The estimate life calculations for the loaded bearings B_1 and B_2 follow:

By resolution of moments and orthogonal gear reaction forces,

$$X_1 = (2.75/4.25)(1848) = 1196 \text{ lbs}$$

$$X_2 = (1.5/4.25)(1848) = 652 \text{ lbs}$$

$$X_3 = -(.51/4.25)(1023) = -123 \text{ lbs}$$

$$X_4 = -(3.74/4.25)(1023) = -900 \text{ lbs}$$

$$Y_1 = (2.75/4.25)(682) = 441 \text{ lbs}$$

$$Y_2 = (1.5/4.25)(682) = 241 \text{ lbs}$$

$$Y_3 = (.51/4.25)(390) = 47 \text{ lbs}$$

$$Y_4 = (3.74/4.25)(390) = 343 \text{ lbs}$$

the load (P) on bearing B_1 is

$$P_1 = \sqrt{(X_2 + X_4)^2 + (Y_2 + Y_4)^2} = 634 \text{ lbs}$$

the load on B_2 is

$$P_2 = \sqrt{(X_1 + X_3)^2 + (Y_1 + Y_3)} = 1178 \text{ lbs}$$

The bearing B_1 is an AFBMA size 305 of capacity, C = 5130 lbs. The C/P ratio is 8.09, and the resultant L_{10} life is 1700 hours.

The bearing B_2 is an AFBMA size 307 of C = 8830 lbs.

C/P = 7.4 and L_{10} = 1000 hours. Check to see if the EHD lubrication regime warrants use of a life increase factor

From Reference 9, the relative film index must exceed the value of 2 for increased life.

For B_1

$$\Lambda = (7 \times 10^4)(3 \times 10^{-8})(725)(.56) = .8$$

For B_2

$$\Lambda = \Lambda \quad (1.27) = 1.02$$

Both bearings are in the region of asperity contact distress. This effectively offsets any advantages gained through increased cleanliness material ratings.

DOCUMENT CONTROL DATA - R & D

(Security classification of title, body of abstract and indexing annotation must be entered when the overall report is classified)

1. ORIGINATING ACTIVITY *(Corporate author)*	2a. REPORT SECURITY CLASSIFICATION
Bell Helicopter Company A Division of Bell Aerospace Corporation Fort Worth, Texas	Unclassified
	2b. GROUP

3. REPORT TITLE

INSTALLATION OF A HIGH-REDUCTION-RATIO TRANSMISSION IN THE UH-1 HELICOPTER

4. DESCRIPTIVE NOTES *(Type of report and inclusive dates)*

5. AUTHOR(S) *(First name, middle initial, last name)*

C. W. Bowen
C. E. Braddock
R. D. Walker

6. REPORT DATE	7a. TOTAL NO. OF PAGES	7b. NO. OF REFS
May 1969	311	25

8a. CONTRACT OR GRANT NO. DA 44-177-AMC-411(T) b. PROJECT NO. Task 1G121401D14414 c. d.	9a. ORIGINATOR'S REPORT NUMBER(S) USAAVLABS Technical Report 68-57 9b. OTHER REPORT NO(S) *(Any other numbers that may be assigned this report)* BHR Report 299-099-112

10. DISTRIBUTION STATEMENT

▮▮

11. SUPPLEMENTARY NOTES	12. SPONSORING MILITARY ACTIVITY US Army Aviation Materiel Laboratories Fort Eustis, Virginia

13. ABSTRACT

This report presents the results of an engineering design study to determine the feasibility of utilizing a high-speed roller gear transmission in a turbine-powered helicopter drive system. In such a transmission, the total speed reduction from the engine power turbine to the main rotor is through one bevel gear stage and a single "planetary" stage. The salient advantages of this concept are derived from the use of pitch-line rollers in lieu of antifriction bearings in the "planetary" stage. The study was directed toward the design of an optimized system adaptable to the UH-1 helicopter. Five different roller gear planetary systems were devised and analyzed during this refinement period. Manufacturing tolerance requirements commensurate with reliable operation were also determined. The primary study criteria were cost, weight, efficiency, and reliability as compared to the existent UH-1 system. The comparison results were greatly influenced by the obvious inherent inefficiencies of the two separate speed reduction units and lubrication systems now employed in the UH-1. However, the magnitude of the gains achieved through elimination of the integral engine gearbox was surprisingly large. This fact suggested the need for the further study of a relatively conventional planetary system designed within a comparable premise and utilization of current technological skills. As an extension of the scope of this study, a three-stage planetary adaptation of the UH-1 transmission was designed in order to provide a creditable comparative basis for evaluating the roller gear system.

DD FORM 1473 REPLACES DD FORM 1473, 1 JAN 64, WHICH IS OBSOLETE FOR ARMY USE.

14. KEY WORDS	LINK A		LINK B		LINK C	
	ROLE	WT	ROLE	WT	ROLE	WT
High-speed roller gear transmission						
Turbine-powered helicopter drive system						
UH-1 helicopter						
Bevel gear						
Roller gear planetary systems						
High-reduction-ratio transmission						